29th International conference on atomic collisions in solids &
11th International symposium on swift heavy ions in matter

ICACS & SHIM 2022

Book of Abstracts

June 19–24, 2022
University of Helsinki, Finland

Welcome to ICACS & SHIM 2022

It is with great pleasure, and without hesitation, that we welcome you, on site and virtual, to the jointly arranged 29th International conference on atomic collisions in solids (ICACS) and the 11th International symposium on swift heavy ions in matter (SHIM). While both conferences have been long running, and especially the ICACS conference has already been arranged during extraordinary turns in world history, never before have world events necessitated postponing the conference twice, first from 2020 to 2021, then again from 2021 to 2022. The reason for this is, as all of those reading this text now, in 2022, well know, the COVID-19 pandemic, that brought travel and physical meetings to a halt all across the globe.

We are very pleased that we can now, in June 2022, finally arrange the conference without any local limitations due to the pandemic situation. Yet on a global level many countries still have rules in place that make travel difficult. To enable participation from all countries, we chose to arrange the conference for the first time in a hybrid format, supporting both on site and virtual participation. This solution, necessitated by the present circumstances, can also be considered an experiment that will guide the organization format of future meetings.

We firmly believe that face-to-face scientific discussions during the conferences will inspire many new collaborations, build new bonds, inspire new daring unprecedented ideas. This is particularly important in times that are difficult from both a global health and political viewpoint.

We welcome you all to a week of high-level science and good-spirited community building during the white summer nights of Finland.

Helsinki, June 10, 2022

Flyura Djurabekova	Kai Nordlund
Professor	Professor
Chairperson	Co-chairperson

Contents

Committees

Local Organizing Committee

Flyura Djurabekova	Chairperson
Kai Nordlund	Co-chairperson
Aleksi Leino	Scientific secretary
Xin Jin	Scientific secretary
Aslak Fellman	Webmaster
Ville Jantunen	Webmaster (in 2021)
Christoffer Fridlund	Webmaster (in 2020)
Jesper Byggmästar	
Fredric Granberg	
Alvaro Lopez Cazalilla	
Eryang Lu	
Guanying Wei	
Jintong Wu	
Victor Lindblad	
Milad Ghaemikermani	
Rasmus Nilsson	
Chloé Nozais	
Saana Vihuri	

ICACS International Scientific Committee

Bhupendra Dev	Kharagpur (India)
Flyura Djurabekova	Helsinki (Finland)
Stefan Facsko	Dresden (Germany)
Pedro Grande	Porto Alegre (Brazil)
Platon Karaseov	St. Petersburg (Russia)
Christoph Lemell	Vienna (Austria)
Claudia Montanari	Buenos Aires (Argentina)
Hidemi Ogawa	Nara (Japan)
Daniel Primetzhofer	Uppsala (Sweden)
Pierfrancesco Riccardi	Cosenza (Italy)
Hermann Rothard	Caen (France)
Thomas Schenkel	Berkeley (USA)
Károly Tökési	Debrecen (Hungary)
Christina Trautmann	Darmstadt (Germany)
Hidetsugu Tsuchida	Kyoto (Japan)
Zhiguang Wang	Lanzhou (China)

SHIM International Scientific Committee

Hiro Amekura	Tsukuba (Japan)
Pavel Apel	Dubna (Russia)
Devesh Avasthi	New Dehli (India)
Michael Beuve	Lyon (France)
Wolfgang Bolse	Stuttgart (Germany)
Flyura Djurabekova	Helsinki (Finland)
Norito Ishikawa	Ibaraki (Japan)
Patrick Kluth	Canberra (Australia)
Maik Lang	Knoxville (USA)
Xinwen Ma	Lanzhou (China)
Nikita Medvedev	Prague (Czech Republic)
Isabelle Monnet	Caen (France)
Ricardo Papaleo	Porto Alegre (Brazil)
Hermann Rothard	Caen (France)
Daniel Severin	Darmstadt (Germany)
Christina Trautmann	Darmstadt (Germany)

Maps

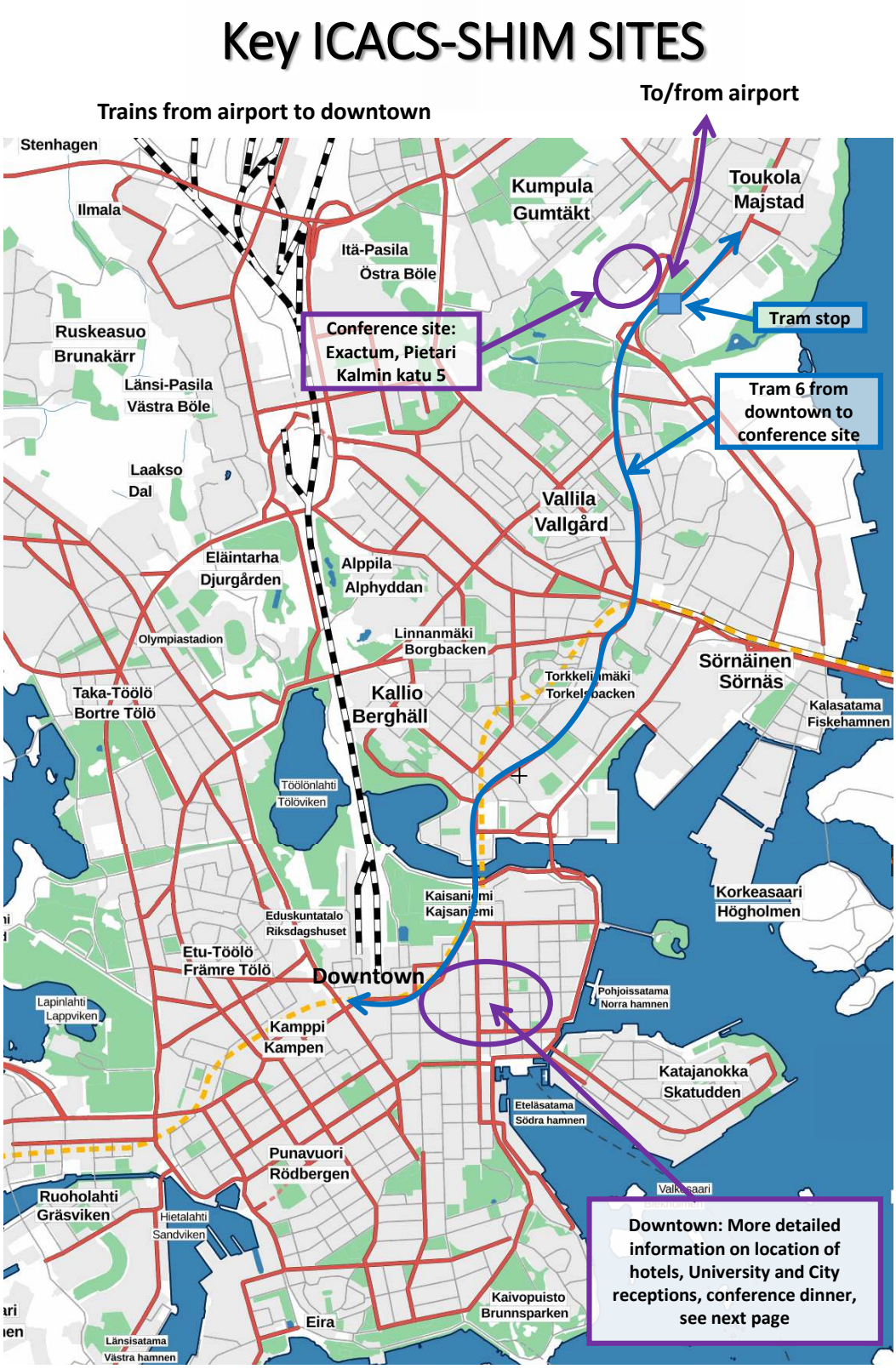
Key ICACS-SHIM SITES
Trains from airport to downtown
To/from airport
Stenhagen
Ilmala
Kumpula
Gumtäkt
Toukola
Majstad
Itä-Pasila
Östra Böle
Tram stop
Conference site:
Exactum, Pietari
Kalmin katu 5
Ruskeasuo
Brunakärr
Länsi-Pasila
Västra Böle
Tram 6 from
downtown to
conference site
Laakso
Dal
Vallila
Vallgård
Eläintarha
Djurgården
Alppila
Alphyddan
Olympiastadion
Linnanmäki
Borgbacken
Sörnäinen
Sörnäs
Taka-Töölö
Bortre Tölö
Kallio
Berghäll
Kalasatama
Fiskehamnen
Töölönlahti
Tölöviken
Korkeasaari
Högholmen
Eduskuntatalo
Riksdagshuset
Etu-Töölö
Främre Tölö
Downtown
Pohjoissatama
Norra hamnen
Lapinlahti
Lappviken
Kamppi
Kampen
Katajanokka
Skatudden
Eteläsatama
Södra hamnen
Punavuori
Rödbergen
Ruoholahti
Gräsviken
Hietalahti
Sandviken
Kaivopuisto
Brunnsparken
Eira
Länsisatama
Västra hamnen
Downtown: More detailed
information on location of
hotels, University and City
receptions, conference dinner,
see next page

Zoom-in on downtown

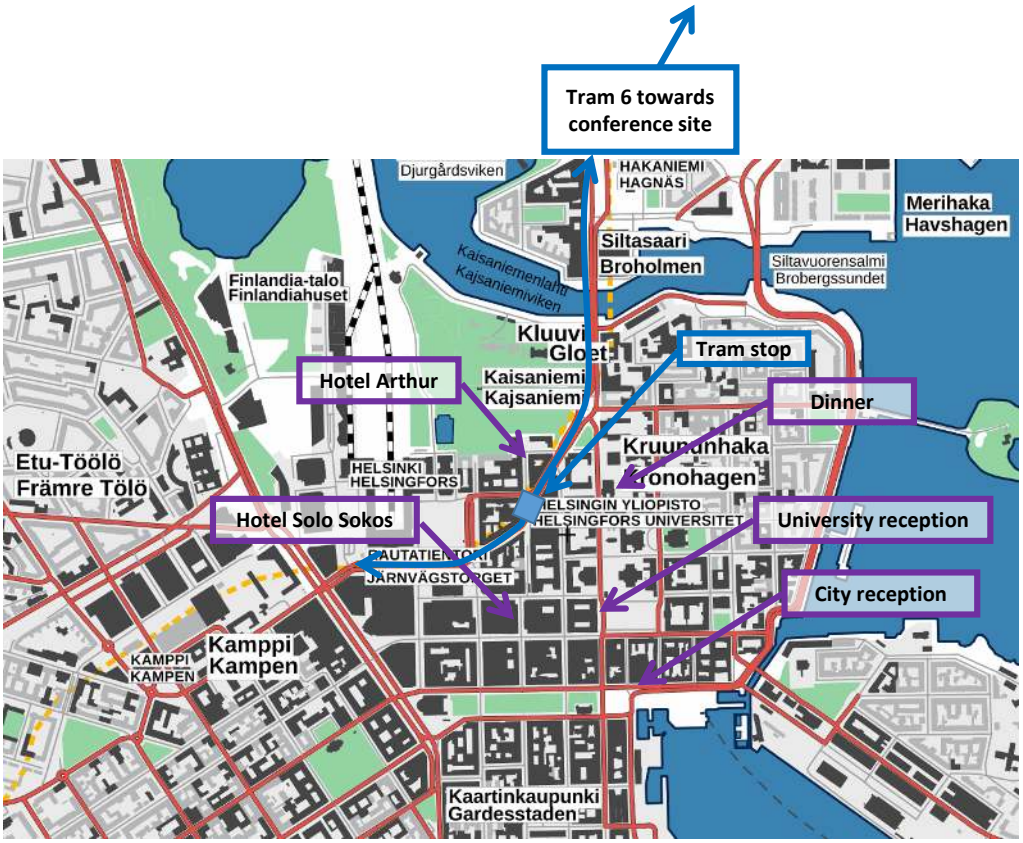

Addresses of key sites, all work in google maps:

- Conference room: Exactum building, Pietari Kalmin katu 5
- Welcome reception*: Accelerator laboratory, Pietari Kalmin katu 2
- University reception: Main building, Senate square, Unioninkatu 34
- City reception: Pohjoisesplanadi 11-13
- Conference dinner: Unionkatu 33
- Hotel Arthur: Vuorikatu 19
- Hotel Solo Sokos Helsinki, Kluuvikatu 8

The direction advices for public transport generally work very accurately in google maps and the free public transport service app HSL.
We will provide a public transportation ticket to attendees.
Before receiving it, you can buy single tickets in the HSL app.

Conference programs

16:00 **Registration and welcome reception**

17:00 Tours to Accelerator Laboratory

19:00 Registration desk is closed

8:00 **Registration and Information desk**

8:40 **Opening of conference**
Chairs: Flyura Djurabekova, Kai Nordlund

Session A1 Sputtering and materials modification

9:00 Particle emission and secondary ion formation in sputtering: a personal view LLp
Andreas Wucher

9:40 Effect of surface roughness on ion induced sputtering O1p
Christian Cupak, Paul Stefan Szabo, Martina Fellinger, Herbert Biber, Johannes Brötzner, Andreas Mutzke, Wolfhard Möller, Richard Arthur Wilhelm, Friedrich Aumayr

10:00 Single-ion induced surface modifications on hydrogen-covered Si(001) surfaces - significant difference between slow highly charged and swift heavy ions O2p
Christian Länger, Philipp Ernst, Markus Bender, Daniel Severin, Christina Trautmann, Marika Schleberger, Michael Dürr

10:20 Ion-beam-induced phase transitions in gallium oxide: impact of the implantation temperature O3p
Alexander Azarov, Calliope Bazioti, Vishnukanthan Venkatachalapathy, Ponniah Vajeeston, Edouard Monakhov, Andrej Kuznetsov

10:40 Coffee break

Session A2 Theoretical foundation of interactions of SHI with materials

11:00 Comprehensive model of SHI impacts: from ion passage to track formation I1p
Ruslan Rymzhanov, Jacques O'Connell, Nikita Medvedev, Marko Ćosić, Vladimir Skuratov, Arno Janse van Vuuren, Sergey Gorbunov, Alexander Volkov

11:30	On the role of oxygen impurities in the synergy between electronic excitations and nuclear collisions on point defect creation in AlN *Mamour Sall, Clara Grygiel, Ons Yahyaoui, Hoda Alassaad, Florian Aubrit, Yvette Ngono-Ravache, Stéphane Guillous, Emmanuel Balanzat, Isabelle Monnet*	O4p
11:50	Paradox resolved: slow electron-phonon coupling vs. fast ion track heating *Nikita Medvedev, Alexander E. Volkov*	O5v
12:10	Annealing of ion tracks in amorphous SiO2 *Shankar Dutt, Christian Notthoff, Xue Wang, Alexander Kiy, Maria Eugenia Toimil-Molares, Christina Trautmann, Pablo Mota-Santiago, Nigel Kirby, Patrick Kluth*	O25p
12:30	Lunch	

Session A3 Experimental observations of SHI induced effects I

13:30	Exploring ion tracks and nanopores using small angle X-ray scattering *Shankar Dutt, Christian Notthoff, Alexander Kiy, Pavel Apel, Nikolay Lizunov, Pablo Mota-Santiago, Nigel Kirby, Maria Eugenia Toimil-Molares, Christina Trautmann, Ilya Korolkov, Maxim Zdorovets, Patrick Kluth*	I2p
14:00	Multi-scale investigation of heterogeneous swift heavy ion tracks in pyrochlore oxides *Eric O'Quinn, Cameron Tracy, William Cureton, Ritesh Sachan, Joerg Neuefeind, Christina Trautmann, Alexandre Solomon, Maik Lang*	O7p
14:20	Swift Heavy Ions interaction with GaN - Relationship between long-range strain fields and track morphologies	O8p

	Miguel C. Sequeira, Isabelle Monnet, Clara Grygiel, Christina Trautmann, Patrick Kluth, Flyura Djurabekova, Kai Nordlund, Eduardo Alves, Katharina Lorenz	
14:40	Ionoacoustic detection and energy-loss measurement of GeV ion pulses *Leon Kirsch, Walter Assmann, Markus Bender, Katia Parodi, Jörg Schreiber, Christina Trautmann*	O9p
15:00	Coffee break	
Session A4	**Atom-surface interactions**	
15:30	Phonon-mediated decoherence in atom-surface collisions *Leandro Frisco, María Silvia Gravielle*	I3v
16:00	Stopping power in heavy atoms: lanthanides, heavy transition metals and beyond *Alejandra Mendez, Jesica Peralta, Dario Mitnik, Claudia Montanari*	O10v
16:20	Electronic excitation by electron promotion during binary atomic collisions in solids *Pierfrancesco Riccardi*	O11v
16:40	Radiolysis and sputtering of amino acids by MeV ions and keV electrons *Cintia Aparecida Pires da Costa, Christian Mejía, Jorge Souza Corrêa, Enio Frota da Silveira*	O12v
17:00	Effect of simulation technique on the defect production and defect evolution in tungsten *Fredric Granberg, Jintong Wu, Daniel R. Mason, Jesper Byggmästar*	O13p
18:00	**Reception by the University of Helsinki**	

Session B1 Low dimensional materials

9:00	Effect of negative ion implantation on optical and surface electronic response of hBN nanosheets *Vidyotma Yadav, Tanmay Mahanta, Tanuja Mohanty*	I4v
9:30	Low energy ion beam induced modifications in optical, structural, chemical and morphological properties of nanostructures MoS2 thin films *Deepika Gupta, Rajesh Kumar*	O14v
9:50	Electronic excitations by keV ions in single crystalline self-supporting targets *Eleni Ntemou, Radek Holeňák, Svenja Lohmann, Daniel Primetzhofer*	O15p
11:10	Radiation Resistance and Cascade Density Effect in α-Ga2O3 *Andrei Titov, Konstantin Karabeshkin, Andrei Struchkov, Alex Pechnikov, Vladimir Nikolaev, Platon Karaseov*	O16v
10:30	Coffee break	

Session B2 Fundamentals of electronic stopping power

10:50	Radiation-induced electronic excitations for defect mobility engineering *Andre Schleife*	I5p
11:20	Application of the PASS code on stopping of slow ions *Peter Sigmund, Andreas Schinner*	O17p
11:40	Non-linear ion stopping calculations for a classical free-electron gas *Pedro Luis Grande, Raul Carlos Fadanelli*	O18p
12:00	Contribution of molecular orbital promotion to the electronic stopping cross section	O19v

Aleksandr Zinoviev, Pavel Babenko, Daria Tensin, Andrey Shergin

12:20 Lunch

Session B3 Atomistic modelling of defects in materials

13:30 Electronic energy losses in two-temperature molecular dynamics simulations of collision cascades I6p
Andrea E. Sand

14:00 Machine Learning modelling the IAEA stopping power database O20v
Dario Mitnik, Felipe Bivort Haiek, Alejandra Mendez, Claudia Montanari

14:20 Energies and volumes of defects and dislocations produced by irradiation: From microscopic to component-scale models. O21p
Sergei Dudarev, Max Boleininger, Peter Derlet, Pui-Wai Ma, Daniel Mason, Luca Reali

14:40 Atomistic simulations of growth mechanisms of hydrogen blisters in copper O22p
Alvaro Lopez-Cazalilla, Flyura Djurabekova, Catarina Filipa Da Palma Serafim, Ana Teresa Perez-Fontenla, Sergio Calatroni, Walter Wuensch

15:00 Explosive desorption induced by radical-radical interaction in methane-doped Ar matrices O23p
Elena V Savchenko, Ivan V Khyzhniy, Sergei A Uyutnov, Mikhail A Bludov, Vladimir E Bondybey

15:20 Coffee break

Session Pp Posters - onsite (See page 26)

18:00 **City reception**

Session C1 Properties of SHI tracks I

9:00	Color centers induced by swift heavy ions and their application as Qubits *Arun Persaud, Kaushalya Jhuria, Qing Ji, Wei Liu, Thomas Schenkel*	I7p
9:30	Density changes in amorphous silicon provoked by swift heavy ions *Sjoerd Roorda, Stéphanie Codsi, Amélie Lacroix, Gabrielle G Long, Fan Zhang, Steven J Weigand, Christina Trautmann*	O24p
9:50	Highly rectifying tunable conical nanopores in amorphous SiO2 *Alexander Kiy, Shankar Dutt, Christian Notthoff, Maria Euginia Toimil-Molares, Patrick Kluth*	O43p
10:10	Ion-tracks and nano-porosity in swift heavy ion irradiated GaSb and InSb *Christian Notthoff, Pablo Mota-Santiago, Andrea Hadley, Taleb Alwadi, Nigel Kirby, Raquel Giulian, Christina Trautmann, Patrick Kluth*	O26p
10:30	Coffee break	

Session C2 Highly charged ions

10:50	Electron emission from freestanding 2D materials during slow highly charged ion irradiation *Anna Niggas, Matthias Werl, Karsten Balzer, Michael Bonitz, Friedrich Aumayr, Richard A Wilhelm*	I8p
11:20	Particle emission from two-dimensional MoS2 induced by highly charged ion impact *Lucia Skopinski, Philipp Ernst, Lars Breuer, Marika Schleberger*	O27p
11:40	Potential sputtering in freestanding van-der-Waals heterostructures	O28v

Richard A. Wilhelm, Anna Niggas, Friedrich Aumayr, Jani Kotakoski

12:00 Probing surface magnetism with highly charged ions by X-ray spectroscopy O29p
Perla Dergham, Matthias Werl, Friedrich Aumayr, Emily Lamour, Stéphane Macé, Christophe Prigent, Sébastien Steydli, Dominique Vernhet, Richard A. Wilhelm, Martino Trassinelli

12:20 Velocity correlated emission of large clusters by fullerene-surface impact O30p
Eli Kolodney, Eran Armon, Anatoly Bekkerman, Erez Zemel, Victor Bernstein, Boris Tsipinyuk

12:40 Lunch

Session C3 Experimental observations of SHI induced effects II

13:40 Local Structure of Ion Tracks in Spinel Compounds by X-ray Spectroscopy I9p
Satoru Yoshioka, Kazuhiro Yasuda, Syo Mastumura, Eiichi Kobayashi, Norito Ishikawa

14:10 Much lower track formation threshold of MeV C60 ions in Si than those of swift heavy monoatomic ions O31v
Hiro Amekura, Kazumasa Narumi, Atsuya Chiba, Yoshimi Hirano, Keisuke Yamada, Shunya Yamamoto, Norito Ishikawa, Nariaki Okubo, Yuichi Saitoh

14:30 On the formation of x-ray waveguide structure in thin films via ion irradiation O32v
Bhupendra Nath Dev, Nasrin Banu, S Roy, B Satpati, S Singh, S Basu

14:50 Velocity distribution of sputtered neutrals under swift heavy ion bombardment O33v

	Tobias Heckhoff, David Theuner, Lars Breuer, Marika Schleberger, Andreas Wucher	
15:10	Elongation of embedded Au nanoparticles in various materials by swift heavy ion irradiation and their plasmonic characterization *Spyridon Korkos, Ville Jantunen, Kosti Tapio, Kai Arstila, Jari Jussi Toppari, Timo Sajavaara, Aleksi Leino, Kai Nordlund, Flyura Djurabekova*	O34p
15:30	Coffee break	
Session Pv	**Posters - virtual**	(See page 31)
19:00	**Conference dinner**	

Session D1 Novel method development

9:00	Single Ion Localization Microscopy for Imaging of Irradiation Effect in Microelectronics *Guanghua Du*	I10v
9:30	He ion channeling contrast investigations using Scanning Transmission Helium Ion Microscopy *Saba Tabean, Michael Mousley, Olivier De Castro, Tom Wirtz, Santhana Eswara Moorthy*	O35p
9:50	Scanning transmission ion microscopy and time of flight energy loss spectroscopy with keV helium ions *Michael Mousley, Saba Tabean, Olivier Bouton, Tom Wirtz, Santhana Eswara*	O36v
10:10	Generation of picosecond ion pulses using a fast pulse electron beam ion source *Gabriel Lukas Szabo, Alexander Sagar Grossek, Anna Niggas, Richard Arthur Wilhelm*	O37p
10:30	Coffee break	

Session D2 Biological and organic applications

10:50	Status and Future Perspectives of Particle Therapy *Christian Graeff*	I11v
11:20	Nanoparticle-assisted radiosensitization in human glioblastoma cells exposed to high-energy photon and charge-particle beams *Danieli B. Guerra, Rafael D. Weimer, Elisa M. N. de Oliveira, Fernanda B. Morrone, Lara Barazzuol, Rob P. Coppes, Ricardo M. Papaléo*	O38p
11:40	Fabrication of Organic Nanowires with Designated Physical Properties via High-Energy Charged Particles	O39p

Masaki Nobuoka, K. Kamiya, Shu Seki

12:00 Reducing uncertainties in particle therapy – status and perspectives I12v
Katia Parodi

12:30 Lunch

Session D3 Astrophysical phenomena and studies of HEA

13:30 Heavy Ion Bombardment of Silicate Targets Relevant to Planetary Surfaces I13v
Rafael Martinez, Alicja Domaracka, Maria E. Palumbo, Giovanni Strazzulla, Philippe Boduch, Hermann Rothard, Enio F. da Silveira

14:00 Sputtering of planets and moons by impact of solar wind ions O40p
Herbert Biber, Paul S. Szabo, Johannes Brötzner, Noah Jäggi, Andre Galli, Peter Wurz, Friedrich Aumayr

14:20 Helium-induced nano-structuring in an FeCoCrNiV high-entropy alloy O41p
Svenja Lohmann, Russell Goodall, Gregor Hlawacek, René Hübner, Le Ma, Amy S. Gandy

14:40 Enhancement of vacancy diffusion by foreign interstitials in FeMnNiCoCr high-entropy alloy O42p
Eryang Lu, Junlei Zhao, Ilja Makkonen, Kenichiro Mizohata, Zhiming Li, Filip Tuomisoto

15:00 **Outing**

Session E1 Properties of SHI tracks II

9:00	SHI induced bulk rotation in non-amorphizable targets *Jacques Herman O'Connell, Danielle Douglas-Henry*	I14P
9:30	Insights into swift heavy ion-induced modification processes in a-SiO2 and a-Ge using molecular dynamics *Aleksi Leino, Ville Jantunen, Flyura Djurabekova*	O6p
9:50	High-Pressure Irradiation Platform at GSI *Ioannis Tzifas, Kay-Obbe Voss, Toimil-Molares Eugenia-Maria, Maik Kurt Lang, Christopher Schröck, Christina Trautmann*	O44p
10:10	Atomic-scale analysis of the swift heavy ion-induced monoclinic-to-tetragonal phase transformation in zirconia *Alexandre P. Solomon, Eric C. O'Quinn, Gianguido Baldinozzi, Maria E. Toimil-Molares, Maik K. Lang*	O45p
10:30	Coffee break	

Session E2 SHI in nanomaterials

10:50	Nanostructuring materials by not-so-swift heavy ion beams *Marko Karlušić*	I15P
11:20	Moderation of SHI induced structure modification of Y4Al2O9 nanoparticles by a surrounding ODS matrix *Anel Ibrayeva, Jacques O'Connell, Alisher Mutali, Ekaterina Korneeva, Alexander Sohatsky, Vladimir Skuratov*	O46p
11:40	Surface nano- and micro-structuring with swift heavy ions in grazing incidence at high fluences *Radia Rahali, Clara Grygiel, Abdenacer Benyagoub, Isabelle Monnet, Mamour Sall, Henning Lebius*	O47p
12:00	Surface nanostructures on Nb-doped SrTiO3 irradiated with swift heavy ions at grazing incidence	O48v

Norito Ishikawa, Yuki Fujimura, Keietsu Kondo, Gabriel L. Szabo, Richard A. Wilhelm, Hiroaki Ogawa, Tomitsugu Taguchi

12:20 Electrochemical Conversion of Cu Nanowires synthesized by electrodeposition in track-etched templates to HKUST-1 O49p
Jia Luo, Michael Wagner, Nils Ulrich, Peter Kopold, Christina Trautmann, Maria Eugenia Toimil-Molares

12:40 **Closing**

List of posters - onsite

P1p The structure and phase composition stability of amorphous Zr irradiated with He ions
Aysha AlNeyadi, Sergey Zlotski, Nicolas Mora, Vladimir V. Uglov

P2p Surface and bulk modifications of 14 MeV Au ion-irradiated diamond
Katja Dorothee Bunk, Igor Alencar, Philipp Bolz, Wolfgang Morgenroth, Florian Bertram, Christian Schmidt, Christina Trautmann, Björn Winkler

P3p Fast and accurate machine-learned interatomic potentials for high-entropy alloys
Jesper Byggmästar, Kai Nordlund, Flyura Djurabekova

P4p Ion implantation, nano-carbon, doping
Boitumelo Joyce Matsoso, Daniel Wamwangi, Rudolph Martinus Erasmus, Neil John Coville, Trevor Ernest DERRY

P5p Bond-specific fragmentation of oligopeptides via electronic stopping of swift heavy ions in molecular films
Pascal Schneider, Philip Keller, Ina Schubert, Markus Bender, Christina Trautmann, Michael Dürr

P6p Simulation and characterization of hot spots generated in plasmas by fast quasi-monoenergetic ion beams
Juan Miguel Gil de la Fe, Pablo Rodríguez Beltrán, Rafael Rodríguez Pérez, Guadalupe Espinosa Vivas

P7p Sputtering of highly corrugated and oriented surfaces
Martina Fellinger, Christian Cupak, Herbert Biber, Johannes Brötzner, Alvaro Lopez-Cazalilla, Raquel Gonzalez-Arrabal, Friedrich Aumayr

P8p An atomistic simulation for the study of Nb-coated SRF cavities by HiP-IMS method
Milad Ghaemikermani, Alvaro Lopez Cazalilla, Flyura Djurabekova

P9p Measurement of oxygen charge state distribution from injected BeO-molecules for Be AMS

Basil Chacko Gonsalves, Kenichiro Mizohata, Kerttuli Helariutta, Pertti Tikkanen, Filip Tuomisto, Jyrki Räisänen

P10p Bunching effects for the electronic straggling of H and He in the matter
Felipe Ferreira Selau, Andreia Mollling, Henrique Trombini, Raul Carlos Fadanelli, Maarten Vos, Pedro Luis Grande

P11p Neutron total scattering analysis of radiation effects in weberite-type oxides
Igor M. Gussev, Eric C. O'Quinn, Gianguido Baldinozzi, Christina Trautmann, Jörg Neuefeind, Changyong Park, Maik Lang

P12p Sequential ion irradiation of GaN studied by MD simulations
Juraj Hanžek, Aleksi Leino, Henrique Vázquez, Flyura Djurabekova, Marko Karlušić

P13p Effect of helium (He) and silver (Ag) co-implanted into SiC: structural evolution and migration behaviour
Thulani Hlatshwayo

P14p Trajectory dependent charge state distribution for keV ions transmitted through crystalline materials
Radek Holeňák, Eleni Ntemou, Svenja Lohmann, Daniel Primetzhofer

P15p Controlled modification of the Au: YSZ structures by high-energy ion irradiation: Structural and optical response in different crystallographic orientations
Adela Jagerova, Romana Miksova, Jakub Cajzl, Vaclav Holy, Marek Vronka, Anna Mackova

P16p RBS dechanneling induced by perfect voids: W as a test-case material
Xin Jin, Flyura Djurabekova, Kai Nordlund

P17p Surface Characterization of CaF2 Crystals Irradiated with MeV Ions Below Charge State Equilibrium
Rajdeep Kaur, Petter Ström, Daniel Primetzhofer

P18p Orientational relationship between SHI induced tetragonal ZrO2 tracks and the monoclinic matrix
Michael Emmanuel Lee, Jacques Herman O'Connell, Vladimir Skuratov

P19p Deuterium's effect on defect accumulation in tungsten during irradiation
Victor Lindblad, Fredric Grandberg, Jesper Byggmästar, Kai Nordlund

P20p Trajectory dependence of electronic energy-loss straggling at keV ion energies
Svenja Lohmann, Radek Holeňák, Pedro L. Grande, Daniel Primetzhofer

P21p Platinum silicide formation on silicon carbide substrates due to thermal annealing and swift heavy ion irradiation
Eric Njoroge, Thulani Hlatshwayo, Vladimir Skuratov

P22p Nuclear stopping power of antiprotons: theory and experimental confirmation
Kai Nordlund, Masaki Hori, Dage Sundholm

P23p Ultrashort pulsed beams of keV ions for materials science at Uppsala University – a status report
Eleni Ntemou, Radek Holeňák, Dan Wessman, Svenja Lohmann, Daniel Primetzhofer

P24p Electronic Sputtering from H2O:C2H6 ice bombarded by energetic heavy ions
Pablo Ramón Batista Oliveira, Rafael Martinez, Enio Frota da Silveira

P25p Applying the inelastic thermal spike model to the investigation of ion tracks in polymers
Max S. da Rocha, João P. M. May, R. S. Thomaz, Ricardo M. Papaléo, Marcel Toulemonde

P26p Trends in electronic stopping powers: the case of period 6
Marcos V. Moro, Eduardo Pitthan, Daniel Primetzhofer

P27p Beam-plasma interaction in fast ignition nuclear fusion: hot-spot gains for different initial conditions

Pablo Rodríguez Beltrán, Juan Miguel Gil de la Fe, Rafael Rodríguez, Guadalupe Espinosa Vivas

P28p Radiolysis of nucleobases by 230 MeV Ca ion beams: temperature dependence (17 - 335 K)
P.C.J. Ada Bibang, Z. Kanuchova, G.S.V Muniz, M. Bender, F. Koch, B. Merk, I. Schubert, D. Severin, C. Trautmann, G. Strazzulla, P. Boduch, A. Domaracka, Hermann Rothard

P29p Adenine irradiated by 800 keV/u proton and helium beams: temperature dependent radiolysis
P.C.J. Ada Bibang, Z. Kanuchova, G.S.V. Muniz, P. Herczku, D.V. Mifsud, Z. Juhasz, S.T.S. Kovacs, S. Ioppolo, N.J. Mason, B. Sulik, P. Boduch, A. Domaracka, H. Rothard

P30p Atomistic model of wet chemical etching of SHI tracks in olivine
Sergey A Gorbunov, Ruslan A Rymzhanov, Alexander E Volkov

P31p Clocking the relaxation of hollow atoms in solids by x-rays
Łukasz Jabłoński, Dariusz Banaś, Paweł Jagodziński, Aldona Kubala-Kukuś, Daniel Sobota, Ilona Stabrawa, Karol Szary, Marek Pajek

P32p Application of the XPS and TRXPS techniques for the analysis of Ti and TiO2 surfaces after modification with slow highly charged Xeq+ ions
Aldona Kubala-Kukuś, Dariusz Banaś, Martyna Piwowarczyk, Ilona Stabrawa, Karol Szary, Daniel Sobota, Regina Stachura, Jolanta Wudarczyk-Moćko, Janusz Braziewicz, Marek Pajek

P33p Analysis of TiO2 and Ti nanolayers irradiated with Xeq+ ions using synchrotron radiation induced XRR and GIXRF methods
Regina Stachura, Aldona Kubala-Kukuś, Dariusz Banaś, Ilona Stabrawa, Karol Szary, Paweł Jagodziński, Giuliana Aquilanti, Iva Božičević Mihalić, Janusz Braziewicz, Marek Pajek, Jacek Semaniak

P34p Molecular Dynamics Simulations of Electronic Sputtering in Amorphous Silica induced by Swift Heavy Ions

Francisco Sánchez-Pérez, Alejandro Prada, Mathieu Bailly-Grandvaux, Eduardo Bringa, María José Caturla, José Manuel Perlado, Jorge Kohanoff, Ovidio Peña Rodríguez, Antonio Rivera

P35p Analytical model for the temperature field of a plasma heated by fast and monoenergetic ion beams
Guadalupe Espinosa Vivas, Juan Miguel Gil de la Fe, Rafael Rodríguez Pérez, Pablo Rodríguez Beltrán

P36p The Effects of SHIs on Si3N4
Arno Janse van Vuuren, Anel Ibrayeva, Vladimir Skuratov, Maxim Zdorovets

P37p A computational approach to the formation and free decay of hollow atoms
Matthias Werl, Anna Niggas, Károly Tőkési, Friedrich Aumayr, Richard Arthur Wilhelm

P38p High-dose high-energy irradiation effects on the defect evolution in tungsten
Jintong Wu

P39p Investigation of He and Kr ion irradiation effects on NiCoFeCr and NiCoFeCrMn high entropy alloys
Ali Yaqoob, Nicolas Mora, Vladimir V. Uglov

P40p Chemical damage and surface roughness induced by 1 MeV/u C and 9 MeV/u Ne ions in thin polymer films of different thickness
R. S. Thomaz, J.P. May, F. V. Filho, Y. Ngono-Ravache, R. M. Papaléo

List of posters - virtual

P1v Observation of ion latent tracks in semicrystalline polymers by scanning electron microscopy
Pavel Apel, Irina Blonskaya, Olga Kristavchuk, Sergey Mityukhin, Alexandr Nechaev, Olga Polezhaeva, Oleg Orelovich

P2v The mechanism of formation of ion-selective channels in PET foils subjected to ion irradiation, photo-oxidation and aqueous extraction
Pavel Apel, Irina Blonskaya, Oleg Ivanov, Olga Kristavchuk, Alexandr Nechaev, Katarzyna Olejniczak, Olga Polezhaeva, Oleg Orelovich, Serguei Dmitriev

P3v Influence of low energy (80 keV) ion beam modifications in structural optical and morphological properties of tungsten oxide thin films deposited by RF sputtering
Deepika Deepika, Deepika Gupta, Vishnu Chauhan, Rashi Gupta, Aman Mahajan, Rajesh Kumar

P4v Effect of high dose gamma radiation on physico-chemical and photoluminescence, surface morphological properties of WO3 thin films
Deepika Deepika, Deepika Gupta, Vishnu Chauhan, Aman Mahajan, Rajesh Kumar

P5v Surface Modifications by Fast Heavy Ions and Slow Highly Charged Ions: Similarities and Differences
Ayman Sherif El-Said

P6v Soft potential and van der Waals effects in He-KCl(001) grazing-incidence fast atom diffraction.
Gisela Anahí Bocan, Hanadi Breiss, Samir Szilasi, Anouchah Momeni, Elena Magdalena Staicu Casagrande, Esteban Alejandro Sánchez, María Silvia Gravielle, Hocine Khemliche

P7v Local structure and hardness change in the amorphization process of Zr-CuAl alloys by heavy ion irradiation
Fuminobu Hori, Yuto Morikuni, Hiroya Obayashi, Akihiro Iwase, Toshiyuki Matsui, Yasuyuki Kaneno, Takeshi Wada, Hidemi Kato, Norito Ishikawa

P8v Density enhancement of ion microbeams with miniature quadrupole magnets for tapered glass capillary optics
Kotoko Inayoshi, Tokihiro Ikeda, Keisuke Ono, Wei-Guo Jin

P9v Analysis of ion-track overlapping effects using Poisson distribution function and Monte Carlo simulation
Akihiro Iwase, Shigeru Nishio, Norito Ishikawa, Fuminobu Hori

P10v Gold nanowire network fabricated by ion-track nanotechnology and its electrochemical properties
Mohan Li, Nils Ulrich, Michael Florian Wagner, Ina Schubert, Christina Trautmann, Maria Eugenia Toimil-Molares

P11v The Variation of Pinning Efficiency in Swift Heavy Ions Irradiated YBCO Superconducting Films
Li Liu, Jie Liu, PengFei Zhai, ShengXia Zhang, Jian Zeng, PeiPei Hu, LiJun Xu, ZongZhen Li

P12v Heavy ion irradiation effects on microstructural properties of amorphous HfO2 thin films
Zongzhen Li, Jie Liu, Pengfei Zhai, Li Liu, Lijun Xu, Shengxia Zhang, Peipei Hu, Jian Zeng

P13v Type and size of the nanostructure formed on a metal surface by an impact of highly charged ions
N.N. Nedeljković, M.D. Majkić, M.A. Mirković, I. Stabrawa, D. Banaś

P14v TREKIS-4: concurrent MC-MD modelling of ion track formation
Nikita Medvedev, Fedor Akhmetov, Ruslan A. Rymzhanov, Roman Voronkov, Alexander E. Volkov

P15v Radiation effects on thymine at low temperature
Christian Mejia, Gabriel Vignoli Muniz, Markus Bender, Daniel Severin, Christina Trautmann, Aditya Narain Agnihotri, Basile Augé, Alicja Domaracka, Boduch Philippe, Hermann Rothard

P16v Radiation damage, conductivity type conversion and p-n nanojunction formation induced by low-energy Ar+ ion collisions with the n-GaAs surface
Valery Mikoushkin

P17v Room-temperature radiation-induced diffusion in the GaAs-oxide irradiated by low-energy Ar+ ion beam
Valery Mikoushkin, Elena Makarevskaya, Anna Solonitsyna

P18v Theory and simulations for plasma created by swift heavy ions
Kengo Moribayashi

P20v Nonlinear effect on Au sputtering by C60- and C70-ion bombardment
Kazumasa NARUMI, Keisuke YAMADA, Yoshimi HIRANO, Atsuya CHIBA, Yosuke YURI, Yuichi SAITOH

P21v Stopping power in lanthanides, from Ce to Lu
Jesica Paola Peralta, Alejandra M. P. Mendez, Claudia C. Montanari

P22v The Levine-Mermin dielectric function to describe stopping of inner-shells.
Jesica Paola Peralta, Marcelo Fiori, Claudia C. Montanari, Alejandra M. P. Mendez

P23v Application of multiple scattering approximation to the calculation ion-atom and ion-molecular collision
Serg Pozdneev

P24v Few-body approximation in chemical physics
Serg Pozdneev

P25v Dissociative electron attachment
Serg Pozdneev

P26v Physics Education and outreach using ion and electron beams
Pierfrancesco Riccardi

P27v Swift heavy ion irradiation of bismuth nanowires pressurized in diamond anvil cells

Christopher Schröck, Ioannis Tzifas, Kay-Obbe Voss, Lkhamsuren Bayarjargal, Wilfried Sigle, Ina Schubert, Maria Eugenia Toimil-Molares, Björn Winkler, Christina Trautmann

P28v Mechanisms of ion irradiated MWNT antibacterial activity: experiment and calculation
Anton V. Stepanov, Andrew A. Shemukhin, Anton V. Nazarov, Anastasia I. Dimitrieva, Alexander P. Popov, Dmitriy S. Yumanov, Alyona V. Kovalenko, Ekaterina Vorobyeva

P29v Si doping of beta-Ga2O3 defect calculation
Anton Stepanov, E. Okulich, D. Tetelbaum

P30v Radiation tolerance of GaN and Ga2O3: role of the defect generation rate
Andrei Titov, Konstantin Karabeshkin, Andrei Struchkov, Alexander Azarov, Platon Karaseov

P31v A graphical user interface for SDTrimSP
Paul S. Szabo, David Weichselbaum, Herbert Biber, Christian Cupak, Andreas Mutzke, Richard A. Wilhelm, Friedrich Aumayr

P32v Projectile dependence in dissociation on biomolecules by swift heavy ion irradiation
Tomoya Tezuka, Mizuki Hongo, Takuya Majima, Manabu Saito, Hidetsugu Tsuchida

P33v Development of analytical methods in the sputtering theory of solids
Luigi Forlano, Alexander Tolmachev

P34v Effect of molecular axis orientation of 3.6 MeV Si2+ on secondary electron emission from carbon foils
Naruki Uno, Takuya Majima, Manabu Saito, Hidetsugu Tsuchida

P35v Surface treatment procedures to mitigate desorption processes induced by swift heavy ions
Verena Velthaus, Trautmann Christina, Bender Markus

P36v Molecular Dynamics Simulations of Silicon Vacancy and Nitrogen Vacancy Color Centers in Diamond
WEI ZHAO, ZONGWEI XU, FEI REN, JINTONG WU, TIANZE SUN

P37v A novel method for preparing highly sensitive graphene room temperature gas detectors
Jian Zeng, Pengcheng Ma, Shengxia Zhang, Lijun Xu, Peipei Hu, Jie Liu

P38v Phase Stability of Pre-irradiated CeO2 with Swift Heavy Ions under High Pressure up to 45 GPa
Jianxiong Lan, Pengfei Zhai, Shuai Nan, Lijun Xu, Jingjing Niu, Cheng Tian, Zongzhen Li, Weixing Li, Jie Liu, Rodney Ewing

P39v Swift Heavy Ion Tracks in CeO2
Jianxiong Lan, Pengfei Zhai, Shuai Nan, Lijun Xu, Jingjing Niu, Cheng Tian, Zongzhen Li, Weixing Li, Jie Liu, Rodney Ewing

P40v Trion Emission in WSe2 Tuned by Swift Heavy Ion Irradiation
Shengxia Zhang, Lijun Xu, Peipei Hu, Khan Maaz, Jian Zeng, Pengfei Zhai, Zongzhen Li, Li Liu, Jie Liu

P41v Dependence of the electronic stopping on the method of measurement
Pavel Babenko, Aleksandr Zinoviev

P42v Fast electron contribution to electronic stopping
Pavel Babenko, Aleksandr Zinoviev

P43v On the problem of Be and W impurities in ITER plasma
Aleksandr Zinoviev, Pavel Babenko, Maxim Mironov, Andrey Shergin

P44v Reflected particles energy spectra during bombarding a tungsten surface with hydrogen atoms
Vladislav Mikhailov, Pavel Babenko, Daria Tensin, Aleksandr Zinoviev

P45v Hydrogen atoms reflection coefficient from the beryllium surface saturated with hydrogen
Vladislav Mikhailov, Pavel Babenko, Daria Tensin, Aleksandr Zinoviev

P46v Channeling of hydrogen isotopes in gold and tungsten
Daria Tensin, Pavel Babenko, Andrey Shergin, Aleksandr Zinoviev

P47v Modeling the interaction of hydrogen and helium isotopes with the first wall of a tokamak reactor
Daria Tensin, Pavel Babenko, Andrey Shergin, Aleksandr Zinoviev

P48v Molecular dynamics simulations of tungsten and beryllium sputtering near threshold
Daria Tensin, Aleksandr Zinoviev, Pavel Babenko, Andrey Shergin

P49v Nuclear stopping powers for DFT potentials
Aleksandr Zinoviev, Pavel Babenko, Kai Nordlund

P50v The potential determination for the H-Au system from experimental data
Pavel Babenko, Aleksandr Zinoviev, Vladislav Mikhailov, Daria Tensin, Andrey Shergin

P51v Photoionization of a Quantum Grating formed by a Single Atom
S.F. Zhang, B. Najjari, Xinwen Ma

P52v Selective Bond Cleavage of ArCO by Electron Impact
Shuncheng Yan, Dong Liu, Songbin Zhang Xinwen Ma

Abstracts

Comprehensive model of SHI impacts: from ion passage to track formation

R.A. Rymzhanov[1,2,*], **J.H. O'Connell**[3], **N. Medvedev**[4,5], **M. Ćosić**[6], **V.A. Skuratov**[1,7,8], **A. Janse van Vuuren**[3], **S.A. Gorbunov**[9], **A.E. Volkov**[1,9]

[1]*Joint Institute for Nuclear Research, Dubna, Russia;*
[2]*The Institute of Nuclear Physics, Almaty, Kazakhstan;*
[3]*Nelson Mandela University, Port Elizabeth, South Africa;*
[4]*Institute of Physics, Czech Academy of Sciences, Prague, Czech Republic;*
[5]*Institute of Plasma Physics, Czech Academy of Sciences, Prague, Czech Republic;*
[6]*Vinča Institute of Nuclear Science, Belgrade, Serbia;*
[7]*National Research Nuclear University MEPhI, Moscow, Russia;*
[8]*Dubna State University, Dubna, Moscow Region, Russia;*
[9]*P.N. Lebedev Physical Institute of the Russian Academy of Sciences, Moscow, Russia;*
[*]*rymzhanov@jinr.ru*

A combined Monte Carlo (MC) and Molecular Dynamics (MD) approach enables us to study in detail effects of different stages of swift heavy ion (SHI) track formation. The MC model (TREKIS [1]) describes excitation of the electronic system and energy transfer to the lattice providing initial conditions for the MD simulations of subsequent lattice response. We discuss here the kinetics of individual track formation, tracks overlap and surface modifications in some amorphizable (YAG, Mg_2SiO_4) and non-amorphizable (Al_2O_3, MgO, CaF_2) solids irradiated with SHIs. High-resolution transmission electron microscopy analysis of samples irradiated with Xe and Bi ions is used to validate the developed model and to investigate the link between the basic properties of the studied materials and the kinetics of structural changes of the targets. We demonstrate the following:

1) The size and morphology of individual latent tracks and tracks overlap at high fluences are strongly affected by recrystallization of the transiently disordered zone [2].
2) Different spectra of electrons generated by ions of different energies result in a velocity effect of track formation and a mismatch between the position of the maximal damage and the Bragg peak of the projectile energy loss [3].
3) Protrusion of molten material and a final structure of surface defects induced by an SHI are governed by mobility of target atoms, surface tensions and recrystallization of a material during the ultra-short cooling period [4].
4) A target thickness affects formation of surface defects under SHI irradiation: the thinnest layers form a through hole, semispherical and spherical hillocks are created after an ion impact at medium thicknesses, whereas nanoparticle emission occurs from thick layers [5].
5) Impact of an SHI under a grazing incidence results in formation of a groove-like structure vs. a chain of nanohillocks depending on material and irradiation properties. It can be concluded that hydrodynamic (Rayleigh) instability of molten material on the surface dominates in hillock chain formation over the effect of the dependence of ion energy loss on the impact parameter.

References

[1] N.A. Medvedev, J.Phys. D 48 (2015) 355303
[2] R.A. Rymzhanov et al. Sci. Rep. 9 (2019) 3837
[3] R.A. Rymzhanov et al. NIMB 440 (2019) 25–35
[4] R.A. Rymzhanov et al. J. Appl. Phys. 127 (2020) 015901
[5] R.A. Rymzhanov et al. Appl. Surf. Sci. 566 (2021) 150640

Exploring ion tracks and nanopores using small angle X-ray scattering

S. Dutt[1,*], C. Notthoff[1], A. Kiy[1], P. Apel[2], N. Lizunov[2], P. Mota-Santiago[3], N. Kirby[3], M.E. Toimil-Molares[4], C. Trautmann[4,5], I. Korolkov[6], M. Zdorovets[6] and P. Kluth[1]

[1]*Department of Materials Physics, Research School of Physics, Australian National University, Canberra, Australia*
[2]*Flerov Laboratory of Nuclear Reactions, Joint Institute for Nuclear Research, Dubna, Moscow region, Russia*
[3]*ANSTO-Australian Synchrotron, Melbourne, Australia*
[4]*GSI Helmholtzzentrum für Schwerionenforschung, Planckstr. 1, Darmstadt, Germany*
[5]*Technische Universtät Darmstadt, Darmstadt, Germany*
[6]*L.N. Gumilvov Eurasian National University, Kazakhstan*
[*]*shankar.dutt@anu.edu.au*

Small angle X-ray scattering (SAXS) is an intriguing tool to study the structure of unetched and etched ion-tracks in a variety of organic and inorganic materials. SAXS is a non-destructive technique and can yield measurements with high precision. SAXS can provide accurate and statistically reliable data since the measured scattering intensity originates from hundreds of thousands of ion-tracks/nanopores. This talk will give an overview of some recent results from our group on synchrotron-based SAXS measurements to explore the morphology of ion-tracks and track-etched nanopores.

Already more than 40 years ago it was noticed that track-etched nanopores in polycarbonate (PC), which are largely cylindrical, may have a tapered structure towards the surfaces. Many more investigations have since followed, indicating that nanopores in PC membranes vary from a perfect cylinder and narrow towards both surfaces. However, due to the inherent difficulty of imaging nanopores using microscopy methods, the quantification of their exact shape has remained elusive. Using SAXS, we were able to quantitatively measure this structure [1]. The high aspect-ratio nanopores were fabricated in PC by irradiating 20 μm thick PC foils with 2.3 GeV Pb ions followed by UV sensitization and etching in 5M NaOH at 60°C. The etch rates for both the radius at the polymer surface and inside the pore were extracted. Both etch rates decrease slightly with increasing fluence, which indicate a track halo radius of approximately 120 nm. Results for the ion-track morphology in polypropylene will also be discussed.

Nanopores with different shapes such as conical, hourglass, cylindrical, and funnel-shaped, fabricated in free-standing silicon dioxide (SiO_2) membranes have interesting applications including bio-sensing (DNA and protein sensing) and charge-based protein separation. We have developed methods for fabricating such nanopore membranes using standard MEMS processing and ion track etching [2,3]. Ion irradiation was performed with 185 MeV Au, 200 MeV Xe, and 1.6 GeV Au ions and subsequent etching using a variety of etching conditions. The novel fabrication methods enable us to create nanopores with lengths ranging from ~50 to 3000 nm with pore opening angles ranging from ~10 to ~110 degrees. The presentation will detail the characterization of the pores using SAXS and explore their potential for bio-sensing and charge-based protein separation.

References

[1] S. Dutt et al., *Journal of Membrane Science*, 638 (2021) 119681
[2] A. Hadley et al., *Physical Review Materials,* 5 (2020) 1-13
[3] S. Dutt, C. Notthoff and P.Kluth, *PCT Patent Application (No. 2021903960) submitted*

Phonon-mediated decoherence in atom-surface collisions

L. Frisco[1] **and M.S. Gravielle**[1,*]

[1] *Instituto de Astronomía y Física del Espacio (UBA-CONICET), Buenos Aires, C1428EGA, Argentina*
[*] *msilvia@iafe.uba.ar*

Grazing-incidence fast atom diffraction (GIFAD) is an exceptionally sensitive method for surface analysis, which can be applied not only at room temperature but also at higher temperatures. However, even though thermal vibrations of surface atoms were often suspected of deteriorating the quantum coherence, most of the theoretical descriptions of GIFAD assume an ideal and static crystal surface, whereas articles dealing with the decoherence introduced by lattice vibrations are scarce.

In this talk, the influence of phonon-mediated processes on the visibility of GIFAD patterns will be analyzed by considering an insulator surface - LiF(001) - for which thermal lattice vibrations are expected to represent the main decoherence mechanism. The theoretical description is based on the phonon-surface initial value representation (P-SIVR) approximation [1], which is a semiquantum method that incorporates the effect of phonon transitions into the SIVR approach [2]. Within the P-SIVR approximation, the main features introduced by thermal lattice vibrations on the angular distributions of scattered projectiles are investigated as a function of the incidence conditions and the crystal temperature T. We found that the azimuthal and polar spectra are strongly affected by thermal fluctuations, which modify the relative intensities and the polar spread of the interference structures, even at room temperature [1,3].

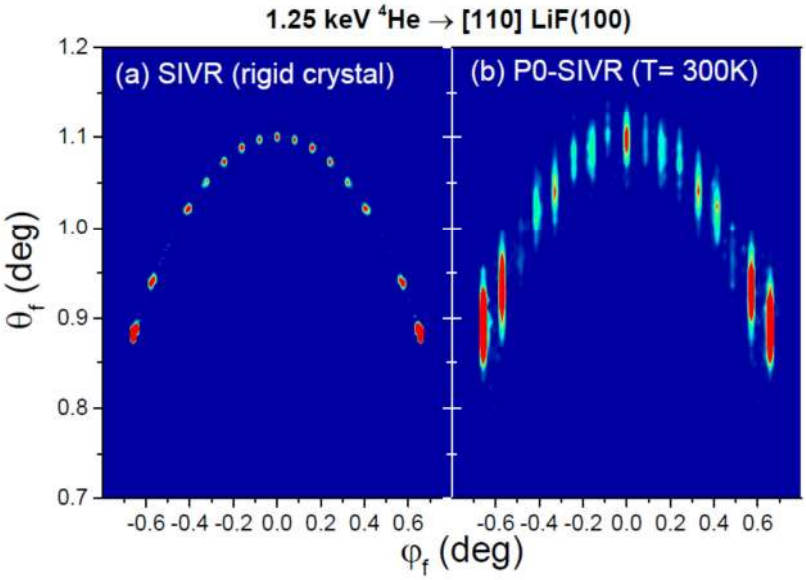

Figure 1: GIFAD distributions derived within (a) SIVR (static crystal) and (b) P0-SIVR (including thermal vibrations) approaches, for a normal incidence energy $E_\perp$ = 0.46 eV.

References

[1] L. Frisco and M.S. Gravielle, *Phys. Rev. A*, 100 (2019) 062703
[2] M.S. Gravielle and J.E. Miraglia., *Phys. Rev. A*, 90 (2014) 052718; *Phys. Rev. A*, 92 (2015) 062709
[3] L. Frisco and M.S. Gravielle, *Phys. Rev. A*, 102 (2020) 062821

Effect of Negative Ion Implantation on Optical and Surface Electronic Response of hBN Nanosheets

V. Yadav[1], **Tanmay Mahanta**[1], **and T. Mohanty**[1,*]

[1]*School of Physical Sciences, Jawaharlal Nehru University, India*
[*]*tanujajnu@gmail.com*

Graphene related wide band gap 2D materials such as hexagonal boron nitride (hBN) nanosheets provide new prospects of device performance. Luminescent centres in the 2D hBN have potential applications in quantum technology. Irradiation with low energy ion beam in keV range is expected to create luminescent defects in a controllable manner in these materials. In this work chemically/physically synthesized hBN nanosheets were then deposited on suitable substrates and irradiated by low energy (30 KeV) negative ion beam irradiation.

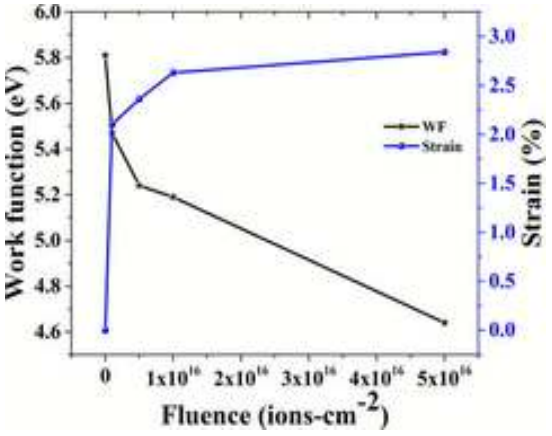

The variation in work function and strain is recorded for hBN nanosheets using different fluences of low energy Au^{-1} ion beam. The work function is decreasing gradually with fluence and strain is showing the exact opposite behavior. Lowering of atomic distances caused by compressive strain leads to decrease in work function. The strain is thus modulating the fermi level of hBNNS while exposing it to low energy ion beam. The XRD and optical response results are also supporting the calculated Strain values using work function values. Surface electronic properties of hBN are mainly due to finite charge transfer between nitrogen and boron atoms.

Ion irradiation in low energy introduces deep level defects in hBN nanosheets thus generating luminescent centers which can play an important role as quantum emitters. The fluence dependent optical response of luminescence centers will be presented.

References

[1] A. K. Geim and K. S. Novoselov, *Nature Materials*, 6 (2007) 183–191
[2] T. Mahanta and T. Mohanty, *AIPApplied Physics Letter,*119 (2021)

Radiation-induced electronic excitations for defect mobility engineering

A. Schleife[1]

[1]*Department of Materials Science and Engineering, University of Illinois at Urbana-Champaign, Urbana, IL 61801, USA*

[*]*schleife@illinois.edu*

Materials modification with atomic precision is a persistent challenge in materials science with great promise: While accurately controlling defect concentrations and defect atomic geometries is difficult, achieving such control enables applications in the context of modern quantum materials and for controlling diffusion in battery applications. Using particle or laser beams to achieve such control is promising, but more understanding of the fundamental interactions and time scales is required.

In this talk, I will present our recent work on two-dimensional and thin materials to understand initial energy deposition, secondary electron emission, and excited-state forces that follow irradiation with energetic ions and lasers. Using real-time time-dependent density functional theory we develop insight into the femtosecond electron dynamics in monolayer graphene and thin slabs of aluminum as test systems and emphasis will be on interesting non-equilibrium effects that occur only for thin target materials. I will also point out connections to carrying over this information into molecular dynamics simulations of systems with larger length and time scales, by exploiting machine learning. Possible applications related to manipulation of defects in materials will be discussed.

References

[1] 1. Phys. Rev. B 103, 224306 (2021)
[2] 2. Nano Lett. 21, 4816-4822 (2021)
[3] 3. Phys. Rev. B 102, 024107 (2020)
[4] 4. Phys. Rev. B 102, 165401 (2020)
[5] 5. Nano Lett. 19, 3939-3947 (2019)

Electronic energy losses in two-temperature molecular dynamics simulations of collision cascades

A. E. Sand

Department of Applied Physics, School of Science, Aalto University, Finland
andrea.sand@aalto.fi

The treatment of electronic effects in multi-million atom simulations of radiation induced collision cascades presents a long-standing challenge in the study of primary radiation damage formation. On the one hand, it is known that energetic projectiles lose energy through electronic stopping as they pass through a material. On the other hand, in near-equilibrium conditions, electrons and ions couple through the electron-phonon interaction. During collision cascades, atoms undergo a continuous transition from the high-energy regime to the equilibrium regime, while at the same time experiencing a highly disordered, under-dense state, surrounded by a higher pressure region. Neither electronic stopping theory nor electron-phonon coupling is suitable for fully describing this whole process.

A recently developed model [1] employing an electron density-dependent coupling term within a two-temperature molecular dynamics (TTMD) scheme is able to describe energy losses during the full evolution of the highly non-equilibrium cascade process, from the early ballistic stage through to the relaxation and cooling phase. In addition, the electronic thermal conductivity, which is important in metals, is captured by the two-temperature framework. I will show that simulations using this model agree with SRIM predictions in the high energy limit, while the cascade recrystallization rate, which controls the degree of atomic mixing, gives agreement with ion beam mixing experiments. I will present recent results from cascade simulations in nickel and tungsten.

Simulations predict a transition in the rate of electronic energy losses occurring between the ballistic phase and the recrystallization phase of cascade evolution, thus capturing both the electronic stopping and electron-phonon interaction regimes without the use of separate coupling terms and cut-off parameters.

This newly developed dissipation model thus offers a significant improvement over current state-of-the-art cascade simulation methodology, by avoiding the use of arbitrary or adjusted thresholds for different ion-electron coupling terms, and replacing them with a more complex physically-informed model of electronic energy dissipation.

References

1 M. Caro, A. Tamm, A. A. Correa, and A. Caro, *Phys. Rev. B,* **99** (2019) 174301

Color centers induced by swift heavy ions and their application as qubits

A. Persaud[1,*], **K. Jhuria**[1], **Q. Ji**[1], **W. Liu**[1], **and T. Schenkel**[1]

[1]*Accelerator Technology & Applied Physics, Lawrence Berkeley National Laboratory, 1 Cyclotron Road, Berkeley, CA 94720, USA*

[*]*apersaud@lbl.gov*

In this talk we give an overview of the application of color centers in quantum information processing. We report on results from recent studies of defect evolution and color center formation in diamonds and single crystalline silicon. In diamond, we are developing a method to create self-aligned NV-centers along the tracks of a swift heavy ion (Au, $1\,\mathrm{GeV}$). As we reported in [1], we found that NV centers are formed along the tracks of swift heavy ions where the formation is dominated by energy deposited by electronic stopping of the ions and do not correlate with the end-of-range of the ions where mostly vacancies are created. Extracting single ion tracks in a lift-out process is expected to enable further insight into the NV centers along the track. Our earlier measurements indicate an average spacing of NV centers on the order of a few nanometers and chain length of tens or more NV centers. Chains with this spacing and length can become resources for quantum sensing applications and for studies of spin coupling. However, alignment and quality of the NV center arrays have to be investigated.

Color centers with photon emission in the telecommunication bands promise to enable large-scale integration of quantum communication between local quantum computer nodes. Attractive candidates are color centers in silicon including the W, G, or T-centers. These might have long electron spin coherent times and narrow linewidths in ^{28}Si enriched SOI-wafers, which we are also exploring. Potential application of such color centers for quantum networks can leverage the established silicon-based manufacturing processes of integrated electronics and photonics platforms. We report on experimental measurements and theoretical calculations (density functional theory) of color centers formed in silicon with intense ion pulses that locally heat and simultaneously dope silicon samples.

The work is supported by the U.S. Department of Energy Office of Science, Office of Fusion Energy Sciences, under Contract No. DEAC02-05CH11231. We acknowledge support through coordinated research project F11020 of the International Atomic Energy Agency (IAEA).

References

[1] R. E. Lake, A. Persaud, C. Christian, E. S. Barnard, E. M. Chan, A. A. Bettiol, M. Tomut, C. Trautmann, T. Schenkel, "Direct formation of nitrogen-vacancy centers in nitrogen-doped diamond along the trajectories of swift heavy ions.", *Appl. Phys. Lett.* 118, 084002 (2021).

Electron emission from freestanding 2D materials during slow highly charged ion irradiation

A. Niggas[1,*], **M. Werl**[1], **K. Balzer**[2], **M. Bonitz**[3], **F. Aumayr**[1], **and R.A. Wilhelm**[1]

[1] *TU Wien, Institute of Applied Physics, 1040 Vienna, Austria*
[2] *Computing Center of Kiel University, 24118 Kiel, Germany*
[3] *Kiel University, Institute for Theoretical Physics and Astrophysics, 24098 Kiel, Germany*
[*] *niggas@iap.tuwien.ac.at*

Upon impact on a material surface, highly charged ions transfer large amounts of their potential energy to the electronic system of the solid. The deposited energy can amount to several tens of keV and triggers a material response, e.g. the emission of x-rays or electrons. Ideal systems to study these effects are freestanding 2D materials: they do not only represent a model system consisting of one material layer only, naturally they also limit the interaction with a transmitting ion to a few fs. This allows for an experimental access to the lifetime of ion-induced electronic decay processes leading to the emission of x-rays and electrons.

Here we present our experimental results on the electron emission from freestanding monolayers of graphene and MoS_2, respectively, both irradiated with slow highly charged Xe ions. All measurements were carried out in coincidence, i.e. corresponding ions and electrons are detected together with information on the ion energy loss, charge state and scattering angle as well as the electron energy and yield.

We recently showed that graphene and MoS_2 behave similar with regard to the ions' neutralisation dynamics [1]. However the electron emission yields from both materials differ strongly: we find up to 100 electrons to be emitted from graphene upon Xe^{40+} impact, but less than 10 from MoS_2. By means of a Green functions approach to the in-plane charge mobility [2] this can qualitatively be explained by a positive charge patch which dissipates within $\sim$fs in graphene. In MoS_2 it stays for the duration of electron emission and thereby prevents low-energy ($< 10\,\mathrm{eV}$) electrons from escaping the material.

In fact, our experiments show a bimodal electron energy distribution ($\sim 4\,\mathrm{eV}$ and $\sim 10\,\mathrm{eV}$) for graphene, but only one peak at $\sim 10\,\mathrm{eV}$ for MoS_2 in agreement with the charge patch suppressing the emission of $\sim 4\,\mathrm{eV}$ electrons [3]. To explore the origin of these distributions we consider calculations of the de-excitation cascade of highly charged ions that take into account both intra-atomic Auger and radiative decay [4].

References

[1] S. Creutzburg, J. Schwestka, A. Niggas *et al.*, *Phys. Rev. B* 102 (2020) 045408
[2] K. Balzer, and M. Bonitz, *Contrib. Plasma Phys.* 62 (2021) e202100041
[3] A. Niggas, J. Schwestka *et al.*, *submitted*
[4] K. Tökesi *et al.*, *Phys. Rev. A* 64 (2001) 042902

Local Structure of Ion Tracks in Spinel Compounds by X-ray Spectroscopy

S. Yoshioka[1,*], K. Yasuda[1], S. Matsumura[1], E. Kobayashi[2] and N. Ishikawa[3]

[1] *Department of Applied Quantum Physics and Nuclear Engineering, Kyushu University, Fukuoka, Japan*
[2] *Kyushu Synchrotron Light Research Center, Saga, Japan*
[3] *Nuclear Science and Engineering Center, Japan Atomic Energy Agency, Tokai, Ibaraki, Japan*
[*] *syoshioka@nucl.kyushu-u.ac.jp*

Spinel oxides with the general formula AB_2O_4 can be formed with a wide variety of divalent A and trivalent B cations. Interestingly, some of the compounds accommodate for a large degree of cation disorder. Under swift heavy ion (SHI) irradiation, structural changes related to the cationic disorder of $MgAl_2O_4$ have been reported using diffraction technique and transmission electron microscopy observation. X-ray absorption near edge structure (XANES) spectroscopy is a powerful structure characterization method that provides local atomistic coordination and electronic structures. Moreover, XANES has great advantage for the elemental selectivity of the multi-cation compounds such as spinels. In this study, we investigated the local structure of $MgAl_2O_4$ spinel induced by SHI irradiation (200 MeV and 100 MeV Xe ions) to quantitatively evaluate the disorder degree. For interpretations of experimental XANES spectra, we perform DFT calculations and adopt theoretical XANES spectra to compare with them [1].

Figure 1(a) shows the experimental difference spectrum of Mg *K*-edge XANES between the pristine and the irradiated sample irradiated with 100 MeV Xe ions to a fluence of 1×10^{13} cm^{-2}. In the calculation, the spectral difference was also evaluated by subtraction of the spectrum of the ideal spinel configuration and that of the disordered configuration. As shown in Fig. 1(b), the difference between the calculated spectra successfully reproduced the experimental difference spectra as well as relative peak energies of peaks *a* to *d*. The spectral change was found to correlate to the increase of the inversion degree of the cations, and the quantitative analysis of the XANES spectra revealed the preferential occupation of cations at the octahedral sites at high fluence [2].

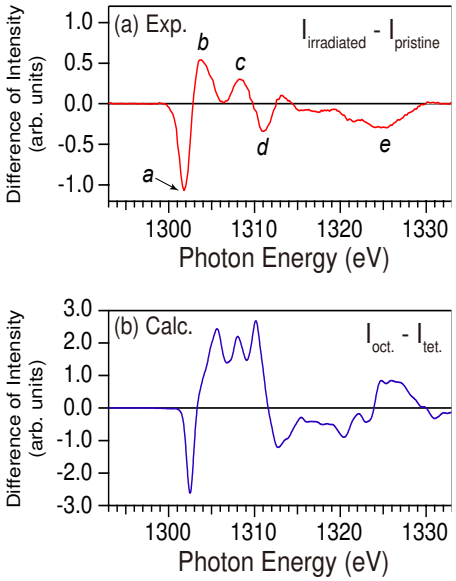

Fig. 1 Differences of Mg *K*-edge XANES. (a) The difference of experimental spectrum between the pristine $MgAl_2O_4$ and the irradiated $MgAl_2O_4$ with 100 MeV Xe ions. (b) The difference of calculated spectra between the ideal spinel configuration and disordered configuration.

References

[1] S. Yoshioka, K. Tsuruta, T. Yamamoto, K. Yasuda, S. Matsumura, N. Ishikawa and E. Kobayashi. *Phys. Chem. Chem. Phys.* 20 (2018) 4962-9.
[2] S. Yoshioka, K. Tsuruta, T. Yamamoto, K. Yasuda, S. Matsumura, T. Sugiyama, Y. Oba, N. Ishikawa and E. Kobayashi and K. Okudaira, *J. Am. Ceram. Soc.* 103 (2020) 4654-63

Single Ion Localization Microscopy for Imaging of Irradiation Effect in Microelectronics

J . Guo[1], **G. Mao**[1,2], **and G. Du**[1,*]

[1]*Institute of Modern Physics, Chinese Academy of Science, China*
[2]*School of Material Science and Engineering, Lanzhou University, China*
[*]*gh_du@impcas.ac.cn*

Cosmic rays in space environment contain high flux heavy ions and protons with energy of tens MeV up to tens GeV. Their ionizing interaction with microelectronics in spacecraft induces single event errors and malfunctions, which is one critical and major cause of in-orbit mission failures. The resolution of the present microbeam facilities for single event effect imaging using high energy heavy ion cannot meet the demand of radiation hardening technique and single event effect study with modern microelectronics with nanoscale fabrication technology. This work targets the development of a new concept of imaging technique for irradiation effect using high energy heavy ions. Based on the high energy heavy ion microbeam facility at HIRFL, single ion scintillation localization microscopy method was developed which allows imaging the single event upset and ion beam induced charge collection with submicron resolution using a slightly focused beam. Such a single ion localization microscopy brings the ion beam imaging technique towards a higher ion energy regime.

Keywords: microbeam, single event effect, single ion localization, ion beam induced charge collection

Status and Future Perspectives of Particle Therapy

Christian Graeff[1,*]

[1]*GSI and TU Darmstadt, Germany*
[*]*C.Graeff@gsi.de*

The finite range of charged particles in tissue permits highly conformal dose delivery to tumors, while sparing healthy tissue and critical organs at risk located nearby. Developments in clinical knowledge, accelerator technology as well as dose delivery and treatment planning strategies have led to a rapid expansion of the number of proton centers in clinical operation both in Europe and worldwide. Also the more complex ion beam centers are being built in Asia, with one planned in the US and four in operation in Europe. The associated cost, technical complexity and lack of hard clinical evidence remain challenges.

Technical and physical developments of modern particle therapy will be presented addressing these challenges. Compact accelerator and facility layouts reduce costs, while advanced delivery strategies are used to exploit the physical precision. This includes imaging and beam range monitoring as well as techniques to compensate target motion due to respiration. These developments aim to reduce uncertainties in the interface of delivery machine and patient, so that the theoretical accuracy of particle therapy can be leveraged for clinical reality and improved patient outcome.

Reducing uncertainties in particle therapy – status and perspectives

K. Parodi[1,*]

[1] *Department of Medical Physics, Faculty of Physics, Ludwig-Maximilians-Universität München, Munich, Germany*

[*] *Katia.Parodi@lmu.de*

Particle therapy is an emerging form of advanced external beam radiation therapy, which particularly exploits the advantageous physical properties of swift ions in matter compared to the widely used X-rays. Due to the predominant electronic energy loss in Coulomb collisions, the deposition of dose (i.e., energy per unit mass) in matter results in a well localized maximum, so called Bragg peak, which can enable a precise targeting of the dose to the tumour, while considerably reducing the burden to the surrounding healthy tissue.

Despite the continued technological evolution of particle therapy, remaining uncertainties in treatment planning and delivery restrict our knowledge in the precise localization of the Bragg peak position within the patient, forcing practitioners to choose more conservative and potentially less effective treatment approaches in current clinical practice. To overcome this issue and unlock the full potential of ion beams for high precision irradiation, extensive research is ongoing. Of particular interest are novel imaging methods which aim at either improving our knowledge of the patient anatomy and stopping power properties at the treatment site prior to irradiation, or utilization of different physical emissions during or shortly after irradiation to infer the beam stopping position inside the patient.

This presentation will give an overview of new approaches and detector technologies under development or already at the stage of initial testing in pre-clinical and clinical research to pave the way for precision image-guided irradiation and advanced adaptive treatment strategies in modern particle therapy.

Parts of the presented work are funded by the European Research Council, the European Commission and the German Research Foundation.

Heavy Ion Bombardment of Silicate Targets Relevant to Planetary Surfaces

R. Martinez[1,2,4], A. Domaracka[2], M.E. Palumbo[3], G. Strazzulla[3], P. Boduch[2], H. Rothard[2], E.F. da Silveira[4]

[1] *Departamento de Física, Universidade Federal do Amapá, Brazil*
[2] *Centre de Recherche sur les Ions, les Matériaux et la Photonique CIMAP Normandie Univ, ENSICAEN, UNICAEN, CEA, CNRS, 14000 Caen, France*
[3] *INAF-Osservatorio Astrofisico di Catania, Italy*
[4] *Departamento de Física, Pontifícia Universidade Católica do Rio de Janeiro, Brazil*
[*] *rafael.mr@unifap.br*

Silicates are ubiquitous in space. They occur in grains in the Interstellar Medium (ISM) and dominate surfaces of inner rocky planets (Mercury in the case of the Solar System), the Moon, and asteroids; silicates constitute the major part of the non-volatile material. Their physical and chemical properties are determined not only on their initial composition but also by processes induced on them. In particular, energetic cosmic particles induce several effects, among them structural changes and sputtering, the latter contributing to the formation of exospheres. As a laboratory approach, several silicate targets were irradiated by energetic (~MeV/u) highly charged projectile ions, and sputtering yields were measured by using the TOF-MS technique (time-of-flight mass spectrometry). Several positive secondary ionic species were identified: Na^+, K^+, Al^+, Ca^+. A predominance of Na and K ions in the sputter flux was observed and their energy distributions were determined with maxima around ~3 eV for Na and ~2 eV for K [1]. From these distributions, escaping fraction of Na^+ and K^+ from planetary surfaces can be estimated. As well, high yields of negative secondary ions were observed, mainly as cluster series: $(SiO_2)_n^-$, $(SiO_2)_nO^-$, $(SiO_2)_nOH^-$ and $(AlSi)O_m^-$. This is unexpected, since due to the prompt secondary electron emission, anion emission is supposed to be some orders of magnitude less intense and softer than cation emission. Current results show similar positive and negative ion yields, for instance, nepheline produces $Y_{i,pos} \sim 0.67$ ions/impact and $Y_{i,neg} \sim 0.13$ ions/impact. This is probably due to relatively low secondary electron emission and/or due to high electron capture by Si containing molecules. The Total Ion Yield (Y) for different materials induced by swift heavy ions, at the low electronic stopping power (S_e), is expected to follow a power law as a function of S_e: $Y = \xi (S_e)^n$, where $n \sim 2$ [2]. Assuming that this law also holds for high S_e values ($S_e = 850$ eV/Å) and considering the experimental results for Y, the ξ value for silicates is determined as being for SiO_2: 9.1E-7 (Å/eV)^2, anorthite: 7.9E-7, jadeite: 9.1E-7 (Å/eV)^2 and nepheline: 0.1E-7 (Å/eV)^2. Also *sputtering rates* of 6.3×10^{-2} particles cm^{-2} s^{-1} at cosmic ray energies of 0.46 MeV/u are determined, and the corresponding *sputtering timescale* is around $\tau \sim 15.9$ s cm^2 ion^{-1}. These results indicate that the evolution of planetary silicates surfaces subjected to cosmic rays is relatively resilient against sputtering by cosmic rays [2].

References

[1] Martinez, R.; et al. NIM B 406 (2017) 523
[2] Martinez, R.; et al. Icarus, 375 (2022) 114830

SHI induced bulk rotation in non-amorphizable targets

J. O'Connell[1,*] **and D. Douglas-Henry**[1]

[1]*CHRTEM, Nelson Mandela University, South Africa*
[*]*joconnell@mandela.ac.za*

An interesting and relatively under studied effect of SHI irradiation at off normal incidence is that of induced rotation in materials. The effect was first observed in amorphous glasses and was explained via a continuum mechanics approach in [1]. Since then, rotation has been observed in several polycrystalline and single crystalline systems using mainly surface shifts and X-ray diffraction to measure rotation angle [2, 3]. Without directly imaging the microstructure it was suspected that crystalline specimens would partially amorphize under irradiation and that grain rotation was facilitated by the amorphous matrix in which the remaining crystallites were suspended. Recent electron microscope-based analysis proved this assumption to be incorrect and instead it is believed that rotation is a consequence of complex dislocation motion due to off normal ion hammering stresses.

A case study of 593 MeV Au irradiated single crystal (001) oriented NiO will be presented as the simple NaCl structure limits the number of required slip systems when the irradiation geometry is suitably symmetric. In order to gain insight on the rotation mechanism, depth (and thus S_e) dependent rotation curves were extracted from electron backscatter diffraction maps of cross sectionally polished specimens and TEM was used to study the microstructure of irradiated specimens. Comparison of SEAD rotation vs depth profiles to those obtained through EBSD which do not require electron transparent lamellae shows that little to no relaxation occurs upon thinning indicating a mostly plastic deformation and relaxed microstructure.

References

[1] S. Klaumünzer, *Nucl. Inst. Meth. B*, 215 (2004) 345-352
[2] I. Zizak, N. Darowski, S. Klaumünzer, G. Schumacher, J. W. Gerlach, and W. Assmann, *Nucl. Inst. Meth. B*, 267 (2009) 944–948
[3] I. Zizak, G. Schumacher, N. Darowski, and S. Klaumünzer, *Phys. Rev. Lett.,* 101 (2008) 1–4

Nanostructuring materials by not-so-swift heavy ion beams

M. Karlušić[1]

[1]*Ruđer Bošković Institute, Bijenička 54, 10000 Zagreb, Croatia*
[*]*marko.karlusic@irb.hr*

Swift heavy ion irradiation is generally considered as an established technique for materials nanostructuring. Permanent damage along each ion trajectory, i.e. an ion track, can be exploited for diverse applications like track etch membrane production, fission track dating and radiation hardness testing. However, ion tracks are formed only when the density of deposited energy exceeds certain material-dependent threshold. This presents a challenge for ion track research at small and medium sized accelerator facilities, where available ion types and ion energies are insufficient to produce ion tracks in wider range of materials.

In this contribution, recent examples of ion track experiments using ion beams that are generally not considered swift (E < 1 MeV/u) nor heavy (m < 20 u) will be presented. These include ion irradiation of graphene, graphite, GaN, MgO and Al_2O_3 [1-3].

References

[1] M. Karlušić, R.A. Rymzhanov, J.H. O'Connell, L. Bröckers, K. Tomić Luketić, Z. Siketić, S. Fazinić, P. Dubček, M. Jakšić, G. Provatas, N. Medvedev, A.E. Volkov, M. Schleberger, Mechanisms of surface nanostructuring of Al_2O_3 and MgO by grazing incidence irradiation with swift heavy ions, *Surf. Interf.* 27 (2021) 101508.

[2] K. Tomić Luketić, M. Karlušić, A. Gajović, S. Fazinić, J.H. O'Connell, B. Pielić, B. Radatović, M. Kralj, Investigation of Ion Irradiation Effects in Silicon and Graphite Produced by 23 MeV I Beam, *Materials* 14 (2021) 1904.

[3] M. Karlušić, M. Mičetić, M. Kresić, M. Jakšić, B. Šantić, I. Bogdanović-Radović, S. Bernstorff, H. Lebius, B. Ban-d'Etat, K. Žužek Rožman, J. H. O'Connell, U. Hagemann, M. Schleberger, Nanopatterning surfaces by grazing incidence swift heavy ion irradiation, *Appl. Surf. Sci.* 541 (2021) 148467.

Effect of surface roughness on ion induced sputtering

C. Cupak[1*], P. S. Szabo[1,2], M. Fellinger[1], H. Biber[1], J. Brötzner[1], A. Mutzke[3], W. Möller[4], R. A. Wilhelm[1], and F. Aumayr[1]

[1] *Institute of Applied Physics, TU Wien, Vienna, 1040, Austria*
[2] *Space Sciences Laboratory, University of California, Berkeley, CA 94720, USA*
[3] *Max–Planck Institute for Plasma Physics, 17491 Greifswald, Germany*
[4] *Helmholtz-Zentrum Dresden-Rossendorf e.V. (HZDR), 01328 Dresden, Germany*
[*] *cupak@iap.tuwien.ac.at*

The sputter yields of solids under ion bombardment are highly sensitive to the roughness of their surfaces. Most laboratory experiments on sputtering have so far been performed on polished, ideally flat samples. However, realistic materials such as the walls of fusion reactors [1] or the rocky surfaces of moons or planets without an atmosphere [2], either are rough or become rough due to prolonged bombardment by plasma or solar wind ions. On rough surfaces effects of local ion incidence angles, shadowing, redeposition and secondary sputtering by reflected ions can influence the sputter yield both in its magnitude and dependence on the projectiles' incidence angle [3, 4].

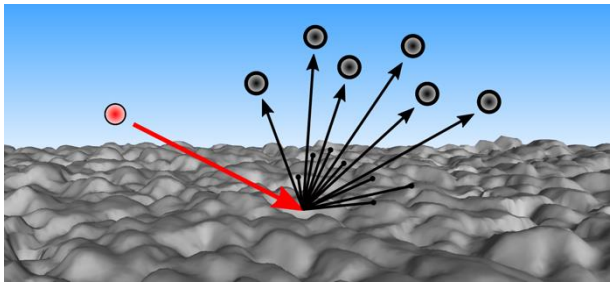

Figure 1: Surface roughness changes the local impact angles of the ions. Some areas of the surface cannot be hit by ions at all (shadowing effect). In addition, sputtered atoms may be redeposited on neighbouring slopes [3].

We have therefore investigated metallic samples of largely different roughness, characterized by atomic force and confocal microscopy. A highly sensitive quartz crystal microbalance was used to determine sputter yields during ion irradiation. Low ion fluences were applied to ensure that the surface morphology did not change during irradiation. The results were used to benchmark the new ray-tracing simulation code SPRAY, which can take microscopy images without limitations in size as input. SPRAY was furthermore applied to perform systematic simulations for artificially roughened and computer-generated surfaces. A clear result was that the governing parameter for the description of the sputtering behavior is the mean value of the surface inclination angle distribution, rather than the commonly used root mean square roughness [4]. Our simulations - supported by a recent analytical model [5] - show that this parameter is universally applicable for a wide range of different surface structures, particularly for randomly rough surfaces with Gaussian distributed height values.

References

[1] S. Brezinsek, et al., *Nucl. Fusion* 57 (2017) 116041
[2] P. S. Szabo, et al. *The Astrophysical J.* 891 (2020) 100
[3] M. Küstner, et al., *Nucl. Instr. Meth. B* 145 (1998) 320; U. von Toussaint et al, *Phys. Scr.* T170 (2017) 014056
[4] C. Cupak, et al., *Appl. Surf. Sci.* 570 (2021) 151204
[5] P. S. Szabo, et al., *Surf. & Interf.* (2022) submitted

Single-ion induced surface modifications on hydrogen-covered Si(001) surfaces – significant difference between slow highly charged and swift heavy ions

C. Länger[1], P. Ernst[2], M. Bender[3,4], D. Severin[3], C. Trautmann[3,5], M. Schleberger[2], and M. Dürr[1,*]

[1]*Institut für Angewandte Physik, and Zentrum für Materialforschung, Justus-Liebig-Universität Giessen, Germany*
[2]*Fakultät für Physik and CENIDE, Universität Duisburg-Essen, 47057 Duisburg, Germany*
[3]*GSI Helmholtzzentrum für Schwerionenforschung, Germany*
[4]*Fachbereich Ingenieurwissenschaften, Hochschule RheinMain, Germany*
[5]*Fachbereich Materialwissenschaften, Technische Universität Darmstadt, Germany*
[*]*michael.duerr@ap.physik.uni-giessen.de*

The formation of nanostructures on the surface of solids by either swift heavy ions (SHI) or slow highly charged ions (HCI) has been observed for many different materials [1]. Both ion types interact primarily with the electronic subsystem of the target material; it has therefore been suggested that the subsequent relaxation mechanisms might be similar and, as a consequence, should lead to similar modifications. Crystalline silicon is a most interesting test case for the comparison of SHI and HCI, as no track formation was observed in crystalline silicon in the case of irradiation with monoatomic SHI up to a stopping power of 21 keV nm^{-1} [2]; in contrast, HCI irradiation of a Si(111) surface was shown to induce damage in areas of several nanometers in diameter [3].

For the further investigation of ion-induced modifications in crystalline silicon, we made use of hydrogen passivated Si(001) surfaces in combination with scanning tunneling microscopy (STM) [4]. As hydrogen desorption from these surfaces leads to distinct signatures in STM measurements, ion-induced surface modifications can be resolved on the atomic scale. Furthermore, desorption of hydrogen under ultra-high vacuum conditions is an irreversible process. Thus, if a thermal spike would lead to hydrogen desorption at the surface at any time after ion impact, this modification would be observable even if the substrate itself recrystallizes during the further process.

For SHI ($^{238}U^{28+}$, 4.8 MeV/u) with a stopping power of 27 keV nm^{-1}, the upper limit for single-ion induced damage on these surfaces was determined to be in order of 1-2 silicon atoms in size. In contrast, the impact of single HCI with a potential energy between 40 and 60 keV resulted in surface pits of 1-3 nm in diameter. As we exclude recrystallization of silicon after SHI impacts, the striking difference between the effect of HCI and SHI is attributed to a high stopping power threshold operative in the case of SHI. This high threshold could result from fast spatial energy redistribution in combination with low electron phonon coupling for the electrons excited in crystalline silicon by swift heavy ion impact.

References

[1] F. Aumayr, et al., J. Phys.: Condens. Matter. 23, 393001 (2011).
[2] A. Kamarou, et al., Phys. Rev. B 78, 054111 (2008); O. Osmani et al., Nucl. Instrum. Methods Phys. Res. B 282, 43 (2012).
[3] M. Tona et al., Surf. Sci. 601, 723 (2007).
[4] C. Länger, et al., New J. Phys. 23, 093037 (2021).

Ion-beam-induced phase transitions in gallium oxide: impact of the implantation temperature

A. Azarov*, C. Bazioti, V. Venkatachalapathy, P. Vajeeston,

E. Monakhov and A.Yu. Kuznetsov

University of Oslo, Centre for Materials Science and Nanotechnology,
PO Box 1048 Blindern, N-0316 Oslo, Norway
*alexander.azarov@smn.uio.no

Gallium oxide (Ga_2O_3) is an ultra-wide bandgap semiconductor exhibiting a number of unique properties applicable in power electronics and optoelectronics. Importantly, Ga_2O_3 can be crystallized in different polymorphs having different structure and, consequently, different physical properties to exploite, if gaining control over the polymorph transitions. Recently, we have demonstrated that the ion-beam-induced disorder can trigger the phase transition from the monoclinic β-Ga_2O_3 to the orthorhombic κ-Ga_2O_3 [1]. In the present contribution we use a combination of several experimental methods (RBS/C, XRD and STEM) to investigate the role of the irradiation temperature on the β-to-κ phase transition induced by ion implantation. As a starting point, Fig.1 illustrates the formation of the orthorhombic layer on the top of the monoclinic substrate by 400 keV 1×10^{16} Ni/cm^2 ion bombardment at room temperature. Further, a range of different ion implants were performed at elevated temperatures too (up to 400°C). These data revealed a threshold-like dependence of the ion-induced β-to-κ phase transition as a function of the irradiation temperature, which is discussed in terms of the interplay between several relevant activation processes.

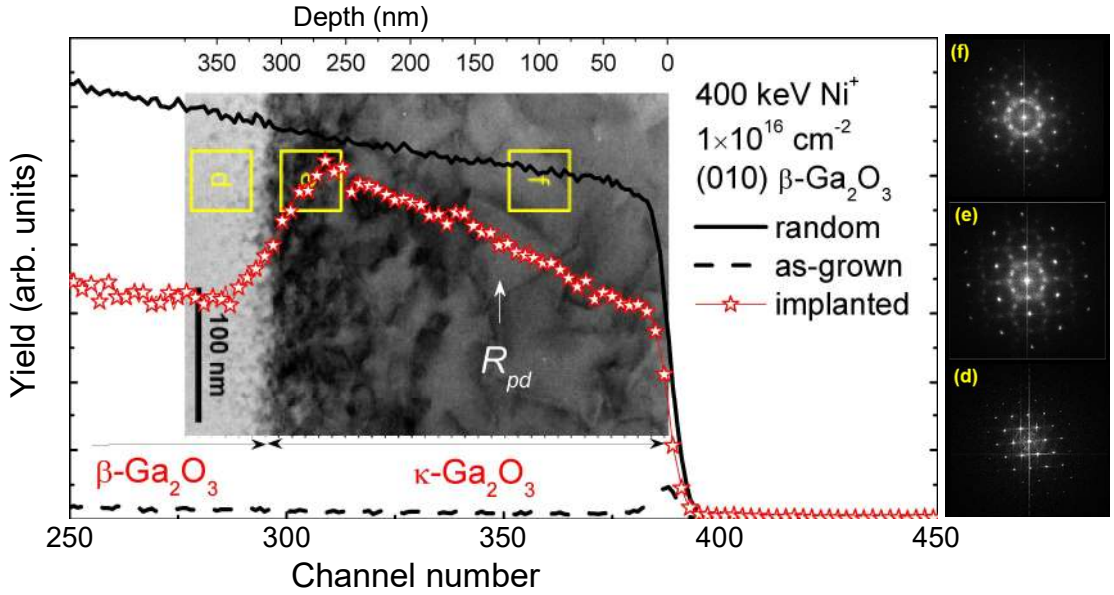

Figure 1 RBS/C spectra with corresponding STEM image of the Ga_2O_3 sample implanted with 400 keV $^{58}Ni^+$ ions to a dose of 1×10^{16} cm^{-2} at room temperature. The right-hand panels show the fast Fourier transforms from high-resolution STEM image taken from (d) β-phase, (f) κ-phase and (e) β/κ interface regions of the sample [1].

References

[1] A. Azarov, C. Bazioti, V. Venkatachalapathy, P. Vajeeston, E. Monakhov, and A. Kuznetsov, *Phys. Rev. Lett.* 128, 015704 (2022)

On the role of oxygen impurities in the synergy between electronic excitations and nuclear collisions on point defect creation in AlN

M. Sall[1,*], C. Grygiel[1], O. Yahyaoui[1], H. Alassaad[1], F. Aubrit[1], Y. Ngono-Ravache[1], S. Guillous[1], E. Balanzat[1] and I. Monnet[1]

[1]*CIMAP (CEA, CNRS, ENSICAEN, UCN), Caen, France*
[*]*sall@ganil.fr*

AlN thanks to its wide bandgap is used as a native material substrate for optoelectronic devices operating in the deep UV range [1]. The effect of oxygen impurity has been actively studied due to the formation of UV absorbing Al-vacancy and oxygen complex defects that could hinder the development of applications [2]. Under Swift Heavy Ion (SHI) irradiation, we reported in AlN a positive synergy between electronic excitations (S_e) and nuclear collisions (S_n) for the creation of defects absorbing at 4.7 eV [3] that could tentatively be assigned to the aforementioned oxygen complex related defects.

In the present study, we have performed SHI irradiation in different controlled atmospheres (vacuum, oxygen or argon partial pressure) to investigate the coupled effects of the S_e/S_n synergy for point defect creation and SHI induced impurity introduction/diffusion into the AlN layer. We found a huge effect of oxygen on the creation of the absorbing defects. The synergy parameter so far considered only dependent on S_e and S_n, must be also linked to the presence of oxygen during irradiation (Fig. 1). At the same S_e, the synergy parameter (kβ) [3] is increased by up to two orders of magnitude with irradiation under O_2 compared to irradiation under vacuum. We will discuss the mechanism of this new-coupled effect (S_e/S_n synergy and oxygen content) and the effect of other impurity types on the synergy.

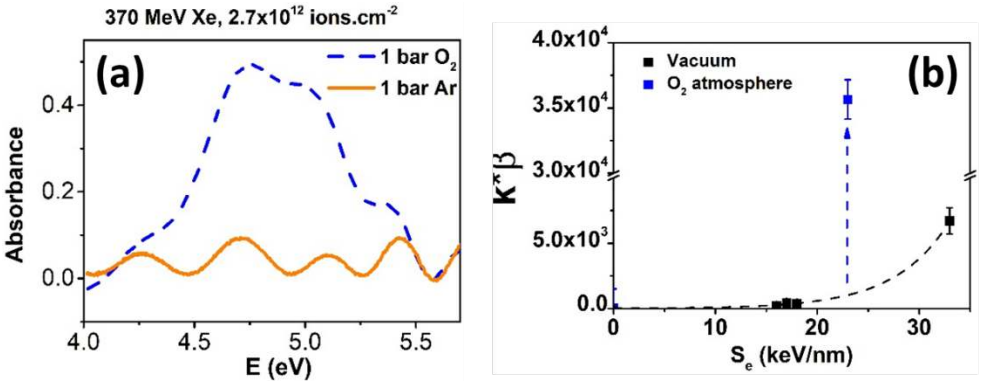

Figure 1: (a) Absorption band at 4.7 eV in AlN irradiated with 370 MeV ^{129}Xe ion at 2.7x10^{12} ions.cm^{-2} either under O_2 or under Ar atmosphere. (b) Evolution of the synergy parameter (kb) as a function of the electronic stopping power (S_e). The dashed lines are for guiding the eye.

References

[1] A. Pandey, J. Gim, R. Hovden, and Z. Mi, Appl. Phys. Lett., 117 (2020) 241101

[2] Kai, C., Zang, H., Ben, J., Jiang, K., Shi, Z., Jia, Y., Cao, X., Lü, W., Sun, X., Li, D., J. Lumin., 235 (2021) 118032

[3] Sall, M., Monnet, I., Grygiel, C., Ban D'Etat, B., Lebius, H., Leclerc, S., Balanzat, E., Europhys. Lett., 102 (2013) 26002

Paradox resolved: slow electron-phonon coupling vs. fast ion track heating

N. Medvedev[1,2,*], **A.E. Volkov**[3]

[1] *Institute of Physics, Czech Academy of Sciences, Na Slovance 2, 182 21 Prague 8, Czech Republic*
[2] *Institute of Plasma Physics, Czech Academy of Sciences, Za Slovankou 3, 182 00 Prague 8, Czech Republic*
[3] *P.N. Lebedev Physical Institute of the Russian Academy of Sciences, Leninskij pr., 53,119991 Moscow, Russia*
[*] *nikita.medvedev@fzu.cz*

For over two decades, there has been a puzzling discrepancy between slow electron-phonon coupling and a fast creation of swift heavy ion (SHI) tracks. Track formation requires extremely fast energy transfer from the excited electrons to atoms [1]. In contrast, laser-irradiation experiments measured much too slow electron-phonon energy exchange rate, which is supported by various calculations [2]. This paradox lead to a widespread use of electron-phonon coupling as a fitting parameter in calculations of SHI track creation.

We resolve this contradiction noticing that electron-phonon coupling is not the sole mechanism of energy exchange between electrons and atoms in solids. Heating of electrons alters potential energy surface of atoms. Appearing forces due to modification of the interatomic potential accelerate atoms increasing their kinetic energy (”nonthermal heating”) [2]. This nonthermal mechanism may be extremely fast, significantly faster than the electron-phonon coupling. At high deposited doses it may even lead to ultrafast nonthermal structure transformations.

It suggests that the estimates of the ”electron-phonon coupling parameter” extracted from the data on SHI track sizes with help of the two-temperature (inelastic thermal spike) model do not reflect the electron-phonon coupling *per se*, but must be interpreted as a quantity reflecting the nonthermal heating of atoms (with a contribution of non-phononic elastic scattering of fast electrons and valence holes) [2]. This notion reconciles the much debated problem of extremely fast atomic heating in swift ion impacts (at hundred femtosecond timescales) with slow electron-phonon coupling (acting at picosecond timescales).

Our results suggest that the nonthermal heating of atoms is a universal effect in nonmetallic crystalline materials under ultrafast energy deposition, and thus must be taken into account in appropriate models and interpretation of experiments [2].

References

[1] A.E. Volkov, V.A. Borodin, Nucl. Instruments Methods Phys. Res. B. 146 (1998) 137–141
[2] N. Medvedev, A.E. Volkov, (2021) https://arxiv.org/abs/2109.04401v1

Insights into swift heavy ion-induced modification processes in a-SiO_2 and a-Ge using molecular dynamics

A. A. Leino[1*], **V. Jantunen**[1], **and F. Djurabekova**[1]

[1]*Department of Physics, University of Helsinki, Finland*
[*]*aleksi.leino@helsinki.fi*

Molecular dynamics simulations are indispensable for understanding swift heavy ion-induced effects in materials. We have modeled two well-known effects - the elongation of embedded Au nanoparticles in silica [1], and the formation of voids in a-Ge [2] - by using new, accurate potentials and including the long-timescale evolution in the materials.

The refinements of the simulation model led to new insights into the elongation process, and we show that it is more elaborate than thought previously. The simulations suggest that the embedding matrix has an active role and that the adhesion between gold and silica affects the process significantly. These results can be used as a starting point to understand the behavior of metal NPs in other embedding matrices.

Modeling results in amorphous germanium explain a peculiar self-organization process of the voids and swelling of the samples during the irradiation. Both examples illustrate the importance of accounting for the macroscopic timescales in the simulation models.

References

[1] A. A. Leino, O. H. Pakarinen, F. Djurabekova, K. Nordlund, P. Kluth and M. C. Ridgway, *Materials Research Letters* (2014) 37

[2] M. C. Ridgway, T. Bierschenk, R. Giulian, B. Afra, M. D. Rodriguez, L. L. Araujo, A. P. Byrne, N. Kirby, O. H. Pakarinen, F. Djurabekova, K. Nordlund, M. Schleberger, O. Osmani, N. Medvedev, B. Rethfeld, and P. Kluth, *Phys. Rev. Lett.*, (2013) *245502*

Multi-scale investigation of heterogeneous swift heavy ion tracks in pyrochlore oxides

Eric C. O'Quinn[1,*], Cameron L. Tracy[2], William F. Cureton[3], Ritesh Sachan[4], Joerg C. Neuefeind[5], Christina Trautmann[6,7], Alexandre Solomon[1], and Maik K. Lang[1]

[1]*Department of Nuclear Engineering, University of Tennessee, Knoxville, TN, 37996, USA*

[2]*Center for International Security and Cooperation, Stanford University, Stanford, CA, 94305, USA*

[3]*Nuclear Energy and Fuel Cycle Division, Oak Ridge National Laboratory, Oak Ridge, TN, 37831, USA*

[4]*Mechanical and Aerospace Engineering, Oklahoma State University, Stillwater, OK, 74078, USA*

[5]*Neutron Sciences Directorate, Oak Ridge National Laboratory, Oak Ridge, TN, USA*

[6]*GSI Helmholtzzentrum für Schwerionenforschung, 64291 Darmstadt, Germany*

[7]*Technische Universität Darmstadt, 64287 Darmstadt, Germany*

[*]*ericoquinn@utk.edu*

Pyrochlore oxides were irradiated with swift heavy ions at the UNILAC accelerator of the GSI Helmholtz Centre using ions with specific energy of 11.4 MeV/u, and the induced structural modifications were systematically examined using conventional characterization techniques including transmission electron microscopy (TEM) and X-ray diffraction (XRD)[1]. The use of GeV ions with very high penetration depths, however, also produces a large irradiated sample mass (~150 mg) enabling bulk structural characterization with neutron total scattering and pair distribution function (PDF) analysis[2]. Each technique reveals unique aspects and length scales of the ion-modified material regions. A core–shell ion track morphology, described as an amorphous core surrounded by a disordered, anion-deficient fluorite shell, was identified directly with TEM and indirectly with XRD. Neutron total scattering, with high sensitivity to the oxygen sublattice, yielded fractions of amorphous and disordered fluorite phases and confirmed a third concentric damage region consisting of a defective pyrochlore phase, clearly distinct from the unirradiated pyrochlore matrix. Despite their differing long-range ordering (or lack thereof), the amorphous, disordered, and defective pyrochlore phases are characterized with the same local ordering. Evolution of the material phase fractions with ion fluence was investigated to reveal the phase-to-phase pathways that occur during initial and subsequent ion impacts. This approach extends fundamental knowledge about the response of complex oxides to swift heavy ion irradiation in the electronic energy loss regime across all material length scales and improves existing track-overlap models.

References

1. O'Quinn, E. C. *et al.* Multi-scale investigation of heterogeneous swift heavy ion tracks in stannate pyrochlore. *J. Mater. Chem. A* **9,** 16982–16997 (2021).
2. Lang, M. *et al.* Advanced Experimental Technique for Radiation Damage Effects in Nuclear Waste Forms: Neutron Total Scattering Analysis. in *MRS Advances* **3,** 1735–1747 (2018).

Swift Heavy Ions interaction with GaN - Relationship between long-range strain fields and track morphologies

M. C. Sequeira[1,*], **I. Monnet**[2], **C. Grygiel**[2], **C. Trautmann**[3], **P. Kluth**[4], **F. Djurabekova**[5], **K. Nordlund**[5], **E. Alves**[1], **and K. Lorenz**[6]

[1]*Instituto de Plasmas e Fusão Nuclear, Instituto Superior Técnico, Portugal*
[2]*CIMAP, CEA-CNRS-ENSICAEN-UNICAEN Caen 5, France*
[3]*Materials Research Department, GSI Helmholtzzentrum and TU Darmstadt, Germany*
[4]*Research School of Physics, Australian National University, Australia*
[5]*Department of Physics, University of Helsinki, Finland*
[6]*Instituto de Engenharia de Sistemas e Computadores – Microsistemas e Nanotecnologias, Portugal*
[*]*miguel.sequeira@tecnico.ulisboa.pt*

Group-III nitrides have contributed to some of the most significant upgrades of semiconductor technologies. Their greatest success, so far, was their use in Light Emitting Diodes (LEDs), a device that completely changed the lighting industry. More recently, they are about to cause similar revolution waves in two other fields: the power industry and radiation-hard electronics. The latter has seen increased interest due to the renewed appeal for applications in extreme radiation environments, namely in space and nuclear reactors. Devices in these surroundings face significant technological challenges that can only be overcome with novel semiconductor materials to design more efficient and enduring devices. Thus, it is of utmost priority to understand the response of nitrides to different types of radiation, in particular, the effects of the less studied radiation regime of strongly ionising radiation.

Here, we study the effects of Swift Heavy Ion (SHI) radiation in GaN thin films using Xe, Au, Pb and U ions with energy losses in GaN between 15 – 55 keV/nm. In particular, we look into the impact that defective tracks produced by SHIs have on the strain fields in the crystal. These fields directly influence the material bandgap, for which their formation needs to be well understood. Using the Two-Temperature Model - Molecular Dynamics simulation scheme, we have shown that different SHIs can create tracks with distinct morphologies [1], ranging from small pockets of point defects to continuous amorphous tracks with N_2 bubbles. Each morphology will induce an identifiable strain field that can be measured using high-resolution X-ray diffraction and analysed with appropriate statistics and the stress-strain linear isotropic model.

From the various hypotheses examined, the measurements strongly suggest that strain appears due to the volume expansion following the crystal-amorphous phase transition. Even at very low fluences, where most of the crystal is expected to be unaffected by the radiation, the strain originating from the tracks has a noticeable impact on the entire sample and extends far beyond (> 35 nm) the typical track dimension. Moreover, the intensity of this strain field seems to depend significantly on whether or not the tracks contain N_2 bubbles. This is especially interesting for the cases where N_2 bubbles are formed only upon ion impact overlapping. In these cases, we observe the presence of two strain fields of different magnitudes, which can co-exist for certain fluences.

References

[1] M. C. Sequeira, J.-G. Mattei, H. Vazquez, F. Djurabekova, K. Nordlund, I. Monnet, P. Mota-Santiago, P. Kluth, C. Grygiel, S. Zhang, E. Alves, K. Lorenz, *Communications Physics,* 4 (2021) 51.

Ionoacoustic detection and energy-loss measurement of GeV ion pulses

L. Kirsch[1,2,3*], **W. Assmann**[2], **M. Bender**[1,4], **K. Parodi**[2], **J. Schreiber**[2], **C. Trautmann**[1,3]

[1]*GSI Helmholtz Centre for Heavy Ion Research, Darmstadt, Germany*
[2]*Ludwig-Maximilians-University of Munich, Germany*
[3]*Technical University of Darmstadt, Germany*
[4]*RheinMain University of Applied Sciences, Rüsselsheim, Germany*
[*]*l.kirsch@gsi.de*

New high-power particle accelerators such as the SIS-100 currently under construction at the FAIR facility will deliver relativistic heavy ion beams with extreme intensities [1]. To overcome the problem that traditional in-beam detectors tend to saturate at such extreme conditions, we present an alternative, robust detector solution based on the ionoacoustic effect.

The principle is rather simple: Individual ion pulses are decelerated in a water reservoir and release a thermo-acoustic wave just before they come to a full stop [2]. The acoustic signal is recorded by an axially aligned, commercially available, broadband ultrasound transducer and evaluated in both the time and frequency domain. Quantities such as the ion beam intensity, the range and thus the ion energy can be deduced from the recorded signal [3].

During the last two SIS-18 beamtimes at GSI, a prototype detector was tested with Xe, Pb and U at energies ranging from 200 MeV/u to 1 GeV/u. The measured ion ranges are within 1 % agreement with ATIMA calculations. By inserting various targets of different thickness into the beam trajectory allowed us to determine the energy loss of a variety of materials. Variation of the intensity enabled the identification of a large dynamic range and a linear response to the number of ions per pulse, easily covering the maximum available intensity of $2 \cdot 10^9$ ions per pulse. The results are very promising to implement ionoacoustic detectors as monitors for intensive heavy ion beams.

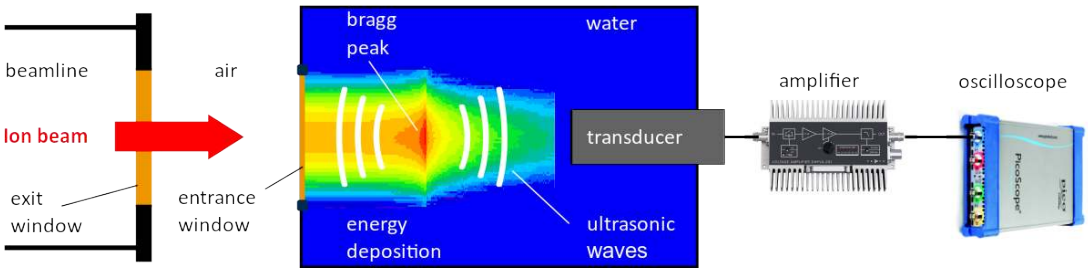

Figure 1: Schematic of the detector, highlighting the ionoacoustic principle and the simplistic signal acquisition chain, consisting mainly of standard lab equipment.

References

[1] Spiller, P. J., Balß, R., Bleile, A., Bozyk, L. Proc. IPAC'14, 1857-1860
[2] Lehrack, S., Assmann, W. et al. (2020) NIM A 950, 162935
[3] Assmann, W., Parodi, K. Nuclear Physics News, Vol. 30, No. 1, 2020

Stopping power in heavy targets: lanthanides, transition metals and beyond

A. Mendez[1], **J. Peralta**[1], **D. Mitnik**[1], **and C. Montanari**[1]

[1] *Instituto de Astronomía y Física del Espacio, Argentina*
[*] *alemendez@iafe.uba.ar*

We present recent calculations for the stopping power of protons in solids composed of heavy atoms. We systematically study lanthanides, from lanthanum to lutetium, transition metals from period 6 of the periodic table and post-transition metals. The electronic stopping power of the targets is described by combining three formalisms. The first one considers a non-perturbative description of the energy loss in the FEG [1], based on the screening potential and the value of r_S. The second one uses the dielectric formalism [2] for the stopping in the FEG, in the energy region where plasmon excitations are important. Finally, the third approach describes the bound electron contribution to the stopping by considering relativistic radial orbitals and binding energy calculations. This contribution is calculated with the shellwise local plasma approximation (SLPA) [3]. We modified the usual SLPA to include inter-shell screening, where required, and a local Mermin dielectric function to consider the mean time between collisions [4]. In this work, we show that the inclusion of relativistic effects on the bound electrons structure is critical to correctly describe the stopping on these targets. In Fig. 1, we compare our results with available experimental data and the SRIM 2013 calculations for three illustrative examples: H on Pr, W and Pt.

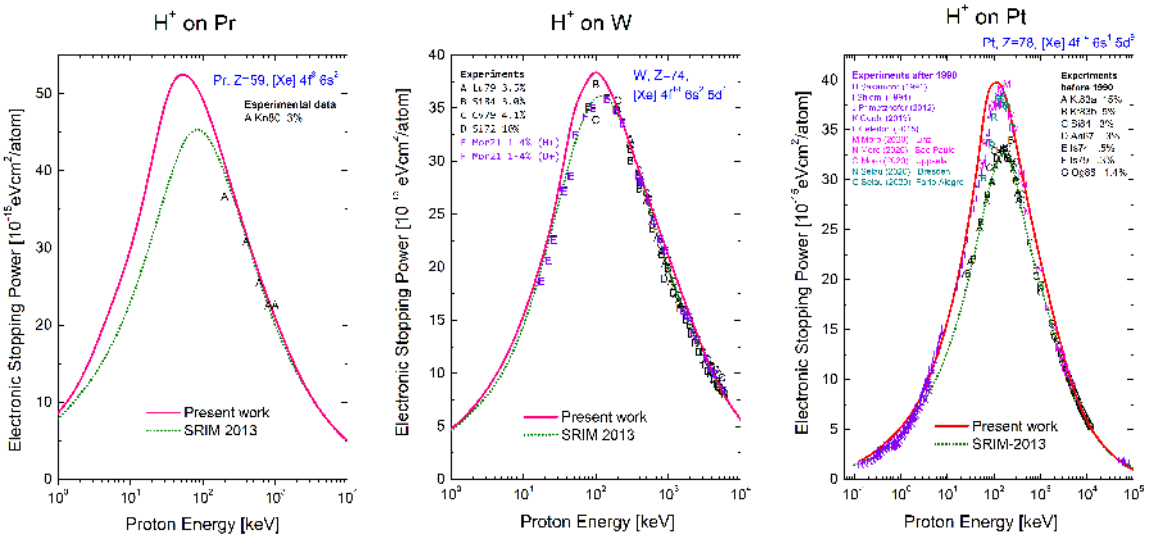

Figure 1: Stopping power of H on Pr, W and Pt. Curves: present work (solid) and SRIM 2013 (dashed). Symbols: experimental data, see references in IAEA database. In color, recent data [5, 6].

References

[1] Montanari, C. C., and Miraglia, J. E. Phys. Rev. A **96**, 012707 (2017).
[2] Mermin, N. D. Phys. Rev. B **1**, 2362 (1970).
[3] Montanari, C. C., and Miraglia, J. E. Nucl. Instrum. Methods Phys. Res. B **460**, 27–29 (2019).
[4] Peralta, J. P. et al. *submitted* (2022).
[5] Moro, M. V. et al. Nucl. Instrum. Methods Phys. Res. B **498**, 1–8 (2021).
[6] Selau, F. F. Phys. Rev. A **102**, 032812 (2020).

Electronic excitation by electron promotion during binary atomic collisions in solids

P. Riccardi[1]

Dipartimento di Fisica – Università della Calabria – Italy
Pierfrancesco.riccardi@unical.it

This work reports on measurements of the energy distributions of electrons emitted by Aluminum and Magnesium surfaces under the impact of low energy singly charged noble gas and sodium ions, focusing on Auger decay of electronic excitations produced in both projectile and target atoms during binary atomic collisions. These excitations are well described by the Fano-Lichten molecular orbital promotion model adopted for gas-phase experiments. For their electronic structure and the larger atomic density, the use of solid targets in experimental studies of inner-shell vacancy production often results in photon and Auger electron emission which differs from the emission observed in experiments with gas target. Many of these solid target effects have been sparsely studied and they are often neglected in studies of ion-solids interaction. In This contribution we present our recent experimental research [1.3] on electron promotion and examine some of these solid target effects, showing their importance within the current context of research in energy loss and energy deposition by ions in solids.

References

[1] D.Runco, P.Riccardi Phys. Rev. A 104 (2021) 042810
[2] D.Runco, P.Riccardi Solid State Communications 340(2021) 114534
[3] P. Riccardi, C. A. Dukes Surface Science 719 (2022) 122025

Radiolysis and sputtering of amino acids by MeV ions and keV electrons

C. A. P. da Costa[1*], **C. Mejía**[2], **J. A. Souza-Corrêa**[3] **and E. F. da Silveira**[3]

[1]*Centre de Recherche sur les Ions, les Matériaux et la Photonique. Normandie Université, ENSICAEN, CIMAP – 14000 Caen, France*
[2]*Facultad de Ciencias Químicas, Universidad de Cuenca, Av. 12 de Abril y Loja, 0101168, Cuenca, Ecuador*
[3]*Departamento de Física, Pontifícia Universidade Católica do Rio de Janeiro, Rua Marquês de São Vicente, 255, Rio de Janeiro 22452-970, Brazil*
[*]*cintia-apc@hotmail.com*

Amino acids have been spotted in space, e.g., in the dust traces of the Comet 81P/Wild 2 and collected by the Stardust spacecraft [1, 2]. Astrophysical materials existent in comets, asteroids and meteorites containing prebiotic molecules such as amino acids could have fallen on Earth and stimulated initial biological processes, such as the formation of nucleobases and other molecular building blocks of life [3]. Determination of amino acid dissociation rates in the laboratory is relevant because it supports astrophysical models on effects produced by the solar wind and galactic cosmic rays in prebiotic material in space.

The experiments were performed at the Van der Graff facilities at PUC-Rio, Rio de Janeiro, Brazil. Radiolysis and sputtering of glycine, valine and phenylalanine, induced by 0.06 – 1 keV electrons, and by 0.5 – 2 MeV H, He and N ion beams, were studied. Their column density evolutions with beam fluences were followed by infrared spectroscopy and their destruction cross sections were determined. Present results show that apparent destruction cross sections (including sputtering), σ_d^{ap}, vary proportionally with the electronic stopping power, S_e, ($\sigma_d^{ap} \approx a\ S_e$), where $1/a$ is ≈ 120, 100 and 65 eV/nm³ for glycine, valine and phenylalanine, respectively. This value corresponds to the average energy density absorbed to dissociate and eject molecules from a solid sample. Assuming the relationship $\sigma_d^{ap} \approx a\ S_e$ to be valid for both ion and electron projectiles, their half-lives are predicted to be ~10 – 40 days in the Solar System (at 1 au), and a million years in the interstellar medium.

References

[1] Sandford S.A, Aléon J, Alexander C. M. D, Araki T, Bajt S, Baratta G. A, and Zolensky M. E. Science 2006; 314, 1720–1724.
[2] Elsila J. E, Glavin D. P, and Dworkin J. P. Meteoritics and Planetary Science 2009; 44(9), 1323-1330.
[3] Oba Y, Takano Y, Naraoka H, Watanabe N, and Kouchi A. Nature communications 2019; 10, 4413.

Effect of simulation technique on the defect production and defect evolution in tungsten

F. Granberg[1,*], **J. Wu**[1], **D. R. Mason**[2], **and J. Byggmästar**[1]

[1] *Department of Physics, University of Helsinki, Post-office box 43, FIN-00014 University of Helsinki, Finland*
[2] *UK Atomic Energy Authority, Culham Science Centre, Oxfordshire OX14 3DB, UK*
[*] *fredric.granberg@helsinki.fi*

Tungsten is the material of choice for some of the most demanding parts of proposed fusion test facilities and power plants. The harsh environment in form of irradiation present will affect the wall and structural materials during operation. For decades studies have been conducted on the effect of cascades in metals by molecular dynamics simulations. Many factors have been seen to affect the defect production and the morphology of the defects produced. However, the doses achieved in a single cascade is very low, not comparable to most experiments and neither to the conditions in the proposed test facilities and reactors. In order to understand the defect build-up at higher doses, overlapping cascades have been simulated [1, 2], and revealed the defect evolution at higher doses, more comparable to realistic ones. It has also been found that the results obtained with this method is agreeing very well with experimental studies at similar doses and under similar conditions.

The main drawback of this technique is that one needs to cumulatively add the dose, resulting in a limit on how large doses can be feasibly achieved. To remedy this, we have studied the effect of utilizing different speed-up techniques to more efficiently obtain higher doses. We found that different methods will yield different results, not agreeing with the slower full molecular dynamics simulations. However, conducting so-called cascade annealing (overlapping cascades) on the structures obtained by more efficient methods, we can reach the same result as conducting only MD simulations, but with a speed-up of orders of magnitude [3, 4]. The sped-up simulations combined with cascade annealing shows that for simple pure metals we can achieve high doses at a reasonable CPU cost.

References

[1] F. Granberg et al, *Physical Review Letters*, 116 (2016) 0135504
[2] F. Granberg, J. Byggmästar, and K. Nordlund, *Journal of Nuclear Materials*, 556 (2021) 153158
[3] D. R. Mason et al. *Physical Review Materials* 5 (2021) 095403
[4] F. Granberg, D. R. Mason and J. Byggmästar *Submitted for publication* (2022)

Low energy ion beam induced modifications in optical, structural, chemical and morphological properties of nanostructures MoS_2 thin films

Deepika Gupta, Rajesh Kumar*

University School of Basic and Applied Sciences,
Guru Gobind Singh Indraprastha University, New Delhi-110078, India
*Corresponding author: rajeshkumar@ipu.ac.in

Abstract

The promising optical and semiconducting peculiarities of few-layer and monolayer transition metal dichalcogenides (TMDCs) as illustrated by MoS_2, prevailed as encouraging candidate for optoelectronic device applications. Ion beam modifications impeccably efficient for patterning of two-dimensional (2D) TMDC materials, but optimization of ion beam implantation parameters demand full microscopic conception of defect origination mechanisms. Contrary to 2D freestanding systems, characteristics of creation of defects in supported 2D TMDCs materials are not completely studied. In the present work we have fabricated nanostructure MoS_2 thin films on silicon and glass substrate utilizing DC magnetron sputtering technique and following ion implantation treatment. Ion beam implantation of MoS_2 thin films were grown at room temperature with 80 keV Au ions with distinct fluence (1E15 and 5E15 ions/cm^2) at Inter-University Accelerator Center (IUAC), New Delhi, India. By regulating ion beam fluence structural defects were introduced in the MoS_2 thin films. The crystal structure and morphology of pristine and ion implanted nanostructure MoS_2 thin films are characterized by Raman, Atomic force microscopy (AFM), X-ray photoelectron spectroscopy (XPS) and X-ray diffraction (XRD) techniques. AFM study demonstrated that the thin films surface exhibit dense nano-level grains, also escalation in average roughness (2.98 to 4.29 nm) and grain size (15-30 nm) have been inferred in a sample implanted with Au ion with fluence of 5E15 ions/cm^2. XRD study of pristine MoS_2 thin films exhibit hexagonal phase parallel to the (100), (103) and (112) planes, also alteration in the crystalline nature of ion implanted specimens were inferred. Optical peculiarities of pristine and ion implanted thin films of MoS_2 were demonstrated by UV-Vis spectroscopy and alteration in optical bandgap have been remarked upon implantation. Photoluminescence (PL) spectra of pristine and ion implanted specimens were taken at 330 nm excitation wavelength and the findings illustrated the emission at 402 nm wavelength, enhancement in PL intensity remarked after ion implantation on account of induction of defects which act as radiative recombination centers. In XPS, two peaks centered at 227.7 eV (Mo $3d_{5/2}$) and 230.93 eV (Mo $3d_{3/2}$) remarked, corresponding to the Mo 3d doublet, also S 2p doublet inferred at 161.64 eV (S $2p_{3/2}$) and 162.51 eV (S $2p_{1/2}$), for the sputtered pristine MoS_2 thin films, peak shifting, alteration in FWHM and intensity is remarked corresponding to the ion implanted samples corroborates that ion implantation influence structural arrangement and local electron density around the atoms in thin films. RBS technique was utilized to calculate the thickness of pristine and ion beam implanted specimens. For qualitative analysis of induction of defects by ion beam implantation Raman spectroscopy was used, two phonon modes of MoS_2 i.e. A_{1g} and E^1_{2g} observed at peak position of 411 and 379 cm^{-1}, corresponding to the out-of–plane and in-plane vibrational modes along with hexagonal phase, alteration in FWHM and intensity of vibrational modes have been remarked. Also, illustration of distinct functional groups and their removal after ion implantation was studied by Fourier transport infra-red (FTIR) spectroscopy technique. Detailed results will be discussed during the presentation.

References:

1. M. Chhowalla, H.S. Shin, G. Eda, L.J. Li, K.P. Loh, H. Zhang, Nat. Chem. 5 (2013) 263–275.
2. Deepika Gupta, V. Chauhan, N. Koratkar, Rajesh Kumar, Ceram. Int. 48 (2022) 2999–3019.
3. K. Lee, R. Gatensby, N. McEvoy, T. Hallam, G.S. Duesberg, Adv. Mater. 25 (2013) 6699–6702.
4. M.A. Baker, R. Gilmore, C. Lenardi, W. Gissler, Appl. Surf. Sci. 150 (1999) 255–262.
5. Rajesh Kumar, V. Chauhan, N. Koratkar, S. Kumar, A. Sharma, K.H. Chae, S.O. Won, J. Alloys Compd. 831 (2020) 154698.

Electronic excitations by keV ions in single crystalline self-supporting targets

E. Ntemou[1,*], **R. Holeňák**[1], **S. Lohmann**[1,2] **and D. Primetzhofer**[1]

[1] *Department of Physics and Astronomy, Uppsala University,751 20 Uppsala, Sweden*
[2]*Institute of Ion Beam Physics and Materials Research, Helmholtz-Zentrum Dresden-Rossendorf e.V. (HZDR), 01328 Dresden, Germany*
[*]*eleni.ntemou@physics.uu.se*

Different energy dissipation mechanisms of ions in matter are crucial not only for applied science and technology but also of interest from a fundamental point of view. The energy loss of ions moving through solids depends mostly on the ion velocity as well as the atomic number of the ion and the target nuclei. In the high velocity regime, the energy loss is well described by the Bethe and Bloch theory. However, at low velocities (around the Bohr velocity, v_0), the situation becomes more complex since trajectory dependent [1], electronic excitations develop a more dynamic character as formation of molecular orbitals and charge exchange in atomic collisions become increasingly important. These processes are, due to their dependence on the interaction distance between ion and target nuclei accessible to a different extent along channeling trajectories in comparison to random trajectories in crystalline targets.

When considering electron-hole pair excitations in binary collisions exclusively, in the low energy regime, the specific energy loss is expected to be proportional to velocity for a free electron gas (FEG). However, deviations associated with the target electronic structure and contributions of charge exchange processes have been observed [2]. These deviations are expected to be minimized in channeling trajectories where interaction is limited to large internuclear distances with the main remaining energy dissipation channel being the excitation of electron-hole pairs.

Experiments were carried-out using the Time-of-Flight Medium Energy Ion Scattering System in transmission geometry at the 350 kV Danfysik Implanter at the Uppsala University. Pulsed beams of H, He, N and Ne, with typical pulse length of ~1-2 ns, were directed on Si and SiC single crystalline self- supporting foils with energies between 10 – 300 keV. The transmitted ions were detected by a large-angle, position-sensitive detector. We employed Si (100) and SiC (100) foils with nominal thickness of 50 nm and 200 nm (Norcada Inc.).

Energy loss was measured along random and several different channeling trajectories for both Si and SiC. For all studied cases the energy loss in channeling orientation was found lower than in random orientation. The specific electronic energy loss for different ions in Si and SiC in random and channeling geometries was extracted, following the calculation and subtraction of the nuclear energy loss using the Monte Carlo package TRBS. Data were also compared with SRIM predictions for random geometries. The experimental results can serve for benchmarking theoretical models for electron dynamics in solids e.g. Time Dependent-Density Functional Theory (TD-DFT) [3].

References

[1] S. Lohmann and D. Primetzhofer, Phys. Rev. Lett. 124 (2020) 096601
[2] D. Primetzhofer, Phys. Rev. B 86 (2012) 094102
[3] A. Kononov and A. Schleife, Nano Lett. 21 (2021) 4816.

Radiation Resistance and Cascade Density Effect in α-Ga_2O_3

A.I. Titov[1], K.V. Karabeshkin[1], A.I. Struchkov[1], A.I. Pechnikov[2,3] V.I. Nikolaev[2,3], P.A. Karaseov[1,*]

[1]*Peter the Great St.-Petersburg Polytechnic University, St-.Petersburg, Russia*
[2]*Perfect Crystals LLC, , St.-Petersburg Russia*
[3]*Ioffe Institute, St-.Petersburg, Russia*

[*]*platon.karaseov@spbstu.ru*

Gallium oxide is an ultra-wide bandgap semiconductor, having a high breakdown field value (a theoretical estimation is ~8 MV×cm^{-1}). It is the most attractive material for the next generation power electronics as well as for solar blind UV photo-detectors and sensors. Several polymorphs of this compound were successfully synthesized with a good crystalline quality. Among them, β-phase with E_g = 4.7 eV is known as thermostable at ambient conditions, which pushed a lot of research to be conducted on it. On the other hand, its native rival α-Ga_2O_3 has even wider bandgap (E_g = 5.3 eV) and higher density. Despite this polymorph is stable only up to 500-550 ºC, it is possible to create a new generation of power devices on its base. Systematic investigation of irradiation-induced effects in metastable α-Ga_2O_3 polymorph is missing. In this contribution, we study formation of structural disorder in undoped HVPE-grown α-Ga_2O_3 single crystal layers [1] under room temperature irradiation with monatomic P^+ and molecular PF_4^+ions. All the implants were carried out at 7° off the channeling direction to similar doses expressed in displacements per target atom (DPA). Ion energy was kept at 1.3 keV/amu, which is equal to 40 and 140 keV for P and PF_4 ions respectively. Implantation-produced disorder was measured by RBS/C spectrometry.

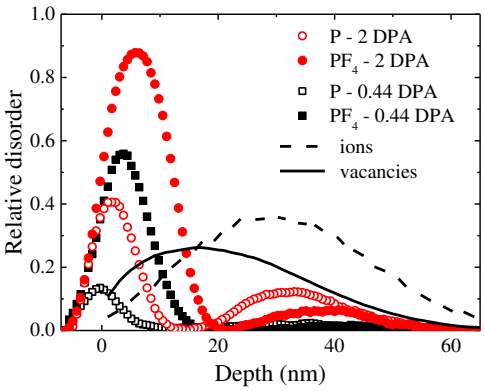

Figure 1. Relative disorder created in α-Ga_2O_3 by different ions as indicated in the legend (symbols) and vacancy and implanted ion distributions as simulated by TRIM (line).

Fig. 1 presents typical depth distributions of structural disorder formed in α-Ga_2O_3 after irradiation with different ions to doses of 0.44 and 2 DPA. It is seen that created damage consists of two distinct peaks, one located at the sample surface, and the second formed in the bulk. The maximum of bulk defect peak in α-Ga_2O_3 originates close to the maximum of the implanted ions distribution and slightly shifts deeper towards the crystal bulk with increasing ion dose. Further, the damage does not reach the amorphization level at the surface as well as in the bulk, saturating at ~ 80 – 90%. This is consistent with our earlier result [2].

Complementary analysis of the results reveals that α-Ga_2O_3 is more radiation resistant as compared to β-Ga_2O_3.

Work was supported by Russian Science Foundation grant # 22-19-00166.

References

[1] Pechnikov A.I. et al. Semiconductors, 53 (2019) 780
[2] Karabeshkin K.V. et al. Springer Proceedings in Physics 268 (2022) 247.

Application of the PASS code on stopping of slow ions

P. Sigmund[1] **and A. Schinner**[2]

[1]*Department of Physics, Chemistry and Pharmacy, University of Southern Denmark, Odense, Denmark*
[2]*Department of Experimental Physics, Johannes Kepler University, Linz, Austria*

The PASS code was originally developed [1] to characterize electronic stopping of ions heavier than helium over an energy range from 25 keV/u upward [2]. More recently we also applied the code to stopping of lighter ions and at lower energies. This included studies of experimental techniques [3, 4] and a widely ignored correction to standard stopping theory [5] which invokes a coupling term between electronic energy loss and nuclear scattering.

Incorporating these effects into the PASS code leads to

- Substantial corrections in calculated, measured and tabulated stopping cross sections,
- Isotope dependence of the electronic stopping cross section and
- Gas-solid and conductor-insulator differences in the electronic stopping cross section.

We distinguish between two main corrections,

- The RM correction [5], which accounts for the effect of angular deflection of colliding particles on electronic excitation, and
- The RED correction [3], which accounts for dependence of measured energy losses on the detector geometry due to multiple angular scattering.

Both effects are negligible if the target is an electron gas. This implies that at low beam energies, where weakly-bound electrons dominate electronic energy loss, the distinction between inner and outer electrons becomes critical.

As an example, measured stopping cross sections for protons in silicon show strict proportionality in the velocity dependence down to very low energies, whereas RM-corrected values would show a steeper depence, as is found in reported measurements on SiO_2.

While RM [5] is a negative correction to stopping cross sections calculated in the conventionaly way, the RED correction, as explored in refs. [3, 6], is likewise negative but specific for transmission measurements. As a rough rule of thumb, RM dominates for light ions, whereas RED, for transmission measurements, dominates for heavy ions.

These findings are tested by comparison with measurements on gases, insulating and conducting solids as well as compounds.

References

[1] P. Sigmund, A. Schinner, Binary theory of electronic stopping, Nucl. Instrum. Methods B 195 (2002) 64–90.
[2] ICRU, Stopping of ions heavier than helium, Vol. 73 of ICRU Report, Oxford University Press, Oxford, 2005.
[3] P. Sigmund, A. Schinner, Note on measuring electronic stopping of slow ions, Nucl. Instrum. Methods B 410 (2017) 78–87.
[4] V. I. Shulga, A. Schinner, P. Sigmund, Effect of impact-parameter-dependent electronic energy loss on reflected-ion spectra, Nucl. Instrum. Methods B 467 (2020) 91–96.
[5] A. Schinner, V. Shulga, P. Sigmund, Threshold behavior and isotope effect in low-energy electronic stopping of light ions, J. Appl. Phys. 129 (2021) 183304.
[6] P. Sigmund, A. Schinner, Is electronic stopping of ions velocity-proportional in the velocity-proportional regime?, Nucl. Instrum. Methods B 440 (2019) 41–47.

Non-linear ion stopping calculations for a classical free-electron gas

P.L.Grande* **and R. C. Fadanelli**

Ion Implantation Laboratory, Instituto de Física, Universidade Federal do Rio Grande do Sul, Av. Bento Gonçalves, 9500, CP 15051, CEP 91501-970, Porto Alegre, RS, Brazil

*grande@if.ufrgs.br

The free-electron gas (FEG) model has been used to evaluate the electronic stopping because its simplicity and reliability [1]. It has been also used as a starting point and a reference for more advanced calculations to check convergence and predictions. The main physical ingredient in this model is the electron-ion interacting potential. It is well known in the framework of dielectric formalism or linearized Vlasov-Poisson equation for a classical plasma. For non-linear calculations the self-consistent electron-ion interacting potential is still unknown and therefore central potentials determined from the Friedel sum rule has been used [2] to calculate the electronic stopping power and the corresponding the Barkas effect [1] as a function of the projectile energy. In this work we solve the non-linear, self-consistent, classical equations for a FEG at T=0 interacting with a stationary ion to calculate the full non-central electron-ion potential, and thus the ion stopping power. We clearly show the origin of the Barkas effect, namely the first non-linear effect for projectiles at high velocities responsible. This effect is strongly enhanced by the multipolar part of the electron-ion potential, and we did not observe any contribution from the non-conservation of the angular momentum in electron-ion collisions as proposed by Lindhard [3]. In addition, Bohr's stopping-power formula is rederived [4] for a free electron gas (FEG) system within the framework of nonrelativistic classical mechanics. A simple and more concise expression for the stopping power of charged particles in FEG is demonstrated on classical grounds. Using semiclassical arguments and the Euler-Maclaurin well-known mathematical formula, Bloch's correction that links Bethe's quantum theory to Bohr's classical model is also recovered. These non-linear calculations are applied to understand the stopping of protons in different materials.

References

[1] P. Sigmund, *Particle Penetration and Radiation Effects*, Vol. 1 (Springer Berlin Heidelberg New York, 2006)
[2] N.R. Arista, *Nuclear Instruments and Methods*, 195, (2002) 91-105.
[3] J. Lindhard, *Nuclear Instruments and Methods*, 132, (1976) 1-5.
[4] P.L. Grande, *Phys. Rev. A*, 104, (2021) 012807.

Contribution of molecular orbital promotion to the electronic stopping cross section

A.N. Zinoviev[1,*], **P.Yu. Babenko**[1], **D.S. Tensin**[1], **and A.P. Shergin**[1]

[1] *Ioffe Institute, St Petersburg (Russia)*
[*] *zinoviev@inprof.ioffe.ru*

It is shown that the MO promotion during collisions of keV-energy ions with a solid plays a determining role in the formation of autoionization states. Corresponding inelastic energy losses strongly contribute to the electronic stopping cross sections S_e. It is proposed to estimate the S_e values using the relation between the cross section for autoionization state excitation and the ionization cross section. For cases where the ionization cross sections are unknown, scaling [1] is used to calculate the ionization cross sections when the L and M shells are excited.

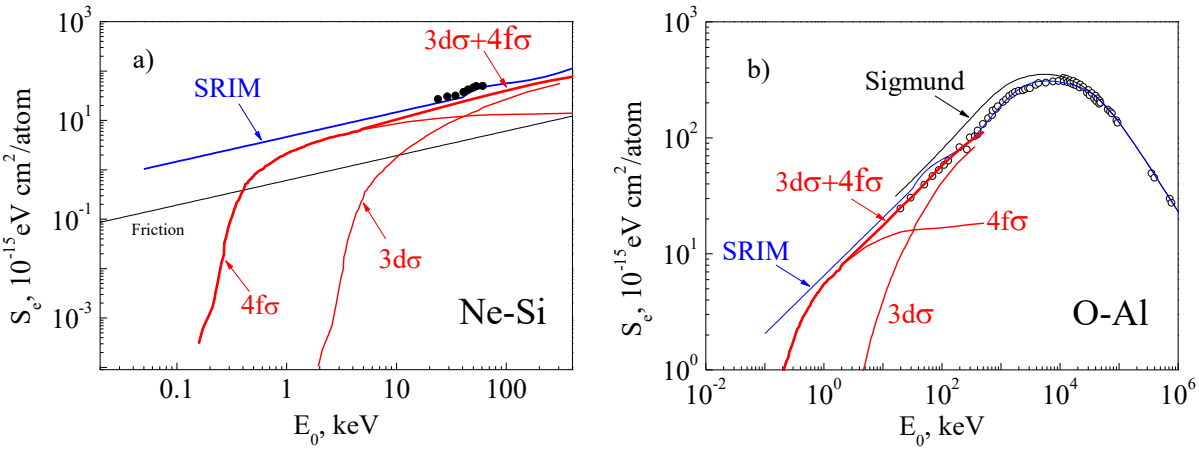

Fig. 1. Electronic stopping cross sections for the Ne-Si (a) and O-Al (b) systems.
(a) Black circles – experimental data from work [2]. Blue line – the SRIM code data [3]. Our estimates of the contribution from the extension of the 3dσ and 4dσ orbitals are shown by thin red lines. Thin black line shows the estimate of the contribution of conduction electrons to stopping. Thick red line shows the resulting curve.
(b) Open circles – experimental data from [4]. Blue line – the SRIM code data [3]. Thin black line – calculation from [5]. Our estimates of the contribution from the promotion of the 3dσ and 4dσ orbitals are shown by thin red lines; thick red line is the resulting curve.

These figures demonstrate the threshold behavior of the electronic stopping cross section S_e. In both considered cases, our approach based on MO promotion model predicts a dominant contribution of autoionization state formation to the electronic stopping cross section S_e.

References

[1] P.Yu. Babenko, A.N. Zinoviev, A.P. Shergin, *Nucl. Instr. Meth. B*, 354 (2015) 142.
[2] G. Grahmann, S. Kalbitzer, *Nucl. Instr. Meth.*, 132 (1976) 119.
[3] J.F. Ziegler, J.P. Biersack, SRIM - http://www.srim.org.
[4] H. Paul, *Stopping Power for Light Ions*. http://www.exphys.uni-linz.ac.at/stopping.
[5] P. Sigmund, A. Schinner, *Nucl. Instr. Meth. B*, 195 (2002) 64.

Machine Learning modelling the IAEA stopping power database

D. M. Mitnik[1,*], **F. Bivort Haiek**[1], **A. M. P. Mendez**[1], **and C. C. Montanari**[1]

[1] *Instituto de Astronomía y Física del Espacio, CONICET and Universidad de Buenos Aires, Buenos Aires, Argentina.*

[*] *dario@iafe.uba.ar*

The International Atomic Energy Agency (IAEA) stopping power database [1] is a highly valuable public resource, making available compilations of the majority of the experimental measurements published over the last nine decades. The database is continuously updated, and being accessible to the global scientific community. Our purpose is to extend the database, allowing to apply machine learning methods to predict the electronic stopping power cross section for any ion and target combination for a wide range of incident energies.

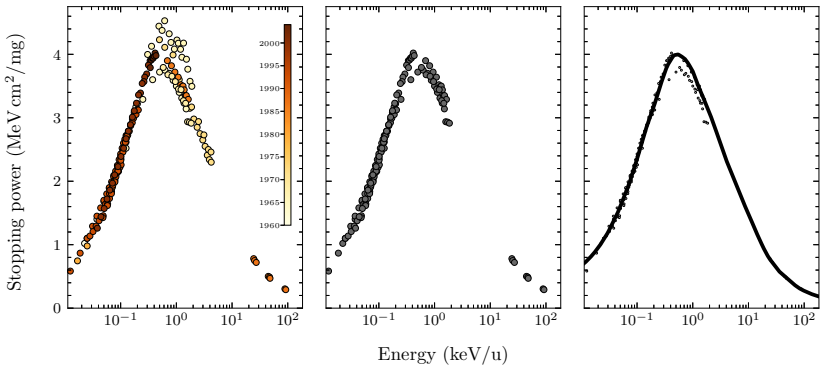

Figure 1: (color online). Left: Experimental results for stopping power cross sections for O in Ag. The colors indicate the year of publication of the data. Middle: Machine–Learning filtered data. Right: Machine–Learning Neural Network predicted results.

The IAEA database was build gathering published articles by diverse authors. Hence, it is not standarised in its original form and in many cases different experiments are not consistent to one another. The data may have been presented in distinct units and formats. We devoted a significant effort in the reorganization of the database, unifying units, and arranging the data in a standard (csv) format, enabling the obtention of the information to be easily and quickly accesible. Considering that the database contains several dozen of thousands input values, purging manually this data requires also a considerable amount of work. To this purpose, we developed a machine learning method to clean up the database, based on an unsupervised clustering technique (DBSCAN) which identifies outlier values, and determines which data to keep in cases of overlapping, taking into account the year of production. The refined data is used to train a deep neural network, able to accurately reproduce the input experimental results, and to predict new results in cases which have never been seen in the training procedure (the test set). The code ESPNN (Electronic Stopping Power with Neural Network), performing all these mentioned tasks, is presented in this work.

References

[1] C.Montanari and P. Dimitriou, Nuclear Inst. and Meth in Phys. Res. B **408**, 50 (2017).

Energies and volumes of defects and dislocations produced by irradiation: From microscopic to component-scale models.

S.L. Dudarev[1*], **M. Boleininger**[1], **P.M. Derlet**[2], **P.-W. Ma**[1], **D.R. Mason**[1], **L. Reali**[1]

[1]*UKAEA, Culham Science Centre, Oxfordshire OX14 3DB, UK*
[2]*Condensed Matter Theory Group, Paul Scherrer Institut, CH-5232 Villigen PSI, Switzerland*
[*]*sergei.dudarev@ukaea.uk*

The multiscale modelling methodology, aiming at delivering predictive simulation capabilities at the macroscopic scale and implemented numerically in the form of finite element models (FEM), over the past several decades has been attempting to find solutions by focusing primarily on the evaluation of energies of defects, their transition energy pathways, and energy barriers controlling the rates of thermally activated processes. This fundamentally physics-based approach proved to be largely detached from the notions of macroscopic elasticity, plasticity, and their FEM implementations, which involve computing internal and external forces acting on components, and the resulting stresses and deformations.

A remarkable illustration of the fact that energies and lattice distortions generated by the defects are not directly related is provided by the case of point defects, where the divergence of the elastic self-energy at the centre of a defect shows that it is the electronic structure at the core and non-linear effects associated with short-range interatomic bonding, as opposed to purely elastic self-energy of harmonic stretching and bending of the chemical bonds that control the structure of defects and their dynamics. At the same time, the macroscopic phenomenological models often used in the context of FEM simulations suffer from the lack of transferability and predictive capacity when applied to simulating the response of materials to the previously unknown operating nuclear environments, including nuclear fusion.

The recognition of the need to identify the differences and synergies in the treatment of energies and deformations associated with defects and dislocations has led to new fundamental developments in multiscale models for radiation effects in nuclear reactor components, and enabled formulating an FEM approach where defects and dislocations act as microscopic distributed sources of macroscopic elastic strain and stress fields [1,2,3,4,5], providing a basis for a self-consistent, as opposed to purely hierarchical, approach to the simulation of the effect of irradiation on the macroscopic engineering properties of materials for fusion reactor components.

References

[1] P.M. Derlet and S. L. Dudarev, *Physical Review Materials,* 4 (2020) 023605
[2] P.-W. Ma, D.R. Mason, and S.L. Dudarev, *Physical Review Materials,* 4 (2020) 103609
[3] D.R. Mason, F. Granberg, M. Boleininger, T. Schwarz-Selinger, K. Nordlund, and S.L. Dudarev, *Physical Review Materials,* 5 (2021) 095403
[4] L. Reali, M. Boleininger, M.R. Gilbert, and S.L. Dudarev, *Nuclear Fusion,* 62 (2022) 016002
[5] M. Boleininger, S.L. Dudarev, D.R. Mason, and E. Martinez, http://arxiv.org/abs/2203.05282

Atomistic simulations of growth mechanisms of hydrogen blisters in copper

Alvaro Lopez-Cazalilla[1,*], **Flyura Djurabekova**[1], **Catarina Filipa Da Palma Serafim**[1,2], **Ana Teresa Perez-Fontenla**[2], **Sergio Calatroni**[2], **and Walter Wuensch**[2]

[1]*Department of Physics, P.O. Box 43, FI-00014 University of Helsinki, Finland*
[2]*CERN, European Organization for Nuclear Research, 1211 Geneva, Switzerland*
[*]*alvaro.lopezcazalilla@helsinki.fi*

Blistering is a process which usually takes place close to the surface of metals when they are irradiated, as can be seen in radio-frequency quadrupoles accelerating structures. This pronounced change of the surface morphology has been measured when the extended irradiation is done with energetic light ions.

The mechanism of continuous growth of a small bubble to a quantifiable size blister is not completely understood. Frequently, such procress is associated to the prismatic dislocation loop punching, which takes place in very short timescale and cannot be covered by experimental techniques. In FCC metals, the pressurized voids yield emitting shear loops, which were suggested to provide explanation on the plastic growth of the bubbles. However, the detachment of these loops has not been demonstrated.

We use molecular dynamics to address the fast bubble growth in Cu, associated with blistering, when exposed to H- irradiation [1]. To do that, we employ a methodology which allows us to closely follow the formation of prismatic loops at different H concentrations. Moreover, we also analyze the interaction of these loops with the different surface orientations of copper. This study sheds light on the mechanism of blister production and, also, to its effect on the surface exposed to irradiation.

We observe the emission of a complete prismatic loop composed by several shear loops, which Burgers vectors are aligned with the gliding direction of the prismatic loop. We show that the prismatic loops are not necessarily smaller than the bubble cross-section. In addition to this, we note that these loops travel toward defects-sinks such as grain boundaries or surfaces, and in the latter case, are creating different shape protrusions. These protrusions' shapes are different depending on the grain orientation, as observed experimentally, and we verify it by our computational method.

References

[1] Alvaro Lopez-Cazalilla, Flyura Djurabekova, Fredric Granberg, Kenichiro Mizohata, Ana Teresa Perez-Fontenla, Sergio Calatroni, Walter Wuensch *Acta Materialia*, 225 (2022) 12

Explosive desorption induced by radical-radical interaction in methane-doped Ar matrices

E. Savchenko[1,*], I. Khyzhniy[1], S. Uyutnov[1], M. Bludov[1], V. Bondybey[2]

[1]*B.Verkin Institute for Low Temperature Physics and Engineering of NASU, Kharkiv, Ukraine*
[2]*Lehrstuhl für Physikalische Chemie II TUM, Garching, Germany*
[*] *elena.savchenko@gmail.com*

Oscillations of particle yield from solid methane subjected to long-term irradiation by an electron beam, have been observed and discussed recently [1, 2]. In these experiments two types of self-oscillations were observed – long-period bursts (on a time scale of about 25 min) and short-period oscillations (of about 10 s). To get more insight into the phenomenon we started research of the phenomenon in solid Ar doped with CH_4 [3].

Here we present an outgrowth of this research promoting in addition the developed methods of nonstationary luminescence (NsL) [4] and nonstationary desorption NsD in combination with thermally stimulated exoelectron emission (TSEE) and optical emission spectroscopy (OES). Spectra were detected concurrently in VUV and visible ranges at CH_4 concentration from 1 to 10%. Registration of the optical emission spectra from CH_4-containig Ar matrices excited with 1.5 keV electron beam revealed following products of radiation-induced methane transformation: H, CH and C. Measurements of the NsD and NsL at the characteristic wavelengths of these species emissions were performed in a correlated manner.

As it was shown [5] the CH radical can be considered as a signature of the CH_3 species. The antibate behavior of the CH NsL and the NsD was observed at all concentrations of CH_4, that was interpreted as a result of the recombination of CH_3 radicals with the formation of C_2H_6 and the energy release spent for the desorption. The NsL of H radical shows the antibate behavior with the the NsD yield only at concentrations of CH_4 as high as 10%. The decrease in the intensity of the characteristic H radical's band points to depletion of atomic H at higher concentrations likely due to their diffusion and nonradiative recombination with the release of energy. Short-period oscillation along with long-period ones were found in Ar matrix doped with 5 and 10% of CH_4. We were able to observe two bursts of long-period self-oscillations during stationary irradiation of methane-doped Ar matrices at low temperatuires. Processes leading to the self-oscillations of particle yield are discussed.

References

[1] E. Savchenko, I. Khyzhniy, S. Uyutnov, M. Bludov, G. Gumenchuk and V. Bondybey, *Nucl. Instrum. Meth*ods *B,* **460** (2019) 244
[2] M.A. Bludov, I.V. Khyzhniy, E.V. Savchenko, V.I. Sugakov, S.A. Uyutnov, *Nuclear Physics and Atomic Energy*, **21** (2020) 312
[3] E. Savchenko, I. Khyzhniy, S. Uyutnov, M. Bludov, and V. Bondybey, *Nucl. Instrum. Methods B*, **469** (2020) 37
[4] E. V. Savchenko, I. V. Khyzhniy, S. A. Uyutnov, A. N. Ponomaryov, G. B. Gumenchuk, V. E. Bondybey, *Procedia Physics*, **76** (2015) 111
[5] E.V. Savchenko, I.V. Khyzhniy, S.A. Uyutnov, M.A. Bludov**,** and V.E. Bondybey, *J. Mol. Structure*, **1221** (2020) 128803

Density changes in amorphous silicon provoked by swift heavy ions

Sjoerd Roorda[1,*], **Stéphanie Codsi**[1], **Amélie Lacroix**[1], **Gabrielle G. Long**[2], **Fan Zhang**[3], **Steven J. Weigand**[4], **and Christina Trautmann**[5]

[1]*Département de physique, Université de Montréal, 2900 Boulevard Edouard Montpetit, Montréal QC Canada*
[2]*X-Ray Science Division, Argonne National Laboratory, Argonne, IL 60439, USA*
[3]*Material Measurement Laboratory, National Institute of Standards and Technology, Gaithersburg, MD 20899, USA*
[4]*DuPont-Northwestern-Dow Collaborative Access Team Synchrotron Research Center, Northwestern University, Argonne National Laboratory, Argonne, IL 60439, USA*
[5]*GSI Helmholtzzentrum, Materials Research, Planckstr. 1, 64291 Darmstadt and Technical University of Darmstadt, 64289 Darmstadt, Germany*
[*]*sjoerd.roorda@umontreal.ca*

Pure and gold-doped amorphous silicon membranes were irradiated with swift heavy ions (75 MeV Ag or 1.1 GeV Au ions) and studied by small angle X-ray scattering. The samples that were irradiated with 1.1 GeV Au ions produced a scattering pattern consistent with core-shell type ion tracks of 2.0 $\pm$ 0.1 nm (core) and 7.0 $\pm$ 0.3 nm (total) radius irrespective of gold doping and consistent with radii previously observed [1]. However the core must be less dense than the original amorphous silicon, not more dense as argued in the Ref. [1], because its density is nearly 4 % different from that of the surrounding material. The compressive stress required to maintain the core 4 % more dense would exceed the yield strength of amorphous Si. The entire track (core + shell) is slightly less dense than the surrounding material, putting it under a lateral stress consistent with the macroscopic "hammering" deformation seen when tracks overlap. No tracks were found in samples irradiated with 75 MeV Ag ions, and no signature specific to the gold impurity doping could be observed.

References

[1] T. Bierschenk *et al.*, *Physical Review B*, 88 (2013) 174111

Annealing of ion tracks in amorphous SiO_2

S. Dutt[1], C. Notthoff[1], X. Wang[1,2], A. Kiy[1], M.E. Toimil-Molares[3], C. Trautmann[3,4], P. Mota-Santiago[5], N. Kirby[5], and P. Kluth[1,*]

[1]*Department of Materials Physics, Research School of Physics, Australian National University, Canberra, Australia*
[2]*State Key Laboratory of Nuclear Physics and Technology, Peking University, Beijing 100871, China*
[3]*GSI Helmholtzzentrum für Schwerionenforschung, Planckstr. 1, Darmstadt, Germany*
[4]*Technische Universtät Darmstadt, Darmstadt, Germany*
[5]*ANSTO-Australian Synchrotron, Melbourne, Australia*
[*]patrick.kluth@anu.edu.au

The annealing induced recovery of swift-heavy ion damage in amorphous SiO_2 (a-SiO_2) is interesting for a fundamental understanding of track annealing in amorphous materials with important implications for materials used for nuclear waste immobilization. However, measuring track annealing in amorphous materials is challenging and little is known about track annealing in SiO_2 [1,2]. Here we present a systematic study of track annealing in a-SiO_2 using a combination of track etching and synchrotron based small-angle x-ray scattering (SAXS) measurements. We have used 2 µm thick a-SiO_2, thermally grown on Si(100) substrates. The films were irradiated with 1.6 GeV Au ions at the UNILAC accelerator at GSI. Annealing was performed between 200 and 900°C. Etching in diluted HF results in the formation of conical etch pits. Using a geometrical track etch model, we can link the size of the etch pits at the surface to the etch rate along the ion tracks, which provides a measure for the damage recovery. By controlled removal of surface layers prior to etching we find that the damage recovery proceeds significantly faster closer to the sample surface and appears to level out at a certain depth. This is apparent from Figure 1, which shows the etch pit radius as a function of the initial etch depth for annealing under different conditions. Annealing in oxidizing atmosphere as compared to reducing atmosphere leads to slightly faster damage recovery near the surface indicating oxygen diffusion contributes to the recovery. SAXS measurements indicate only a small change in the radial track density profile up to 600°C with negligible change in the total track radius. This suggests that no significant material flow is taking place as part of the track recovery and the core-shell density structure with a low-density core and high-density shell remains up to this temperature [3,4]. At 700°C no remaining tracks have been observed.

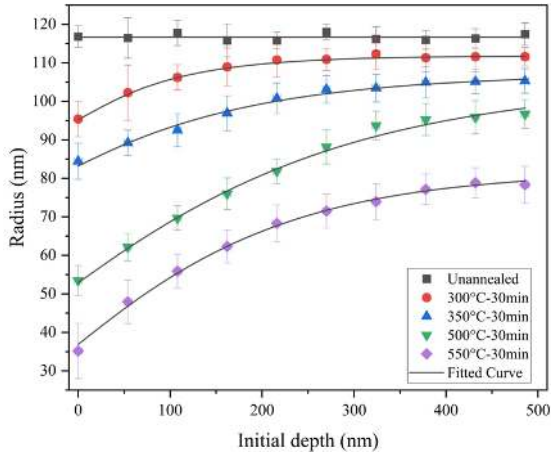

Figure 1: Etch pit radius as a function of initial etch depth.

References

[1] A. Aframian, Radiat. Eff. 33 (1977) 95–100.
[2] S.L. Koul *et al.*, Int. J. Radiat. Appl. Instrum. Part Nucl. Tracks Radiat. Meas. 19 (1991) 185–188.
[3] P. Kluth *et al.*, Phys. Rev. Lett. 101 (2008)
[4] P. Mota-Santiago *et al.*, Nanotechnology. 29 (2018).

Ion-tracks and nano-porosity in swift heavy ion irradiated GaSb and InSb

C. Notthoff[1,*], P. Mota-Santiago[1,2], A. Hadley[1], T. Alwadi[1], N. Kirby[2], R. Giulian[3], C. Trautmann[4,5], and P. Kluth[1]

[1]*Research School of Physics, The Australian National University, ACT 2601, Australia*
[2]*Australian Synchrotron, ANSTO, Clayton VIC 3168, Australia*
[3]*Institute of Physics, UFRGS, Av. Bento Gonçalves 9500, Porto Alegre – RS, cep 91501970, Brazil*
[4]*Materials Research Department, Gesellschaft für Schwerionenforschung (GSI), 64291 Darmstadt, Germany*
[5]*Technische Universtät Darmstadt, 64291 Darmstadt, Germany*
[*]*christian.notthoff@anu.edu.au*

Antimony based semiconductors are narrow band gap semiconductors used in many optoelectronic devices such as light emitting diodes, photodetectors, and diode lasers. We have studied the evolution of nano-porous structures in Ga- and InSb following swift heavy ion irradiation [1, 2, 3]. Nano-porous semiconductors differ significantly in their physical and chemical properties from their bulk counterparts, due to their microstructure [4]. The controlled fabrication of porous semiconductors thus paves the way for the development of new materials with application specific properties.

GaSb and InSb films grown on Si/SiO_2, InP, and GaAs substrates as well as bulk specimens were irradiated with different fluences, incidence angles, and ion energies at the ANU Heavy Ion Accelerator Facility and at GSI. Samples irradiated to low fluences are used to investigate ion track formation as a function of ion energy. With increasing fluence the formation of nano-porous structures is observed in both GaSb and InSb. A combination of high resolution structural characterisation techniques including synchrotron based small- and wide-angle x-ray scattering (SAXS/WAXS), imaging (SEM) and optical measurements (Raman- and FTIR-spectroscopy) have been used to investigate ion track formation and nano structure evolution as a function of ion energy, incidence angle, and fluence.

We will present our recent results on the energy dependence of the ion track formation in GaSb and InSb. Furthermore, we will present how the micro structure evolution depends on extrinsic properties such as the sample thickness. Fig. 1 shows bulk InSb irradiated at 30° incidence anglewith different fluences. The microstructure of the porous material is highly dependent on the fluence as well as the incident angle of the ion irradiation. The results aid in understanding the processes operational during pore formation in GaSb and InSb.

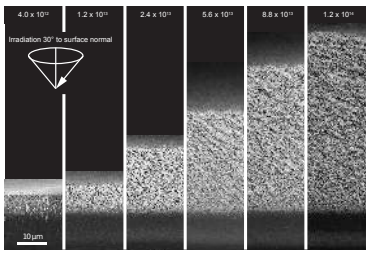

Figure 1: Bulk InSb irradiated to different fluences with 185 MeV Au Ions at 30° relative to the surface normal.

References

[1] P. Kluth, et al., *Appl. Phys. Lett.* **104**, 023105 (2014).
[2] C. Notthoff, et al., *Nuclear Inst. and Methods in Physics Research B*, **435**, 126 (2018).
[3] C. Notthoff, et al., *Phys. Rev. Materials*, accepted (2020).
[4] L. T. Canham, Appl. Phys. Lett. 57, 1046 (1990)

Particle emission from two-dimensional MoS_2 induced by highly charged ion impact

L. Skopinski[1,*], **P. Ernst**[1], **L. Breuer**[1], **and M. Schleberger**[1]

[1] *Fakultät für Physik and CENIDE, AG Schleberger, Universität Duisburg-Essen*
[*] *lucia.skopinski@uni-due.de*

Two-dimensional materials such as graphene or transition metal dichalcogenides have attracted much attention lately due to their huge potential for novel applications. However, they are also very interesting from a basic science point of view because their reduced dimensionality makes them ideal samples for studies in the field of ion-solid interaction. The irradiation with highly charged ions (HCIs) can be used to fabricate pores in freestanding single layers of MoS_2, the diameter of which can be tuned via the potential energy of the primary ion [1] enabling DNA sequencing or desalination. However, for many attractive applications the sample is supported by a substrate which plays an important role for the damage formation due to indirect sputtering [2] and thus has not yet been investigated experimentally in detail.

Here, we report on HCI induced damage of supported single layer MoS_2. We used Au substrates to minimize potential sputtering of the substrate and analyzed the emission of secondary ions and atoms under irradiation. Using laser-assisted time of flight (ToF) mass spectrometry,

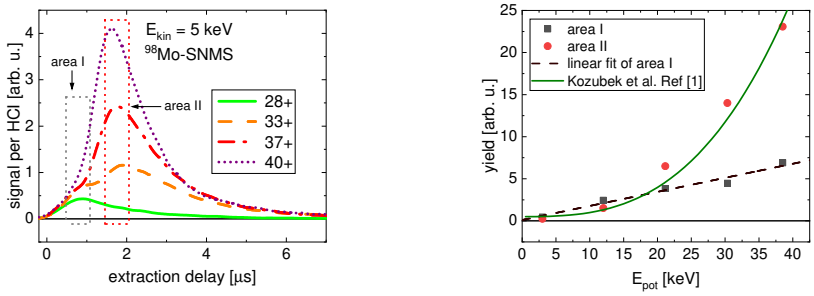

(a) Extraction delay measurements with a ToF mass spectrometer of emitted particles by Xe^{q+} impact.

(b) Yield of particles emitted in area I and area II depending on the potential energy of the projectile.

Figure 1: Analysis of emitted neutral ^{98}Mo particles sputtered by HCI impact from two-dimensional MoS_2 sample supported on a gold substrate. Evaluation of the yield in area I and II from (a) in (b).

the mass spectra are detected with different extraction delays allowing the transformation into a velocity or energy distribution. [3] In Fig. 1 (a) the signal dependence on the extraction delay shows two contributions at around 0.83 μs and 1.75 μs for the measured distributions. While the first one, assigned to kinetic sputtering, increases only slightly the latter contribution in area II increases strongly with the potential energy and is therefore considered to be caused by potential sputtering (Fig. 1 (b)). Further, the intensity of the signal caused by potential sputtering (area II) can be approximated by an addition of the kinetic effects from area I and the potential effects found for freestanding material by Kozubek et al.

References

[1] R. Kozubek et al. *J. Phys. Chem. Lett.*, 10 (2019) 904-910
[2] S. Kretschmer et al. *ACS Appl. Mater. Interfaces*, 10 (2018) 30827-30836
[3] L. Skopinski et al. *Rev. Sci. Instrum.*, 92 (2021) 023909

Potential sputtering in freestanding van-der-Waals heterostructures

R.A. Wilhelm[1,*], **A. Niggas**[1], **F. Aumayr**[1], **and J. Kotakoski**[2]

[1] *TU Wien, Institute of Applied Physics, Austria, EU*
[2] *University Vienna, Faculty of Physics, Austria, EU*
[*] *wilhelm@iap.tuwien.ac.at*

There exists a demand for highly surface-sensitive methods for defect engineering in order to tune the properties of 2D materials post growth. Slow and fast ions, electrons or photons typically possess an interaction cross section which is too small to confine the interaction to the first layer only and therefore multiple layers of a van-der-Waals (vdW) stack may be altered in an unfavourable way. Consequently, to achieve a certain morphological and/or electronic modification in a particular layer, one needs to apply high fluences which increases damage to other layers as well.
Using the feature of a high degree of charge exchange of slow highly charged ions we can confine the deposition of the potential energy to one layer only. Fig. 1 shows a freestanding

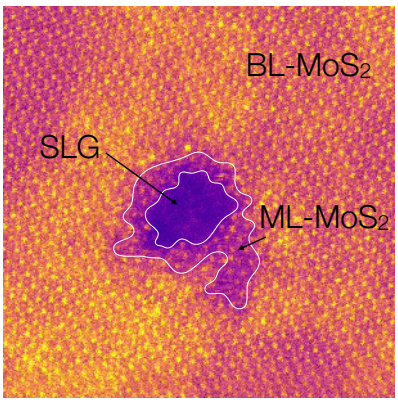

Figure 1: MoS_2/graphene heterostructure irradiated with 170 keV Xe^{38+} ions. The MoS_2 area is covered with a bilayer, where the ion carves a hole with different sizes in the first and second layer exposing the single layer of graphene (SLG).

bilayer MoS_2 on graphene stack, where the MoS_2 faced the incoming highly charged ion beam [1]. The MoS_2 is perforated in the top layers due to individual ion impacts, but the graphene underneath stays intact. Using a triple-layer MoS_2 reveals, that only the two topmost layers are perforated and the third layer is not damaged. Even more so, when turning the sample around such that the graphene faces the ion beam, no damage is observed in either layer. Therefore, we can conclude, that (a) the potential energy is deposited in one or two layers, but not more and (b) graphene can protect the MoS_2 from potential sputtering. It was shown previously, that the individual graphene [2] and MoS_2 [3] layers show different susceptibilities towards charge-exchange-driven damage.
In this contribution we show recent results on HCI-driven perforation of vdW structures and discuss the possible damage mechanism.

References

[1] J. Schwestka, H. Inani, M. Tripathi, A. Niggas, N. McEvoy, F. Libisch, F. Aumayr, J. Kotakoski, R.A. Wilhelm, *ACS Nano*, 14 (2020) 10536
[2] E. Gruber, R.A. Wilhelm *et al.*, *Nat. Commun.*, 7 (2016) 13948
[3] R. Kozubek, M. Tripathi *et al.*, *J. Phys. Chem. Lett.*, 10 (2019) 904

Probing surface magnetism with highly charged ions by X-ray spectroscopy

P Dergham[1*], M Werl[2], F Aumayr[2], E Lamour[1], S Macé[1], C Prigent[1], S Steydli[1], D Vernhet[1], R A Wilhelm[2], M Trassinelli[1]

[1] *Institut des NanoSciences de Paris (INSP), UMR 7588 CNRS- Sorbonne Université, Paris, 75005, France*
[2] *Institute of Applied Physics, TU Wien, Vienna, 1040, Austria*
*dergham@insp.jussieu.fr

The goal of the present project is to probe the magnetic state of the very first surface atomic layers, taking advantages of the interaction between slow highly charged ions (HCI) and the surface. The developed method will provide an alternative to conventional methods such as the Kerr effect, the X- ray dichronism and the neutron scattering more sensitive to bulk magnetization properties. Indeed, grazing collisions of HCI on surfaces are known to be sensitive to the first atomic layers offering the possibility to characterize the surface magnetic state. The experiment is based on electron transfer from the surface to the ion excited states when a highly charged ion gets close enough to the surface. Following this electron capture, hollow atoms are produced [1]. They then relax via radiative and Auger processes that partially conserve the initial spin state but also via the interatomic Coulombic decay (recently highlighted by R.A. Wilhelm et al. [2]) that is spin-insensitive. The surface magnetization properties can still be extracted through a careful study of the ion relaxation and coincidence measurements between the X-ray emission and the final ion charge state "Fig. 1".

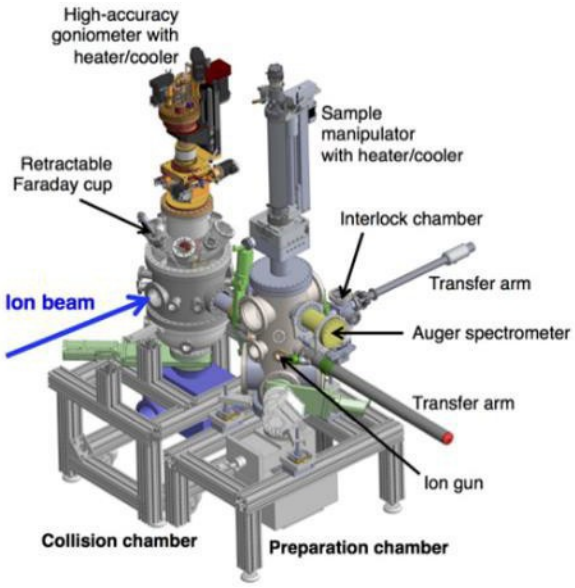

Figure 1: New setup of the ion collision and sample preparation chambers.

References

[1] HP. Winter, F. Aumayr, J. Phys. B: At. Mol. Opt. Phys. 32, R39 (1999).

[2] R.A. Wilhelm et al. 2017 Phys. Rev. Lett. 119, 103401.

Velocity correlated emission of large clusters by fullerene-surface impact

E. Kolodney[1,*], E. Armon[1], A. Bekkerman[1] , E. Zemel[1] , V. Bernstein[1], and B. Tsipinyuk[1]

[1] *Schulich Faculty of Chemistry, Technion–Israel Institute of Technology Haifa 32000, Israel*
[*] eliko@technion.ac.il

One of the intriguing aspects of ion-solid impact interactions at the keV kinetic energy range is the emission of large secondary clusters. Here we describe our recent observations of a new mechanism of velocity correlated clusters emission from a variety of metallic targets following impact of a *large polyatomic ion* (C_{60}^-). Measurements of the kinetic energy distributions (KEDs) of the emitted secondary clusters revealed a behaviour which is very different from that observed for the case where the impacting keV projectile is a *heavy monoatomic ion*. We have measured the KEDs of large clusters emitted from six different targets, ranging from group 5 (Nb and Ta carbidic clusters $Nb_nC_n^+$ and $Ta_nC_n^+$) [1,2] to group 11 coin metals (Cu_n^+ , Ag_n^+ and Au_n^+) [1,2] and group 13 (Al_n^+) [3] following a single impact of C_{60}^- ion at 14 keV.

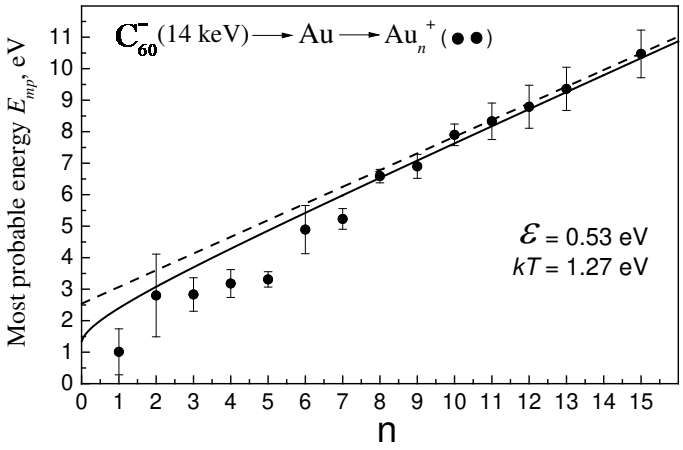

Fig. 1. Most probable energies $E_{mp}(n)$ of Au_n^+ (n=1-15) cluster ions sputtered from a gold target following 14 keV C_{60}^- impact. Measured (solid circles) and calculated (solid and dashed lines) dependences are shown. The calculated dependences are based on ε and *kT* parameters extracted from a shifted Maxwellian fit to the respective families of the measured cluster KEDs. The ε parameter is the kinetic energy of a single Au atom in the cluster moving with the prcursor velocity.

All the large clusters emitted (from a given target) move with nearly the same velocity (see Fig.1 for Au_n^+) with KEDs described as shifted Maxwellians where some precursor moving with a common center-of-mass velocity is the source for the emitted clusters. These observations are supported by a model for the formation of the precursor and molecular dynamics simulations [2,4]. Target mass effect as well as using the measurements for subpicosecond probing of extreme initial spike conditions will be discussed.

References

[1] E. Armon , A. Bekkerman, Y. Cohen , J. Bernstein , B.Tsipinyuk and E. Kolodney , Phys. Rev. Lett. **113**, 027604 (2014).
[2] E. Armon, E. Zemel, A. Bekkerman, V. Bernstein, B. Tsipinyuk and E. Kolodney, J. Chem. Phys. **150**, 204705 (2019).
[3] A. Bekkerman, B. Tsipinyuk and E. Kolodney, *Nucl. Instrum. Methods Phys. Res. B,* **481**, 24 (2020).
[4] E. Armon, A. Bekkerman, V. Bernstein, B. Tsipinyuk and E. Kolodney, submitted

Much lower track formation threshold of MeV C_{60} ions in Si than those of swift heavy monoatomic ions

H. Amekura[1,*], K. Narumi[2], A. Chiba[2], Y. Hirano[2], K. Yamada[2], S. Yamamoto[2], N. Ishikawa[3], N. Okubo[3], and Y. Saitoh[2]

[1]*National Institute for Materials Science (NIMS), Tsukuba, Japan*
[2]*National Institutes for Quantum Science and Technology (QST), Takasaki, Japan*
[3]*Japan Atomic Energy Agency (JAEA), Tokai, Japan*
[*]*amekura.hiroshi@nims.go.jp*

When a high energy heavy ion in the electronic stopping (S_e) regime is injected into some kinds of solids, a damaged region of cylindrical shape with high aspect ratio is formed along the nearly straight trajectory of the ion, which is called ion track. Crystalline silicon (c-Si) is one of the most important materials in today's technology, and is also known as a radiation-hard material in the electronic stopping regime: Up to the present, any swift heavy *monoatomic* ions do not form ion tracks in c-Si.

The track formation in c-Si was succeeded in utilizing fullerene (C_{60}) ions, since a C_{60} ion provides much higher energy deposition than the U ion. Since all the sixty C atoms are injected at the same time into almost the same position, i.e., within the diameter of C_{60} molecule of 0.7 nm, roughly sixty times greater energy than the carbon monomer is deposited. In the late 1990s, Canut et al. and Dunlop et al. simultaneously succeeded in producing ion tracks in c-Si using 40 and 30 MeV C_{60} ions from the Orsay facility in France. From these data, the threshold S_e of 30 keV/nm (C_{60} energy of 17 MeV) was extrapolated, below which the ion tracks were believed not to be formed in c-Si.

Here we report that the ion track formation in c-Si under 6 MeV C_{60}^+ ion irradiation [1], which corresponds to S_e of 18.0 keV/nm, i.e., much lower than the extrapolated threshold of 30 keV/nm. Even decreasing the C_{60} energy down to 1 MeV (S_e = 7.5 keV/nm), still tracks were observed [1]. In this paper, the track formation in c-Si under much lower energy deposition than the extrapolated threshold of 30 keV/nm are discussed in terms of non-negligible nuclear energy deposition and recrystallization of transiently molten tracks. The inelastic thermal spike model with assumptions clearly explains both the behaviour observed below and above the threshold of 30 keV/nm.

References

[1] H. Amekura, et al., *Scientific Reports*, 11 (2021) 185.

On the formation of x-ray waveguide structure in thin films via ion irradiation

B. N. Dev[1,*], Nasrin Banu[2], S. Roy[3], B. Satpati[4], S. Singh[5], and S. Basu[5]

[1] *Centre for Quantum Engineering, Research and Education (CQuERE), TCG Centres for Research and Education in Science and Technology, Kolkata 700091, India*
[2] *Department of Condensed Matter Physics and Materials Science, Weizmann Institute of Science, Israel*
[3] *Department of Physics and Astrophysics, University of Delhi, Delhi 110007, India*
[4] *Surface Physics and Material Science Division, Saha Institute of Nuclear Physics, Kolkata 700064, India*
[5] *Solid State Physics Division, Bhabha Atomic Research Centre, Mumbai 400085, India*
[*] *bhupen.dev@tcgcrest.org*

Materials modification using interactions of energetic ions with materials over a wide range of ion energies (keV to GeV) has been extensively used to fabricate optical waveguide structures. Among other techniques of optical waveguide fabrication, ion implantation/ irradiation is a general and flexible method to achieve this goal with several advantages over the other techniques [1]. However, there was no report on the waveguide fabrication in the x-ray regime using ion beams. Recently, we reported the first results on x-ray waveguide formation by ion irradiation of cobalt thin films on silicon [2]. In this case, Co(25 nm)/ Si(111) was irradiated with 1 MeV Si^+ ions in the 10^{16} ions/cm^2 fluence range. The irradiated samples were investigated with x-ray reflectivity (XRR), SIMS and TEM measurements. Although Co thin films on Si is a simple system, Co thin films, grown on clean Si, has shown formation of high-density (HD) Co as well as normal-density Co layers in the film [3, 4]. These interesting observations led us to undertake the ion irradiation work. (It is worth mentioning here that, while normal Co is ferromagnetic, the HD Co layers are nonmagnetic [3, 4] as well as superconducting [5]).

X-ray reflectivity experiments were carried out on both as-deposited and irradiated samples. For the irradiated sample, dips in the total reflectivity region were observed [2]. These dips are signatures of resonant modes generation in an x-ray waveguide [6]. The lost intensity in the reflected beam at dips tunnels into the wave-guiding layer. Our calculation from the XRR results also shows a 15-fold x-ray flux enhancement in the guiding layer. Flux enhancement is also a characteristic of x-ray waveguides [6]. Details of further experiments will be presented.

References

[1] P.D.Townsend, P. J. Chandler, and L. Zhang, *Optical Effects of Ion Implantation* (Cambridge, UK: Cambridge University Press, 1994)
[2] Nasrin Banu, S. Roy, B. Satpati, S. Singh, A. Bhukta, P. Chakraborty, S. Basu, and B. N. Dev, *Mater. Res. Express* 6 (2019) 056419
[3] Nasrin Banu, S. Singh, B. Satpati, A. Roy, S. Basu, P. Chakraborty, H. C. P. Movva, V. Lauter and B. N. Dev, *Scientific Report* 7 (2017) 41856
[4] Nasrin Banu, S. Singh, S. Basu, A. Roy, H. C. P. Movva, V. Lauter, B. Satpati, and B. N. Dev, *Nanotechnology* 29 (2018) 195703
[5] Nasrin Banu, M. Aslam, A. Paul, S. Banik, S. Das, S. Datta, A. Roy, I. Das, G. Sheet, U. V. Waghmare, and B. N. Dev, *EPL*, 131 (2020) 47001
[6]Y. P. Feng, S. K. Sinha, H. W. Deckman, J. B. Hastings, and D. P. Siddons, *Phys.Rev.Lett.* 71 (1993) 537

Velocity distribution of sputtered neutrals under swift heavy ion bombardment

T. Heckhoff[1], **D. Theuner**[1], **L. Breuer**[1], **C. Böttger**[1], **M. Schleberger**[1] **and A. Wucher**[1,*]

[1]*Universität Duisburg-Essen, Germany*
[*]*andreas.wucher@uni-due.de*

Experiments measuring velocity distributions of sputtered atoms are well known. Utilizing time-of-flight (TOF) secondary ion and neutral mass spectrometry (SIMS and SNMS) experiments, it is also possible to measure those distributions in a mass resolved manner. For that purpose, two things are needed, namely i) a well-defined starting point in space and time and ii) a well-defined finish line for sputtered particle detection. Usually, a short primary ion pulse is used as a starting point. For our experiments, making use of swift heavy ion (SHI) projectiles for SIMS and SNMS, however, this is not applicable. Compared to the nanosecond timescale of the experiment, the swift heavy ion pulse, which has a duration in the range of milliseconds, is a quasi-stationary (dc) ion beam.

In this work, a method is described to measure the velocity distribution of sputtered neutrals under bombardment with a dc ion beam. For our experimental setup we use swift heavy ions (e.g. 4.8 MeV/u $^{197}Au^{26+}$) delivered by the UNILAC at the GSI Helmholtz Centre in Darmstadt. Sputtered particles can be ionized by single-photon ionization using a pulsed 157-nm excimer laser (photon energy 7.9 eV) or a tightly focused high-intensity femtosecond laser beam. Using laser post-ionization as a starting point in space and time, a confined sensitive volume of the TOF spectrometer as a finish line and delayed extraction, one can determine how many of the post ionized particles have left the sensitive volume by a certain time. By varying the delay between the laser pulse and the switched extraction of ions into the TOF spectrometer, it is possible to probe the velocity distribution of the post-ionized sputtered neutral particles.

As a proof of principle for this method, a dataset is presented, which was acquired using a tightly focused high-intensity femtosecond laser beam for post-ionization. Under 20 keV C_{60}^+ ion bombardment, the method delivers a velocity distribution of sputtered Indium atoms which matches that measured with the conventional method using a pulsed primary ion beam as well as a theoretically expected "Thompson"-like distribution.

Furthermore, we will demonstrate the application of the method for the analysis of data sets acquired under swift heavy ion bombardment. The resulting velocity spectra of neutral particles emitted under SHI impact are directly compared to those measured *in-situ* under 5-keV Ar^+ ion bombardment. The results obtained for a number of metal, semiconductor and organic film targets indicate a strong contribution of extremely slow emitted neutral particles under SHI as compared to keV ion bombardment. Particularly for metals, however, this contribution appears to strongly depend on the oxidation state of the surface in, however, a fundamentally different way as compared to keV ion bombardment.

Elongation of embedded Au nanoparticles in various materials by swift heavy ion irradiation and their plasmonic characterization

S. Korkos[1,2], V. Jantunen[3], T. Kosti[2], K. Arstila[1,2], J. J. Toppari[2], T. Sajavaara[1,2] A. A. Leino[3], K. Nordlund[3], F. Djurabekova[3]

[1]*Accelerator Laboratory, Department of Physics, University of Jyvaskyla, P.O. Box 35, FI-40014 Jyvaskyla, Finland*

[2]*Nanoscience Center, Department of Physics, University of Jyvaskyla, P.O. Box 35, FI-40014 Jyvaskyla, Finland*

[3]*Department of Physics, University of Helsinki, P.O. Box 43, FI-00014 Helsinki, Finland*

[*]*spyridon.s.korkos@jyu.fi*

Swift Heavy Ion (SHI) irradiation of nanoparticles (NPs) embedded in solid-state matrix is a promising method to fabricate novel nanostructure morphologies for a wide variety of applications. Except for the transformation of metallic spherical NPs to nanorods at high ion fluences >10^{13} ions/cm^2 [1-3], SHI irradiation can be used to "rotate" embedded nanorods along the ion beam direction [4]. This phenomenon can be explained by the formation of the ion track in the matrix resulting in lower density (underdense) material and by melting of the NP caused by deposited ion energy. As a result, the elongation occurs after the flow of the molten metal to the underdense matrix. However, the elongation has been observed in metallic NPs embedded in a small number of matrix materials, such as SiO_2, Si_3N_4 and sapphire.

In this work, we have developed a new experimental approach allowing for imaging the same NPs before and after the irradiation with TEM (Transmission Electron Microscopy). In this way we can study the elongation as a function of the initial size and shape of the particle. In our study, we investigated the elongation process of SHI irradiated Au spherical NPs of various diameter (5-80 nm) embedded in amorphous SiO_2 [5], Si_3N_4 and Al_2O_3. Au nanorods of 20-45 nm diameter and 30-90 nm length were investigated as well [4]. The samples were irradiated with 50 MeV $^{127}I^{9+}$ ions at 45° angle of incidence and ion fluences from 10^{13} to 5x10^{14} ions/cm^2. Moreover, atomistic simulations [4] were applied to give insight on the experimental results.

It is well known that metallic NPs embedded in dielectric matrices exhibit localized surface plasmon (LSP) modes. These modes have a resonance frequency (LSPR) showing a scattering peak in spectroscopic measurements. Dark-Field (DF) optical microscopy was performed after the irradiation to study the impact of the particle shape deformation to the LSP modes.

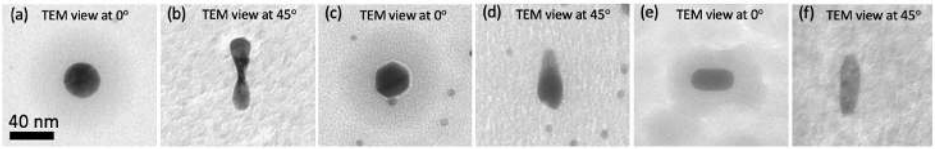

Figure 1: TEM images of (a), (b) a spherical NP embedded in SiO_2 before and after the irradiation, respectively, at 5x10^{14} ions/cm^2 fluence, (c), (d) a spherical NP embedded in Al_2O_3 before and after the irradiation at 2x10^{14} ions/cm^2 fluence, (e), (f) a nanorod embedded in SiO_2 before and after the irradiation at 10^{14} ions/cm^2 fluence.

References

[1] C. D' Orleans, et al., *Physical Review B,* **67** (2003) 220101.
[2] G. Rizza, et al., *Physical Review B,* **86** (2012) 035450.
[3] P. Mota-Santiago, et al*, Physical Review Materials,* **4** (2020) 096002.
[4] S. Korkos et al., *Applied Physics Letters* (submitted).
[5] S. Korkos, et al., (manuscript in preparation).

He^+ ion channeling contrast investigations using Scanning Transmission Helium Ion Microscopy

S. Tabean[1,*], M. Mousley[1], O. De Castro[1], T. Wirtz[1], S. Eswara[1]

[1] *Advanced Instrumentation for Nano-Analytics (AINA), MRT Department, Luxembourg Institute of Science and Technology (LIST), L-4422 Belvaux, Luxembourg*

[*]saba.tabean@list.lu

In order to demonstrate advanced structural and chemical imaging modalities at nanometer scale using Helium Ion Microscopy, we have developed the npSCOPE prototype at the Luxembourg Institute of Science and Technology(LIST)[1]. This prototype incorporates the Gas Field Ion Source (GFIS) technology as key enabler for high lateral resolution Ion Microscopy using Helium in combination with three different detection/analysis modes in single platform, namely a Secondary Electron (SE) detector for SE imaging, a position sensitive Delay-line detector (DLD) for Scanning Transmission Helium Ion Microscopy (STIM) imaging, and a continuous focal plane microchannel plate delay line (MCP-DL) detector for Secondary Ion Mass Spectrometry. This paper presents the possibility to perform STIM imaging using a keV He^+ ion beam to investigate channeling in nanoscale structures including crystalline defects and crystal orientations. STIM imaging captures sub-surface features such as defects or precipitates within crystalline structures whereas conventional SE imaging is not able to provide this information. We have reported the details of the STIM imaging capability using the npSCOPE prototype elsewhere[2,3].

In this talk, we will present examples of STIM images captured in npSCOPE to demonstrate the possibility to perform quantitative analysis of transmission ion channeling with nanoscale lateral resolution. As an example, a STIM image taken from a polycrystalline Au as a model sample using 25 keV He^+ with 60fA beam current and a dwell time of 110µs is shown in Fig. 1a. Dark lines (e.g. the blue arrows in Fig.1a) within the crystalline grains indicate twin bands. Also, channeling efficiencies along different grain orientations manifest as channeling contrast in the STIM image revealing hidden structures hardly visible in the SE image in Fig. 1b.

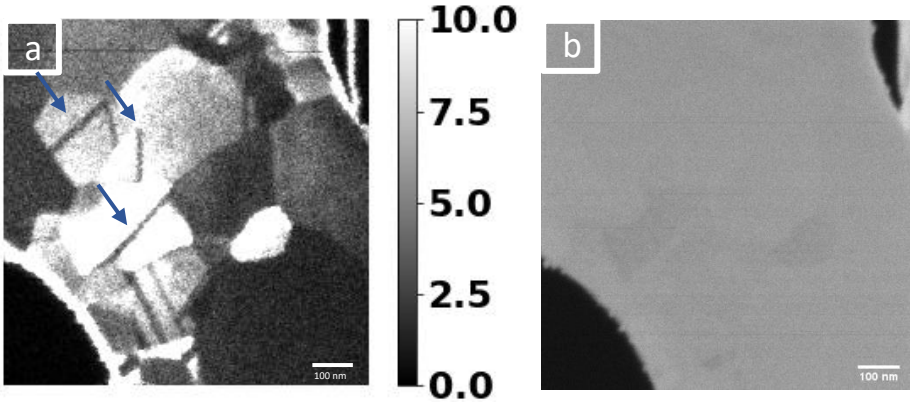

Figure 1: An example comparison of a (a) Scanning Transmission Helium Ion Microscopy(STIM) image with (b) SE image for a polycrystalline gold with a thickness ~ 50 nm. Both images were taken from the same region of the sample. The straight dark lines seen within bright grains in the STIM image correspond to twin bands (blue arrows in figure a).

Refrences

1. De Castro, O. *et al.* npSCOPE: A New Multimodal Instrument for in Situ Correlative Analysis of Nanoparticles. *Anal. Chem.* **93**, 14417–14424 (2021).

2. Serralta, E. *et al.* Scanning transmission imaging in the helium ion microscope using a microchannel plate with a delay line detector. *Beilstein J. Nanotechnol.* **11**, 1854–1864 (2020).

3. Tabean, S. *et al.* Quantitative nanoscale imaging using transmission He ion channelling contrast: Proof-of-concept and application to study isolated crystalline defects. *Ultramicroscopy* **233**, 113439 (2022).

Scanning transmission ion microscopy and time of flight energy loss spectroscopy with keV helium ions

M. Mousley[1*], **S. Tabean**[1] **and O.Bouton**[1], **T. Wirtz**[1], **S. Eswara**[1]

[1]*Advanced Instrumentation for Nano-Analytics (AINA)*
Materials Research and Technology Department, Luxembourg Institute of Science and Technology
[*]*michael.mousley@list.lu*

Over the last decades, advances in gas field ion source technology have led to keV helium ion beams, with sub-nm probe sizes, being commercially available in helium ion microscope (HIM) instruments. When measuring the signals coming back from the sample, the HIM has already been proven to be a versatile instrument [1], providing multiple imaging modes including secondary electron imaging with excellent lateral resolution, time of flight (TOF) back scatter spectroscopy and nanoscale secondary ion elemental mapping. However, detectors to measure the transmission signal using keV helium ions, are not readily available in commercial instruments meaning previous studies required bespoke experimental equipment [2]–[5]. The use of a delay line detector (DLD) has only recently been explored with efforts performing (scanning) transmission ion microscopy ((S)TIM), an analogous technique to (scanning) transmission electron microscopy ((S)TEM)[6][7]. Despite renewed interest in energy loss of keV helium ions [8], there is currently a lack of research into the imaging capabilities of keV STIM ion energy loss spectroscopy (IELS) in direct analogy to STEM-electron energy-loss spectroscopy (EELS) experiments. Results from a helium ion TOF energy loss spectroscopy experiment will be shown. 20 keV He^+ ions from a duoplasmatron source were focussed onto a 15nm Si membrane substrate. A 50nm Au layer was deposited onto some regions of the membrane. The beam was scanned over the sample whilst recording the TOF values with a DLD. The detector records the TOF and position on the detector for every count, producing a 5D dataset when the beam is scanned over the sample. The different delays in arrival time due to the sample are visible in the TOF spectra. Different time windows can be used to map out regions of different materials, producing energy selective STIM-IELS maps in a similar manner to STEM-EELS maps.

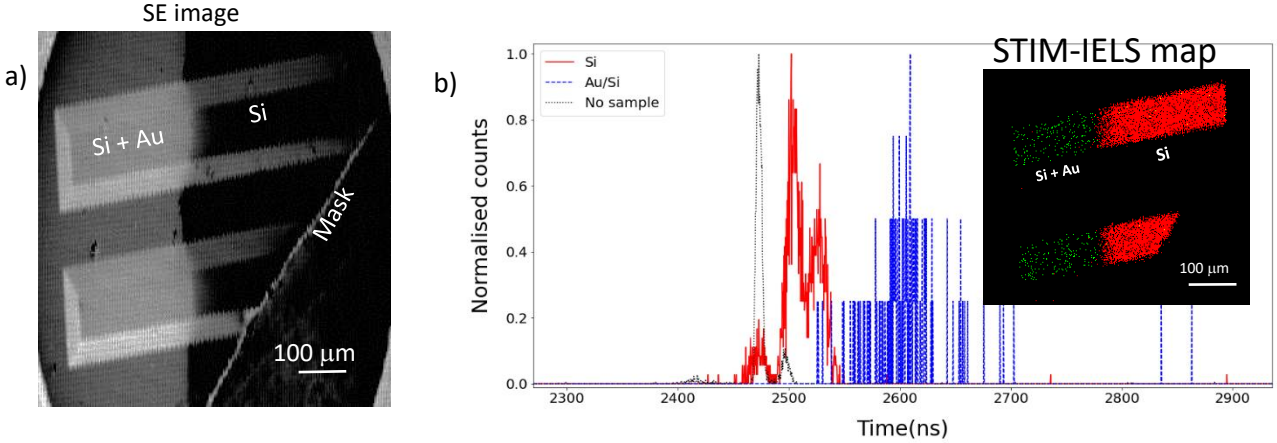

Figure 1 a) A HIM-SE image of the 15nm Si membrane sample partially coated with 50nm Au b) the TOF data from the different regions of the sample and, inset, a reconstructed STIM-IELS overlay image of the sample.

References

[1] T. Wirtz O. De Castro J.-N. Audinot and P. Philipp, “Imaging and Analytics on the Helium Ion Microscope,” *Annu. Rev. Anal. Chem.*, vol. 12, no. 1, 2019, doi: 10.1146/annurev-anchem-061318-115457.

[2] M. Mousley *et al.*, “Stationary beam full-field transmission helium ion microscopy using sub-50 keV He+: Projected images and intensity patterns,” *Beilstein J. Nanotechnol.*, vol. 10, pp. 1648–1657, Aug. 2019, doi: 10.3762/bjnano.10.160. [Online]. Available: https://www.beilstein-journals.org/bjnano/articles/10/160

[3] J. Wang *et al.*, “Focussed helium ion channeling through Si nanomembranes,” *J. Vac. Sci. Technol. B, Nanotechnol. Microelectron. Mater. Process. Meas. Phenom.*, vol. 36, no. 2, p. 021203, 2018, doi: 10.1116/1.5020667. [Online]. Available: http://avs.scitation.org/doi/10.1116/1.5020667

[4] T. J. Woehl R. M. White and R. R. Keller, “Dark-Field Scanning Transmission Ion Microscopy via Detection of Forward-Scattered Helium Ions with a Microchannel Plate,” *Microsc. Microanal.*, vol. 22, no. 3, pp. 544–550, 2016, doi: 10.1017/s1431927616000775.

[5] D. Emmrich *et al.*, “Scanning transmission helium ion microscopy on carbon nanomembranes,” *Beilstein J. Nanotechnol.*, vol. 12, pp. 222–231, 2021, doi: 10.3762/bjnano.12.18.

[6] E. Serralta *et al.*, “Scanning transmission imaging in the helium ion microscope using a microchannel plate with a delay line detector,” *Beilstein J. Nanotechnol.*, vol. 11, pp. 1854–1864, 2020, doi: 10.3762/BJNANO.11.167.

[7] S. Tabean *et al.*, “Quantitative nanoscale imaging using transmission He ion channelling contrast: Proof-of-concept and application to study isolated crystalline defects,” *Ultramicroscopy*, vol. 233, no. June 2021, p. 113439, 2022, doi: 10.1016/j.ultramic.2021.113439. [Online]. Available: https://doi.org/10.1016/j.ultramic.2021.113439

[8] R. Holeňák S. Lohmann and D. Primetzhofer, “Contrast modes in a 3D ion transmission approach at keV energies,” *Ultramicroscopy*, vol. 217, no. April, pp. 0–5, 2020, doi: 10.1016/j.ultramic.2020.113051.

Generation of picosecond ion pulses using a fast pulse electron beam ion source

G.L. Szabo[1,*], **A.S. Grossek**[1], **A. Niggas**[1], **and R.A. Wilhelm**[1]

[1] *Institute of Applied Physics, TU Wien, 1040 Vienna, Austria*
[*] *gszabo@iap.tuwien.ac.at*

Ion beams in the range from few keV up to MeV are used to change and analyse material properties from experiments. While the structure changing processes are well understood, little is known about the timescale at which ion-solid interaction and subsequent collisional cascades take place. For this, a pump-probe experiment is required, consisting of a fs-laser that is utilised on one hand to generate pulsed ions (pump) and on the other hand to analyse the surface around the ion impact (probe). To realise such an experiment, the pulse width of the ion beam has to be in the order of a few ps, which is the expected lifetime of such a collisional cascade.

We present first results of ion pulses in the ps range, obtained with a modified concept of an electron beam ion source (EBIS), such that a pulsed electron beam generates ions by electron impact ionisation. We also present simulations on improving the pulse width to only a few ps and on a new approach to measure ion pulses in the ps range, using an energy-filtered streak-camera. For the experiment and the simulations, we used a ultra-compact fast-pulse EBIS from D.I.S Germany [1], where the electrons are generated from a photo-cathode with a fs-laser (12 fs laser pulse duration). We first analysed the electrons emitted from the cathode. In Fig. 1 a time-of-flight (TOF) spectrum of pulsed electrons, with a pulse width of 276 ps, can be seen. The electron pulses are detected by a standard Chevron MCP stack, pre-amplified and time-stamped by a constant-fraction discriminator. The TOF spectrum is generated with the help of a time-to-digital converter. With these pulsed electrons, we were able to produce pulsed ions with a pulse width significantly below 1 ns. Additional simulations for the same geometry predict a possible pulse width below 100 ps at room temperature and even lower pulse widths at gas temperatures in the mK regime can be realised by a gas jet [2]. In order to measure such short pulse lengths, an adapted streak-camera will be utilised and its concept will be presented as well.

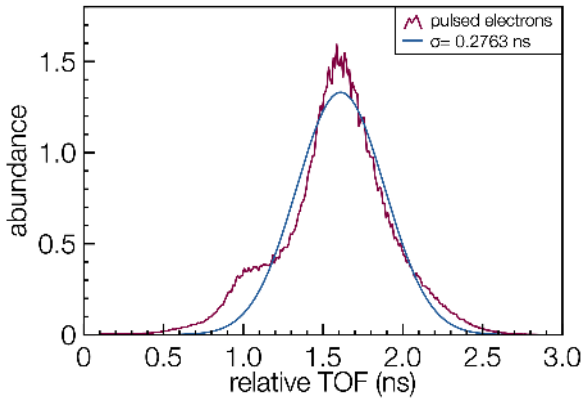

Figure 1: In this figure, a relative TOF spectrum of pulsed electrons with a pulse width of 276 ps is shown.

References

[1] https://www.dis-eng.de, last opened: 10.03.2022
[2] A. Golombeket al. *New J. Phys.*, 23 (2021) 033023

Nanoparticle-assisted radiosensitization in human glioblastoma cells exposed to high-energy photon and charged-particle beams

D. B. Guerra[1,2], **R. D. Weimer**[1], **E. M. N. de Oliveira**[1], **F. M. Diz**[3], **F. B. Morrone**[3], **L. Barazzuol**[2], **R. P. Coppes**[2], **and R. M. Papaléo**[1,*]

[1]*Interdisciplinary Center of Nanoscience and Micro-Nanotechnology,School of Technology,Pontifical Catholic University of Rio Grande do Sul, Brazil*

[2]*Dept. of Biomedical Sciences of Cells and Systems, University Medical Center Groningen, Groningen, The Netherlands*

[3]*Applied Pharmacology Laboratory, School of Health and Life Sciences,Pontifical Catholic University of Rio Grande do Sul, Brazil*

[*]*papaleo@pucrs.br*

Metal-based nanoparticles have been proved to be a promising class of new radiosensitizer agents for radiotherapy of cancer. Although, a substantial amount of data has already been collected on the sensitization action of nanomaterials, the reported effects show a large variability. Results, even at the in vitro level, are far from being conclusive, and both, the underlying mechanisms and the role of key parameters involved in NP-enhanced radiotherapy are not fully understood. In this contribution, we report on an intercomparison of radiosensitization effects produced by gold (GNP) and dextran-coated superparamagnetic iron oxide nanoparticles (SPION-DX) in human glioblastoma (GBM) cells irradiated by beams of 6 MV photons (from a clinical linear accelerator in Brazil) and 150 MeV protons (at the UMCG PARTREC cyclotron facility in the Netherlands). The nanoparticle treatment concentration was varied from 20 up to 100 μg/mL. We monitored cell viability after nanoparticle exposure alone, the actual NP uptake by the cells with ICP-MS, post-irradiation cell survival via the clonogenic assay, and DNA damage and repair by means of immunofluorescence studies with γH2AX and 53BP1. The linear-quadratic model was used to extract the α and β parameters, the α/β ratio, and the enhancement sensitization factor at 10% survival ($SER_{10\%}$), which were all obtained as a function of NP concentration.

GNP-treated cells irradiated by 6 MV-photons displayed large sensitization enhancement ratios ($SER_{10\%}$ up to 2.04). More modest effects were induced by SPION-DX, but still significant reductions in survival were achieved (maximum $SER_{10\%}$ =1.61). For both NPs $SER_{10\%}$ increased with the degree of metal uptake, but not necessarily with treatment concentration. The α/β ratios extracted from the survival curves are reduced by the presence of SPION-DX, but strongly increased by GNPs, suggesting that sensitization by GNPs occurs mainly via promotion of lethal complex damage, while for SPION-DX repairable damage dominates. Preliminary data from radiosensitive and a radioresistent strains, revealed that the combination of the nanoparticles with RX radiotherapy was more effective in eliminating the radioresistant cells. The use of GNPs in combination with the proton beam also resulted in an increase in radiation-induced cell death, with $SER_{10\%}$ values close to 1.5 and a fold change of 1.62 in the α/β ratio. Immunofluorescence studies showed an increase in the number of DNA double strand breaks (DSBs) in the presence of NPs. GNPs induced a higher number of cells with residuals DSBs, suggesting NP-induced inhibition of DNA repair. Sensitization efficacy increased linearly with GNP concentration, but not for iron oxide NPs. A general comparison of the NP action under the two types of radiation fields will be presented. Similar experiments are also planned using C beams and may also be reported.

Fabrication of Organic Nanowires with Designated Physical Properties via High-Energy Charged Particles

M. Nobuoka[1], **K. Kamiya**[1], **and S. Seki**[1*]

[1]*Department of Molecular Engineering, Graduate School of Engineering, Kyoto University, Japan*
[*]*seki@moleng.kyoto-u.ac.jp*

Semiconductors and the related optoelectronic devices are in the midst of rapid development, which can be attributed to the nanotechnology advancements resulting from the miniaturization of these devices. Nanowires, which have quantum-sized structures restricted into one dimension, are attracting attentions as materials platforms because of their 1) huge specific surface area, and 2) energy/charge/spin transport along the axes. Although inorganic nanowires have been already well-developed, organic nanowires with explicitly defined 1D structures have been reported rarely in spite of expectations for extra-wide range of their applications such as electro-luminescence and organic photovoltaics. Convensional lithography techniques has been often the major choice for fabrication of organic nanostructures, however the reality of the technique is still in the formation of nanostructures with high aspect ratio.

We have developed a nanowire (NW) fabrication technique using high-energy particle beams: single particle induced linear solid-phase polymerization (STLiP) technique (Fig. 1). In this process, a high-energy ion beam is irradiated onto a organic-molecular thin film to induce intermolecular polymerization reactions in a nm-sized cylindrical space along the particle trajectory, and the polymerized material is obtained as organic NWs through isolation operations. Since one particle gives a corresponding NW, we are intrinsically free from focusing limit defined by beam optics or space charge effects. In addition, the thickness of the starting material film is perfectly reflected by the NW length, as well the particle fluence define clearly the number density of NWs in unit area; this is suggestive of its feasibility to lead structurally uniform NW assemblies. Recently, we reported facile and universal formation protocols of nanowire array (NA) structures, where perfect-uniform NWs were oriented perpendicularly to the substrate by an use of sublimation of small organic molecules as the NW isolation scheme (removal of unreacted molecules from the irradiated film).[1] NWs with ordered heterojunctions[1], core-shell (coaxial)[1], and multi-linkage [2] structures have been demonstrated as addressable by the simple STLiP technique, giving electrical devices such as nano diodes and transistors. We believe the STLiP technique is a powerful and unique choice for the future nanomaterial platforms exhibiting widespread dynamic range in designated physical propeties reflecting the nature of organic molecules.

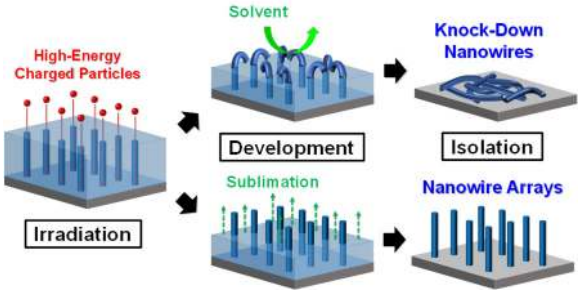

Figure 1. Schematic illustration of fabrication organic nanowires by STLiP technique.

References

[1] K. Kamiya, et al. *Nat. Commun.* 12 (2021) 4025
[2] M. Nobuoka, et al. *J. Photopolym. Sci. Technol.* 34 (2021) 167.

Sputtering of planets and moons by impact of solar wind ions

H. Biber[1], P. S. Szabo[1,2], J. Brötzner[1], N. Jäggi[2], A. Galli[2], P. Wurz[2], and F. Aumayr[1*]

[1] *Institute of Applied Physics, TU Wien, Vienna, 1040, Austria*
[2] *Space Sciences Laboratory, University of California, Berkeley, CA 94720, USA*
[3] *Physics Institute, University of Bern, Bern, 3012, Switzerland*
[*] *aumayr@iap.tuwien.ac.at*

The sputtering of planetary surfaces by ions is a dominant contributor to the space weathering of airless planets and moons [1]. The main source of ion precipitation is the solar wind (see Fig. 1), a steady stream of mainly H^+ and He^{2+} ions with kinetic energies of typically 1 keV/amu. The Martian moon Phobos is also exposed to a stream of oxygen ions from the Martian magnetosphere with energies of several keV [2]. The erosion dynamically alters the composition and optical properties of the surface of such atmosphere-free celestial bodies while the ejected atoms contribute to the formation of a very thin exosphere around them [3]. Many aspects of this process are currently not well understood and are simulated with inadequate sputtering codes.

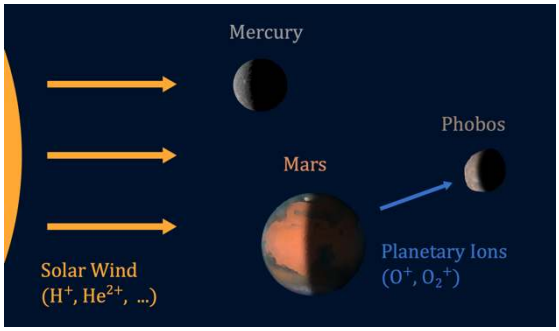

Figure 1: Airless bodies in the solar system are primarily sputtered by ions of the solar wind. Phobos is also exposed to a flux of oxygen ions from the Martian atmosphere.
(Image credit: NASA/JPL/USGS/David Crisp and the WFPC2 Science Team/University of Arizona)

To get a better understanding of the effects responsible for the interaction between ions and planetary surfaces, laboratory experiments were performed using a quartz crystal microbalance (QCM). This approach allows for real-time measurements of mass changes in situ [4]. Thin films of various silicate minerals were used as analog materials for the surfaces of the Moon, Mercury, and Phobos [5, 6]. He^{2+} potential sputtering was found to increase the total sputtering of planetary surfaces by around 40% [5], due to additional release of O atoms in accordance with the defect-mediated theory of potential sputtering [7]. Sputtering by oxygen ions was found to significantly contribute to the alteration of the surface of Phobos [6]. These results provide new insights into space weathering and will help to understand the history of the airless bodies in the solar system.

References

[1] C. M. Pieters and S. K. Noble, *J. Geophys. Res.: Planets* 121 (2016) 1865
[2] Q. Nenon et al., *Nature Geoscience* 14 (2022) 61, & *J. Geophys. Res.: Planets* 124 (2019) 3385
[3] P. Wurz, et al., *Sp. Sci. Rev.* (2022) in press
[4] G. Hayderer et al *Rev. Sci. Instrum.* 70 (1999) 3696
[5] P. S. Szabo et al., *Astrophys. J.* 891 (2020) 100
[6] P. S. Szabo et al., *J. Geophys. Res.: Planets* 125 (2020) e2020JE006583
[7] M. Sporn et al., *Phys. Rev. Lett.* 79 (1997) 945

Helium-induced nano-structuring in an FeCoCrNiV high-entropy alloy

S. Lohmann[1,*], **R. Goodall**[2], **G. Hlawacek**[1], **R. Hübner**[1], **L. Ma**[2], **and A. S. Gandy**[2]

[1] *Institute of Ion Beam Physics and Materials Research, Helmholtz-Zentrum Dresden-Rossendorf, Germany*
[2] *Department of Materials Science and Engineering, University of Sheffield, United Kingdom*
[*] *s.lohmann@hzdr.de*

High-entropy alloys (HEAs) are a relatively new class of metal alloys composed of several principal elements, usually at (near) equiatomic ratios. It has previously been reported that some HEAs display superior radiation damage resistance, with composition and microstructure being cited as contributing factors, though the precise mechanism is still unknown. To study the influence of the crystal structure on the response to radiation, we have chosen FeCoCrNiV as a model system. While FeCoCrNi has a face-centred cubic (fcc) structure, adding V leads to a structural transformation towards a body-centred tetragonal (bct) structure with both phases present at near-stochiometric composition [1].

The as-cast sample was characterised by energy-dispersive X-ray spectroscopy (EDXS) and electron backscatter diffraction in a scanning electron microscope confirming the presence of both phases. Irradiations were performed with a focussed He beam provided by a helium ion microscope (HIM) at temperatures between $20\,^{\circ}\mathrm{C}$ and $500\,^{\circ}\mathrm{C}$. The fluence was varied between $6 \times 10^{17}\,\mathrm{ions/cm^2}$ and $1 \times 10^{20}\,\mathrm{ions/cm^2}$. High-resolution images of the irradiated areas were taken with the same HIM as shown in Fig. 1a. Selected irradiated areas were additionally studied by transmission electron microscopy (TEM) in combination with EDXS.

Under irradiation, pores start to be generated in the material with pore sizes differing significantly between the two phases. At higher fluences and above a critical temperature, a tendril structure as exemplary shown for the bct phase in Fig. 1a forms in both phases. TEM images reveal that these tendrils span the whole depth of the irradiated area (Fig. 1b) and are accompanied by bubbles of various sizes. Scanning TEM-based EDXS of these structures indicates a He-induced change in composition.

A.G. acknowledges support by the Royal Academy of Engineering and the Leverhulme Trust.

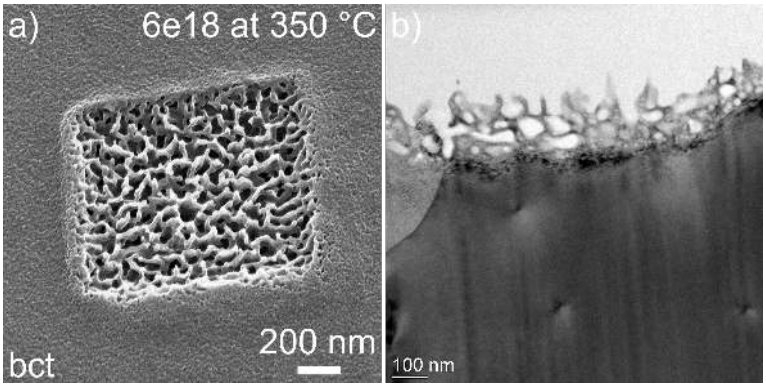

Figure 1: bct phase of FeCoCrNiV sample after irradiation by a focussed He beam. The He energy was $5\,\mathrm{keV}$ and the irradiation fluence $6 \times 10^{18}\,\mathrm{ions/cm^2}$ under normal incidence. The sample was kept at $350\,^{\circ}\mathrm{C}$ during irradiation. a) HIM image b) TEM cross section.

References

[1] Z. Leong et al., *Scientific Reports*, 7 (2017) 39803

Enhancement of vacancy diffusion by foreign interstitials in FeMnNiCoCr high-entropy alloy

E. Lu[1, *], **J. Zhao**[2], **I. Makkonen**[1], **K. Mizohata**[1], **Z. Li**[3, 4], **and F. Tuomisto**[1]

[1]*Department of Physics and Helsinki Institute of Physics, University of Helsinki, Finland*
[2]*Department of Electrical and Electronic Engineering, Southern University of Science and Technology, China*
[3]*School of Material Science and Engineering, Central South University, China*
[4]*Max-Planck-Institut für Eisenforschung, Max-Planck-Straße 1, 40237 Düsseldorf, Germany*
[*]*eryang.lu@helsinki.fi*

In recent decade, high entropy alloys have gained much research interest. They are promising candidate materials to replace the traditional engineering alloys in harsh environment due to their promising mechanical properties [1–3]. In this study, we present evidence of homogenization of atomic diffusion properties caused by C and N interstitials in an equiatomic single-phase high entropy alloy (FeMnNiCoCr). This phenomenon is manifested by an unexpected interstitial-induced reduction and narrowing of the migration barrier distribution of mono-vacancy defects introduced by particle irradiation. The experimental observation by positron annihilation spectroscopy is explained by state-of-the-art theoretical calculations that predict preferential localization of C/N interstitials in regions rich in Mn and Cr, leading to a narrowing and reduction of the mono-vacancy size distribution in the random alloy. This phenomenon is likely to have a significant impact on the mechanical behavior under irradiation, as the local variations in elemental motion have a profound effect on the solute strengthening in high entropy alloys.

References

[1] Z. Li, K. G. Pradeep, Y. Deng, D. Raabe, and C. C. Tasan, *Nature,* **534** (2016) 227
[2] B. Gludovatz, A. Hohenwarter, D. Catoor, E. H. Chang, E. P. George, and R. O. Ritchie, *Science,* **345** (2014) 1153.
[3] C. Lu, L. Niu, N. Chen, K. Jin, T. Yang, P. Xiu, Y. Zhang, F. Gao, H. Bei, S. Shi, M. R. He, I. M. Robertson, W. J. Weber, and L. Wang, *Nat. Commun,* **7** (2016) 1.

Highly rectifying tunable conical nanopores in amorphous SiO_2

A. Kiv[1,*], **S. Dutt**[1], **C. Notthoff**[2], **M.E. Toimil-Molares**[3], **and P. Kluth**[1]

[1]*Department of Materials Physics, Australian National University, Canberra ACT, Australia*
[2]*Department of Physics and Accelerator Applications, Australian National University, Canberra ACT, Australia*
[3]*GSI Helmholtzzentrum für Schwerionenforschung, Planckstr. 1, 64291 Darmstadt, Germany*
[*] *alexander.kiy@anu.edu.au*

When a highly energetic heavy ion passes through a target material, the damaged region left in its wake often exhibits preferential chemical etching over the undamaged material. This etch-anisotropy can be used to create pores with nanometer sizes and different shapes such as cylindrical or conical in a wide range of materials. Track etched nanopores have been used for a wide range of applications such as ultrafiltration, bio- and medical sensing, nanofluidic and nanoelectronic devices.

One of the major challenges in current nanopore technology is to combine the high throughput rates that nanopores in ultrathin membranes provide with the highly asymmetric transport properties characteristic of long, conical nanopores. Especially translating the performance of single pores to a multipore system has proven to be challenging.

We present a method for fabrication of conical nanopores in thin amorphous SiO_2 membranes using ion track etching. Our system features conical nanopores that exhibit opening angles far greater than those in track etched polymers, while being an order of magnitude thinner. The technique enables us to fabricate single pores or multiple pores with adjustable pore density over large areas.

The transport characteristics and surface properties were measured by using a KCl solution and monitoring the ionic current across the membrane. We find that at neutral pH the surface is negatively charged due to SiO^- radicals present at the pore surface. The geometrical asymmetry of conical pores combined with a strongly charged surface that can be tuned by adjusting the pH and electrolyte concentration causes a large ionic current rectification (ICR), *i.e.* the ratio of positive to negative current for a given voltage, of up to 10 as shown in Fig. 1. This indicates a very high selectivity towards cations (or anions in acidic environments). The surface charge and hence ICR changes in polarity when exposing the nanopores to acidic environments. This allows to create novel electroosmotic pumps or energy harvesting systems and is marking an important milestone towards the development of novel microfluidic diodes and separation membrane technologies.

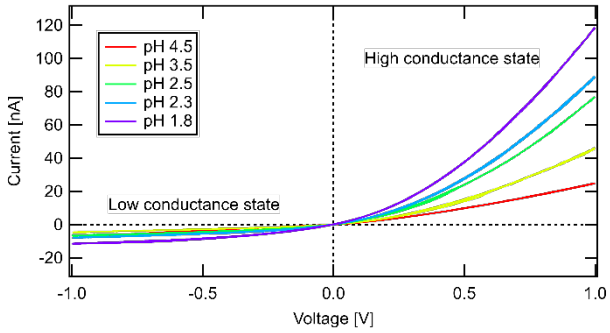

Figure 1: *I – V* curves for in 100 mM KCl for different pH values in acidic conditions.

High-Pressure Irradiation Platform at GSI

I. Tzifas[1*], K.O. Voss[1], M.E. Toimil-Molares[1], M. Lang[3], Ch. Schröck[1,2,4], C. Trautmann[1,2]

[1]*GSI Helmholtzzentrum für Schwerionenforschung, 64291 Darmstadt, Germany*
[2]*Materialwissenschaften, Technische Universität Darmstadt, 64287 Darmstadt, Germany*
[3]*University of Tennessee, Knoxville, Tennessee 37996, U.S.A.*
[4]*Institute of Geosciences, Goethe University Frankfurt 60438, Germany*
i.tzifas@gsi.de

Over the past few decades, high-pressure research has been advancing rapidly due to its great impact on fundamental physics, chemistry, condensed matter physics as well as Earth and materials sciences. It has been shown that the pressure itself can trigger the formation of novel phases and structures with fascinating properties. In this contribution, we present the high-pressure irradiation facility at GSI, where materials are simultaneously exposed to high static pressures and high energy heavy ion irradiation. Pioneering experiments at the SIS-18 accelerator at GSI revealed that the combination of pressure and ion irradiation can lead to the synthesis of new phases far from the thermodynamic equilibrium and to the possibility to recover a high-pressure phase upon pressure release [1,2].

The compression of a miniaturized sample (size *ca* 100 µm) is achieved by squeezing it between two opposite diamonds, while a metallic gasket (W, Re) with a drilled hole in its centre keeps the sample anchored. To prevent possible ion damage of the diamonds, the samples are irradiated through the gasket by using a remote controlled adjustable collimating system. Online analysis of beam-induced structural changes on the sample in the DAC is provided for the first time by means of Raman spectroscopy through the two diamond anvils. The aim of this development is to provide a high-pressure user platform in Cave A (GSI) with SIS-18 beams and at a later stage in the APPA Cave of the new FAIR facility. Coupling high pressures with ion irradiation and including at a later stage also high sample temperatures opens new possibilities for material science as well as for the simulation of radioactive decay events in planet's interiors.

References

[1] Lang, M., Zhang, F., Zhang, J., Wang, J., Schuster, B., Trautmann, C., Neumann, R., Becker, U., Ewing, R.C. Nanoscale manipulation of the properties of solids at high pressure with relativistic heavy ions. Nature. Materials 2009, p. 793-797 https://doi.org/10.1038/nmat2528.

[2] Lang, M., Zhang, F., Lian, J., Trautmann, C., Neumann, R. and Ewing, R.C. Combined high pressure and heavy-ion irradiation: a novel approach. Journal of Synchrotron Radiation, 2009, pp.773-777 https://doi.org/10.1107/S0909049509034384.

Atomic-scale analysis of the swift heavy ion-induced monoclinic-to-tetragonal phase transformation in zirconia

Alexandre P. Solomon[1,*], Eric C. O'Quinn[1], Gianguido Baldinozzi[2], Maria E. Toimil-Molares[3], and Maik K. Lang[1]

[1]*Department of Nuclear Engineering, University of Tennessee, Knoxville, TN, 37996, USA*

[2]*SPMS, CNRS CentraleSupélec, Université Paris-Saclay, 91190 Gif-sur-Yvette, France*

[3]*GSI Helmholtzzentrum für Schwerionenforschung, 64291 Darmstadt, Germany*

[*]*asolomo6@vols.utk.edu*

Monoclinic ZrO_2 was irradiated by 1.5 GeV Au ions using the UNILAC accelerator at the GSI Helmholtz Centre for Heavy Ion Research (Darmstadt, Germany), and the irradiated material was structurally characterized by high-resolution synchrotron X-ray and neutron total scattering experiments coupled with pair distribution function (PDF) analysis. The monoclinic-to-tetragonal phase transformation of swift heavy ion-irradiated ZrO_2 has been widely studied, yet details of how irradiation drives the transformation at the nanoscale remain unclear. Using PDF analysis, we have probed the local structure of ZrO_2 before and after irradiation to a fluence of 5×10^{12} and 1×10^{13} ions cm^{-2} and confirmed that the long-range structure is described best using the previously reported tetragonal high-temperature phase; however, the local atomic arrangement cannot be fully described by this structural model as it cannot explain the observed nearest neighbor bonds and coordination polyhedra. A metastable, orthorhombic high-temperature phase, distinct from the monoclinic and tetragonal phases, must be included in the refinement of the local structure after ion irradiation. This phase was predicted in the structural transformation pathway between the monoclinic and tetragonal polymorphs but never observed because of its inherent metastable character[1]. The orthorhombic phase, which quickly loses correlation beyond the nanoscale, is an essential ingredient to explain the structure of zirconia across the relevant range of length-scales. This study contributes to an improved understanding on the mechanisms of the ion beam-induced polymorphism in ZrO_2 and describes how orthorhombic structural building blocks organize across the mesoscale to yield the tetragonal long-range ZrO_2 structure. Interestingly, this structural heterogeneity has also been reported in complex oxides after swift heavy ion irradiation[2].

References

[1] D. Simeone, G. Baldinozzi, D. Gosset, M. Dutheil, A. Bulou, and T. Hansen. "Monoclinic to Tetragonal Semireconstructive Phase Transition of Zirconia." *Physical Review B* 67, no. 6 (Feb 2003): 8 064111.

[2] R. Sherrod, E. C. O'Quinn, I. M. Gussev, C. Overstreet, J. Neuefeind, and M. K. Lang. "Comparison of Short-Range Order in Irradiated Dysprosium Titanates." *Npj Materials Degradation* 5, no. 1 (Apr 2021): 7 19.

Moderation of SHI induced structure modification of $Y_4Al_2O_9$ nanoparticles by a surrounding ODS matrix

A. Ibrayeva[1,2,*], **J. O'Connell**[1], **A. Mutali** [2,3,4], **E. Korneeva**[4], **A. Sohatsky**[4], **and V. Skuratov**[4,5,6]

[1]*Center for High Resolution Transmission Electron Microscopy, Nelson Mandela University, South Africa*
[2]*Institute of Nuclear Physics, Kazakhstan*
[3]*L.N. Gumilyov Eurasian National University, Kazakhstan*
[4]*Flerov Laboratory of Nuclear Reactions, JINR, Russia*
[5]*National Research Nuclear University MEPhI, Russia*
[6]*Dubna State University, Russia*
[*]*a.d.ibrayeva@gmail.com*

$Y_4Al_2O_9$ (YAM) nanocrystalline ceramics is a key component of the Fe-15Cr-4Al-2W-0.35Y_2O_3 oxide dispersion strengthened (KP4 ODS) steel [1,2], a promising structural material for next generation fission power plants. Investigations on their radiation tolerance, particularly to swift heavy ion (SHI) impact have received increased interest recently [3,4]. SHI irradiation is known to stimulate the formation of specific defects called latent tracks. To date, no latent tracks and only partial amorphization have been found in YAM nanoparticles in the KP4 alloy, even after irradiation with 700 MeV Bi up to a fluence of 1.5×10^{13} cm^{-2} corresponding to the overlapping track regime [4]. On the contrary, the same energy ion bombardment has produced TEM visible tracks with a radius of 4.8±0.3 nm in isolated nanoparticles (without metal matrix) [5], and the threshold stopping power for formation of continuous tracks was estimated at much lower electronic stopping power ~8 keV/nm. These results suggest a crucial role of the metallic matrix in the formation of structural changes induced via high-energy ion irradiation in YAM nanocrystals. Additionally, full amorphization and associated critical fluence have not yet been reported.

In this work we present and discuss results of HRTEM examination of structural and morphological changes in YAM nanocrystals embedded into KP4 steel and in isolation after irradiation with Xe and Bi ions over a wide range of energy losses and fluences.

References

[1] L.L. Hsiung, M.J. Fluss, S.J. Tumey, B.W. Choi, Y. Serruys, F. Willaime, and A. Kimura, *Physical Review B*, 82 (2010) 184103.
[2] L. Hsiung, M. Fluss, S. Tumey, J. Kuntz, B. El-Dasher, M. Wall, B. Choi, A. Kimura, F. Willaime, and Y. Serruys, *Journal of Nuclear Materials,* 409 (2011) 72-79
[3] S.V .Rogozhkin, A.A Khomich, A.A. Bogachev, A.A. Nikitin, A.A. Lukyanchuk, O.A. Raznitsyn, A.S. Shutov, A.L. Vasiliev, and M.Y. Presniakov, *Physics of Atomic Nuclei,* 83 (2020) 1425-1433
[4] V.A. Skuratov, V.V. Uglov, J. O'Connell, A.S. Sohatsky, J.H. Neethling, and S.V. Rogozhkin, *Journal of Nuclear Materials,* 442 (2013) 449-457
[5] A. Ibrayeva, A. Mutali, J. O'Connell, A. Janse van Vuuren, E. Korneeva, A. Sohatsky, R. Rymazhanov, V. Skuratov, and I. Ivanov, *Nuclear Materials and Energy,* 30 (2022) 101106.

Surface nano- and micro-structuring with swift heavy ions in grazing incidence at high fluences

R. Rahali[1], **C. Grygiel**[1,*], **A. Benyagoub**[1], **I. Monnet**[1], **M. Sall**[1], **and H. Lebius**[1]

[1]*CIMAP (CEA, CNRS, ENSICAEN, UCN), University of Caen Normandy, France*
[*]*grygiel@ganil.fr*

Swift heavy ion (SHI) irradiation is one of the most used techniques for structural modifications of materials such as morphological changes, amorphization, or even surface nanostructuring. This technique plays a key role in enhancing material properties through the various created patterns, widening the range of exploitation in scientific and industrial fields [1, 2]

Usually, in a low fluence regime where the single impact dominates, different nano-structures can appear whose dimension and morphology depend on the irradiation parameters and the type of targets, and surface nanostructuring can thus be controlled [3, 4].

We present a first interesting measurement with $SrTiO_3$ single crystals, irradiated with SHI at grazing incidence in the high fluence regime where tracks are overlapping several times.

The results show a modification and a reorganization of the surface, with the formation of two types of structures of different scales. This transformation appears in the form of quasi-periodic patterns like waves at the micrometric scale bristling with smaller protrusions with size of the order of ten to a few hundred nanometers (see Figure), and whose characteristics depend on the irradiation parameters, such as incidence angle and ion beam fluence. Different characterization techniques, in particular XRD, AFM and TEM, are undertaken on these irradiated materials to highlight the original surface nanostructuring created under SHI at high fluence and all details will be discussed during the communication.

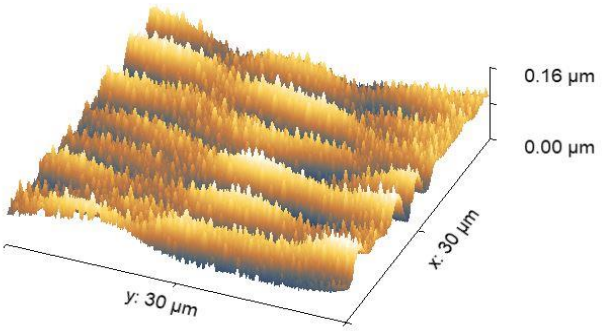

AFM image of $SrTiO_3$ (100) surface after SHI irradiation with 75 MeV Xe ions under $\theta = 3°$ and $\Phi = 5e13$ cm^{-2}

References

[1] N. Toyoda, B. Tilakaratne, I. Saleem, and W.-K. Chu, *Appl. Phys. Rev*, 6, 020901 (2019).
[2] F. Chen, J. *Appl. Phys*. 106, 081101 (2009).
[3] M.Karlušić, M. Mičetić, M. Kresić, *Applied Surface Science* 541 (2021): 148467
[4] S.Akcöltekin, E.Akcöltekin, T.Roll, *Nucl. Inst. Meth. Phys. Res. B* (2009) 267 (8–9), 1386–1389.

Surface nanostructures on Nb-doped $SrTiO_3$ irradiated with swift heavy ions at grazing incidence

N. Ishikawa[1,*], Y. Fujimura[1], K. Kondo[1], G.L. Szabo[2], R.A. Wilhelm[2], H. Ogawa[1], and T. Taguchi[3]

[1] *Japan Atomic Energy Agency (JAEA), Tokai, Japan*
[2] *TU Wien, Vienna, Austria*
[3] *National Institutes for Quantum Science and Technology (QST), Tokai, Japan*
[*] *ishikawa.norito@jaea.go.jp*

A single crystal of $SrTiO_3$ doped with 0.5 wt% niobium (Nb-STO) was irradiated with 200 MeV Au^{32+} ions at grazing incidence to characterize the irradiation-induced hillock chains. Exactly the same hillock chains are observed by using atomic force microscopy (AFM) and scanning electron microscopy (SEM) to study the relation between irradiation-induced change of surface topography and corresponding material property changes. As expected, multiple hillocks as high as 5-6 nm are imaged by AFM observation in tapping mode. It is also found that the regions in between the adjacent hillocks are not depressed, and in many cases they are slightly elevated.

Line-like contrasts along the ion paths are found in both AFM phase images and SEM images, indicating the formation of continuous ion tracks in addition to multiple hillocks. Validity of preexisting models for explaining the hillock chain formation is discussed based on the present results.

In order to obtain new insights related to the ion track formation, cross-sectional transmission electron microscopy (TEM) observation was performed. The ion tracks in the near-surface region are found to be relatively large, whereas buried ion tracks in the deeper region are relatively small. The results suggest that recrystallization plays an important role in the formation of small ion tracks in the deep region, whereas formation of large ion tracks in the near-surface region is likely due to the absence of recrystallization. TEM images also show shape deformation of ion tracks in the near-surface region, suggesting that material transport towards the surface is the reason for the absence of recrystallization.

References

[1] N. Ishikawa et al., Nanotechnology (2022). In press.

Electrochemical Conversion of Cu Nanowires synthesized by electrodeposition in track-etched templates to HKUST-1

J. Luo[1,2 *], **M. Wagner**[2], **N. Ulrich**[2,3], **P. Kopold**[4], **C. Trautmann**[2,3], **M.E. Toimil-Molares**[2]

[1] *School of Physical Science and Technology, Southwest Jiaotong University, Chengdu, China*
[2] *Materials Research Department, GSI Helmholtz Centre for Heavy Ion Research, Darmstadt, Germany*
[3] *Material Science, Technische Universität Darmstadt, Darmstadt, Germany*
[4] *Stuttgart Center for Electron Microscopy (StEM), MPI for Solid State Research, Stuttgart, Germany*
[*] *J.Luo@gsi.de*

Metal-organic frameworks (MOFs) are a novel type of nanoporous materials that have attracted widespread attention over the past two decades [1]. Cu-based metal-organic frameworks such as $Cu_3(BTC)_2$ (also known as HKUST-1) are one of the most famous MOF representatives, which exhibit a huge open porosity and thus a remarkably capacity to store and uptake different gases [2, 3]. Recently, increasing efforts are devoted toward finding synthetic routes that enable downsizing MOF crystals to the nanoscale. Achieving control over the size and shape of nanoMOFs and finding ways to assemble them is essential for their exploitation in integrated devices such as sensors, gas separation membranes or photoelectrodes.

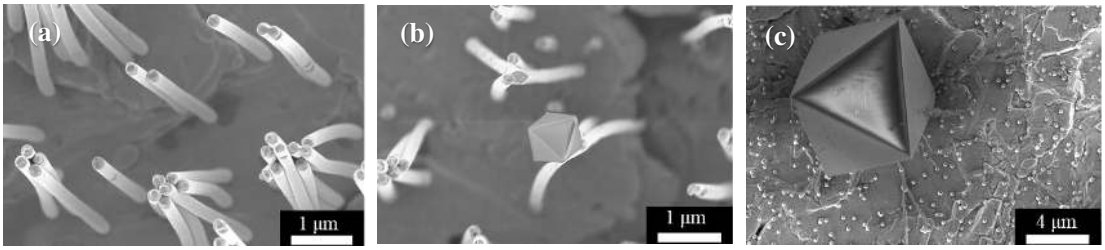

Figure 1: SEM images of cylindrical Cu nanowires (a) before and (b) during the electrochemical conversion process, and (c) of a representative octahedral particle after complete conversion to HKUST-1.

In this study we explore the conversion of free-standing arrays Cu nanowires with controlled diameter and length synthesized by electrodeposition in etched ion-track membranes into HKUST-1. In a first process step, free-standing Cu wires are produced by dissolving the ion-track polymer template. In a second step, the wires are converted into HKUST-1 structures by electrochemical oxidation. Applying 2.5 V versus a Cu counter electrode, the Cu nanowires are oxidatively dissolved and the MOF is built up as the as-formed Cu^{2+} ions bind to the BTC^{3-} ligands in the electrolyte solution. The morphology and crystallinity of the samples at different transformation stages is investigated by scanning electron microscopy (Fig. 1) and transmission electron microscopy, respectively. X-ray diffraction spectra measured at different conversion times reveal the appearance of the characteristic reflections of HKUST-1. These results will be compared with previous studies of the transformation of Cu nanowires to HKUST-1 nanowires inside the polymer membrane [4].

References

[1] Freund R, Canossa S, Cohen SM, Yan W, Deng et al. *Angewandte Chemie International Edition*. (2021) 2: 23946-23974
[2] Chui SS-Y, Lo SM-F, Charmant JP, Orpen AG, Williams ID. *Science.* (1999) 283:1148-50.
[3] Li H, Li L, Lin R-B, Zhou W, Zhang Z, Xiang S, et al. *EnergyChem*. (2019) 1:100006.
[4] Caddeo F, Vogt R, Weil D, Sigle W, Toimil-Molares ME, Maijenburg AW. *ACS applied materials & interfaces* . (2019)11:25378-87.

The structure and phase composition stability of amorphous Zr irradiated with He ions

A. AlNeyadi[1,2*], **S. Zlotski**[1], **N. Mora**[2], **and V.V. Uglov**[1]

[1] *Faculty of Physics, Belarusian State University, Minsk, Belarus.*
[2] *Directed Energy Research Center, Technology Innovation Institute, Abu Dhabi, UAE.*
[*] *Aysha.AlNeyadi@tii.ae*

Alloy structures characterization, production technology, and performance monitoring are considered essential requirements in developing nuclear energy. Amorphous alloys based on several metal components are very common materials for different industrial applications. They exhibit unique physical and mechanical properties that cannot be reached in materials with crystalline structures.

In this work, amorphous alloy samples based on Zr with different metals were irradiated using He ions at operating energy of 40 keV under room temperature conditions with two different fluences: 5 x 10^{17} and 7 x 10^{17} cm^{-2}. The phase analysis of the samples is conducted using an X-ray diffractometer (XRD). The XRD analysis revealed the formation of amorphous, crystalline, and amorphous-crystalline structures of Zr base foils. It was found that irradiation with He ions (1) does not lead to a change in the structure of the foils; (2) it leads to a shift in the diffraction peaks of crystalline phases to the region of smaller angles for all crystalline and crystalline amorphous foils; and (3) to a decrease in the angular position of the amorphous halo. Additionally, it was also found an increase (about 1.6%) in the lattice parameter of Zr in crystalline alloys at a fluence of 5 x 10^{17} cm^{-2} and a decrease after the second dose of 7 x 10^{17} cm^{-2} (around 1.6%). Finally, it was found that the free volume decreases with an increase in the amorphousness of the alloys [1].

References

[1] A. AlNeyadi, V. Uglov, S. Zlotski, N. Mora, and A. Bouchalkha, "The Structure and Phase Composition Stability of Amorphous Zirconium Irradiated with Helium Ions." 510-512, 2021. Available: http://vitt.bsu.by/publication_4_e.files/510.pdf. [Accessed 18 December 2021].

Surface and bulk modifications of 14 MeV Au ion-irradiated diamond

K. Bunk[1,*], I. Alencar[2], P. Bolz[3], W. Morgenroth[4], F. Bertram[5], C. Schmidt[6], C. Trautmann[3,7], and B. Winkler[1]

[1]*Institute of Geoscience, University of Frankfurt, Germany*
[2]*Department of Physics, Federal University of Santa Catarina, Brazil*
[3]*GSI Helmholtz Centre for Heavy Ion Research, Germany*
[4]*Department of Geosciences, University of Potsdam, Germany*
[5]*Deutsches Elektronen-Synchrotron DESY, Germany*
[6]*GFZ German Research Center for Geosciences, Germany*
[7]*Institute of Materials Science, Technical University of Darmstadt, Germany*
[*]*bunk@kristall.uni-frankfurt.de*

Diamond is known for its outstanding physical and optical properties, as well as its radiation hardness [1]. It is used in many applications in science and technology, e.g. as a sensor material in radiation detectors [2]. Hence, changes of morphology, structure, and physical properties of diamond due to irradiation are of great interest.

Ion irradiation was carried out with $14\,\mathrm{MeV}\ \mathrm{Au}^{6+}$ ions (penetration depth of $1.7\,\mu\mathrm{m}$) and a maximal fluence of $2.4 \times 10^{15}\ \mathrm{ions/cm}^2$ on various synthetic diamond samples [3]. The surface of the samples was characterized by atomic force microscopy, which provided information of topography changes, including increased roughness and swelling. X-ray reflectivity experiments revealed the formation of modified layers on the samples surfaces (Fig. 1 a). Structural changes were investigated with Raman spectroscopy which showed significant changes in the lattice dynamics and the formation of sp^3 bonded amorphous carbon (Fig. 1 b). The change of hardness was obtained from nanoindentation as a function of irradiation fluence and was found to linearly decrease with the fluence. The electrical resistivity of the irradiated diamonds exponentially decreases with increasing fluence. The effect is ascribed to density changes as calculated from swelling measurements. A correlation of hardness and density decrease is observed which is caused by the amorphization of diamond during irradiation.

A comprehensive picture of radiation-induced changes on the diamond surfaces and the bulk material due to Au ion irradiation is provided.

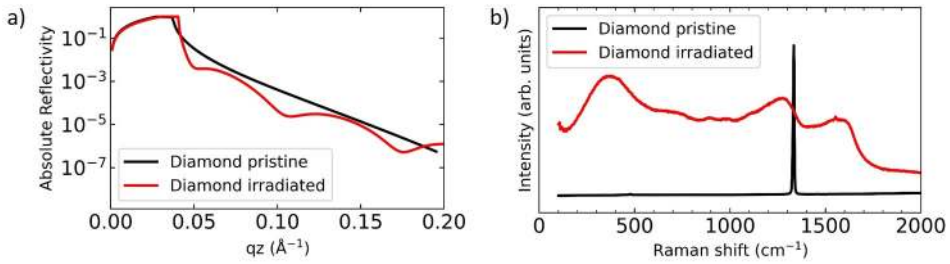

Figure 1: (a) X-ray reflectivity as a function of momentum transfer q_z and (b) Raman spectra for pristine and irradiated diamond.

References

[1] B. Campbell et al., *Nuclear Instruments and Methods in Physics Research Section A: Accelerators, Spectrometers, Detectors and Associated Equipment*, 476 (2002) 680-685
[2] R. Tapper, *Reports on progress in Physics*, 63 (2009) 1273
[3] K. Bunk et al., *Journal of Applied Physics*, 130 (2021) 105303

Fast and accurate machine-learned interatomic potentials for high-entropy alloys

J. Byggmästar[1,2,*], **K. Nordlund**[1], **and F. Djurabekova**[1]

[1] *Department of Physics , University of Helsinki, Finland*
[2] *FCAI: Finnish Center for Artificial Intelligence*
[*] *jesper.byggmastar@helsinki.fi*

Refractory high-entropy alloys have shown promising tolerance to irradiation, yet little is still known about the atom-level changes and damage caused by irradiation. For molecular dynamics simulations, developing data-driven machine-learned interatomic potentials for high-entropy alloys is challenging due to the vast configuration space that needs to be sampled by the fitting data. We show that simple potentials based on low-body descriptors for the local atomic environments can achieve remarkable accuracy for Mo–Nb–Ta–V–W alloys. The potentials are based on the Gaussian approximation potential framework (GAP) and subsequently tabulated and evaluated using cubic splines (tabGAP), yielding a speedup of two orders of magnitude. The potential contains accurate repulsive parts that makes it applicable to radiation damage simulations of Mo–Nb–Ta–V–W alloys. We discuss the potential development and simulate properties of radiation-induced defects in the equiatomic MoNbTaVW high-entropy alloy. Simulations reveal that MoNbTaVW shows a strong tendency for segregation around radiation-induced defects, which is mainly driven by the size difference of the atoms [1]. Interstitial configurations are most stable when containing the smallest atom, V. V also shows strong preferential segregation to compressed environments in the lattice such as interstitial dislocation loops. In contrast, the inner surface of voids are preferentially decorated by Nb, as it is the largest atom and because pure Nb has the lowest surface energy.

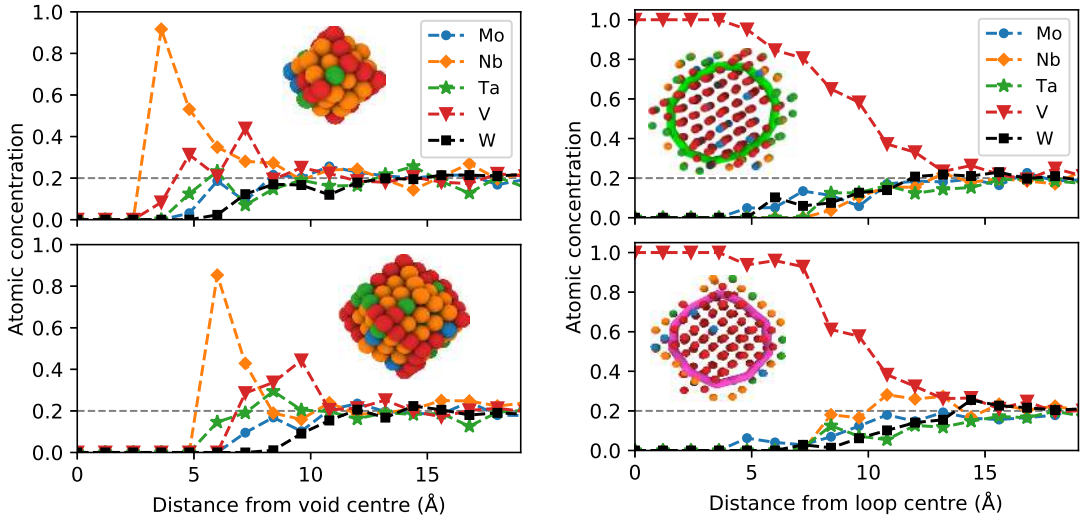

Figure 1: Segregation of (a) Nb to voids and (b) V to interstitial dislocation loops.

References

[1] J. Byggmästar, K. Nordlund, F. Djurabekova, *Phys. Rev. B* 104 (2021) 104101

Modulating properties of solid carbon nanospheres via ion implantation with heteroatoms

B.J. Matsoso[1], D. Wamwangi[2], R.M. Erasmus[2], N.J. Coville[1] and T.E. Derry[2]*

[1]*DSI-NRF Centre of Excellence in Strong Materials and Molecular Sciences Institute, School of Chemistry, University of the Witwatersrand, South Africa*
[2]*DSI-NRF Centre of Excellence in Strong Materials and Materials Physics Research Institute, School of Physics, University of the Witwatersrand, South Africa*
**Trevor.Derry@wits.ac.za*

Solid carbon nanospheres of about 200 nm diameter have been prepared and then doped by ion implantation, using a specialized end-station adapted for the uniform implantation of powders. Boron, nitrogen and neon ions were chosen initially, the latter for control purposes. Herein, the dependence of the physicochemical properties of solid carbon spheres on the fluence of the implanted ions was investigated by controlling the dosage of the 100 keV B^+, N^+ and Ne^+ ions into the carbon shell over 7h and 14h implantation periods at room temperature. SEM analysis revealed significant surface deformation in the form of cracks for the N^+ implanted samples, whilst little structural deformation was observed with Ne^+ and B^+ implanted samples. On the other hand, TEM micrographs showed formation of varying thicknesses of the amorphous carbon depending on the implantation period. In particular, both N^+ and Ne^+ implanted samples exhibited thicker amorphous layers of ~21 ± 2 nm and ~12 ± 3 nm, respectively, whilst a reduction to ~12 ± 2 nm was observed after the 14h implantation period with B^+ ions. Raman spectroscopy indicated significant structural changes upon implantation, as evident by large values for the defect density ratios. Moreover, compromised BET surface area was observed for B^+ and N^+ implanted samples, whereas an improved thermal stability was recorded for both Ne^+ and B^+ implanted samples. Finally, electrical measurements were carried out. The study showed the importance of the choice of the heteroatom ion on the properties of the solid carbon spheres for the development of next generation carbon-based electronic devices.

Bond-specific fragmentation of oligopeptides via electronic stopping of swift heavy ions in molecular films

P. Schneider[1], P. Keller[1], I. Schubert[2], M. Bender[2,3], C. Trautmann[2,4], and M. Dürr[1,*]

[1]*Institut für Angewandte Physik, and Zentrum für Materialforschung, Justus-Liebig-Universität Giessen, Germany*
[2]*GSI Helmholtzzentrum für Schwerionenforschung, Germany*
[3]*Fachbereich Ingenieurwissenschaften, Hochschule RheinMain, Germany*
[4]*Fachbereich Materialwissenschaften, Technische Universität Darmstadt, Germany*
[*]*michael.duerr@ap.physik.uni-giessen.de*

Fragmentation of oligopeptides induced by single swift heavy ions (SHI) was investigated by means of soft cluster-induced desorption/ionization mass spectrometry (Figs. 1(a,b)) [1,2]. Mass spectra of SHI-irradiated samples show a high abundance of specific fragments, i.e., cleavage took place at the peptide bonds of the peptide backbone (Fig. 1(c)). This is in clear contrast to previous experiments with keV ions, for which the majority of fragments was observed to be non-specific [3]. It indicates that the fragmentation process is largely influenced by the respective energy loss mechanism, i.e., nuclear stopping in the case of keV ions versus electronic stopping in the case of SHI. keV ions interact directly with the nuclear subsystem, which implies a stronger local correlation between the interaction site and the breaking bond, thus leading to non-specific fragments. In the case of electronic stopping, first the electronic subsystem is excited on the (sub-)femtosecond timescale, followed by spreading of the energy through the electronic subsystem and excitation of the nuclear subsystem via electron-phonon coupling (Fig. 1(c)). As a consequence, excitation of the nuclear subsystem is more evenly distributed over the whole molecule, leading to preferential breaking of weaker bonds, i.e., specific fragmentation of the peptide backbone. However, the amount of different fragment species observed, as well as the sensitivity of the intact molecules to the SHI irradiation, are strongly dependent on the oligopeptide investigated, thus suggesting an influence of the details of the electronic subsystem on the ion-molecule interaction and on the excitation of the nuclear subsystem via electron-phonon coupling.

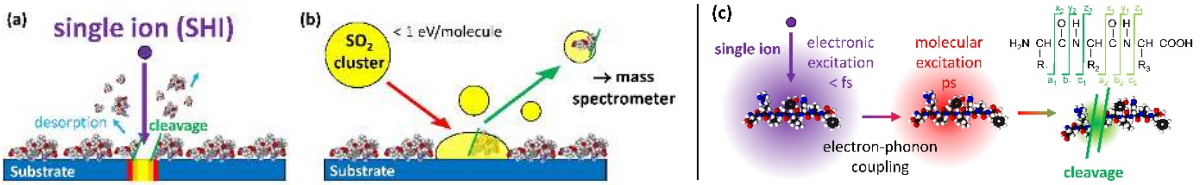

Figure 1: (a) and (b): sketch of the experimental procedure. (a) Single ion impacts lead to fragmentation and desorption of some of the peptide molecules on the sample. (b) The fragments are analyzed by means of SO_2 cluster-induced desorption/ionization which does not induce further fragmentation thus directly revealing the molecular fragments formed in the sample during SHI irradiation. From these fragments, the relevant excitation and cleavage processes as shown in (c) can be deduced.

References

[1] C. R. Gebhardt, A. Tomsic, H. Schröder, M. Dürr, and K.-L. Kompa, Ang. Chem. Int. Ed. 48, 4162 (2009).
[2] M. Baur, C. R. Gebhardt, and M. Dürr, Rapid Commun. Mass Spectrom. 28, 290 (2014).
[3] P. Schneider, F. Verloh, A. Portz, S. Aoyagi, M. Rohnke, and M. Dürr, Anal. Chem. 92, 15604 (2020).

Simulation and characterization of hot spots generated in plasmas by fast quasi-monoenergetic ion beams

J.M. Gil [1,*], P.R. Beltrán[1,2], R. Rodriguez[1], and G. Espinosa[1]

[1] *Department of Physics, University of Las Palmas de Gran Canaria, Las Palmas de G.C. 35017, Spain*
[2] *Instituto de Astrofísica de Canarias (IAC), E-38200 La Laguna, Tenerife, Spain*
* *juanmiguel.gil@ulpgc.es*

Fast ignition (FI) scheme was proposed 25 years ago as an alternative to the standard central ignition of inertial fusion targets [1]. FI scheme intends to reduce the drive requirements by separating target compression and ignition. Due to the large divergences and the high energies found in electron-driven fast ignition (EFI) experiments and simulations [2], ion-driven fast ignition (IFI) has been taking an increasing interest. IFI scheme offers several advantages, such as generation of collimated beams, well known interaction with the plasma or localized energy deposition on compressed deuterium-tritium (DT) plasma. On the other hand, the potential of monoenergetic, Maxwellian and Gaussian ion beams has been extensively investigated, as for example, the optimal energies and radius of proton, lithium, carbon, aluminium and vanadium beams [3,4,5].

In this work we present a numerical model for the calculation of the temperature field reached by a compressed DT target plasma due to its interaction with fast quasi-monoenergetic ion beams. From simulations performed on a wide range of vanadium ion beam parameter values such as mean energy, spread energy or radius, an analysis of the main parameters of the generated hot spot is carried out. We focus the analysis on the maximum temperature, average temperature and range or length reached by the hot spot as well as its self-heating and ignition conditions or its burn efficiency. In our problem, the compressed DT fuel has spherical geometry with homogeneous temperature and density distribution $\rho(r) = \rho_m Exp(\text{-}\alpha(r/R)^4)$, where $\alpha = log2$, r is the distance to center, ρ_m is the maximum density (300, 500 or 1000 g/cm^3) and R is the dense core radius (40 μm). We assume perfectly collimated cylindrical ion beam with constant flux (within its cross section) impinging on radial direction of a spherical plasma. Therefore, due to the symmetry, the interaction beam-target can be described as one-dimensional. On the other hand, it is assumed that the characteristic time of the interaction is considerably shorter than the characteristic hydrodynamic time and the plasma heating can be considered as isochoric. Therefore, the change in the plasma temperature depends only on the energy deposited by the beam projectiles, since the mechanical work and conduction can be neglected.

This work has been supported by the Spanish Government through the Project PID2019-110678-I00 and by the Consejería de Economía, Industria, Comercio y Conocimiento del Gobierno de Canarias.

References

[1] M. Tabak et. Al., Phys. Plasmas **1**, 1626 (1994).
[2] A.P.L. Robinson et. Al., Nucl. Fusion **54**, 054003 (2014).
[3] P.R. Beltrán et al., *X-Ray Spectrom.,* **49** (2020)
[4] J. Fernández et. al., Nucl. Fusion **54**, 054006 (2014).
[5] J.J. Honrubia and M. Murakami, Physics of Plasmas **22**, 012703 (2015)

Sputtering of highly corrugated and oriented surfaces

M. Fellinger[1*], C. Cupak[1], H. Biber[1], J. Brötzner[1], A. Lopez-Cazalilla[2], R. Gonzalez-Arrabal[3], and F. Aumayr[1]

[1] *Institute of Applied Physics, TU Wien, 1040 Vienna, Austria*
[2] *Department of Physics, University of Helsinki, 00014 Helsinki, Finland*
[3] *Instituto de Fusión Nuclear, Universidad Politécnica de Madrid, 28006 Madrid, Spain*
[*] *fellinger@iap.tuwien.ac.at*

Dependencies of the sputter yield on ion kinetic energy, incidence angle and mass ratio between target and ion species are already well described by existing theoretical models [1] or numerical simulation codes, often based on the Binary Collision Approximation (BCA) [2]. However, surface roughness remains a challenging property for sputter yield calculation. Although modern 3D versions of BCA codes are able to handle rough surface input already, the usage of large-scale topographies larger than several 100x100nm² is often too demanding for accessible computational infrastructure.

Recently, we were able to develop a new raytracing code called SPRAY [3], which is capable of quickly simulating sputter yields for rough topographies (as e.g. derived from atomic force microscopy - AFM or from computer-generated structures) independent of size. Using a precise quartz crystal microbalance (QCM) technique in combination with a low-flux ion source, we could benchmark SPRAY with experimental sputtering data. W samples with a wide spread in roughness were irradiated with 2 keV Ar^+ bombardment. On this basis, we could show that the mean inclination angle δ_m is a much more reliable parameter than, e.g., the root mean square roughness (RMS) for sputter yield predictions [3].

In this work, we extend our studies from isotropically rough surfaces with Gaussian distributed height values towards more corrugated and oriented structures. For this purpose, a dense assembly of tungsten nanocolumns with about 500nm height and 50nm diameter was deposited by oblique-angle magnetron sputtering on our quartz sample surfaces, so that direct investigations with our QCM experiment under Ar^+ bombardment were possible. In parallel, AFM images were used as input for SPRAY simulations of these complex nanostructured surfaces. Additionally, computer-generated structures, which mimic the surface of our sample found in SEM images, were used as input. As an important first result we notice from our experiments that our nanocolumnar W surfaces not only show a significantly reduced sputter yield in comparison to a flat W surface, but that the yield is also nearly independent of the ion's incidence angle. The SPRAY simulation results also compare well to the experimental data and to recent molecular dynamics simulations (using PARCAS [4]) of the nanostructured surface.

References

[1] P. Sigmund, *Phys. Rev. Lett.*, 184 (1969) 383-416
[2] H. Hofsäss et al., *Appl. Surf. Sci.* 310 (2014) 134-141
[3] C. Cupak et al., *Appl. Surf. Sci.* 570 (2021) 151204
[4] K. Nordlund, *Comp. Mat. Sci.* 3, 448-456 (1995)

An atomistic simulation for the study of Nb-coated SRF cavities by HiPIMS method

M.Ghaemi[1], **A.L.Cazalilla**[1,*], **and F. Djurabekova**[1,*]

[1]*Department of Physics, University of Helsinki, P.O. Box 43, FIN-00014, Finland*
[*]*alvaro.lopezcazalilla@helsinki.fi, flyura.djurabekova@helsinki.fi*

The Nb/Cu combination has shown high performance for superconducting radio-frequency (SFR) elliptical cavities. However, the proper deposition of Nb on Cu is crucial to obtain a good performance. In recent years, miscellaneous processes have been utilized to deposit Nb thin layers over Cu. Among a number of techniques, high power impulse magnetron sputtering (HiPIMS) has significantly attracted attention, since it provides a smooth surface and high density of deposited films [1]–[4]. Herein, molecular dynamics (MD) simulations were performed to investigate the properties of Nb deposition on Cu, mimicking HiPIMS conditions with/without Ar. Introducing Nb with different energies, i.e., 50, 75, 85, and 100eV, at different deposition angles, i.e., 0°, 45°, and 75°, we investigated the growth of Nb films on the copper substrate with different geometries (flat and step-like structure) and crystallographic orientations, i.e., (100), (110), and (111). Additionally, these series of simulations were conducted under different substrate temperatures. Then, the thin-film structure, microhardness, and difference of angle between Cu [100] and Nb [110] were studied. Our results show that with the increase of temperature, the order in the Nb surface improves. It is also found that on Cu (100) and Cu (111), the Nb accumulates forming grains with different orientations and, on the other hand, on Cu (110), Nb is deposited creating almost a single crystal. Moreover, in the normal-to-substrate deposition, no void formation was observed. Nevertheless, at grazing deposition on the step-like structure, some voids appeared in the bottom corner of the MD cell, especially when the height of the step-like structures is sufficiently high.

References

[1] M. Arzeo *et al.*, "Enhanced radio-frequency performance of niobium films on copper substrates deposited by high power impulse magnetron sputtering," *Supercond. Sci. Technol.*, 2022.

[2] G. Rosaz, A. Bartkowska, C. P. Carlos, T. Richard, and M. Taborelli, "Niobium thin film thickness profile tailoring on complex shape substrates using unbalanced biased High Power Impulse Magnetron Sputtering," *Surf. Coat. Technol.*, p. 128306, 2022.

[3] M. Kateb, J. T. Gudmundsson, P. Brault, A. Manolescu, and S. Ingvarsson, "On the role of ion potential energy in low energy HiPIMS deposition: An atomistic simulation," *Surf. Coat. Technol.*, vol. 426, p. 127726, 2021.

[4] E. Uhlmann, D. Hinzmann, K. Kropidlowksi, P. Meier, L. Prasol, and M. Woydt, "Substitution of commercially coated tungsten carbide tools in dry cylindrical turning process by HiPIMS coated niobium carbide cutting inserts," *Surf. Coat. Technol.*, vol. 354, pp. 112–118, 2018.

Measurement of oxygen charge state distribution from injected BeO^- molecules for Be AMS

B. C. Gonsalves, K. Mizohata, K. Helariutta, P. O. Tikkanen, F. Tuomisto, and J. A. Räisänen

Department of Physics, University of Helsinki, Finland

basil.gonsalves@helsinki.fi

There is an interest in our laboratory to measure ^{10}Be due to a time scale wider than the limit of radiocarbon dating for geological applications. The most suitable way to measure ^{10}Be is via AMS. ^{10}Be samples are typically prepared from fluoride (BeF) or oxide (BeO). However, low BeF^- currents mean that it is preferable to prepare BeO samples for Be accelerator mass spectrometry (AMS) analysis. The procedure to prepare BeO samples is well known and practical for routine analysis. At Helsinki Accelerator Mass Spectrometry facility (HAMS), BeO samples are put into a Source of Negative Ions by Cesium Sputtering ion-source (SNICS), resulting in BeO negative ions being injected into our accelerator. These are mass selected at the injector magnet and broken down into their constituent elements in the stripper canal. These subsequently pass through an analysing magnet where only ions of a set energy can pass through. These ions then proceed to the AMS end station. Ions are then detected by a particle detector or a Faraday cup.

Following on previous work on the measurement of Be charge state distribution [1], in this work we measure charge state distribution of positive oxygen ions (q = +1, ..., +8) in Ar and SF_6 stripping gases. This is useful for Be AMS facilities as knowledge of O charge state yields is useful in Be AMS e.g. measurement of $^{17}O^{+5}$ yield is used to determine $\frac{^{10}\mathrm{Be}}{^{9}\mathrm{Be}}$ ratio [2]. An understanding at a molecular level of the break up of BeO^- is interesting in its own right and has applications in different fields. Similar studies have been done for molecular ions in radiocarbon AMS, but not so far for beryllium AMS. Finally, comparisons against theoretical predictions and literature values are presented.

References

[1] Gonsalves, B. C., Mizohata, K., Tikkanen, P. O., Räisänen, J. A. (2020), *Nuclear Instruments and Methods in Physics Research Section B: Beam Interactions with Materials and Atoms*, 469 (2020) 33-36

[2] Tuniz, C., Kutschera, W., Fink, D., Herzog, G. F., Bird, J. R., *Accelerator mass spectrometry: ultrasensitive analysis for global science*, 1998

Bunching effects for the electronic straggling of H and He in the matter

F.F. Selau[1], A. Molling[1], H. Trombini[1,2], R.C. Fadanelli[1], M. Vos[3] and P.L. Grande[1,*]

[1]*Ion Implantation Laboratory, Instituto de Física, Universidade Federal do Rio Grande do Sul (UFRGS), Brazil*
[2]*Medical Physics Laboratory, Universidade Federal de Ciências da Saúde de Porto Alegre Brazil*
[3]*Electronic Materials Engineering, Research School of Physics, Australian National University, Australia*
[*]*grande@if.ufrgs.br*

The energy-loss straggling is an important quantity, which describes the energy loss fluctuations of ions traversing the matter [1,2]. Typically, the variance σ^2 and the mean energy-loss $\langle\Delta E\rangle$ are proportional to the ion path length and therefore the effect of energy-loss fluctuations $\sigma/\langle\Delta E\rangle$ is more important for short traveled distances and low-medium projectile energies.

We have investigated, in this work, the energy-loss straggling of low and medium energy H and He on available simple materials and demonstrate the well-known Yang-O'Connor-Wang [3] empirical formula for the energy-loss straggling of protons in the matter has a clear physical interpretation. This formula predicts, on empirical grounds, energy-loss straggling values that exceed the values of traditional straggling formulas (e.g., by Lindhard and Chu) at energies around 0.3 MeV/amu by a factor of 2–3. This excess is correlated to the bunching effect [4-6], which comes from the inhomogeneity feature of the electron density.

We show that the well-known Yang-O'Connor-Wang straggling formula has captured bunching effects from the experimental data in an empirical way [7]. This formula was further refined in this work to consider the subsequent experimental data. The bunching effect and the straggling excess are like each other and are highly correlated for both solid and gas targets. The influence of packing effects was also investigated for amorphous and polycrystalline solids.

References

[1] P. Sigmund, *Particle Penetration and Radiation Effects*, Vol. 1, Springer-Verlag, Berlin Heidelberg, Heidelberg (2006).
[2] P. Sigmund, *Particle Penetration and Radiation Effects*, Vol. 2, Springer, Berlin (2014).
[3] Q. Yang, D. O'Connor, Z. Wang. *Nucl. Instr. Meth. B* 61 (2) (1991) 149–155.
[4] F. Besenbacher, J.U. Andersen, E. Bonderup. *Nucl. Instrum. Methods* 168 (1–3) (1980) 1–15.
[5] P. Sigmund, A. Schinner. *Eur. Phys. J. D* 58 (1) (2010)
[6] F.F. Selau, H. Trombini, G.G. Marmitt, A.M.H. de Andrade, J. Morais, P.L. Grande, I. Alencar, M. Vos, R. Heller. *Phys. Rev. A* 102 (3) (2020), 032812.
[7] F.F. Selau, H. Trombini, R.C. Fadanelli, M. Vos, and P.L. Grande. *Nucl. Instr. Meth. B* 497 (2021) 70-77.

Neutron total scattering analysis of radiation effects in weberite-type oxides

Igor M. Gussev[1*], Eric C. O'Quinn[1], Gianguido Baldinozzi[2], ChristinaTrautmann[3], Jörg Neuefeind[4], Changyong Park[5] and Maik Lang[1]

1 Department of Nuclear Engineering, University of Tennessee, Knoxville, TN, USA

2 Laboratoire Structures, Propriétés et Modélisation des Solides, CNRS, CentraleSupélec, Université Paris-Saclay, 91190 Gif-sur-Yvette, France

3 GSI Helmholtzzentrum für Schwerionenforschung and Technische Universität Darmstadt, Darmstadt, Germany

4 Neutron Sciences Directorate, Oak Ridge National Laboratory, Oak Ridge, TN, USA

5 HPCAT, X-ray Science Division, Argonne National Laboratory, Argonne, IL, USA

* *igussev@vols.utk.edu*

Progress in advanced fuel and wasteform materials requires unprecedented control of the design and organization of systems at the micro-, meso-, and nanoscale. These materials must maintain structural stability in harsh working conditions, such as intense radiation fields and extreme heat fluxes. In recent years, weberite-type oxides, with general formula A_3BO_7 (where A is a trivalent rare earth element and B is a pentavalent cation, such as Ta, Nb), have sparked interest for a number of technological applications due to their chemical and structural flexibility, which leads to a broad spectrum of physical properties, such as high ionic conductivity, ferroelectricity, and photocatalytic activity. In addition, weberite-type oxides have recently been linked to pyrochlore oxides ($A_2B_2O_7$) as atomic building blocks that form after exposure to swift heavy ions. Here, we present the comprehensive ion irradiation study on weberite-type tantalate oxides (A_3TaO_7, A = Pr, Tb, Dy, Y, Yb), covering three major structural families with various degrees of order/disorder level. Irradiation experiments were performed using 1.6 GeV Au ions at the X0 beamline of the GSI Helmholtz Center (Darmstadt, Germany). Samples were analyzed using neutron total scattering technique at the Nanoscale Ordered Materials Diffractometer (NOMAD) at Oak Ridge National Laboratory and X-ray diffraction technique at the Advanced Photon Source (APS) at Argonne National Laboratory, respectively. The data shows a clear trend between the amorphization resistance of the material and the ionic radius of the A-site cation, with smaller cations being more radiation-resistant (i.e. less observed amorphization). Neutron pair distribution function (PDF) analysis revealed that the local atomic arrangement in these materials, and in particular the level of pre-existing order/disorder, plays a critical role in structural response with the ordered, orthorhombic Pr_3TaO_7 (*Cmcm*) being much more susceptible to ion-beam induced amorphization than Tb_3TaO_7 (*Ccmm*). Disordered, cubic Yb_3TaO_7 (*Fm-3m*) shows the highest degree of structural stability and irradiation triggers, besides minor amorphization, a transformation to a different cubic structure, which has been previously reported for swift heavy ion irradiated sesquioxides (A_2O_3).

Sequential ion irradiation of GaN studied by MD simulations

J. Hanžek[1], **A. Leino**[2], **H. Vazquez**[2], **M. Karlušić**[1], **F. Djurabekova**[2]

[1]*Ruđer Bošković Institute, Bijenička 54, 10000 Zagreb, Croatia*
[2]*University of Helsinki, Pietari Kalmink katu 2, 00560 Helsinki, Finland*
[*]*marko.karlusic@irb.hr*

By means of sequential ion irradiations, response of damaged gallium nitride to swift heavy ion irradiation can be investigated. In this contribution, we present results of molecular dynamics simulations that help us understand results obtained in ion irradiation experiments on GaN. First, we present results of MD simulations when defects are introduced in GaN via nuclear stopping. In this case, we find damaged GaN to be more sensitive to ion track formation than pristine GaN. Next, we present results of MD simulations when ion tracks are produced by very high ion energy irradiation of GaN. In this case, subsequent swift heavy ion irradiation can induce partial recovery of the ion track produced by previous ion impact.

Effect of helium (He) and silver (Ag) co-implanted into SiC: structural evolution and migration behaviour

T.T. Hlatshwayo[1], S. Mtsi[1], C.E. Maepa[1], M. Msimanga[2], V.A. Skuratov[3] and T. Mokgadi[1]

[1]*University of Pretoria, Department of Physics, South Africa*
[2]*Tshwane University of Technology, Physics Department, South Africa*
[3]*Joint Institute for Nuclear Research, Dubna, Russia*
[*]*thulani.hlatshwayo@up.ac.za*

The effect of He in the migration behaviour of radiological important fission products (FPs) in SiC is crucial for improving safety of generation IV nuclear reactors, where fission products co-exist in the presence of He. In this study, the structural evolution of SiC co-implanted with He and Ag ions and the migration behaviour of the implants were investigated. Ag ions of 360 keV were individually implanted into polycrystalline SiC to a fluence of 2×10^{16} cm^{-2} at room temperature (RT) and 350 ^{o}C. Some of the implanted SiC were then implanted separately with He ions of 17 keV to a fluence of 1×10^{17} cm^{-2} also at RT and 350 ^{o}C. The implanted samples were annealed at 1100 ^{o}C for 5 hours. Both implanted and annealed samples were characterized by transmission electron microscopy (TEM), Raman spectroscopy and heavy ion elastic recoil detection analysis (ERDA). Ag implantation at RT resulted in the formation of amorphous SiC layer while co-implantation of He in the formation of He nano-bubbles in the amorphous layer. Ag implantation retained some defects in SiC without amorphization and co-implantation of He resulted in the formation of bigger bubbles and cavities. No migration of Ag was observed in both Ag implanted SiC annealed at 1100 ^{o}C. Migration of Ag governed by trapping in cavities was observed in the as co-implanted and annealed co-implanted samples. Hence, He does play a role in the migration behaviour if implanted Ag.

Trajectory dependent charge state distribution for keV ions transmitted through crystalline materials

R. Holeňák[1*], E. Ntemou[1], S. Lohmann[1,2], and D. Primetzhofer[1]

[1]*Department of Physics and Astronomy, Uppsala University, 751 20 Uppsala, Sweden*
[2]*Institute of Ion Beam Physics and Materials Research, Helmholtz-Zentrum Dresden-Rossendorf e.V. (HZDR), 01328 Dresden, Germany*
[*]*radek.holenak@physics.uu.se*

Studying energy deposition of keV projectiles in solid matter permits to further advance our understanding of fundamental aspects of electronic excitations in matter. The velocity of the projectiles being comparable to the one of electrons in the target valence and conduction bands renders the interactions highly dynamic and above all trajectory dependent [1]. Several charge exchange processes including Auger neutralization and collision-induced reionization lead to an oscillatory alternation of the projectile charge and together with creation of molecular orbitals directly affect the specific energy loss. Ion transmission through self-supporting single-crystalline targets was shown to be an excellent model system to study the trajectory dependence of the interactions due to the geometrical simplicity of the experimental set-up. In combination with the crystallinity of the target, it allows an exclusive choice of projectile trajectories and interaction distances, thus switching on and off the processes mentioned above. The transmission experiments, in particular those in channelling geometry, moreover serve as a benchmark for Time Dependent-Density Functional Theory (TD-DFT) calculations that currently provide the closest theoretical description of the keV ion-solid interaction [2].

While distinct differences in the specific energy loss between different trajectories in the crystal were already reported, we have recently implemented a time-of-flight approach for the detection of transmitted projectiles discriminated based on their exiting charge states [3]. In this contribution, we present evidence for a dependence of charge state distributions of the projectiles emerging from different crystal directions. Experiments were performed by simultaneous detection of the exit charge fractions of He, N and Ne projectiles with velocities below 0.7 a.u. transmitted through 50 nm and 200 nm thick single-crystalline silicon membranes. The comparison was made between a number of low-index crystal orientations along the (110) plane including <100>, <311>, <211>, <111> and so-called random orientation. Variations in the final charge distributions were found for all projectiles across the measured energy range in accordance with expectations from measurements of the specific energy loss. Moreover, the extrapolation of the mean charge state data acquired in channelling geometry towards lower velocities suggests an existence of a velocity threshold below which all projectiles would remain neutral along their entire trajectory.

Experimental data are presented along with the evaluation of the time scales and the interaction distances necessary for specific charge exchange processes to occur. In this way, we are able to assess the weight of their individual contribution to the electronic excitation.

References

[1] S. Lohmann, and D. Primetzhofer, *Phys. Rev. Lett.*, 124 (2020) 096601
[2] S. Lohmann, R. Holeňák, and D. Primetzhofer, *Phys. Rev. A*, 102 (2020) 062803
[3] R. Holeňák, S. Lohmann, F. Sekula, and D. Primetzhofer, *Vacuum*, 185 (2021) 109988

Controlled modification of the Au: YSZ structures by high-energy ion irradiation: Structural and optical response in different crystallographic orientations

A. Jagerová[1,2], R. Mikšová[1,*], J. Cajzl[3], V. Holý[4,5], M. Vronka[6], A. Macková[1,2]

[1]*Nuclear Physics Institute of the Czech Academy of Sciences, PRI, 250 68 Řež, Czech Republic*
[2]*Department of Physics, Faculty of Science, J.E. Purkyně University, Pasteurova 3544/1, 400 96 Ústi nad Labem, Czech Republic*
[3]*Department of Inorganic Chemistry, University of Chemistry and Technology in Prague, 166 28 Prague, Czech Republic*
[4]*Department of Condensed Matter Physics, Faculty of Mathematics and Physics, Charles University, Ke Karlovu 2026/5, 121 16 Prague 2, Czech Republic*
[5]*Institute of Condensed Matter Physics, Faculty of Science, Masaryk University, Kotlářská 2, 61137 Brno, Czech Republic*
[6]*Department of Material Analysis, Institute of Physics of the Czech Academy of Sciences, Na Slovance 1999/2, 182 21 Prague*
**miksova@ujf.cas.cz*

Gold nanoparticles (Au-NPs) modified metallic oxides offer significant improvement of optical properties applied in ultrafast optical switches or optical gas sensors. Within this work, (100)-, (110)- and (111)-oriented crystalline yttria-stabilized zirconia oxide (YSZ) was implanted with 1 MeV Au^+ ions at room temperature and fluences from 1.5×10^{16} cm^{-2} to 7.5×10^{16} cm^{-2} to prepare the Au-NPs. Coalescence of Au-NPs and structure recovery of implanted YSZ was carried out by thermally annealing at 1100 °C for 1 h in air. Additionally, prepared Au-NPs in YSZ crystals were modified using 10 MeV Si^{3+} ion-irradiation with a fluence of 5.0×10^{14} cm^{-2}. Au-depth profiles, as well as structural changes in YSZ crystals with embedded Au-NPs, at particular preparation steps, were monitored via Rutherford backscattering spectrometry in channelling mode (RBS-C) showing the gold distribution in the layer about 50-300 nm below the surface. At this depth, Au ions aggregate into the small Au NPs with sizes from 1 to 3 nm as was confirmed by transmission electron microscopy (TEM). Annealing procedure of the Au-implanted YSZ causes partial structure recovery and the subsequent Si-ion irradiation increased Zr-disorder again, however, the disorder does not reach values before the annealing. The optical properties of Au implanted YSZ analysed by absorption measurement showed the appearance of the new absorption band at 550 nm for the Au-ion fluences above 5.0×10^{16} cm^{-2}. Annealing and Si irradiation of implanted samples lead to the appearance of this absorption peak for all prepared samples in the wavelength range of 530-580 nm in connection with the Au-ion fluence and optical activity of created Au-NPs. The XRD measurement shows evidence of laterally homogeneous deformation after the annealing and Si-ion irradiation. The defects in these samples almost do not deform the host lattice which is in contrast with samples before the annealing and Si-ion irradiation, where the diffuse scattering is caused mainly by the elastic deformation of the host lattice due to the particles.

RBS dechanneling induced by perfect voids: W as a test-case material

Xin Jin[1,*], **Flyura Djurabekova**[1], **and Kai Nordlund**[1]

[1]*Department of Physics, University of Helsinki, Finland*
[*]*xin.jin@helsinki.fi*

Rutherford backscattering spectrometry in channeling mode (RBS/C) is a non-destruction characterization technique that relies on the interaction of probing ions with target atoms. It has been extensively applied to detect radiation defects in solids over past decades. Although the RBS/C technique is sensitive to defects of interstitial-type, it is generally considered that RBS/C signals only have weak response to defects of vacancy-type, for example, voids. Nonetheless, considering that defects of vacancy-type are pervasive, it is of importance to have a better understanding of the effect of vacancy-defects on RBS/C signals.

In this work, we present a computational study of RBS dechanneling induced by perfect voids with W as a test-case material. The study was performed by using a code called RBSADEC [1, 2, 3] which can generate RBS/C signals from arbitrary atomic structures and can take into account the effect of voids on the electronic stopping power of probing ions. We show how the decanneling fraction evolves as a function of void size as well as the energy of probing ions by utilizing voids with different shapes: on the one hand, results obtained from spherical and cubic voids validate theoretical descriptions in literature; on the other hand, results obtained from slab-voids highlight the importance of the spatial distribution of probing ions in a crystal, which tends to be neglected in literature. In addition, it is used to consider that the effect of voids on dechanneling is similar to that of stacking faults. We demonstrate that the dechanneling induced by voids and stacking faults can show significant differences, which could provide a tool to distinguish the signals generated by the two defects in experiments.

References

[1] S. Zhang *et al.*, *Phys. Rev. E*, 94 (2016) 043319
[2] X. Jin *et al.*, *Model. Simul. Mat. Sci. Eng.*, 28 (2020) 075005
[3] RBSADEC. Available at https://gitlab.com/xinJin/rbsadec

Surface Characterization of CaF_2 Crystals Irradiated with MeV Ions Below Charge State Equilibrium

R. Kaur[1,*], **P. Ström**[1], **and D. Primetzhofer**[1]

[1]*Department of Physics and Astronomy, Applied Nuclear Physics, Uppsala University, Uppsala, Sweden*
[*]*rajdeep.kaur@physics.uu.se*

Irradiation of solids by ion beams commonly alters surface and bulk material properties with applications in, for example, thin film electronics, surface nanostructure engineering and modification of 2D materials. In the case of ionic crystals, e.g. CaF_2, irradiation by heavy ions like Xe with high charge states ($q \geq 33+$) and keV impact energy results in formation of surface nanohillocks.[1] For irradiation with MeV Xe ions, the threshold charge state for such hillock formation reduces to between 25+ and 26+ with 3 MeV projectiles and between 21+ and 22+ with 5 MeV projectiles.[2] Furthermore, irradiation by swift heavy ions with initial energy between 0.5 and 13.7 MeV/u is reported to produce near-surface lattice modification in CaF_2 crystals with two different electronic stopping power thresholds for damage creation.[3] These thresholds correspond to (a) quenching of a molten phase, accompanied by swelling and surface nanohillock formation, and (b) quenching of a boiling phase, leading to tracks visible in Transmission Electron Microscopy (TEM). In this contribution, we investigate the threshold energy for surface structure modification in CaF_2 irradiated by different ions below equilibrium charge state in the MeV energy regime (below the electronic stopping power maximum).

Single crystals of CaF_2, cleaved along (111) plane, were irradiated by Au and Br ions with energies from 2 MeV to 48 MeV, charge states from 1+ to 11+ and ion fluences from 2.8×10^{10} to 1×10^{13}. The surface properties of the irradiated samples were studied by means of Atomic Force Microscopy (AFM) in contact mode. Nanoscale surface structures were observed for some surfaces irradiated by Au and Br ions. Electronic stopping power (S_e) and total stopping power (S_t) values for the projectiles were calculated using SRIM [4] and the dependence of the observed surface structure modifications on S_e and S_t was studied.

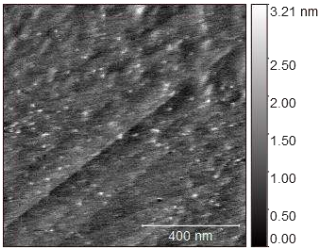

Figure 1. AFM image of CaF_2 surface irradiated by 30 MeV Au^{7+} ions under normal incidence

References

[1] A. S. El-Said, R. A. Wilhelm, R. Heller, S. Facsko, C. Lemell, G. Wachter, and J. Burgdörfer, R. Ritter, F. Aumayr, *Phys. Rev. Lett.*, **109** (2012) 117602

[2] Y. Y. Wang, C. Grygiel, C. Dufour, J. R. Sun, Z. G. Wang, Y. T. Zhao, G. Q. Xiao, R. Cheng, X. M. Zhou, J. R. Ren, S. D. Liu, Y. Lei, Y. B. Sun, R. Ritter, E. Gruber, A. Cassimi, I. Monnet, S. Bouffard, F. Aumayr, M. Toulemonde, *Scientific Reports, Nature Publishing Group*, **4** (2014) 5742

[3] M. Toulemonde, A. Benyagoub, C. Trautmann, N. Khalfaoui, M. Boccanfuso, C. Dufour,1 F. Gourbilleau, J. J. Grob, J. P. Stoquert, J. M. Costantini, F. Haas, E. Jacquet, K.-O. Voss, A. Meftah, *Phys. Rev. B*, **85** (2012) 054112

[4] J. F. Ziegler, M. D. Ziegler, and J. P. Biersack, *Nucl. Instrum. Methods Phys. Res. B*, **268** (2010) 1818

Orientational relationship between SHI induced tetragonal ZrO_2 tracks and the monoclinic matrix

M. Lee[1,*], J. O'Connell[1] and V. Skuratov[2]

[1]*Centre for HRTEM, Nelson Mandela University, South Africa*
[2]*FLNR, JINR, Russia*
[*]*michael.lee@mandela.ac.za*

Pure bulk zirconia (ZrO_2) is a polymorphic oxide that exists in three different low pressure crystal structures below its melting point namely, the high temperature phases cubic and tetragonal as well as the low temperature monoclinic phase [1]. Irradiation of bulk natural zirconia at room temperature along the monoclinic $[100]_m$ crystal axis were shown by transmission electron mocroscopy to produce non-continuos tetragonal latents tracks consisting of segments approximately 30 nm in length and rectangular cross sections of the order 2.5 nm.The segments were aligned along the $[001]_t$ crystal axis and approximately 9° to the $[100]_m$ axis. It was suggested that the mechanism for the stabilization of the high temperature phase could be due to the surface energy of the interface surfaces [3] or the presence of additional vacancies and interstitial oxygen atoms [4]. In this presentation we present results for irradiated bulk monoclinic zirconia along different crystalline directions to determine the influence of interfacial surfaces on the formation and stabilization of latent tracks.

Natural ZrO_2 from the Palaborwa complex in South Africa was irradiated with 167 MeV Xe ions to a fluence of $2x10^{10}$ ions.cm^{-2} at the FLNR, JINR, Dubna. Plan view and cross sectional TEM lamellae were prepared by standard FIB lift out procedure using an FEI Helios NanoLab 650 and imaged in a JEOL ARM 200F TEM operating at 200 kV.

Individual ion tracks were found to be composed of the high temperature stable tetragonal phase. The c axis of the monoclinic and tetragonal regions was parallel with 45° relative rotation about the c axis. Discontinuities in the tetragonal phase together with a slight misalignment relative to the ion path was ascribed to the difference in a-c angle between the tetragonal and monoclinic phase.

Although stressed, the tetragonal inclusions were found to be stable at room temperature for at least several years although thermal excitation as well as excitation by high energy electrons was able to transform the tetragonal phase back into the monoclinic phase leaving behind a train of defect clusters as is typical of ion tracks in non-amorphizable crystals.

References

[1] J.E. Bailey, *Proc. R. Soc. A. Math. Phys. Sci.*, 279 (1964) 395-412
[2] J.H. O'Connell, M.E Lee, V.A Skuratov and R.A. Rymzhanov, *Nucl. Inst. Meth. Phys. Res. B*, 473 (2020) 1-5
[3] M.W. Pitcher, S.V. Ushakov, A. Navrotsky, B.F. Woodfield, G. Li, J. Boerio-Coates and B.M. Tissue, J. Am. Ceram. Soc., 88 (2005) 160–167
[4] X. Lu, K. Liang, S. Gu, Y. Zheng and H.Fang, J. Mater. Sci., 32 (1997) 6653-6656

Deuterium's effect on defect accumulation in tungsten during irradiation

V. Lindblad, F. Granberg, J. Byggmästar, K. Nordlund[1]

[1] *University of Helsinki, Finland*
[*] *victor.lindblad@helsinki.fi*

Experimental studies on irradiation of tungsten with and without deuterium present during irradiation have revealed a huge discrepancy in the retained deuterium. Adding deuterium after irradiation resulted in approximately 1.7 % retained D, whereas the retained deuterium in samples where D was present during irradiation the value is expected to be close to 4 % [1]. In order to explain the discrepancy, we conducted simulations on similar setups.

Our molecular dynamics simulations consisted of three different sets of systems, containing around half a million atoms each. The first set consisted of pure tungsten, while the remaining sets had an addition of either 10,000 or 50,000 deuterium atoms, corresponding to a deuterium fraction of 2 or 10 percent, respectively. For each system, 2000 overlapping cascades were performed, with an initial recoil energy of 10 keV, to obtain a dose of roughly 0.15 dpa. The evolution of vacancy and interstitial build-up was monitored to get a quantitative picture of the produced damage and mechanisms.

An integral part of any molecular dynamics simulation is the interatomic potential deployed. For our systems, we also used three different potentials. By comparing the obtained results, we gained some insight in the suitability of these potentials for irradiation simulations.

References

[1] M. Pečovnik, T. Schwarz-Selinger, S. Markelj, *Journal of Nuclear Materials*, Volume 550, July 2021, 152947

Trajectory dependence of electronic energy-loss straggling at keV ion energies

S. Lohmann[1,2,*], **R. Holeňák**[2], **P. L. Grande**[3], **and D. Primetzhofer**[2]

[1]*Institute of Ion Beam Physics and Materials Research, Helmholtz-Zentrum Dresden-Rossendorf, Germany*
[2]*Department of Physics and Astronomy, Uppsala University, Sweden*
[3]*Physics Department, Institute of Physics, Federal University of Rio Grande do Sul (UFRGS), Brazil*
[*]*s.lohmann@hzdr.de*

We have measured the electronic energy-loss straggling of H, He, B and Si ions in Si using a transmission time-of-flight approach. Figure 1 demonstrates our experimental approach, in which ion energy loss is measured together with angular distributions. Singly charged ions with velocities between 0.25 and 1.6 times the Bohr velocity were transmitted through single-crystalline Si(100) nanomembranes in either channelling or random geometry to study the impact parameter dependence of energy-loss straggling. Contributions from nuclear losses and path length corrections to the straggling were accounted for with Monte Carlo simulations. We discuss the asymmetry of the energy-loss distribution and the extend of the correlation between electronic and nuclear straggling for random geometry. Our results exhibit an increase in straggling with increasing ion velocity for channelled trajectories for all investigated projectiles as well as for H and He in random geometry. In contrast for heavier ions, electronic straggling exhibits a minimum value and increases again for low velocities. We compare our experimental results with transport cross section calculations [1]. The satisfying agreement for He shows that electronic stopping for light ions is dominated by electron-hole pair excitations, and that the previously observed trajectory dependence [2, 3] can indeed be attributed to a higher mean charge state for random trajectories. No agreement is found for B and Si indicating that local losses in charge-exchange events significantly contribute to the energy loss at low velocities.

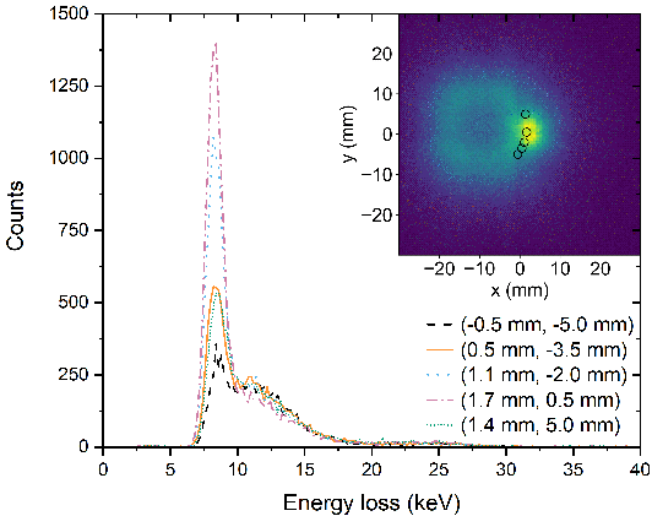

Figure 1: 100 keV Si^+ transmitted through a 53 nm Si(100) nanomembrane turned by (1°,2°) out of channelling geometry. The main plot shows energy-loss curves for different regions of interest on the detector. ROI radius is 1 mm in all cases. The inset shows the spatial distribution of ions with ROIs from the main plot indicated by circles.

References

[1] F. F. Selau et al., *Phys. Rev. A*, 102 (2020) 032812
[2] S. Lohmann, and D. Primetzhofer, *Phys. Rev. Lett.*, 124 (2020) 096601
[3] S. Lohmann, R. Holeňák, and D. Primetzhofer, *Phys. Rev. A*, 102 (2020) 062803

Platinum silicide formation on silicon carbide substrates due to thermal annealing and swift heavy ion irradiation

E. Njoroge[1, 2*], **T. Hlatshwayo**[2], **and V. Skuratov**[3,4,5], **J. Malherbe**[2]

[1]*ENGAGE, University of Pretoria, South Africa*
[2]*Physics Department, University of Pretoria, South Africa*
[3]*Flerov Laboratory of Nuclear Reactions, Joint Institute for Nuclear Research, Russia*
[4]*National Research Nuclear University MEPhI, Russia*
[5]*Dubna State University, Dubna, Moscow Region, Russia*
[*]*eric.njoroge@up.ac.za*

Platinum silicide formation on silicon carbide at relatively low temperatures was investigated. Multi-layered thin films of Pt and silicon of different thicknesses were deposited on SiC substrates. The samples had a 30 nm wide Pt layer on a 20 nm wide Si layer both deposited by e-beam on SiC substrates. The one set of samples was annealed in vacuum from 100 °C to 400 °C and others were irradiated with Xe^{26+} ions with energy of 167 MeV at room temperature to fluences of 3.4×10^{14} and 8.3×10^{14} ions/cm^2.

The interdiffusion, reaction temperature, silicide phase identification and surface morphology were investigated with Rutherford backscattering spectrometry (RBD), X-ray photoelectron spectroscopy (XPS) and scanning electron microscopy (SEM). The RBS and XPS results indicate that interdiffusion starts to occur at Pt/Si interface after annealing at 200 °C for the Pt (30 nm)/Si (20 nm) sample. The solid-state reactions in this sample start at 250 °C with the formation of Pt_2Si. The width of the Pt_2Si phase increased up to 400 °C when the reaction was complete. The irradiated samples did show ion beam mixing at the Pt/Si interface induced by SHI due to high electronic excitations. The reactions in the two samples did not involve the SiC substrate which was still intact. Pt silicides that formed on SiC had good contact with SiC substrate and did not delaminate.

Nuclear stopping power of antiprotons: theory and experimental confirmation

K. Nordlund[1,*], **M. Hori**[2], **and D. Sundholm**[3]

[1]Department of Physics and Helsinki Institute of Physics, P.O. Box 64, University of Helsinki, Finland
[2] Fakultät für Physik, Ludwig-Maximilians-Universität München, 80799 Munich, Germany
[3] Department of Chemistry, P. O. Box 55, University of Helsinki, Finland

[*] *kai.nordlund@helsinki.fi*

The production of stable antihydrogen atoms relies on the slowing down of antiprotons with initial energies of the order of MeV's or keV's to thermal energies. In particular, the antiproton storage ring ELENA just taken into use at CERN produces a 100 keV antiproton beam, that should be further slowed down to energies of 0 -- 5 keV to enable antihydrogen production. The slowing down of energetic ions or antiions is determined by the stopping power. Optimizing the transmission efficiency makes it important to know the low-energy stopping power of antiprotons in materials.

While there are numerous studies of the electronic stopping power of antiprotons, there have been none for the nuclear stopping power. We have now used quantum chemical methods to calculate interparticle potentials between antiprotons and different atoms, and show that these are attractive at all interatomic distances. Using scattering calculations with the obtained potentials, we further derive the nuclear stopping power of antiprotons in solids. The results show that the antiproton nuclear stopping powers are much stronger than those of protons. Moreover, contrary to the case of protons, the antiproton nuclear stopping stopping can be stronger than their electronic one [1].

Using the obtained interparticle potential and experimental electronic stopping powers (including the straggling of the electronic stopping), we simulate with molecular dynamics (MD) the transmission and capture probability of 100 keV antiprotons in nanometer thin foils. The simulations show that after slowing down to keV energies, the antiprotons have a high probability of being captured in a bound orbit with sample atoms. Since the antiproton-atom interaction at small distances is essentially a purely attractive 1/r potential, comparable to the gravitational potential, the antiprotons can even end up in Kepler-like elliptical orbits.

Finally, we hae determined the optimal film thickness of C, mylar, polyethylene naphtaplate, Be, Al an Si foils for the production of 0 - 5 keV antiprotons [1,2,3]. The simulation results are in good agreement with data from two experiments that involve pulsed antiproton beams with incident kinetic energies between 63 keV and 122 keV that traverse polymer foils with thicknesses of ≈ 1.3 μm and 1.8 μm. The 25 nm-thick layers of Ag on the latter foils reduced the transmission of antiprotons. The results will be utilized to design the degrader foils in laser spectroscopy experiments of antiprotonic helium atoms and experiments involving Penning traps that are carried out at the ELENA facility of CERN,

References

[1] K. Nordlund et al, Physical Review A 96, 042717 (2017).

[2] K. Nordlund, Results in physics 8, 683 (2018).

[3] K. Nordlund, M. Hori and D. Sundholm, Phys. Rev A (2022) submitted for publication.

Ultrashort pulsed beams of keV ions for materials science at Uppsala University – a status report

E. Ntemou[1, *], **R. Holeňák**[1*], **D. Wessman**[2], **S. Lohmann**[1,3] **and D. Primetzhofer**[1,2]

[1] *Department of Physics and Astronomy, Uppsala University,751 20 Uppsala, Sweden*
[2] *Tandem Laboratory, Uppsala University, Box 529, S-751 20 Uppsala, Sweden*
[3] *Institute of Ion Beam Physics and Materials Research, Helmholtz-Zentrum Dresden-Rossendorf e.V. (HZDR), 01328 Dresden, Germany*
[*] *eleni.ntemou@physics.uu.se*

The 350 kV Danfysik Implanter at Uppsala University features a ~8 m beamline designed for time-of-flight experiments equipped with an electrostatic chopper, a drift tube bunching unit and associated ion optics delivering a near-parallel beam with divergence lower than 0.056° into a beam spot smaller than 1 mm^2. The end station consists of an ultra-high vacuum chamber equipped with a precise 6-axis goniometer. Scattered or transmitted ions along with the emitted photons, electrons, recoils and desorbed species are detected by a large-solid angle (130 msr), position-sensitive microchannel plate detector (MCP), enabling also crystallographic studies by acquisition of energy-resolved blocking and channeling patterns. The detector is mounted on a rail that can rotate around the sample by 180° at a distance of 290 mm. A second position-sensitive MCP flight time detector with a solid angle of 2 msr is mounted at a distance of 1050 mm from the sample at a scattering angle of 135°.

Continuous atomic and molecular beams in a wide range of chemical elements are produced in the energy range of 5-330 keV for singly charged ions and are chopped in short pulses by an electrostatic chopper using a horizontal 4 MHz sinusoidal scanning combined with a vertical electrostatic gating, resulting in typical pulse lengths of 1 ns [1,2]. These pulses can be further compressed in time using a drift tube buncher distorting the phase space. The buncher is optimized for 100 keV H for which a time resolution of 300 ps was achieved [3]. However only a very limited number of combinations of ions and energies can be tuned in this way. Therefore, the most recent upgrade to the system is a second electrostatic chopper operating at the frequency of 16 MHz. The combination of the choppers offers a pulse repetition rate from 1 Hz to 1 MHz and a time resolution significantly below 300 ps for a wide range of energies and ion species, approaching intrinsic limitations in time-resolution of our detector (~200 ps).

The energy resolution obtained for 60 keV He by the detector with the shorter flight distance and both choppers is ~0.21 keV resulting in a relative energy resolution (δE/E) of ~ 0.0035. By using the second detector the energy resolution is further increased to ~0.06 keV, resulting in a relative energy resolution better than 0.001. The corresponding depth resolution at the surface of amorphous Si is significantly below 10 Å.

The upgrade of the setup leads to higher energy resolution, and along with the additional capabilities of the setup (annealing, charge discrimination and implantation) will facilitate modification and depth profiling studies of superlattices and thin films in the sub-nm range.

References

[1] M. K. Linnarsson et al., Review of Scientific Instruments 83 (2012) 095107
[2] M. A. Sortica et al., Nuclear Inst. And Methods in Physics Research B 463 (2020) 16
[3] D. Primetzhofer et al., Nuclear Inst. And Methods in Physics Research B 332 (2014) 212

Electronic Sputtering from H_2O:C_2H_6 ice bombarded by energetic heavy ions

P. R. B. Oliveira[1,*], **R. Martinez**[2], **and E. F. da Silveira**[1]

[1]*Departamento de Física, Pontifícia Universidade Católica do Rio de Janeiro, Rua Marquês de São Vicente, 255, Rio de Janeiro 22452-970, Brazil*

[2]*Universidade Federal do Amapá – UNIFAP, Departamento de Física, Rod. Juscelino Kubitschek, km 02, 68903-419, Jardim Marco Zero – Macapá – AP, Brazil*

[*]*pablo@aluno.puc-rio.br*

Inside molecular clouds, cosmic rays induce chemical reactions on the surface of ice-covered grains and stimulate the sputtering of the processed material to the gas phase. In particular, cosmic rays trigger secondary ion emission from these surfaces. Consequently, the knowledge of desorption processes helps to understand the formation and composition of different species within molecular clouds. Water (H_2O) has been observed in asteroids, centaurs, scattered disk objects, trans-Neptunian objects and the Solar System planets. It is then expected that, in those environments, condensed gases like H_2O be irradiated by energetic particles. A special case occurs when H_2O is mixed with other gases, like Ethane (C_2H_6), more yet, if the proportion of H_2O:C_2H_6 is less than one. Several laboratory studies demonstrated the effects of energetic processing of ices at low temperature, showing the production of several new molecules and free radicals, among them H^+, H_3O^+, OH^-, O^- [1,2]. In the current work, H_2O:C_2H_6 ice, with a proportion of approximately 100:1, is irradiated at an average temperature of 100 K by energetic multicharged ions (^{252}Cf fission fragments of ~ 65 MeV), and the sputtered positive and negative secondary ions are analyzed by time-of-flight mass spectrometry (PDMS-TOF) [3]. Several ionic species are identified, indicating strong surface fragmentation and clusterization. The bombardment induces the formation of ion cluster series, where the main ones are $(H_2O)_nX_m$, with X = H_2O^+, H_3O^+, O^- and OH^-. Their yield distributions are fitted by the sum of two decreasing exponentials (equation 1):

$$Y = Y_0^F e^{(-k_F m/z)} + Y_0^S e^{(-k_S m/z)} \quad (1)$$

where m/z is the mass-to-charge ratio. This two-exponential decay for the desorbed ionic clusters yields have already been reported in previous works for other ices bombarded by ^{252}Cf fission fragments [4]. This behavior is described by a cluster emission model with two regimes: fast (F) and slow (S) regimes [5]. We have found that most of the yield distributions have similar exponential decays, $k_F = 0.480\ u^{-1}$ and $k_S = 0.063\ u^{-1}$. Such finding may be useful to understand the processes by which, in space, ionized molecular species are delivery to the gas phase.

References

[1] V. M. Collado, et al., *Surface Science,* 569 (2004) 149-162.
[2] A. L. F. de Barros, et al., *J. Phys. Chem. C,* 115 (2011) 12005-12014.
[3] P. R. B. Oliveira, et al., *Monthly Notices of the Royal Astronomical Society,* 502, 1 (2021) 1423-1432.
[4] F. A. Ribeiro, et al. *Monthly Notices of the Royal Astronomical Society,* 492, 2 (2019)
[5] R. Martinez, et al. *International Journal of Mass Spectrometry,* 253, 1-2 (2006) 112-121.

Applying the inelastic thermal spike model to the investigation of ion tracks in polymers

M. S. da Rocha[1], J. P. M. May[1], R. S. Thomaz[1,2], R. M. Papaléo[1], and M. Toulemonde[3]

[1]*Interdisciplinary Center of Nanoscience and Micro-NanoTechnology, School of Technology, Pontifical Catholic University of Rio Grande do Sul, Porto Alegre, Brazil*
[2]*Ion Implantation Laboratory, Federal University of Rio Grande do Sul, Brazil*
[3]*Centre de Recherche sur les Ions, les Matériaux et la Photonique, CEA-CNRS-ENSICAEN-Université de Caen, CIMAP-GANIL, France*
** papaleo @pucrs.br*

In this work, we analyze ion track production in polymers by swift heavy ions within the framework of the inelastic thermal spike model (i-TS). The model is used to describe the track size as a function of energy loss in several polymers: the amorphous poly(methyl methacrylate) (PMMA) and the semi-crystalline poly(p-phenylene sulphide) (PPS), poly(ethylene terephthalate) (PET), and poly(vinylidene difluoride) (PVDF). Track size calculations are compared to experimental data from the literature deduced from measurements of crater size, bond-breaking cross sections, changes in crystallinity and electron density, ion track etching, and electrical depolarization. The use of data obtained from distinct experimental techniques, which probe different types of damage, provides a broad platform to test the applicability of the inelastic thermal spike model to the investigation of ion tracks in polymers. We show that the i-TS describes reasonably well the evolution of track size as a function of electronic energy loss obtained from most experimental probes, when the activation energy of thermal decomposition of the polymers is used as the physical criterion of track formation with an electron-phonon mean free-path value close to 3nm. Amorphization radii of the semicrystalline polymers is not directly correlated to melting in the spike, as often observed in inorganic materials. Only depolarization of β- PVDF appears to be correlated to the size of a molten zone. As the degree of damage is not uniform across the track radial dimension, there are variations in experimental track sizes for a given polymer that can only be accounted for by using multiple activation processes. The electronic energy loss threshold of thermal decomposition deduced from the i-TS model for all polymers investigated is close to or smaller than 1 keV/nm and below 0.5 keV/nm for the appearance of a molten phase. Such values of threshold are very low as compared to inorganic materials, in accordance with the extreme sensitivity of polymeric materials. We will discuss how the thermal spike model may contribute to rationalize different aspects of swift heavy ion irradiation of polymers.

Trends in electronic stopping powers: the case of period 6

M.V. Moro[1], E. Pitthan[1], and D. Primetzhofer[1,2,*]

[1]*Department of Physics and Astronomy, Uppsala University, Box 516, 751 20 Uppsala, Sweden*
[2]*The Tandem Laboratory, Uppsala University, Box 529, 751 21 Uppsala, Sweden*
[*]*daniel.primetzhofer@physics.uu.se*

Electronic stopping powers, i.e. the energy deposited per unit path length by ions traversing matter serve as a key input quantity for depth profiling using ion beams, for calculating energy deposition in irradiation, and ion ranges in implantation. Moreover, the specific dependence of stopping powers on quantities such as ion energy and target material composition or orientation can increase our fundamental understanding of electronic excitation processes in matter.

Despite the huge efforts made in the field under a long period of time, the majority of existing datasets are, however, still limited to only a few reference systems. As an example, the more reactive early transition metals, not to speak of earth-alkali or alkali metals have obtained much less attention from experimentalists, which can be at least partially attributed to difficulties in preparation and characterization of appropriate sample systems.

Nevertheless, early transition and rare-earth metals have become increasingly relevant in materials research in particular in the field of functional coatings increasing the need for accurate stopping powers by applied research, often at low ion energies. At the same time, it has been shown, that the established concepts predicting electronic stopping powers can be found highly inaccurate for materials with only partially occupied d- or f-shells [1].

We have earlier conducted a comparison of early and late transition metals in periods 4-6 of the periodic table [2] to investigate systematic dependencies. To further expand on this topic, we have now determined electronic stopping powers in a wide energy range of energies for a large number of chemical elements in period 6 spanning from lanthanides such as Gd over early and late transition metals, with the first measurements on Os, to post-transition metals such as Pb and Bi.

In this contribution we will present these new results and compare data for protons and He as primary ions for the different well-characterized target materials with a particular focus on energies below the Bragg peak. We aim to draw general conclusions which allow to obtain better predictability of stopping powers for hitherto not investigated systems or energy regimes.

References

[1] D. Roth, B. Bruckner, M.V. Moro, S. Gruber, D. Goebl, J.I. Juaristi, M. Alducin, R. Steinberger, J. Duchoslav, D. Primetzhofer, P. Bauer., *Phys. Rev. Lett.* 118 (2017) 103401.
[2] M.V. Moro, P. Bauer, and D. Primetzhofer, *Phys. Rev. A* 102 (2020) 022808.

Beam-plasma interaction in fast ignition nuclear fusion: hot-spot gains for different initial conditions.

P. Rodríguez-Beltrán[1,2], J.M. Gil[1], R. Rodriguez[1,*] and G. Espinosa-Vivas[1]

[1]*Departament of Physics, Universidad de Las Palmas de Gran Canaria, Spain*
[2]*Instituto de Astrofísica de Canarias, Spain*
[*] *rafael.rodriguezperez@ulpgc.es*

The interaction between an ion beam and a compressed target plasma at stagnation state is expected to be one of the best candidates to operate a future inertial confinement fusion power plant. The fast ignition approach decouples the fusion process: the fuel is compressed with a laser system and then a short beam with high energy is focused on one side of the core, heating it and starting ignition. Therefore, a precise knowledge of the energy deposition of the beam in the target plasma is required to design this scheme [1].

The aim of this work is to study the interaction between an ion beam and a plasma fuel of Deuterium-Tritium (DT), finding the relation between the characteristics of the ion beam and the resulting heated plasma and its properties. For this purpose, we use a numerical model to simulate the stopping of an ion beam in a plasma target, as well as the plasma heating process. We consider a compressed sphere of DT fuel with a 50 μm radius, with temperature and density homogeneous distributions. We assume a perfectly collimated, cylindrical and monoenergetic ion beam with constant flux impacting on a radial direction on the plasma, so the interaction beam-target can be described as 1D [2]. It is assumed that the time of the interaction is considerably shorter than the characteristic hydrodynamic times and thus, the plasma heating can be considered as isochoric. Therefore, the change in the plasma temperature depends exclusively on the energy deposited by the beam projectiles, since the mechanical work and conduction can be neglected [3]. With this numerical model we calculate the temperature field after the interaction and we define a region of special interest named hot spot. From the distribution of temperatures, we extract key parameters, such as the maximum temperature and its position, the length and the mean temperature of both the heated region and the hot spot. Using the parameters of the hot spot we describe the initial evolution of the plasma, studying the self-heating, the ignition and the burning gains of the plasma [3, 4].

Finally, we perform a systematic study for ion beams composed of P^+, C^{6+} and V^{23+}, in a wide range of kinetic energies and number of particles. This study is performed for plasmas of density $\rho = 300$ g/cm^3, with different initial temperatures of the plasma: $T_0 = 0.5$, 1 and 5 keV. These results allow to identify the regions of interest, relating the plasma gain, the characteristics of the created hot-spot and the proper beam to reach this conditions.

This work has been supported by the Spanish Government through the Project PID2019-110678-I00 and by the Consejería de Economía, Industria, Comercio y Conocimiento del Gobierno de Canarias.

References

[1] Tabak, Max, et al. *Phys. Plasmas* 15 (1994): 1626-1634.
[2] O. R. Gasparyan et al., *J. Russ. Laser Res.* 34 (2013), 33.
[3] S.Atzeni, J. Meyer-ter-Vehn. OUP Oxford, 2004.
[4] Gus'kov, S. Yu, et al. *Journal of Experimental and Theoretical Physics* 119 (2014): 958-970.

Radiolysis of nucleobases by 230 MeV Ca ion beams: temperature dependence (17 - 335 K)

P. C. J. Ada Bibang[1], Z. Kanuchova[2], G. S. V. Muniz[1,3], M. Bender[4,5], F. Koch[4], B. Merk[4], I. Schubert[4], D. Severin[4], C. Trautmann[4,6], G. Strazzulla[7], P. Boduch[1], A. Domaracka[1], and H. Rothard[1,*]

[1]*CIMAP-CIRIL-Ganil, Normandie Univ, ENSICAEN, UNICAEN, CEA, CNRS, Caen, France*
[2]*Astronomical Institute of the Slovak Academy of Sciences, T. Lomnica, Slovakia*
[3]*Institute of Physics, University of São Paulo, Brazil*
[4]*GSI Helmholtzzentrum für Schwerionenforschung, Darmstadt, Germany*
[5]*Hochschule Rhein-Main, Rüsselsheim, Germany*
[6]*Technische Universität Darmstadt, Germany*
[7]*INAF Astrophysical Observatory, Catania, Italy*
[*]*rothard@ganil.fr*

Ices are omnipresent in cold regions in space (comets, transneptunian objects, dust grains, surfaces of planets and their satellites). Although the ices mainly contain small molecules (H_2O, carbon oxides, CH_4, NH_3 etc.), larger complex organic molecules (COMs) may be present. Temperatures on objects containing COMs cover a range from as low as 10 K in dense molecular clouds, through 25 to 150 K in the outer Solar system, and up to >300 K in the inner Solar system. Ionizing radiation (UV photons, electrons, ions from solar wind and cosmic rays) induces physicochemical processes such as radiolysis and subsequent formation of new molecules. At UNILAC of GSI (Darmstadt, Germany) the radiolysis and radio-resistance of the nucleobases adenine and cytosine were studied at different temperatures (17 - 335 K). The purine nucleobase adenine consists of two heterocyclic rings, the pyrimidine nucleobase cytosine is formed by just one heterocyclic ring. The swift heavy ion irradiation induced effects in the samples were studied in situ by Fourier transform infrared absorption spectroscopy [1,2]. The samples prepared on infrared transparent windows (ZnSe) were mounted on a closed-cycle helium cryostat. The latter allows cooling them down to about 17 K in order to simulate the conditions inside dense molecular clouds. The setup can also be held at other temperatures up to 335 K to simulate the temperatures occurring in the inner and outer Solar system. The destruction cross sections of nucleobases are determined from the exponential decay of the peak areas of IR absorption lines as a function of the projectile fluence. The destruction cross sections are significantly lower at 300 K than at T < 50 K. Survival times of COMs in space environments can be estimated from the destruction cross sections [1]. The data at temperatures around 300 K can help understanding processes occurring at the molecular level in radiation damage of biological targets (ion beam therapy, radiation protection) [2]. This work was supported by the EU's Horizon 2020 Research and Innovation Programme (grant agreement No. 654002 ENSAR2).

References

[1] G. S. Vignoli Muniz, C. F. Mejía, R. Martinez, B. Augé, H. Rothard, A. Domaracka, Ph. Boduch Radioresistance of adenine to cosmic rays, *Astrobiology* 17(4) (2017) 298-308, doi:10.1089/ast.2016.1488

[2] Prudence C. J. Ada Bibang, Aditya N. Agnihotri, B. Augé, Ph. Boduch, Ch. Desfrançois, A. Domaracka, F. Lecomte, B. Manil, R. Martinez, G. S.V. Muniz, N. Nieuwjaer, H. Rothard Ion radiation in icy space environments: Synthesis and Radioresistance of Complex Organic Molecules *Low Temperature Physics* 45 (2019) 590-597, doi: 10.1063/1.5103250

Adenine irradiated by 800 keV/u proton and helium beams: temperature dependent radiolysis

P. C. J. Ada Bibang[1], Z. Kanuchova[2], G. S. Vignoli Muniz[1,3], P. Herczku[4], D. V. Mifsud[4,5], Z. Juhász[4], S. T. S. Kovács[4], S. Ioppolo[6], N. J. Mason[5], B. Sulik[4], P. Boduch[1], A. Domaracka[1], and H. Rothard[1,*]

[1]CIMAP-CIRIL-Ganil, Normandie Univ, ENSICAEN, UNICAEN, CEA, CNRS, Caen, France
[2]Astronomical Institute of the Slovak Academy of Sciences, T. Lomnica, Slovakia
[3]Institute of Physics, University of São Paulo, Brazil
[4]Institute for Nuclear Research (Atomki), Debrecen, Hungary
[5]Centre for Astrophysics and Planetary Science, School of Physical Sciences, University of Kent, Canterbury, United Kingdom
[6]School of Electronic Engineering and Computer Science, Queen Mary University of London, United Kingdom
[*]rothard@ganil.fr

Complex organic molecules (COMs, including amino acids and nucleobases) can be formed in cold space environments by e.g. UV irradiation and ion bombardment of ices containing simple molecules. COMs formed in space could contribute to the emergence of life; consequently, their radiation resistance should be studied in order to determine their survival times [1,2]. Temperatures on objects containing COMs cover a range from as low as 10 K in dense molecular clouds, through 25 to 150 K in the outer Solar system, and up to >300 K in the inner solar system.We therefore studied the radiolysis and radio-resistance of the purine nucleobase Adenine in solid phase as a function of temperature (20-300 K) with H (0.8 MeV) and He (3.2 MeV) beams (which mimic cosmic rays) at ATOMKI by in situ Fourier transform infrared absorption spectroscopy. The samples deposited on infrared transparent window (ZnSe) are mounted on a closed-cycle helium cryostat which allows cooling them down to about 20 K in order to simulate the conditions inside dense molecular clouds. The samples can also be held at other temperatures up to 300 K to simulate the temperatures occurring in the inner and outer solar system [3]. The apparent destruction cross sections of nucleobases are determined from the exponential decay of the peak areas of IR absorption lines as a function of the projectile fluence. Adenine is found to be significantly (of the order of 50%) more radio-resistant at high temperatures. Furthermore, the destruction cross sections scale with the electronic stopping following a power law with a stronger than linear dependence. This project has received funding from the European Union's Horizon 2020 research and innovation programme under grant agreement No 871149.

References

[1] G. S. Vignoli Muniz, C. F. Mejía, R. Martinez, B. Augé, H. Rothard, A. Domaracka, Ph. Boduch Radioresistance of adenine to cosmic rays, *Astrobiology* 17(4) (2017) 298-308, doi:10.1089/ast.2016.1488

[2] Prudence C. J. Ada Bibang, *et al.*, Ion radiation in icy space environments: Synthesis and Radioresistance of Complex Organic Molecules, *Low Temperature Physics* 45 (2019) 590-597, doi: 10.1063/1.5103250

[3] Péter Herczku, *et al.*, The Ice Chamber for Astrophysics-Astrochemistry (ICA): A New Experimental Facility for Ion Impact Studies of Astrophysical Ice Analogues, Rev. Sci. Instrum. 92 (2021) 084501, doi: 10.1063/5.0050930

Atomistic model of wet chemical etching of SHI tracks in olivine

S.A. Gorbunov[1,*], R.A. Rymzhanov[2,3] A.E. Volkov[1,2,4]

[1]*P.N. Lebedev Physical Institute of the Russian Academy of Sciences, Leninskij pr., 53,119991 Moscow, Russia*

[2]*Joint Institute for Nuclear Research, Joliot-Curie 6, 141980 Dubna, Moscow Region, Russia;*

[3] *The Institute of Nuclear Physics, Ibragimov St. 1, 050032 Almaty, Kazakhstan;*

[4]*National Research Centre 'Kurchatov Institute', Kurchatov Sq. 1, 123182 Moscow, Russia;*

[*] *gorbunovsa@lebedev.ru*

Combination of the swift heavy ion (SHI) irradiation and wet chemical etching is widely applied technology for manufacturing of nano- microstructures: nanopores, nanowires, polymer filters, nano- and micro-diaphragms [1]. The technique is also used for registration of tracks of heaviest galactic cosmic rays nuclei [2] in meteorites and satellite detectors.

Despite of widespread interest to the etching treatment of SHI tracks, etching models face crucial difficulties with description of temporal evolution of pores, especially in anisotropic crystals. For example, etching of tracks of ions with the same dE/dx, but with different velocities may result in a different etched pore shapes [3], which can not be predicted before irradiation & etching experiments in current state of art.

This motivated us to develop an atomistic model of wet chemical etching. In this scheme Monte-Carlo code TREKIS [4] describing electronic excitation in SHI track is combined with MD simulations of subsequent relaxation of the lattice [5]. Application of these models provide initial conditions for transition state theory based algorithm of sequential removal of atoms from etching surface.

We applied this approach to SHI track etching in crystalline olivine (Mg_2SiO_4). We demonstrate dependence of etched pore shape on various crystallographic orientations. The model describes a transition of a rounded pore resulting from cylindrical symmetry of structural damage in SHI track into the polygonal shape.

References

[1] F.F. Komarov, *Physics-Uspekhi*, 60 (2017) 435–471

[2] V. Alexeev, A. Bagulya, V. Alexeev, et al., *Astrophys. J.* 829 (2016) 120

[3] M. Lang, K. Voss, R. Neumann, et al., *GSI Sci. Rep.* 3 (2006) 343

[4] N.A. Medvedev, R.A. Rymzhanov, A.E. Volkov, *J. Phys. D. Appl. Phys*, 48 (2015) 355303.

[5] A.P. Thompson, H.M. Aktulga, R. Berger, et al., *Comput. Phys. Commun*. 271 (2022) 108171.

Clocking the relaxation of hollow atoms in solids by x-rays

Ł. Jabłoński, D. Banaś, P. Jagodziński, A. Kubala-Kukuś, D. Sobota, I. Stabrawa, K. Szary and M. Pajek*

Institute of Physics, Jan Kochanowski University, 25-406 Kielce, Poland
*pajek@ujk.edu.pl

The ultrafast relaxation of highly excited Rydberg ($n \approx$ 20-30) hollow atoms [1], formed in collisions of slow, highly charged Xe^{q+} ions (q=23-36) with metallic Be foil, was studied by observing X-ray emission. The pulsed beams of Xe^{q+} ions were produced in the EBIS facility and the M-X-rays ($nf \rightarrow 3d$) emitted from radiative relaxation of Xe were measured by a Si drift detector. The developed dead-time correction for pulsed X-rays was necessary to consider in order to derive the X-ray yields and, consequently, the decay rates.

The observed X-ray spectra, which were interpreted in terms of the performed MCDF calculations, clearly demonstrate the importance of two-electron relaxation processes in hollow atoms such as the Internal Dielectronic Excitation (IDE) [2], the Two-Electron-One Photon (TEOP) transition and the Interatomic Coulombic Decay (ICD) [3]. By modelling the measured X-ray spectra for different charge states, the relative contributions of discussed processes were obtained as well as the decay rates were estimated. In particular, by observing a cut-off of X-ray emission in the measured Paschen series at $n \approx$ 10-20, it was demonstrated experimentally that ICD plays dominating role in early stage of nonradiative relaxation of hollow atoms in solids [4]. Further fast deexcitation of hollow atoms by Auger and IDE processes, as estimated from the measured fluorescence yields, makes the full relaxation to the ground state an ultrafast process.

References

[1] J.P. Briand et al. , *Phys. Rev. Lett.* 65, 1990, 159.
[2] R. Schuch et al. *Phys. Rev. Lett.* 70, 1993, 1073.
[3] L. S. Cederbaum, J. Zobeley and F. Tarantelli, *Phys. Rev. Lett.* 79, 1997, 4778.
[4] R. A. Wilhelm et al., *Phys. Rev. Lett*. 119, 2017, 103401.

Application of the XPS and TRXPS techniques for the analysis of Ti and TiO_2 surfaces after modification with slow highly charged Xe^{q+} ions

A. Kubala-Kukuś[1,2], D. Banaś[1,2], M. Piwowarczyk[1], I. Stabrawa[1,2,*], K. Szary[1,2], D. Sobota[1], R. Stachura[1], J. Wudarczyk-Moćko[2], J. Braziewicz[1,2], and M. Pajek[1]

[1] *Institute of Physics, Jan Kochanowski University, Uniwersytecka 7, 25-406 Kielce, Poland*
[2] *Holycross Cancer Center, Artwińskiego 3, 25-734 Kielce, Poland*
[*] *ilona.stabrawa@ujk.edu.pl*

In order to improve the biological, chemical and mechanical properties, the surface of materials are often modified [1]. One of the method of the modification is the irradiation of the surface with low-energy (nuclear stopping power regime) highly charged ions (HCI). These ions are characterized by an additional (to the kinetic energy) high potential energy resulting from the removal of electrons from a neutral atom (see [2] and references therein).

In this work, the surfaces of Ti and TiO_2 nanolayers deposited on Si and SiO_2 substrates were analyzed. The samples were modified with slow Xe^{q+} ions delivered by EBIS accelerator at the Institute of Physics of Jan Kochanowski University (Kielce, Poland) [3]. X-ray photoelectron spectroscopy techniques in the non-total (XPS) and total reflection (TRXPS) regimes were used to analyze the surface of the nanolayers before and after their modification with slow HCI Xe^{q+} ions. In the XPS technique, a low energy (Al Kα) X-ray beam is directed towards the studied surface at an angle of several tens of degrees. In the TRXPS technique this angle is lower (or very close) than the critical angle of the X-ray beam, which value depends on the X-ray energy and the type of material being studied. Under such geometrical conditions, X-rays do not penetrate deeper into the sample than the range of the evanescent wave (on the order of 20–40 Å) [4]. The XPS and TRXPS measurements were carried out using XPS system (SPECS) at the Institute of Physics of the Jan Kochanowski University (Kielce, Poland).

In the XPS and TRXPS measurements both survey and detailed spectra (photoelectron peaks C1s, N1s, Ti2p and O1s) were investigated. The measurements gave information about the surface properties of Ti and TiO_2 nanolayers (electron binding energy, elemental composition, chemical environment of the elements). It was shown, that the use of TRXPS geometry increases the intensity of the photoelectron lines and at the same time lowers the background in XPS spectra.

References

[1] T. Rautray, R. Narayanan, T-Y. Kwon, K-H. Kim, *J. Biomed. Mater. Res. Part B, Appl. Biomater.*, 93 (2010) 581-591

[2] F. Aumayr, S. Facsko, A. S. El-Said, C. Trautmann, M. Schleberger, *J. Phys.: Condens. Matter*, 23 (2011) 393001

[3] D. Banaś, Ł. Jabłoński, P. Jagodziński, A. Kubala-Kukuś, D. Sobota, M. Pajek, *Nucl. Instrum. Methods Phys. Res.B*, 354 (2015) 125-128

[4] A. Kubala-Kukuś, D. Banaś, I. Stabrawa, K. Szary, D. Sobota, U. Majewska, J. Wudarczyk-Moćko, J. Braziewicz, M. Pajek, *Spectrochim. Acta Part B At. Spectrosc.*, 145 (2018) 43-50

Analysis of TiO_2 and Ti nanolayers irradiated with low-energy Xe^{q+} ions using synchrotron radiation induced XRR and GIXRF methods

R. Stachura[1,*], A. Kubala-Kukuś[1,2], D. Banaś[1,2], I. Stabrawa[1,2], K. Szary[1,2], P. Jagodziński[1], G. Aquilanti[3], I. Božičević Mihalić[3,4], J. Braziewicz[1,2], M. Pajek[1], J. Semaniak[1]

(1) Institute of Physics, Jan Kochanowski University, Uniwersytecka 7, 25-406 Kielce, Poland
(2) Holycross Cancer Center, Artwińskiego 3, 25-734 Kielce, Poland
(3) Elettra - Sincrotrone Trieste, s.s. 14, km 163.5 in Area Science Park, 34149 Basovizza, Trieste, Italy
(4) Rudjer Boskovic Institute, Bijenicka cesta 54, 10000 Zagreb, Croatia
**e-mail: regina.stachura06@gmail.com*

Modification of metal, semiconductor and insulator surfaces by ion irradiation is of great importance for developing new technologies for manufacturing electronics system with nanometer dimensions. One of promising technologies, which gives possibility for obtaining novel physico-chemical properties of materials, diffcult to achieve with other processing methods, is modification of materials surfaces by irradiation with low-energy highly charged ions (HCI) [1-2].

The main aim of this study is to determine the changes in morphology and physico-chemical properties of TiO_2 and Ti nanolayers caused by irradiation with the HCI ions. The nanolayers were irradiated with Xe^{q+} (q = 25-40) ions of energy in the houndreds of keV range at the Kielce EBIS facility (Jan Kochanowski University, Kielce, Poland) [4]. In order to investigate the changes of nanolayers properties, as a result of the HCI irradiation surface sensitive X-ray spectroscopy techniques were applied. X-ray reflectometry (XRR) method was used to determine density, thickness and roughness of the nanolayers. Grazing Incidence X-ray fluorescence (GIXRF) technique allowed to determine the depth distributions of the elemental composition [3]. The XRR and GIXRF measurements were performed at Elettra Synchrotron X-ray fluorescence beamline, using synchrotron X-ray beam with energy 6.0 keV. In the presented studies characterization of TiO_2 and Ti nanolayers of thickness of 25 nm, 50 nm and 75 nm, deposited on the Si substrate, not implanted and implanted with Xe^{q+}, was performed.

Comparison of the roughness of the TiO_2 and Ti nanolayers, unmodified and irradiated with HCI, shows that irradiation of the nanolayers change the roughness of the outermost surface layer and the change depends on the ion charge states. The results obtained from GIXRF method show changes of the angular dependence of the intensities of Ti-Kα and Si-Kα lines on the thickness of nanolayers and the ion charge states.

References

[1] A. B. Cusick, et al., Nucl. Instrum. Methods Phys. Res. B 407, (2017), 25-33
[2] L. Q. Zhang et al., Nucl. Instrum. Methods Phys. Res. B 269, (2011), 2835-2839
[3] R. Klockenkämper, Spectrochim. Acta B 61 (2006) 1082-1090.
[4] D. Banaś, et al., Nucl. Instrum. Methods Phys. Res. B 354 (2015) 125-128.

Molecular Dynamics Simulations of Electronic Sputtering in Amorphous Silica induced by Swift Heavy Ions

Francisco Sánchez-Pérez[1], Alejandro Prada[2], Mathieu Bailly-Grandvaux[3], Eduardo Bringa[4], María José Caturla[5], José Manuel Perlado[1,6], Jorge Kohanoff[1,6], Ovidio Peña-Rodríguez[1,6], and Antonio Rivera[1,2]

[1]*Instituto de Fusión Nuclear "Guillermo Velarde", Universidad Politécnica de Madrid, Spain*
[2]*Universidad Católica de Maule, Chile*
[3]*University of California San Diego, EE.UU*
[4]*Universidad de Mendoza, Argentina*
[5]*Departamento de Física, Universidad de Alicante, Spain*
[6]*Departamento de Ingeniería Energética, ETSI Industriales, Universidad Politécnica de Madrid, Spain*

The atom emission from surfaces in solids under swift heavy ion irradiation, often named electronic sputtering, is a research field under-investigation. New experimental methodologies and new mathematical models are making possible understand the underlying physical phenomena. Swift heavy ion irradiation produces high electronic excitation followed by multiple processes that eventually lead to energy transfer of the incident ion to the lattice. In the near-surface region, atom emission occurs with a yield several order of magnitude higher than the equivalent emission by physical sputtering.

This work is focused on the study of atomistic simulations by means of molecular dynamics. For validation purposes, these results were compared with experimental data [1-6]. Despite we used a simple model to simulate the energy deposition, the simulations reproduce consistently a broad range of experimental data obtained at different incidence angles (from glancing to normal) and stopping powers. We conclude that three mechanisms dominate the surface evolution: (i) An ejection mechanism that describes the experimentally observed angular distributions of emitted atoms, the total sputtering yield correlation with the electronic stopping power and incidence angle. (ii) A collective mechanism that explains the energy dissipation of bulk atoms and the density changes, residual stress, defect formation and optical variation. (iii) A flow mechanism, responsible for the surface.

References

[1] S. Sugden *et al*., Nucl. Instrum. Methods Phys. Res. Sect. B Beam Interact. Mater. At. **67**, 569 (1992).
[2] M. Toulemonde *et al*., Nucl. Instrum. Methods Phys. Res. Sect. B Beam Interact. Mater. At. **379**, 2 (2016).
[3] N. Matsunami *et al*., Nucl. Instrum. Methods Phys. Res. Sect. B Beam Interact. Mater. At. **193**, 830 (2002).
[4] N. Matsunami *et al*., Nucl. Instrum. Methods Phys. Res. Sect. B Beam Interact. Mater. At. **209**, 288 (2003).
[5] W.M. Arnoldbik *et al*., Nucl. Instrum. Methods Phys. Res. Sect. B Beam Interact. Mater. At. **203**, 151 (2003).
[6] W. Assmann *et al*., Sputtering Part. Bombard. **401** (2007).

Analytical model for the temperature field of a plasma heated by fast and monoenergetic ion beams

G. Espinosa-Vivas[1,*], **J.M. Gil**[1], **R. Rodriguez**[1] **and P.R.Beltrán**[1,2]

[1]*Departament of Physics, Universidad de Las Palmas de Gran Canaria, Spain*
[2]*Instituto de Astrofísica de Canarias, Spain*
[*] *guadalupe.espinosa@ulpgc.es*

In diverse areas of research and applications such as fusion, astrophysics and plasma ion heating, the interaction between fast ion beams and target plasmas is a topic of relevant interest [1]. The study of this phenomenon requires precise knowledge of the energy deposition of the beam particles and the heating of the plasma [2]. In this work we present an analytical model for the calculation of the temperature field of a fully ionized deuterium-tritium (DT) target plasma due to its interaction with a fast ion beam. In our problem, the precompressed DT fuel has spherical geometry, with homogeneous temperature and density. The ion beam is assumed to be formed by point-like fast and monoenergetic fully stripped ions with radial direction. Therefore, due to the symmetry, the interaction beam-target can be described as 1D [2]. Since the characteristic time of the interaction is considerably shorter than the characteristic hydrodynamic time and the plasma is in the stagnation state the plasma can be considered as static. Therefore, the change in the plasma temperature depends only on the energy deposited by the beam projectiles, since the mechanical work and conduction can be neglected, and can be obtained as follows

$$\frac{dT(x,t)}{dt} = \frac{db(t)}{dt}\frac{1}{\rho(x,t)c_v(x,t)}S_p(x,t;E_{k0}), \tag{1}$$

where $b(t)$ is the flux of particles of the beam, $\rho(x,t)$ is the density of matter and $c_v(x,t)$ is the heat capacity (constant since the precompressed plasma is assumed as an ideal gas). Furthermore, the process can be considered as isochoric (the density of the plasma is approximately constant). Finally, $S_p(x,t;E_{k0})$ denotes the stopping power (SP) (with E_{k0} the initial kinetic energy of the projectile) which represents the slowing down of the projectiles due to the plasma particles of the plasma (free electrons and deuterium and tritium nuclei), which allows to obtain the variation of the beam energy per unit length. As said above, an approximated analytical model for the temperature field of the plasma (Eq. (1)) is given. The model is obtained using the asymptotic behaviours at high and low energies of the SP and assuming that the deposition of the energy in the plasma is very fast. Then, the plasma temperature fields are obtained for different kind of beams (changing the ion, the flux of particles and the initial kinetic energy). This analytical model provides relationships between the main variables, which are useful to achieve a better understanding of the phenomenon.

This work has been supported by the Spanish Government through the Project PID2019-110678-I00 and by the Consejería de Economía, Industria, Comercio y Conocimiento del Gobierno de Canarias.

References

[1] S.N. Chen et al., *Sci. Rep.,* 8 (2018) 14586.
[2] P.R. Beltrán et al., *X-Ray Spectrom*., 49 (2020) 173-176.

The Effects of SHIs on Si_3N_4

A. Janse van Vuuren[1,*], **A. Ibrayeva**[1], **V. Skuratov**[2,3,4], **and M. Zdorovets**[5,6]

[1]*Centre for HRTEM, Nelson Mandela University, South Africa*
[2]*Flerov Laboratory of Nuclear Reactions, Joint Institute for Nuclear Research, Russia*
[3]*National Research Nuclear University MEPhI, Russia*
[4]*Dubna State University, Russia*
[5]*Astana Branch of Institute of Nuclear Physics, Kazakhstan*
[6]*Ural Federal University, Russia*
[*]*arnojvv@gmail.com*

Si_3N_4 is the only known nitride ceramic demonstrating microstructural sensitivity to dense electronic excitation effects i.e., latent tracks have been observed only in this nitride material [1-8]. Si_3N_4 has proven useful as a probe for multiple factors which play a role in the formation of latent ion tracks in materials, such as thermal conductivity, dopant levels, phase, temperature, and the stopping power of the incident ion [9,10].

There are clear indications that the number of impurities play a role in the formation of latent ion tracks. In Si_3N_4 with Al impurities of the order of 3 at% tracks form more easily as opposed to its high purity counterparts. It is likely that impurities may enhance phonon scattering which in effect can lead to a reduction in thermal conductivity.

The creation of a radiation induced amorphous phase, due purely to electronic stopping effects, has also been observed in Si_3N_4, the onset of which is also enhanced by a greater amount of impurities. The formation of latent ion tracks in this radiation amorphous phase has also been observed and is compared to those in amorphous thin films of silicon nitride.

The analysis of latent ion tracks in nanocrystalline particles of Si_3N_4 suggests that crystallite size plays little role in the formation of latent ion tracks in this material.

To assess the microstructural response of Si_3N_4 to swift heavy ion irradiation, polycrystalline (Al doped) bulk samples, amorphous thin films and nanoparticles were irradiated with ions of varying stopping power. The samples were irradiated with Bi (710 MeV) and Xe (167, 220, 480 MeV) ions to fluences from 1.1×10^{11} cm^{-2} up to fluences exceeding 1×10^{15} cm^{-2}. Selected samples were also irradiated with 220 MeV Xe ions at temperatures ranging from LNT to 1000 K. The microstructural effects were analysed using transmission electron microscopy techniques.

References

[1] S.J. Zinkle, V.A. Skuratov and D.T. Hoelzer, Nucl. Instrum. Methods Phys. Res. B 191 (2002) 758
[2] A. Janse Van Vuuren, V. Skuratov, A. Ibraeva and M. Zdorovets, Acta Phys. Pol. A 136 (2019) 241
[3] T. Kitayama, et al., Nucl. Instrum. Methods Phys. Res. B 356 (2015) 22
[4] H. Hayashi, et al., Nucl. Instrum. Methods Phys. Res. B 406 (2017) 591
[5] S. Matsuzaki, et al., Nucl. Instrum. Methods Phys. Res. B 406 (2017) 456
[6] B. Canut, et al., Nucl. Instrum. Methods Phys. Res. B 266 (2008) 2819
[7] L.A. Vlasukova, et al., Bull. Russ. Acad. Sci. Phys. 74 (2010) 206
[8] L. Vlasukova, et al., J. Vacuum 129 (2016) 137
[9] M. Toulemonde et al., Nucl. Instrum. Methods Phys. Res. B 166 (2000) 903
[10] G. Szenes, Rad. Effects & Defects in Solids 175 (2020) 241

A computational approach to the formation and free decay of hollow atoms

M. Werl[1,*], **A. Niggas**[1], **K. Tőkési**[2], **F. Aumayr**[1], **and R. A. Wilhelm**[1]

[1]*Institute of Applied Physics, TU Wien, Vienna, Austria*
[2]*Institute for Nuclear Research, Hungarian Academy of Sciences, Debrecen, Hungary*
[*]*Corresponding Author: werl@iap.tuwien.ac.at*

A hollow atom (HA) is formed when a highly charged ion approaches a surface. Its formation can be described using the classical over-the-barrier model [1]. At a certain distance above the surface ($d_c \propto \sqrt{q_{in}} \approx 10 - 25$ Å), electrons are resonantly captured into excited, high-n shells ($n_c \approx q_{in}$), while inner atomic shells initially remain empty. Subsequently, these excited electrons decay through radiative or Auger processes.
Here, a computational approach for the study of free HAs is presented [2]. After its formation due to the resonant capture of electrons, the subsequent decay is calculated using a Monte-Carlo approach with corresponding rate equations for radiative and Auger-decay, giving the evolution of the HA's charge state and shell occupation as well as the energy spectra of emitted particles.
The Auger-transition rates are approximated by using a fit for rates obtained from atomic structure codes [1]. The radiative rates are approximated by fitting a large dataset of experimentally available data [3]. These approximate rates depend on the element with nuclear charge Z as well as the initial shell n_i and the final shell n_f of a decaying electron.
Fig. 1 shows preliminary results of this approach: The time evolution of the average number of excited electrons (red) and the HAs charges state (green) for an ensemble of 10^4 Xe^{40+}-ions colliding with a Ni surface are shown. The HA decay time is the time, after which only $\frac{1}{e}$ of the captured electrons remain in excited states.

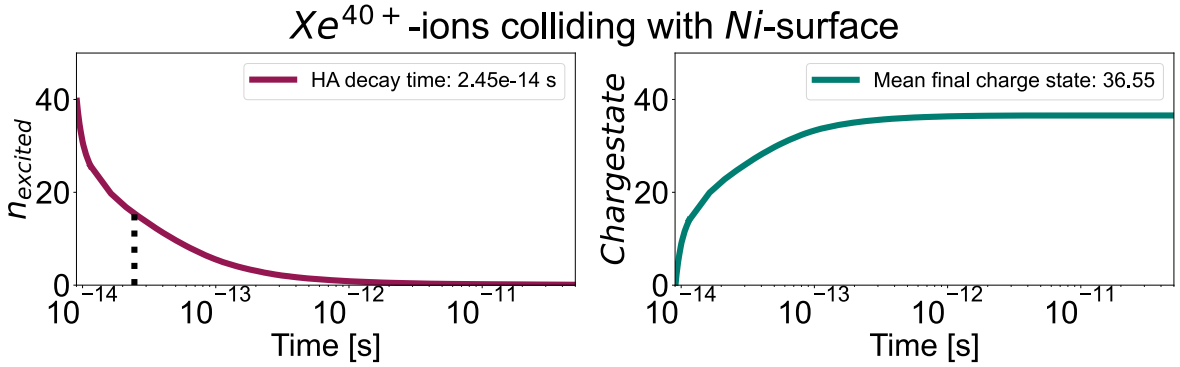

Figure 1: Xe^{40+}-ions impacting onto a Ni-surface. Average values of an ensemble of 10^4 projectiles are shown. a) Remaining number of excited electrons inside the HA. After the decay time, the number of excited electrons has dropped to $\frac{1}{e}$ of its initial value. b) Charge state evolution of the projectile.

A comparison with experimental data on final ion charge states and electron emission spectra is presented.

References

[1] J. Burgdörfer, P. Lerner, F. W. Meyer, *Phys. Rev. A*, **44** (1991) 9
[2] K. Tőkési, L. Wirtz, C. Lemell, J. Burgdörfer, *Phys. Rev. A*, **64** (2001), 042902
[3] NIST Atomic Spectra Database, https://physics.nist.gov/PhysRefData/ASD/lines_form.html, Accessed: 2022-01-05

High-dose high-energy irradiation effects on the defect evolution in tungsten

J. Wu[1,*] **and F. Granberg**[1]

[1] *Department of Physics, University of Helsinki, Post-office box 43, FIN-00014 University of Helsinki, Finland*
[*] *jintong.wu@helsinki.fi*

Tungsten is attractive for fusion applications due to its high melting point and high thermal conductivity. Irradiation of tungsten has been studied computationally for decades, however mainly focusing on single cascades at different energies. Experimental studies and especially production power plants are and will always be at higher doses (i.e. overlapping cascades), causing morphology changes and different defect production compared to single cascades.

One recent study has focused the defect evolution under 10 keV overlapping cascade irradiation in tungsten [1]. Although 10 keV is enough to reach a high dose, the effect of higher energy irradiation, common in fusion-relevant conditions, on the defect evolution, is still an unanswered question. In this study we investigate; 1) The process of defect production and volumetric swelling under higher energy overlapping cascade irradiation; 2) The similarity of the evolution of defects, clusters and dislocations under different energy irradiation conditions; 3) The damage evolution under Full-MD simulations and Cascade annealing on cells damaged by FP insertion (used to speed up the simulations to reach higher doses); 4) Rationality of cascade annealing on cells obtained by FP insertion, and comparison of differences and consistencies between the results of pure thermal annealing and cascade annealing.

References

[1] F. Granberg, J. Byggmästar, and K. Nordlund, *Journal of Nuclear Materials*, 556 (2021) 153158

Investigation of He and Kr ion irradiation effects on NiCoFeCr and NiCoFeCrMn high entropy alloys

A. Yaqoob[1,2,*], **N. Mora**[2], **and V.V. Uglov**[1]

[1] *Faculty of Physics, Belarusian State University*
[2] *Directed Energy Research Center, Technology Innovation Institute, Abu Dhabi, UAE*
[*] *ali.yaqoob@tii.ae*

The possibilities in forming high-entropy alloys (HEAs) are endless, giving new opportunities in advancing material science to find advanced materials to perform better than conventional alloys in extreme conditions such as a high irradiation environment. In this work, NiCoFeCr and NiCoFeCrMn HEAs samples were produced by arc melting and casting in a copper cell, followed by vacuum annealing. The HEAs samples were investigated with i) Energy Dispersive X-ray Spectroscopy (EDS) to obtain their elemental composition, ii) Scanning Electron Microscopy (SEM) to obtain their surface structure, and iii) X-Ray Diffraction (XRD) to obtain their phase composition, interplanar spacing, and lattice parameter. The samples were irradiated at 300° K with He ions with the energy of 40 keV at a fluence of 2 x 10^{17} cm^{-2}, and Kr ions at 300° K with 280 keV at a fluence of 5 x 10^{15} cm^{-2}. Lastly, the samples were irradiated with both He and Kr ions with the previously mentioned energies and fluences. It was found that the HEAs samples have grain sizes smaller than 300 µm. In addition, the samples showed phase stability having a single FCC phase before and after irradiation. Also, the HEAs showed elemental composition stability by being equiatomic before and after irradiation and no surface structure erosion due to irradiation. The results show that HEAs are an excellent candidate for next-generation nuclear plants.

References

[1] Z. Zhang, D. E. Armstrong and P. S. Grant, Progress in Materials, 123 (2021).
[2] B. Murty, J. Yeh and S. Ranganathan, Elsevier (2014).

Chemical damage and surface roughness induced by 1 MeV/u C and 9 MeV/u Ne ions in thin polymer films of different thickness

R. S. Thomaz[1,2*], **J.P. May**[1], **F. V. Filho and Y. Ngono-Ravache**[3] and **R. M. Papaléo**[1*]

[1]*School of Technology, Pontifical Catholic University of Rio Grande do Sul, Porto Alegre, Brazil*
[2]*Institute of Physics, Federal University of Rio Grande do Sul, Porto Alegre, Brazil*
[3]*CIMAP UMR 6252 (CNRS/CEA/ENSICAEN/UNICAEN), France*
[*]*raquel.thomaz@pucrs.br*

In this work, chemical damage induced by 1 MeV/u C ions and 9 MeV/u Ne ions in PMMA and PVC was systematically investigated, following bond breaking rates as a function of the thickness h of the layers (2<h<100 nm). Bond breaking was followed by XPS and FTIR, and morphological changes were investigated by SFM. Marked differences were observed on surface morphology induced in PMMA and PVC films. The effect of both ion beams on the PMMA surface was a pronounced roughening, followed by smoothening at high fluences. This roughening process is thickness dependent for PMMA, but not for PVC. Preliminary data indicate that damage cross sections for bond-breaking in PMMA films, estimated from FTIR, are smaller for thinner layers. There are although several challenges for the quantification of the bond breaking rates, beyond the reduced signal from the thinnest layers. The morphological changes in the films due to ion bombardment (roughness, coverage, density) plus thickness decrease due to sputtering can all play a role in quantification and are going to be discussed.

Observation and characterization of ion latent tracks in semicrystalline polymers by SEM

P.Y.Apel[*], I.V. Blonskaya, O.V. Kristavchuk, S.A. Mityukhin, A.N. Nechaev, O.A. Polezhaeva, O.L. Orelovich

Joint Institute for Nuclear Research, Dubna, Russia
[*] *apel@jinr.ru*

The observation of ion latent tracks using various microscopy methods is an important part of studies on fundamental mechanisms of high LET radiation effects. Transmission electron microscopy (TEM) and scanning probe microscopy have been widely employed to image ion tracks in solids. In contrast, scanning electron microscopy (SEM) has been hardly applicable. In the present study, we show how SEM can be used to observe latent tracks in semicrystalline polymers. The procedure includes the embrittlement of a specimen by controlled photo-oxidation and its subsequent fracture. A proper choice of an ultraviolet (UV) spectrum provides polymer degradation only in amorphous regions. Once this condition is fulfilled, latent tracks are clearly visible on fractured surfaces as structureless stripes surrounded by an inhomogeneous semicrystalline matrix. The FTIR spectroscopy showed that ion irradiation leads to a significant decrease in the intensity of "crystalline" spectral bands as compared to the "amorphous" ones, while the exposure to soft UV light barely affects the crystalline-to-amorphous band intensity ratio. In contrast, stronger UV irradiation leads to homogeneous amorphization and makes latent tracks invisible to SEM imaging.

The latent tracks of Kr, Xe and Bi ions in polyethylene terephthalate (PET) and polypropylene (PP) films were observed (Figure 1). The width of the observed stripes in PET reaches ~40 nm, i.e. considerably larger than the typical track core diameter estimated by TEM. However, the width of tracks in PP is ~ 10 nm, which evidences that the track halo is highly diffuse due to long-range energy migration in polyolefins. Therefore, the developed method makes it possible to image either track core or track halo, depending on polymer nature. Using image analysis software, the track width as a function of ion energy loss was estimated. It can be concluded that SEM observations can complement other commonly used techniques to comprehensively characterize the structure of ion tracks in polymers.

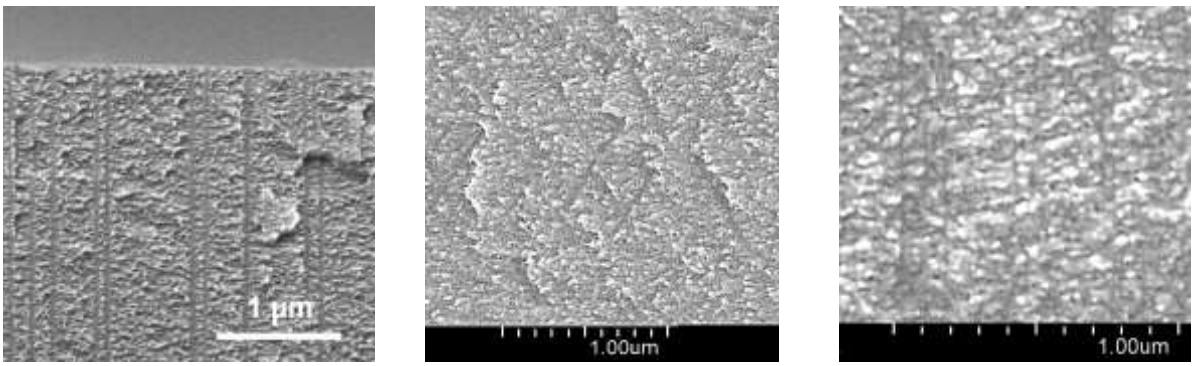

Figure 1. SEM images of fractured surfaces of a PET foil with parallel Xe ion tracks (left); a PET foil with Xe ion tracks crossing each other at an angle of 60° (center); a PP foil with parallel Xe ion tracks (right).

The mechanism of formation of ion-selective channels in PET foils subjected to ion irradiation, photo-oxidation and aqueous extraction

P.Y. Apel[1*], **I.V. Blonskaya**[1], **O.M. Ivanov**[1], **O.V. Kristavchuk**[1], **A.N. Nechaev**[1], **K. Olejniczak**[1,2], **O.A. Polezhaeva**[1], **O.L. Orelovich**[1], **S.N. Dmitriev**[1]

[1]*Joint Institute for Nuclear Research, Dubna, Russia*
[2]*Nicolaus Copernicus University, Gagarina str. 7, 87-100 Torun, Poland*
[*]*apel@jinr.ru*

Recently it was found that a long-time exposure to ultraviolet (UV) radiation followed by extraction of radiolysis and photolysis products from heavy ion tracks allows fabrication of ion-selective membranes from polyethylene terephthalate (PET) films irradiated with heavy ions [1]. The aim of this work was a detailed study of mechanisms responsible for the formation of ion-permeable and ion-selective channels. PET films were irradiated under different angles with accelerated Xe and Bi ions with energy losses of 11 and 18 keV/nm, respectively. The amount of matter removed from the films by energetic ions and by liquid extraction is measured and compared with the amount of carboxyl groups produced by the ion and UV exposure. The change in electrical conductivity of the films during the liquid extraction is studied depending on the atomic number of bombarding ion, ion fluence, temperature, mechanical stress, and properties of starting material. Examination of samples irradiated at different angles shows that interconnection of ion tracks in the membrane bulk drastically enhances the ionic permeability by reducing the intrapore energy barrier. Both external and internal stresses have a pronounced effect on the development of the ion-conductive structure. It can be concluded that

- Swift heavy ions create large free volume in PET foils due to direct evaporation of volatile radiolysis products from tracks
- The number of carboxyl groups created along the ion tracks is of the order of 10^2 per 1 nm of track length
- Aqueous extraction removes several tens of terephthalic acid molecules from 1 nm of track length
- Compared to parallel tracks, arrays of intercrossing tracks have a much higher conductivity and a lower selectivity
- Molecular relaxation and mechanical stress are important factors
- Ion-conducting charged gel-filled channels are much wider than 1 nm
- The resulting structure resembles a heterogeneous ion-exchange membrane

References

[1] P. Wang, M. Wang, F. Liu, S. Ding, X. Wang, G. Du, J. Liu, P. Apel, P. Kluth, C. Trautmann, Y. Wang, *Nature Commun*. 9 (2018) 569.

Influence of low energy (80 keV) ion beam modifications in structural optical and morphological properties of tungsten oxide thin films deposited by RF sputtering

Deepika[1], Deepika Gupta[1], Vishnu Chauhan[2], Rashi Gupta[3], Aman Mahajan[4], Rajesh Kumar[1*]

[1]University School of Basic and Applied Sciences,
Guru Gobind Singh Indraprastha University, New Delhi-110078, India
[2]Materials Science Group, Inter-University Accelerator Centre,
ArunaAsaf Ali Marg, New Delhi - 110067, India
[3]Department of Physics, J.C. Bose University of Science & Technology, YMCA,
Faridabad-121006, India.
[4]Department of Physics, Guru Nanak Dev University, Amritsar-143005, India.
*Corresponding author: kumarrrpi@gmail.com

Abstract

Recently, metal oxides-based nanoparticles are widely used in many fields[1-2]. Among them, Tungsten trioxide (WO_3) is the most promising material exhibiting wide band gap of 2.7 eV making it highly effective for various applications including sensing devices, electrochromic devices, photocatalyst, electrochemical cells, capacitors, and smart windows [3-4]. In the present work, Tungsten oxide (WO_3) thin films were grown by RF Sputtering method on the glass and silicon substrate with a thickness of 100 nm. Tungsten oxide thin films were implanted by Au ion with 80 keV energy at different fluences 5E14, 1E15 and 5E15 at IUAC New Delhi, India. After ion beam implantation, pristine and implanted thin films were characterized by XRD, AFM, UV-Vis., Raman, FTIR, RBS, and Photoluminescence XPS. The grain size, roughness were calculated by AFM. Optical study of thin films includes parameters such as energy band gap, absorption coefficient, skin depth, Urbach energy, optical density and extinction coefficient were calculated by using UV-Vis spectroscopy. The chemical structure and crystal phase of the pristine and irradiated thin films were analyzed by Raman spectroscopy. Rutherford Backscattering Spectroscopy (RBS) is used for analysis of thickness and chemical compositions of elements. Photoluminescence (PL) spectra were used to determine the change in intensity and shifting of strong and broad emission spectra. XPS study shows the binding states and elemental composition in the pristine and implanted thin films. Detailed results will be discussed during the presentation.

References:

1. H. Torvela, T. Jaakola, A. Uusima¨ki, and S. Leppa¨vuori, J. Electron. Mater. 15, 7 (1986).
2. M. Andrzejczuk, A. Roguska, M. Pisarek, M. Hołdyn´ ski, M. Lewandowska, and K.J. Kurzydłowski, Micron 95, 35 (2017).
3. W.J. Lee, Y.K. Fang, J.J. Ho, W.T. Hsieh, S.F. Ting, D. Huang, and F.C. Ho, J. Electron. Mater. 29, 183 (2000)
4. R. Kumar and V. Kumar Optical Materials 88, (2019) 320-332.

Effect of high dose gamma radiation on physico-chemical and photoluminescence, surface morphological properties of WO_3 thin films

Deepika [1], Deepika Gupta[1], Vishnu Chauhan[2], Aman Mahajan[3], Rajesh Kumar[1*]

[1]University School of Basic and Applied Sciences,
Guru Gobind Singh Indraprastha University, New Delhi-110078, India
[2]Materials Science Group, Inter-University Accelerator Centre,
ArunaAsaf Ali Marg, New Delhi - 110067, India
[3]Department of Physics, Guru Nanak Dev University, Amritsar-143005, India.

*Corresponding author: kumarrrpi@gmail.com

Abstract

In the present work Tungsten oxide (WO_3) thin films were deposited by R.F. Sputtering method on glass and silicon substrate with a thickness 200 nm After deposition, thin films were annealed at 550 ^{0}C for 24 hours. Gamma radiation shows good potential and ability to penetrate in the metal oxide-based nanomaterials and influences the *insitu* properties of the nanomaterials based thin films [1-2]. Finally, the annealed Tungsten oxide (WO_3) thin films were exposed to gamma irradiation with different doses (100kGy, 200kGy, 300kGy, 400kGy and 500kGy) by Cobalt-60 source at the room temperature. After gamma irradiation, pristine and gamma irradiation thin films were characterized by Atomic Force Microscopy (AFM), Fourier Transform Infrared Spectroscopy (FTIR), X-ray diffraction (XRD), Photoluminescence (PL) Spectroscopy, Raman Spectroscopy, Rutherford back Scattering (RBS) and UV visible Spectroscopy. Detailed results will be discussed during the presentation.

References:

[1] N. Lavanya *et al.*, "Effect of gamma irradiation on structural, electrical and gas sensing properties of tungsten oxide nanoparticles," *Journal of Alloys and Compounds*,693 (2017) 366-372.

[2] V. Chauhan, R. Kumar et al., Optical Materials 126(2022)112125.

Surface Modifications by Fast Heavy Ions and Slow Highly Charged Ions: Similarities and Differences

Ayman S. El-Said

Physics Department and Interdisciplinary Research Center for Advanced Materials, King Fahd University of Petroleum and Minerals, Dhahran 31261, Saudi Arabia
elsaid@@kfupm.edu.sa

It is well established that the single impact of fast heavy ions can efficiently produce structural modifications not only in the bulk but also in the irradiated material surface. This is confirmed by observing various types of ion-induced surface nanostructures in different materials [1-3]. The creation of these nanostructures is attributed to the deposition of large amount of ion kinetic energy along the ion penetration depth resulting in high energy density. Similar surface nanostructures were recently produced by irradiation with slow highly charged ions [4-6]. Despite the extremely small kinetic energy of these type of ions, they carry a large amount of potential energy (equal to the sum of the ionization potentials of the ion), which is deposited in nanometer-sized volume close to the surface producing strong electronic excitations comparable to the ones induced by fast heavy ions. These electronic excitations are then coupled in a later stage to the phononic system. Comparing the two types of ions in terms of the primary interaction with the surface as well as the subsequent electronic energy transfer to the lattice is of high interest for understanding the underlying mechanisms of nanostructures creation in various materials.

References

[1] N. Ishikawa, Y. Fujimura, K. Kondo, G.L. Szabo, R.A. Wilhelm, H. Ogawa, T. Taguchi, Nanotechnology 3, 235303 (2022).
[2] C. Länger, P. Ernst, M. Bender, D. Severin, C. Trautmann, M. Schleberger, M. Dürr, New J. Phys. 23, 093037 (2021).
[3] F. Aumayr, S. Facsko, A.S. El-Said, C. Trautmann. M. Schleberger, J. Phys. condensed matter 2, 224012 (2011).
[4] S. Facsko, R. Heller, A.S. El-Said, W. Meissl, F. Aumayr, J. Phys.: Cond. Mat. 2, 224012 (2009).
[5] A.S. El-Said, R.A. Wilhelm, R. Heller, and S. Facsko, C. Lemell, G. Wachter, J. Burgduorfer, R. Ritter, F. Aumayr, Phys. Rev. Lett. 109, 117602 (2012).
[6] A.S. El-Said, R. A. Wilhelm, R. Heller, M. Sorokin, S. Facsko, F. Aumayr, Phys. Rev. Lett. 117, 126101 (2016).

Soft potential and van der Waals effects in He-KCl(001) grazing-incidence fast atom diffraction.

G.A. Bocan[1,*], H. Breiss[2], S. Szilasi[2], A. Momeni[2,3], E.M. Staicu Casagrande[2], E.A. Sánchez[1,4], M.S. Gravielle[5], and H. Khemliche[2]

[1] *Instituto de Nanociencia y Nanotecnología (CNEA-CONICET), Centro tómico Bariloche, Argentina*
[2] *Institut des Sciences Moléculaires d'Orsay, University Paris-Saclay, CNRS, France*
[3] *CY Cergy Paris Université, France*
[4] *Instituto Balseiro (U.N. Cuyo), Centro Atómico Bariloche, Argentina*
[5,*] *Instituto de Astronomía y Física del Espacio (UBA-CONICET), Argentina*
[*] *gisela.bocan@cab.cnea.gov.ar*

In our poster we address, both experimentally and theoretically, the very grazing scattering of He atoms off KCl(001), for incidence along the $\langle 100 \rangle$ channel. Our theoretical model combines a semiquantum description of the scattering dynamics and a high-precision interaction potential. By means of a thorough analysis of the quantum phase for in-plane scattering and rainbow trajectories, we are able to connect the presence of a physisorption well with the significant enhancements of the corrugation and rainbow angle, relative to the hard corrugated wall predictions. We trace this connection to soft potential effects on the incident and scattered beams due to their traversing of the physisorption well. Finally, we show that the inclusion of vdW interactions in the potential improves the theoretical accord with experiments for both the corrugation and the rainbow angle [1].

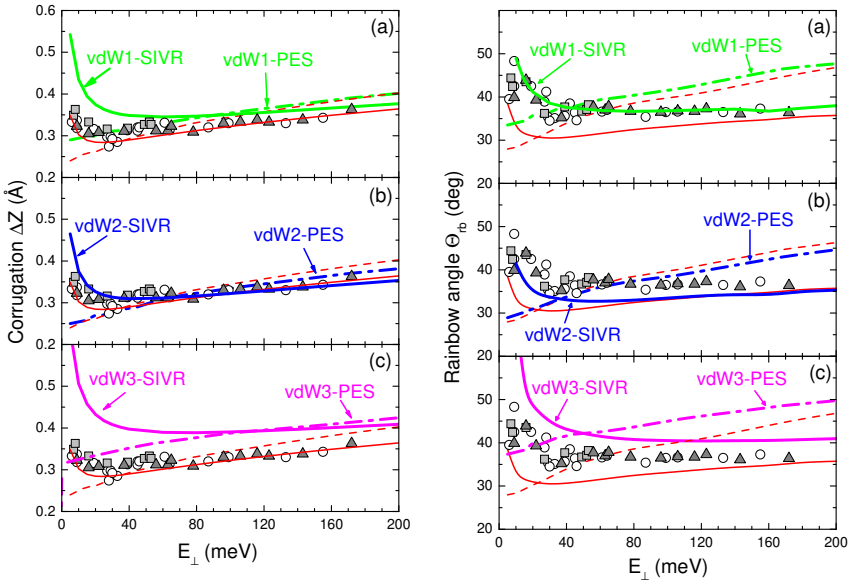

(a) (b)

Figure 1: Corrugation (left) and rainbow deflection angle (right) as functions of $E_\perp$. Symbols: values from experiments. Solid and dashed lines: values respectively obtained from SIVR dynamics and the HCW model, both with (a) vdW1, (b) vdW2, and (c) vdW3 potentials. Red thin lines: PBE-SIVR (solid) and PBE-PES (dashed) results, meant to be used as a reference.

References

[1] G.A. Bocan, H. Breiss, S. Szilasi, A. Momeni, E.M. Staicu Casagrande, E.A. Sánchez, M.S. Gravielle, and H. Khemliche, *Phys. Rev. B* 104 (2021) 235401

Local structure and hardness change in the amorphization process of ZrCuAl alloys by heavy ion irradiation

[*]F. Hori[1], Y. Morikuni[1], H. Obayashi[1], A. Iwase[1,2], T. Matsui[1], Y. Kaneno[1], T. Wada[3], H. Kato[3], N. Ishikawa[4]

[1]*Osaka Prefecture Univ., Sakai, Osaka, Japan*
[2]*Wakasa-wan Energy Research Center, Tsuruga City, Fukui.*
[3] *Institute for Material Research, Tohoku Univ.*
[4]*Japan Atomic Energy Agency, Tokai, Japan*
[*]horif@mtr.osakafu-u.ac.jp

Recently, based on the unique phenomena induced by heavy ion irradiation of materials, we have been researching on material modification by ion irradiation [1]. However, the conditions under which the crystals are amorphized by heavy ion irradiation, such as alloy species, crystal structure and irradiation conditions, are still unknown. ZrCuAl alloy has a wide supercooled liquid region and are known to be able to easily synthesize amorphous by quenching [2,3]. In addition, it has been found that eutectic $Zr_{50}Cu_{40}Al_{10}$ amorphous alloy has quite different properties in other alloy composition, especially hypo-eutectic composition alloys. In this study, heavy ion irradiation was done for eutectic and hypo-eutectic alloys in order to investigate the radiation effects lead to the amorphization by the heavy ion irradiation. Hypo-eutectic alloy of $Zr_{45}Cu_{45}Al_{10}$ was irradiated with 16 MeV from 4×10^{15} to 1×10^{16}/cm^2 and 200 MeV Au ions from 1×10^{13} to 1×10^{14}/cm^2 at room temperature. Before and after irradiation, X-ray diffraction (XRD), X-ray absorption fine structure (XAFS), micro-Vickers hardness and positron annihilation measurements have done. As a result of irradiation, amorphization was confirmed in both energy of the irradiation but the changing behavior of hardness depends on the irradiation energy. That is, the hardness once decreases and increases with increasing the fluence in case of 16MeV irradiation, but in case of 200 MeV irradiation no decreasing trend was observed. During this hardness change, it found that the changing ratio of Cu-Cu and Cu-Zr bonds different for low energy and high energy by XAFS measurement.

References

[1] H. Kojima, Y. Kaneno, M. Ochi, S. Semboshi, F. Hori, Y. Saitoh, N. Ishikawa, Y. Okamoto, A. Iwase, Mater. Trans. Vol.58, 5 (2017) 739-748.
[2] F. Hori, A. Ishii, T. Ishiyama, A. Iwase, Y. Yokoyama, T.J. Konno, J. Alloys and Comp. 707 (2017) 73–77.
[3] Y. Yokoyama T. Ishikawa, J.T. Okada, Y. Watanabe, S. Nanao, A. Inoue, J. Non-Cryst. Solids 355 (2009) 317-322.

Density enhancement of ion microbeams with miniature quadrupole magnets for tapered glass capillary optics

K. Inayoshi[1,2,*], **T. Ikeda**[2,1], **K. Ono**[1,2], **and W.-G. Jin**[1]

[1]*Department of Physics, Toho University, Japan*
[2]*RIKEN Nishina Center for Accelerator-Based Science, Japan*
[*]*kotoko.inayoshi@a.riken.jp*

Ion microbeams are powerful tools to efficiently induce DNA double strand breaks in specific single cells. We have realized a simple microbeam generator for the ion energy of a few MeV to irradiate cultivated cells in liquid medium employing tapered glass capillary optics with an end-window[1, 2]. To avoid mis-hitting the target, the microbeam size should be kept smaller. One of the major reasons of beam size broadening is found to be ion scatting on the inner surface of the capillary during the transmission, according to the simulation including beam divergence inside the capillary and material of the end-window. A set of miniature quadrupole permanent-magnets surrounding a glass capillary was introduced for the first time to reduce the divergence of the traveling ion beam within the capillary. By using the quadrupole magnets, it is expected not only to prevent ions from scattering on the inner surface, but also to increase the density of the extracted microbeam.

Figure 1(a) shows the used beamline in RIKEN Pelletron accelerator facility. An H^+ beam with an energy of 2.4 MeV entered a capillary with an outlet diameter of 50 μm. The thickness of the plastic end-window was 30 μm, which is much smaller than the ion range in plastic. Regarding the analyzing switching magnet, the horizontal beam divergence was larger than the vertical one. The orientation of the quadrupole magnet was selected as shown in Fig. 1(b) so that the horizontal component was focused. The extracted ions were counted by a detector when the quadrupole magnet moved away from or near the capillary at approximately 20 s interval. Figure 1(c) shows low and high count rates corresponding to the magnet positions. The density enhancement was found to be up to 125% to that without the magnet when two quadrupole magnets were installed in the same orientation to increase the high magnetic field region. The extracted beam size will be examined by a plastic tracking detector, CR-39.

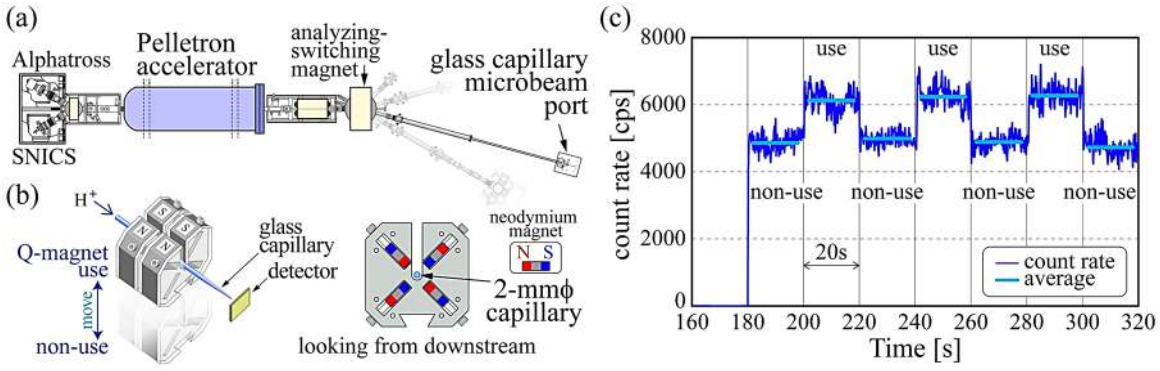

Figure 1: (a) Pelletron accelerator and the used beamline. (b) Location of the quadrupole magnets. (c) Repetition of low / high count rates at the detector corresponding to the states of use / non-use of the quadrupole magnets.

References

[1] T. Ikeda, Quantum Beam Science 4(2), 22 (2020) 1.
[2] T. Ikeda *et al*., Nucl. Instrum. Methods Phys. Res. B 470 (2020) 42.

Analysis of ion-track overlapping effects using Poisson distribution function and Monte Carlo simulation

A. Iwase*[1,2], S. Nishio[1], N. Ishikawa[3] and F. Hori[2]

[1]*The Wakasa Wan Energy Research Center, Fukui, Japan*
[2]*Osaka Prefecture University, Osaka, Japan*
3Japan Atomic Energy Agency, Ibaraki, Japan
aiwase@werc.or jp

It is well known that in various oxides and ceramics irradiated with swift heavy ions, one-dimensional defective structures (ion-tracks) are produced along ion beam paths. The ion-tracks originate from the energetic ion induced high-density electronic excitation. There have been a lot of studies for individual ion-track structures and their dependence on the electronic stopping power, Se, of the irradiating ions. The effects of the ion-track overlapping on lattice structures of target materials, which appear for the high fluence irradiation, have also been investigated so far.

Ishikawa et al. have explained the ion track overlapping effect on the TiO_2 amorphization by using the binomial distribution function[1]. The Poisson distribution function, which is the approximated formula of the binomial distribution function can also describe the ion-track overlapping effect on the evolution of the irradiation induced magnetization in CeO_2[2]. Such analytical methods, however, only reproduce the total fraction of the areas modified by high energy ions as a function of ion fluence. In the present study, we use the Monte Carlo method in order to simulate the two-dimensional images of the lattice structures and the magnetic states as a result of the ion -track overlapping for some oxides[3]. In the conference, we will also show the description of the overlapping of three-dimensional defetcive areas (cascade damage) and the ion flux dependent irradiaion effect due to the overlapping of short-lived ion-tracks

References

[1] N. Ishikawa, K. Ohhara, Y. Ohta, O. Michikami, *Nucl. Instrum. Methods Phys. Res. Sect. B* **2010**, 268, 3273-3276.
[2] Y. Yamamoto, N. Ishikawa, F. Hori, A. Iwase, *Quantum Beam Sci*, **2020**, 4,26.
[3] A. Iwase, S. Nishio, *Quantum Beam Sci.* **2021**, 5,13.

Gold nanowire network fabricated by ion-track nanotechnology and its electrochemical properties

M. Li[1,2,*], **N. Ulrich**[1,2], **M. Wagner**[2], **I. Schubert**[2], **C. Trautmann**[1,2] **and M.E. Toimil-Molares**[1]

[1] *Materials Research, GSI Helmholtzzentrum für Schwerionenforschung, Germany*
[2] *Materials and Earth Sciences Department, Technische Universität Darmstadt, Germany*
[*] M.Li@gsi.de

The electrochemical characterization of free-standing Au nanowire networks synthesized by ion-track technology and electrodeposition is presented. The fabrication process employs irradiation of polycarbonate foils with heavy ions followed by chemical track etching [1]. In this work, the foils were irradiated sequentially from four directions with 1-2 GeV Au ions at the UNILAC accelerator of GSI. Subsequent chemical etching of the ion tracks results in templates with interconnecting nanochannels which are then filled with gold by potentiostatic electrodeposition. Nanowire growth rate and homogeneity are tuned by varying the deposition potential. The technique provides precise control of the nanowire size, interconnectivity, and composition [2,3]. By dissolving the polymer template, free-standing nanowire networks are obtained showing remarkable mechanical stability (Fig. 1 a, b). Because of their large surface area, the networks are of interest for catalytic processes such as, e.g., the environmental friendly methanol electro-oxidation. The networks are inserted into an electrochemical cell where they act as electrode. The electrochemically active surface area (ECSA) of our Au nanowire networks is systematically measured as a function of nanowire diameter. Their catalytic activity towards methanol oxidation is recorded by cyclic voltammetry (CV) in an alkaline electrolyte (Fig. 1c) and reveals significantly higher current densities than with a planar gold electrode. They also showed very stable long-term performance, with the current density dropping by only 5% during 200 CV cycles of oxidation reaction.

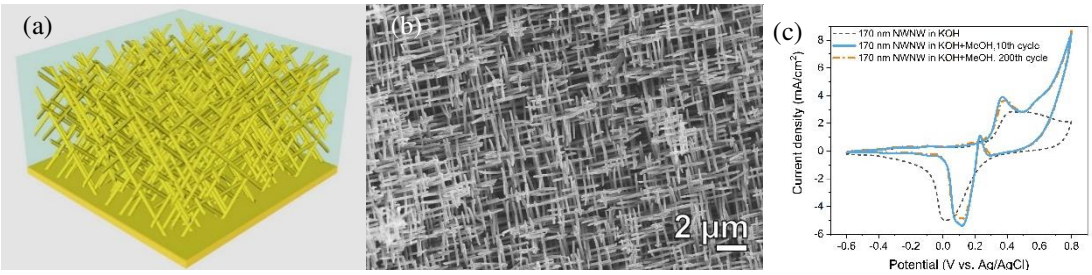

Figure 1. (a) Schematic of nanowire network inside an etched ion-track template, (b) SEM image of a Au nanowire network, (c) CVs recorded for a Au nanowire network in 0.1 M KOH with (solid line) and without (dash line) 1 M methanol.

References

[1] M. E. Toimil-Molares, *Beilstein journal of nanotechnology*, 3.1 (2012) 860-883.
[2] M. Rauber, I. Alber, S. Müller, and et al. *Nano letters*, 11.6 (2011) 2304-2310.
[3] L. Movsesyan, A. W. Maijenburg, N. Goethals, and et al. *Nanomaterials*, 8.9 (2018) 693.

The Variation of Pinning Efficiency in Swift Heavy Ions Irradiated YBCO Superconducting Films

Li Liu[1,2], Jie Liu[1,2,*], PengFei Zhai[1,2], ShengXia Zhang[1], Jian Zeng[1,2], PeiPei Hu[1], LiJun Xu[1], and ZongZhen Li[1]

[1]*Institute of Modern Physics, Chinese Academy of Sciences (CAS), PR China*
[2]*School of Nuclear Science and Technology, University of Chinese Academy of Sciences (UCAS), PR China*
[*]*j.liu@impcas.ac.cn*

A major impediment to the widespread use of high temperature superconductors (HTS) is the dissipation of critical current density in external field. This problem can be solved by swift heavy ion irradiation-induced one-dimensional columnar defects (namely latent tracks), which are thought to be the strongest pinning centers in type II superconductors since it can pin vortices along its entire length, thus enhancing in-field current-carrying capability.

In the present work, $YBa_2Cu_3O_{7-x}$ (YBCO) films were irradiated by ions with different electronic energy loss S_e (17.7 keV/nm Kr ions, 35.8 keV/nm Ta ions and 43.7 keV/nm Bi ions) at identical fluence of 5×10^{10} ions/cm^2 (corresponding to matching field $B_\Phi \approx 1.0$ T). Existences of latent tracks in Ta ions and Bi ions irradiated YBCO films have been confirmed by TEM (transmission electron microscope), respectively. Whereas, there is no visible latent tracks in Kr ions irradiated YBCO films because S_e of Kr ions is lower than $S_{e,th} \approx 35$ keV/nm. Variations of pinning efficiency η, which can be represented as ratio between pinning force density $F_{p,i}$ of irradiated sample and $F_{p,p}$ of pristine sample at the same temperature, with temperature and magnetic field in YBCO films irradiated with different ion species were systematically studied. η in all the irradiated samples show monotonically increasing trend with increasing temperature. Nevertheless, as the number of vortices, i.e. external magnetic field B, increases, η in YBCO film containing latent tracks gradually reaches its maximum value at low magnetic field and then decreases slowly, totally different from YBCO film containing no latent tracks. This phenomenon may provide a fresh idea to judging the existence of columnar defects in YBCO films. Peak position B_p is far below B_Φ and peak value increased with increasing temperature. Moreover, sample containing larger-size columnar defects (which can be produced by ions with higher S_e) exhibits higher but narrower peak in η-B curve, which is also important for future application.

References

[1] S. Foltyn, L. Civale, J. MacManus-Driscoll, Q. Jia, B. Maiorov, H. Wang and M. Maley, *Nature materials*, 6 (2007) 631
[2] L. Civale, *Superconductor Science and Technology*, 10 (1997) A11

Heavy ion irradiation effects on microstructural properties of amorphous HfO_2 thin films

Zongzhen Li[1], Jie Liu[1,2,*], Pengfei Zhai[1,2], Li Liu[1,2], Lijun Xu[1], Shengxia Zhang[1,2], Peipei Hu[1] and Jian Zeng[1,2]

[1] *Institute of Modern Physics, Chinese Academy of Sciences, China*
[2] *Nuclear Science and Technology, University of Chinese Academy of Sciences, China*
[*] *j.liu@impcas.ac.cn*

Amorphous HfO_2 is widely utilized as high-k gate dielectric materials for reducing the tunneling leakage current and improving the reliability to overcome the physical limitation of traditional gate dielectric like SiO_2[1-2]. In this work, we report on swift heavy ion irradiation effects on the structural characteristics of amorphous HfO_2 films on Si (100). Amorphous HfO_2 thin films have been deposited on Si substrate by atomic layer deposition. The structural properties of HfO_2 thin films in relation to heavy ion irradiation are investigated by X-ray diffraction (XRD), high resolution transmission electron microscopy (HRTEM) and X-ray photoelectron spectroscopy (XPS). It is found that the stoichiometric ratio of Hf/O changed from 2.483:1 to 2.154:1 after Fe ions with the energy of 6.3 MeV/u irradiated to 2×10^{14} ions/cm^2, which is closer to the stoichiometric ratio of HfO_2, and the ratio of completely oxidized Hf and lattice oxygen are gradually increased as well. The analysis of XRD indicates that the amorphous HfO_2 films transformed to monoclinic and cubic/tetragonal crystal phases after irradiation, as shown in Figure 1. When the fluence increased from 5×10^{13} ions/cm^2 to 2×10^{14} ions/cm^2, the crystallinity of the film increased from 10.5% to 38.7%, the average grain size increased from 12 nm to 14 nm. The cubic/tetragonal phase of HfO_2 have lager dielectric constant compared to the amorphous one.

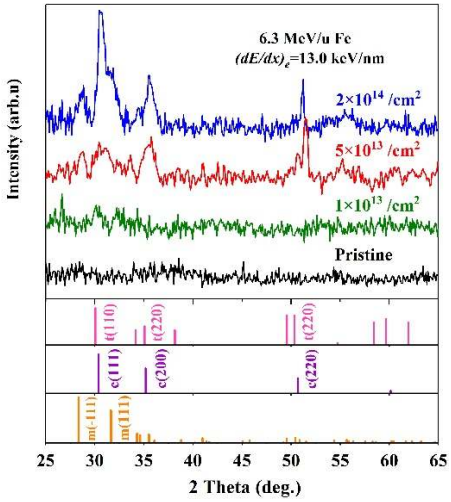

Figure 1: The XRD patterns of the HfO_2 films on Si (100) wafer as a function of ion fluences.

References

[1] M. Houssa, G. Pourtois, M.M. Heyns, and A. Stesmans, *J. Phys. Condens. Matter*, 17 (2005) 2075
[2] A.Y. Kang, P.M. Lenahan, and J.F. Conley, *Appl. Phys. Lett.*, 83 (2003) 3407

Type and size of the nanostructure formed on a metal surface by an impact of highly charged ions

N. N. Nedeljković[1], M.D. Majkić[2,*], M. A. Mirković[3], I. Stabrawa[4], and D. Banaś[4]

[1]*Faculty of Physics, University of Belgrade, P.O. Box 368, 11001 Belgrade, Serbia*
[2]*Faculty of Technical Sciences, University of Priština-Kosovska Mitrovica, Knjaza Miloša 7 38220 Kosovska Mitrovica, Serbia*
[3]*University College of Civil Engineering and Geodesy, Hajduk Stankova 2, 11050, Belgrade, Serbia*
[4]*Institute of Physics, Jan Kochanowski University, Uniwersytecka 7, 25-406 Kielce, Poland*
[*]*milena.majkic@pr.ac.rs*

Nanostructures, created as a result of the highly charged ions (charge $Z \gg 1$) impact on a metal surface (for low to moderate ionic velocities), are studied theoretically. The mechanism of the surface modification is considered within the framework of our model [1]; the approach is based on the quantum two-state vector model accompanied by the micro-staircase model for the calculation of the neutralization energy and the charge dependent ion-atom interaction model for the nuclear stopping power calculation. The neutralization energy and the kinetic energy loss, deposited into the surface during the ionic motion above and below the surface, respectively, are considered. The interplay of these two energies is described by the critical ionic velocity [1]; for the ionic velocities lower than the critical one the model assumes an appearance of the hillocks, while for the larger velocities a dominant surface structures are craters.

The theoretical study is extended to include the analysis of the size (diameter) of the nanostructures as a velocity-dependent quantity. The total deposited energy, consisting of the neutralization energy and the deposited kinetic energy, is considered as the energy necessary to break down the bonds between the target atoms in the intermediate stages of the surface modification. According to the model, the nanostructures are created for lower energy density compared to the energy density of the unmodified surface, in agrement with the Bringa's conclusion [2]. The calculated diameters are in accord with the diameters of the hillocks [3] and craters [4] obtained experimentally by the impact of Xe^{Z+} ions upon the titanium and gold targets. The interpretation of the nanostructure size based on the melting temperature is also discussed within the framework of our model.

References

[1] M.D. Majkić, and N. N. Nedeljković, *Vacuum*, 190 (2021) 110301
[2] E.M.Bringa, K. Nordlund, and J. Keinonen, *Physical Review B*, 64 (2001) 235426
[3] I. Stabrawa, D. Banaś, A. Kubala-Kukuś, K. Szary, J. Braziewicz, J. Czub, Ł. Jabłoński, P. Jagodziński, D. Sobota, M. Pajek, K. Skrzypiec, E. Mendyk, and M. Teodorczyk, *Nucl. Instrum. Methods Phys. Res.B*, 408 (2017) 235-240
[4] I. Stabrawa, D. Banaś, A. Kubala-Kukuś, K. Szary, Ł. Jabłoński, P. Jagodziński, D. Sobota,K. Szary, M. Pajek, K. Skrzypiec, E. Mendyk, and M. Borysiewicz, M.D. Majkić, and N. N. Nedeljković, to be published

TREKIS-4: concurrent MC-MD modelling of ion track formation

N. Medvedev[1,2,*], **F. Akhmetov**[3], **R.A. Rymzhanov**[4,5], **R. Voronkov**[6], **A.E. Volkov**[6]

[1]*Institute of Physics, Czech Academy of Sciences, Na Slovance 2, 182 21 Prague 8, Czech Republic*

[2]*Institute of Plasma Physics, Czech Academy of Sciences, Za Slovankou 3, 182 00 Prague 8, Czech Republic*

[3]*Industrial Focus Group XUV Optics, MESA+ Institute for Nanotechnology, University of Twente, Drienerlolaan 5, 7522 NB Enschede, The Netherlands*

[4]*Joint Institute for Nuclear Research, Joliot-Curie 6, 141980, Dubna, Moscow Region, Russia*

[5]*The Institute of Nuclear Physics, Ibragimov St. 1, 050032 Almaty, Kazakhstan*

[6]*P.N. Lebedev Physical Institute of the Russian Academy of Sciences, Leninskij pr., 53,119991 Moscow, Russia*

[*]*nikita.medvedev@fzu.cz*

We present a concurrent Monte Carlo (MC) – molecular dynamics (MD) approach to modeling of matter response to swift heavy ion (SHI) excitation of its electronic system [1]. The two methods are combined on-the-fly in one new code, TREKIS-4. The MC model describes SHI passage, induced cascades of excitation of secondary particles (electrons, holes, and photons), their ballistic transport and energy exchange with atoms due to scattering. The response of the atomic system is simulated with an MD model. An MC-MD combination allows to account for nonequilibrium processes in the electronic system and their effects on the atomic dynamics.

We also propose a simple model to account for the nonthermal energy exchange between electrons and atoms in covalent materials *via* conversion of the potential energy of electron-hole pairs into kinetic energy of atoms on-the-fly. The advantage of such an approach is that it can readily be implemented into standard MC models, without complex *ab-initio* simulations of the effect. As it is the dominant channel of energy transfer from excited electrons to atoms in SHI tracks [2], the proposed simple model can significantly boost practical applications.

The developed concurrent MC-MD approach potentially enables us to describe effects of material irradiation with intensive beams of relativistic ions, which will be applied in new accelerator facilities (e.g. FAIR-GSI). Its fundamental importance lies in the ability to model SHI track formation without adjustable parameters [1].

References

[1] N. Medvedev, F. Akhmetov, R.A. Rymzhanov, R. Voronkov, A.E. Volkov, (2022) https://arxiv.org/abs/2201.08023

[2] N. Medvedev, A.E. Volkov, (2021) https://arxiv.org/abs/2109.04401

Radiation effects on thymine at low temperature

C. Mejía[1,3,*], G. S. Vignoli Muniz[2,3], M. Bender[4,5], D. Severin[4], C. Trautmann[4,6], A. N. Agnihotri[3,7], B. Augé[3,8], A. Domaracka[3], P. Boduch[3] and H. Rothard[3]

[1]*Facultad de Ciencias Químicas, Universidad de Cuenca, Cuenca, Ecuador.*
[2]*Instituto de Física, Universidade de São Paulo, Rua do Matão, 1371 – 05508-090, São Paulo, Brasil.*
[3]*Centre de Recherche sur les Ions, les Matériaux et la Photonique. Normandie Université, ENSICAEN, UNICAEN, CEA, CNRS, CIMAP – 14000 Caen, France.*
[4]*GSI Helmholtzzentrum für Schwerionenforschung, Darmstadt, Germany*
[5]*Hochschule Rhein-Main, Rüsselsheim, Germany*
[6]*Technische Universität Darmstadt, Germany*
[7]*Indian Institute of Technology Delhi, New Dehli, India*
[8]*University Grenoble Alpes, CNRS, Institut de Planetologie et Astrophysique de Grenoble (IPAG), UMR 5274, , Grenoble, F-38041, France*
**cfmejiag@gmail.com*

Thymine ($C_5H_6N_2O_2$) is a basic N-heterocyclic nucleobase existing in all known organisms. Thymine has also been found in meteorites that were previously exposed to harsh radiation and cold environments of space before falling to Earth's surface [1]. The aim of this study is to investigate the physical and chemical modifications of thymine under irradiation at cryogenic conditions. Space radiation was simulated by irradiating thymine sample at 20 K with 230 MeV Ca ions. The experiments were performed at the M-branch of the UNILAC beamline at GSI in Darmstadt, Germany. Infrared spectroscopy (FTIR) was employed to monitor the degradation of a 2.8 µm thick sample film under irradiation (Fig. 1a). Fig. 1b presents the decreasing amount of thymine as a function of ion fluence. The mean destruction cross-section required to dissociate or eject a thymine molecule is obtained by fitting an exponential function to the data as $\sigma_d^{ap} = (4.6 \pm 0.1) \times 10^{-13}$ cm^2. In comparison with results from the literature [2, 3], the thymine's structural changes, chemical modifications and sputtering yield during irradiation were assessed. This study also provides insight into the chemical synthesis of new molecular species caused by irradiation: CN^-, OCN^-, HCNO, and CO [3].

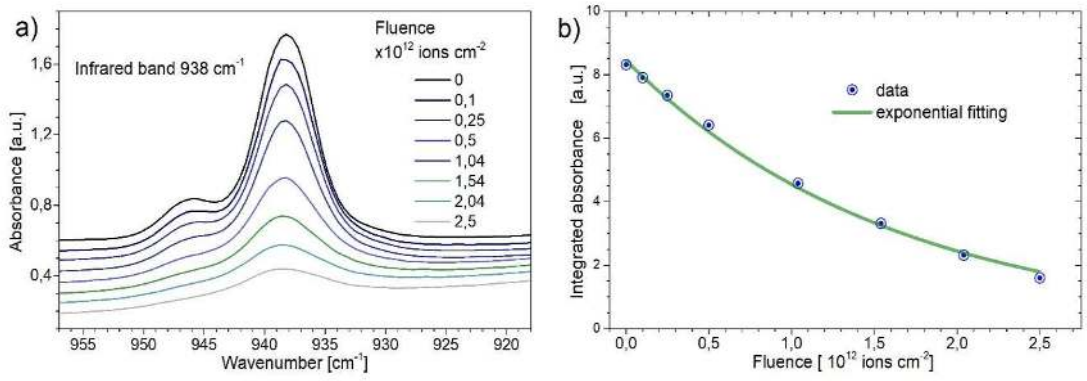

Figure 1. Infrared bands at 938 cm^{-1} of thymine (a) and their integrated absorbance (b) as a function of fluence.

References

[1] Callahan, M. P., Smith, K. E., Cleaves, H. J., Ruzicka, J., Stern, J. C., Glavin, D. P., & Dworkin, J. P. Proceedings of the National Academy of Sciences, 108 (34), 2011, 13995-13998.
[2] Vignoli Muniz G. S., Ph. D. thesis, Normandie Univ- UNICAEN, 2017.
[3] Materese, C. K., Gerakines, P. A., & Hudson, R. L. Astrobiology, 20(8), 2020, 956-963.

Radiation damage, conductivity type conversion and *p-n* nanojunction formation induced by low-energy Ar^+ ion collisions with the *n*-GaAs surface

V.M. Mikoushkin

Ioffe Institute, 194021 Saint-Petersburg, Russia
*V.Mikoushkin@mail.ioffe.ru

Low-energy Ar^+ ion beams are widely used in research and development for removal of natural oxides, preparation of atomically-clean material surfaces, layer-by-layer ion etching and modification of properties of semiconductors, among which GaAs and GaAs-based semiconductors are one of the most important in high-frequency electronics [1]. Therefore, research of physical and chemical modification induced by Ar^+ ion collisions with GaAs has remained a topical task for decades. The main result of this study is that *n*-GaAs with an atomically clean surface bombarded by Ar^+ ions is not a homogeneous amorphous semiconductor restricted by a plane, but a *p-n* nanostructure [2] with diode [3] and photovoltaic [4] properties. The process of the conductivity type conversion of the irradiated layer resulting in formation of a *p-n* structure is illustrated by Fig. 1a. The effect manifests itself in adjoining the valence band edge to the Fermi level in the irradiated layer, which was revealed by photoelectron spectroscopy with using synchrotron radiation of the BESSY-II electron storage ring [2, 5]. Transformation of the conductivity type has been shown to be caused by Ga-antisite point defects generated under irradiation due to preferential sputtering of As atoms, resulting in enrichment of the irradiated layer by Ga (Fig. 1b). The thickness of the *p*- layer and the band diagram of the *p-n* junction determined experimentally show the unexpectedly narrow interface (~ 1 nm) compared to the depth distribution of implanted ions and generated defects (~ 10 nm) [5]. The application potential of the revealed effect can be associated with the creation of 3D diode structures on the *n*-GaAs surface directly by an Ar^+ ion beam without a resist and wet lithography.

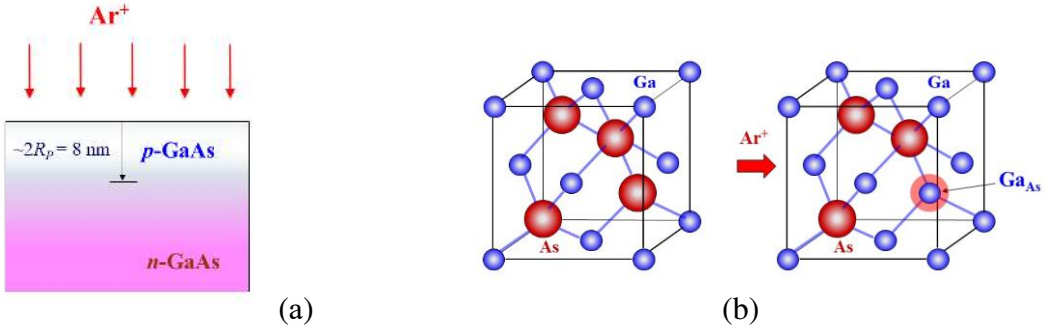

Figure 1. (a) Sceme of a *p-n* structure formation due to Ar^+ ion bombardment of the *n*-GaAs surface. (b) Scheme of the GaAs crystal structure: pristine and with a Ga-antisite (Ga_{As}) defect formed under Ar^+ irradiation.

References

[1] A.G. Baca, C.I.H. Ashby, Fabrication of GaAs devices, IET, London, United Kingdom, 2005.
[2] V.M. Mikoushkin, V.V. Bryzgalov, S.Yu. Nikonov et al., *EPL* 122 (2018) 27002.
[3] V.M. Mikoushkin, V.S. Kalinovskii, E.V. Kontrosh, E.A. Makarevskaya, *Semiconductors* 53 (2019) 56.
[4] V.M. Mikoushkin, V.S. Kalinovskii, E.V. Kontrosh, and K.K. Prudchenko, *J. Mater. Sci.* 56 (2021) 15180.
[5] V.M. Mikoushkin, E.A. Makarevskaya, M. Brzhezinskaya, *Appl. Surf. Sci.* 539 (2021) 148273.

Room-temperature radiation-induced diffusion in the GaAs-oxide irradiated by low-energy Ar^+ ion beam

V.M. Mikoushkin[*], **E.A. Makarevskaya, A.P. Solonitsyna**

[1]*Ioffe Institute, 194021 Saint-Petersburg, Russia*
[*]*V.Mikoushkin@mail.ioffe.ru*

Gallium oxide (Ga_2O_3) is one of the most intensively studied wide-gap semiconductors in the last decade due to high electron mobility [1]. Ga_2O_3 is also a part of the native oxide (Ga_2O_3 + As_2O_3 + As_2O_5) of GaAs which is one of the most important semiconductors in high-frequency electronics [2]. Threfore, the recently revealed effect of the GaAs native oxide conversion into Ga_2O_3 under low-energy Ar^+ ion irradiation seems to be noticeable [3]. The effect was qualitatively explained by ion induced chemical bonds breaking and the diffusion after the irradiation of As atoms from the oxide layer 2.0 -2.5 nm thick [4] to the surface and into the bulk. In this work, diffusion coefficient and length were estimated in dependence of Ar^+ ion fluence. Since the As activation energy in Ga_2O_3 was unknown, the average value of this energy E_m ~ 0.9 eV in GaAs was used [5, 6] for an upper estimate. (The activation energy of an atom in GaAs must be less than in Ga_2O_3, since the covalent bond of atoms in the oxide is stronger.) The density of the oxygen vacancies generated by ions was calculated by TRIM code for GaAs coated with a Ga_2O_3 layer 2 nm thick (Fig.1a). (As and Ga vacancies were considered as traps.) Fig 1b shows the dose dependencies of the As diffusion length in Ga_2O_3 for 10 and 60 min. It is seen that the diffusion length exceeds the oxide layer half-thickness for 10 min at fluences $Q > 2\times10^{14}$ cm^{-2}. Thus, the upper estimate confirmed the assumption about important role of room-temperature radiation-induced diffusion in the process of GaAs native oxide conversion into gallium oxide.

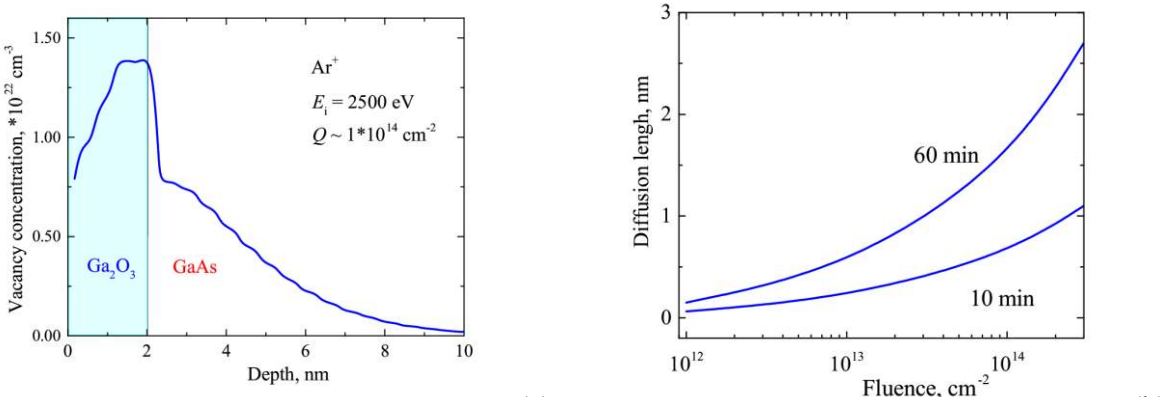

Figure 1. (a) TRIM profile of vacancies formed by Ar^+ ions with energy E_i = 2500 eV and fluence $Q = 10^{14}$ cm^{-2} in GaAs coated with a Ga_2O_3 layer 2 nm thick. (b) Dependence of the diffusion length of As in Ga_2O_3 on the ion irradiation fluence according to the vacancy radiation-enhanced mechanism for 10 and 60 min.

References

[1] S.J. Pearton, J. Yang, P.H. Cary, F. Ren, J. Kim et al., Appl. Phys. Rev. 5 (2018) 011301.
[2] A.G. Baca, C.I.H. Ashby, Fabrication of GaAs devices, IET, London, United Kingdom, 2005.
[3] V.M. Mikoushkin, V.V. Brysgalov, E.A. Makarevskaya at al., *Surf. Coat. Technol.* 344 (2018) 149.
[4] M.R. Vilar, J.E. Beghdadi, F. Debontridder, R. Artzi et al., *Surf. Interface Anal.* 37 (2005) 673.
[5] A.Rim, and R. Beserman, *J. App. Phys*. 74 (1993) 897.
[6] J.F. Wager, *J. Appl. Phys.* 69 (1991) 3022.

Theory and simulations for plasma created by swift heavy ions

Kengo Moribayashi[1*]

[1] *National Institutes for Quantum and Science and Technology, Japan*

[*] *moribayahsi.kengo@qst.go.jp*

Over one century passes since plasma is thought to be produced in swift heavy ion irradiation using the free electron gas model, theoretically. However, it is still unclear if this irradiation forms plasma or not. In simulations, plasma formation was not incorporated using the binary collision model before our simulation model was proposed. In our model based on the binary collision model, a similar mechanism to the free electron gas model is incorporated to produce plasma as mentioned later [1]. The problem of the presence or the absence of the plasm is important to calculate the radial dose distribution, which is employed in the treatment planning system for the cancer therapy to calculate the survival rate of cells [1,2]. Here, the radial dose is the dose as a function of the distance (r) from the incident ion path.

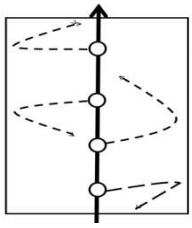

Fig.1 Motion of secondary electron are shown by dashed lines: Molecular ion and Paths of the incident ion are shown by ○ and a solid line, respectively.

In heavy ion irradiation, huge number of molecules are ionized along the incident ion path (IP) and, as a result, a lot of molecular ions are produced. In our model which can be applied only to the insulator target, strong electric field created by these molecular ions and the effect of this electric field on the motion of secondary electrons are incorporated (see Fig.1). The measurement of secondary electron yield measured by Kimura et al. [3] indicated the movement shown in Fig.1. Namely, it was shown that slow secondary electrons were trapped by this electric field. These trapped secondary electrons are expected to form plasma.

We found that simulation results of electron density agree well with the solution of the Poisson's equation [4]. In Fig. 2, one example is shown, that is, the electron density vs. r at $\sigma = 4 \times 10^{-15}$ cm^2 and E_i = 500keV/u, where σ, and E_i are the ion impact ionization cross section and the ion energy, respectively. Further, we found from simulations that $\lambda_D \propto \sigma^{-1/2}$ is approximately satisfied, where λ_D is the Debye length, that is, the length of the plasma. This relationship was also derived from theoretical treatment [4]. We also derived a simple formular which can almost reproduce the simulation results of the probabilities of secondary electrons escaping the electric field produced near the incident ion path [4]. In the presentation, we will show when, where, and how plasma is produced through simulations and theory.

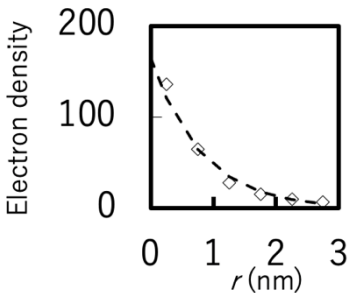

Fig.2 Electron density vs. r at $\sigma = 4 \times 10^{-15}$ cm^2 and E_i = 500keV/u . Simulation results (◇), Solution of theory (the dashed line).

References

[1] K. Moribayashi, *Jpn. J. Applied Phys.,* 59 (2020) SH0801.
[2] Y. Kase et al., Phys. Med. Biol., 53 (2008) 37.
[3] K. Kimura, et.al., *Nuclear Instr. Meth. Phys. Res. B* 193 (2002) 661.
[4] K. Moribayashi, *Radiat. Phys. Chem.*, 184 (2021) 109436

Nonlinear effect on Au sputtering by C_{60}- and C_{70}-ion bombardment

K. Narumi*, K. Yamada, Y. Hirano, A. Chiba, Y. Yuri, and Y. Saitoh

Takasaki Advanced Radiation Research Institute, National Institutes for Quantum Science and Technology
*narumi.kazumasa@qst.go.jp

One of the most remarkable characteristics of molecular- or cluster-ion bombardment of condensed matter is huge sputtering. It has been reported that sputtering yield by cluster ions is not proportional to the number of the constituent atoms. Such an effect is called nonlinear effect on sputtering: One of the typical cases is Au sputtering by Au_n-ion bombardment ($n \leq 13$), where the sputtering yield is proportional to n^2 [1]. Fullerene ions, on the other hand, have much more constituent atoms but a much smaller atomic number than the above Au_n ions. It draws the interest how nonlinear effect on the sputtering by fullerene ions is. In the present study, we have measured Au sputtering yields by 0.03-to-9-MeV C_{60}- and C_{70}-ion bombardment and will discuss nonlinear effect on Au sputtering by C_{60}- and C_{70}-ion bombardment.

Au sputtering yields were measured with a quartz-crystal microbalance technique. A Au thin film, which was one of the electrodes on a quartz crystal, was used as a target as it is and was bombarded with C_{60} and C_{70} ions. These ions were accelerated to 0.03 to 1.08 MeV and to 1.08 to 9 MeV with the 400-kV ion implanter and a 3-MV tandem accelerator of TIARA [2], respectively. Sputtering yields by 18-to-150-keV C^+ ions were also measured.

We have introduced sputtering-yield ratio $R(n)$, which is defined by $Y(n)/nY(1)$, where $Y(n)$ is Au sputtering yield by C_n-ion bombardment. $R(n)$ is a kind of indicator of the nonlinear effect; specifically speaking, $R(n) = 1$ means that the effect is not observed. We have obtained $R(n) = 3$-6 for the energy region of 18 to 150 keV/atom. The result demonstrates obviously that the nonlinear effect is observed; however, the effect is not so much as Au_n ions on a Au target [1] because $R(n)$ is not proportional to n, *i.e.,* the obtained sputtering yields are not proportioanl to n^2. Possible factors for why the present sputtering yields are not proportional to n^2 are as follows: small energy deposition due to the low atomic number of the projectile, and rather low density of energy deposition resulting from a large room inside of C_{60} and C_{70} molecules.

References

[1] S. Bouneau, A. Brunelle, S. Della-Negra, J. Depauw, D. Jacquet, Y. Le Beyec, M. Pautrat, M. Fallavier, J.C. Poizat, and H.H. Andersen, *Phys. Rev. B*, 65 (2002) 14106.
[2] A. Chiba, A. Usui, Y. Hirano, K. Yamada, K. Narumi, and Y. Saitoh, *Quantum Beam Science*, 4 (2020) 13.

Stopping power in lanthanides, from Ce to Lu

J. P. Peralta[1,*], **A. M. P. Mendez**[1], **and C. C. Montanari**[1]

[1]*Instituto de Astronomía y Física del Espacio, CONICET and Universidad de Buenos Aires, Buenos Aires, Argentina.*

[*]*jpperalta@iafe.uba.ar*

The knowledge of electronic stopping is important in many fields, from basic physics to technology and medicine [1]. We focused on lanthanides due to its electronic complexity (open 4f-subshell, need of relativistic description [2]); the importance of rare-earth oxides [3], and discrepancies among experimental data. In this work we perform a systematic study of the stopping cross sections from Ce (Z=58) to Lu (Z=71). Fully relativistic atomic structure calculations were developed for the atomic wave functions and binding energies. These values are the only inputs of our full theoretical calculations for bound electrons using the shellwise local plasma approximation [4]. Our results cover an extended energy region by considering separately the free electron gas (FEG) and the bound electrons as in [4].

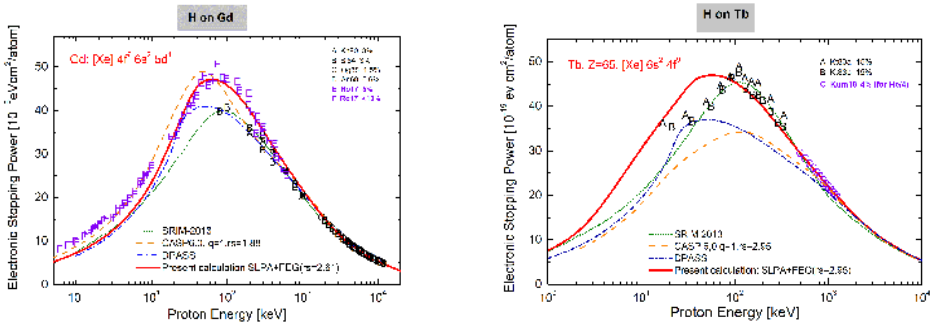

(a) (b)

Figure 1: Stopping cross sections for H in Gd and Tb. Solid-curve: present results, dotted-curve: SRIM semi empirical values [8], dashed-line: CasP 6.0 [7] for proton impact, dash-dotted curve: DPASS [6]. Symbols, experimental data in [9], with the latest measurements in colour.

As example, in Figure 1 we show our results for stopping of proton in Gd and Tb. For Gd the present results describe nicely the latest experimental data around the stopping maximum [5]. We also compare with other theoretical models, such as DPASS [6] and CasP 6.0 [7]. For Tb our curve is quite different from the SRIM [8] and the data around the maximum, but agrees well with the high energy values. We will show that the systematic study of all the lanthanides lets us have some doubts about the SRIM predictions for this type of targets.

References

[1] H. Paul, A. Schinner, At. Data Nucl. Data Tables 85 (2003) 377
[2] A M P Mendez et al, Nuclear Inst. and Meth in Phys. Res. B 460 (2019) 114–118
[3] E. Kennedy et al, arXiv:2101.06794v1 (2021).
[4] C C Montanari et al, Phys. Rev. A 96 (2017) 012707
[5] D Roth et al, Phys. Rev. Lett. 118 (2017) 103401
[6] P. Sigmund and A. Schinner, https://www.sdu.dk/en/dpass
[7] G. Schiwietz and P. L. Grande, http://www.casp-program.org/
[8] J.F. Ziegler http://www.srim.org/
[9] Electronic Stopping Power of Matter for ions, IAEA database, https://www-nds.iaea.org/stopping/

The Levine-Mermin dielectric function to describe stopping of inner-shells

J. P. Peralta[1,*], **M. Fiori**[2], **A. M. P. Mendez**[1], **and C. C. Montanari**[1]

[1] *Instituto de Astronomía y Física del Espacio, CONICET and Universidad de Buenos Aires, Buenos Aires, Argentina.*

[*] *jpperalta@iafe.uba.ar*

[2] *Universidad Nacional de Salta, Salta, Argentina*

The shellwise local plasma approximation (SLPA) has been successfully used to deal with the stopping power due to excitation and ionization of bound electrons [1]. However, for multielectronic relativistic targets (atomic number greater than 54) an overestimation is noted for high impact energies [2]. New measurements in tungsten [3] confirm these differences. In this contribution, we present an improvement of this formalism by using the Levine-Mermin [4, 5] dielectric function (SLPA-LM). This approach considers a more realistic description of the bound electrons by facing the problem of the damping in the collective excitations. We introduce local damping that depends on the density of electrons of each shell, keeping the full-theoretical characteristic of the SLPA. To analyze the dependence of the SLPA-LM with the number of sub-shells we use this model to calculate stopping cross sections $S(v)$ for proton impact on metal targets of group VI of the periodic table (Cr, Mo and W). We also include results of stopping for Hf to highlight the importance of the SLPA-LM description on relativistic targets.

The results are presented as stopping number L, which is proportional to $v^2 S(v)$ to see the high energy region enlarged. Figure 1 shows the improvement obtained. As expected the SLPA-LM improves the Levine-Lindhard model in [1, 2]. We observe that this changes the results for targets with many bound shells, while changes are negligible for targets such as Cr with fewer shells.

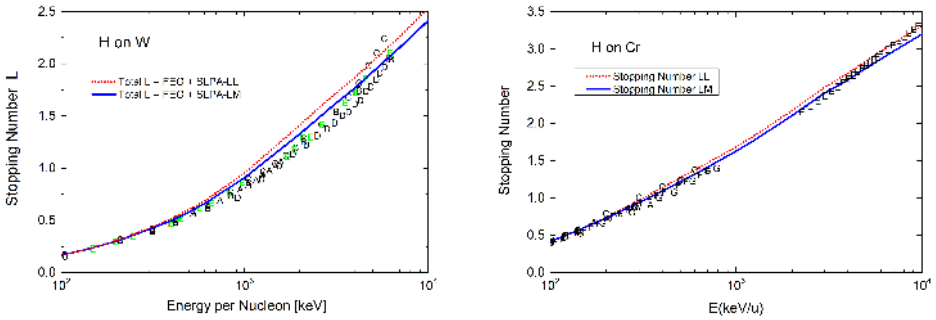

(a) (b)

Figure 1: Stopping number for H in W and Cr. Curves: present result; symbols, experimental data in [6], with the latest measurements in colour.

References

[1] C. C. Montanari, et al, Nucl. Instr. Meth. Phys. Res. B 460 (2019) 27.
[2] C. C. Montanari et al Phys Rev. A 80 (2009) 012901.
[3] M. Moro et al, Nucl. Instr. Meth. Phys. Res. B 498 (2021) 1.
[4] Z. H. Levine and S. G. Louie, Phys. Rev. B 25 (1982) 6310.
[5] N. D. Mermin, Phys. Rev. B 1, 2362 (1970).
[6] Electronic Stopping Power of Matter for ions, IAEA database, https://www-nds.iaea.org/stopping/

Application of multiple scattering approximation to the calculation ion-atom and ion-molecular collision

Pozdneev S.A.[*1]

P.N.Lebedev Physical Institute, Department Quantum Radiophysics, Laboratory of Photochemical Processes, Leninsky pr.53, 119924, Moscow, Russia

Synopsis Ion-atom and ion-molecular collision, multiple scattering approximation, Faddeev-Yakubovsky equations

The quantum theory of few-body scattering based on the modified Faddeev-Yakubovsky equations (FYE) [1] is applied to the calculation of the ion-atom, ion-molecular and atom-molecular collisions [2]. In this approach we consider all channels in this reaction (elastic, inelastic and ionization) simultaneously.

In case of high energy (the velocity of the incoming particle is larger then 1 a.u. ($v \gg 1$)) FYE simplification and may used eikonal approximation [2]. Therefore by virtue of the well know fact that the scattering is concentrated about the principal directions and in calculating the cross sections can be used expand in a parameter characterizing the derivation from the eikonal direction, assuming this parameter to be small. For this case the amplitude may be written in the form: $F_{if}(\vec{k}_f, \vec{k}_i) = (\mu/4\pi) T_{if}(\vec{k}_f, \vec{k}_i) \sim (\mu/4\pi) \int d\vec{R} d\vec{r} f_i(\vec{r}) f_f(\vec{r}) exp[iS(\vec{\Delta}, \vec{R}, \vec{r})] \Gamma(\vec{R}, \vec{r}, \delta)$ where $\vec{r} = \vec{r}_2 - \vec{r}_3; S = \vec{R}\vec{\Delta} + \delta_+; \Gamma(\vec{R}, \vec{r}, \delta) = W(\vec{R}, \vec{r}) exp(-i\delta_-) + V(\vec{R}, \vec{r}) exp(i\delta_-); V = V_{12} + V_{13} + V_{23}; W = V_{12} + V_{13}; \delta_{\pm} = (\delta_i \pm \delta_f)/2; \delta_{i,f} = \int_0^\infty W(\vec{R}, \vec{r}) dt$; $\vec{R}$ - the distance from the center of mass to the target to the particle 1; $\vec{k}_i$, f_i,$\vec{k}_f$, f_f are the momentum and wave functions of particles in initial and final states; $\vec{\Delta} = \vec{k}_f - \vec{k}_i$ is the transfer momentum; T_{if} – is T-matrix [1,2].

In case the $\mid \vec{\Delta} \mid \gg 1$ explicit expression for the differential cross section are presented.

Using this approximation the calculation of the different processes in the collisions H^+, D^+, T^+ with H and He, $He^+ + He$, $H_2^+ + He$ are present. The characteristic features(anomaly) in the ionization spectrum at forward angles (the continuum electron capture and binary encounter peak) and different mechanism of this processes are discussed. Nevertheless even this approximate calculation enables us to achieve satisfactory with experimental data [3].

The eikonal approximation for small angle for the scattering of fast particles not only makes it possible to express the scattering amplitude and cross section in simple form but also preserves many important properties of the exact solution for example it preserves the unitary relation, which the crude Born approximation does not do. In limiting cases the eikonal approximation reduces to the Born and classical approximations for small-angle scattering [3]. Note here that the analogous anomaly was obtained in elastic scattering by charged particles by set of two charges, equal magnitude and opposite to sign using eikonal approximation. According to [2,3] the anomaly angles is determined by the ratio of the interaction of the target to the energy of the incident particles. In case $H^+ + He$ we have $\theta \sim E_{e+He^+}/E_p \sim 24.6eV/20000eV \sim 1.23mrad$.

References

[1] Faddeev L D and Merkuriev S P 1983 Quantum scattering theory for several particles systems, Kluwer, London.

[2] Pozdneev S A 2001 Application on the quantum theory of few-body scattering to the calculation of the different processes in nuclear, atomic and molecular physics, Moscow, Janus-K.

[3] Demkov Yu N 1981 Sov.Phys.-JETP v.53 63 681

[1]E-mail: pozdneev@sci.lebedev.ru

Few-body approximation in chemical physics

Pozdneev S.A.[*1]

P.N.Lebedev Physical Institute, Department Quantum Radiophysics, Laboratory of Photochemical Processes, Leninsky pr.53, 119924, Moscow, Russia

Synopsis Electron scattering by atoms and molecules, multiple scattering approximation, Faddeev-Yakubovsky equations

The main difficulties in the research of few-body problems are bounded with the really many-channels and multidimensional nature of the these problem, impossible applied many well known theories such as adiabatic, impulse, coupled channels, etc.

For this reason we proposed new method for the investigation of the different few-body processes used the mathematically rigorous formalism based on the treatment of collision processes as many body processes, using Faddeev-Yakubovsky equations [1] (FYE) in integral and differential forms. In particular techniques based on FYE have been used successfully in studies of the dynamics of few-particle systems (bound-state properties and elastic, reactive and breakup scattering) [2]. That is why we applied this formalism for the theoretical investigation of the dynamics of the different processes in atomic and chemical physics. The following results are presented and discussed [2].

Calculation of low-energy characteristics in scattering processes like scattering length, effective range parameter, amplitude, cross section etc. in processes $p+d$, $n+d$, $p+He$, electron + molecule etc. for the verification of the fundamental principal of the atomic and chemical interaction.

The theoretical investigation of the quasi-bound, virtual and resonances states in few-body systems such as $p+d$, $n+d$, $e+H$, $e+He$, $p+H$, $p+He$.

Scattering the electrons, protons on the few-centers targets (atoms, molecules etc.) and the estimation the role of many center scattering in these cases.

The calculations of the excitation, rearrangement and ionization H and He atoms and its ions by the electrons and protons impact.

The investigation of the influence of the long range part of pair-wise potentials in FYE on the scattering in few-body systems.

The study on the correlation between low-energy characteristic in few-body scattering.

Scattering electrons by two atomic (H_2, HD, D_2, N_2, Cl_2, F_2, Br_2, J_2, HF, DF, HJ, DJ, HCl, DCl, HBr, DBr,$RbCl$, $RbBr$, $CsCl$, $CsBr$, KI) and few atomic molecules (CO_2, O_3, NF_3).

The investigation the theory of quasimolecule (electron + molecule), the ionization mechanism in quasimolecule and the main characteristics of quasimolecule autoionization states, determination of the bound between these states, the resonance states, potential energy surface (PES) and dynamics of the chemical reaction.

The scattering atoms with two ($O+CS$, $H+H_2$, $O+N_2$, $O+O_2$) and few atomic ($O+CF_3J$, $O+CS_2$, $O+OSC$, $HCl+HCl$) molecules, the many particles interactions, orientations of the reacting molecules etc. on the reactions dynamic, the confection between the interactions in FYE and PES, the investigation of the resonances, virtual states and threshold phenomena in chemical reactions.

The studding the unusual dynamical threshold phenomena in chemical reactions such as Efimov states based on FYE. This research may be obtain the information of the reaction mechanism, PES etc. and may have a strong influence on the scattering observable. Hence the careful studding of these states may be provide better understanding of the control and management of the chemical reaction processes.

The investigations of the possibility of the analytical solution of FYE in the different approximations, the construction of the solvable model in FYE approach are presented.

References

[1] Faddeev L D and Merkuriev S P 1983 Quantum scattering theory for several particles systems, Kluwer, London.

[2] Pozdneev S A 2001 Application on the quantum theory of few-body scattering to the calculation of the different processes in nuclear, atomic and molecular physics, Moscow, Janus-K.

[1]E-mail: pozdneev@sci.lebedev.ru

Dissociative electron attachment

S. Pozdneev

P.N.Lebedev Physical Institute, Department Quantum Radiophysics, Laboratory of Theoretical Radiophysics, Leninsky pr.53, 119924, Moscow, Russia

The dissociative attachment processes is the simplest chemical reaction induced by electrons and therefore a subject of rather theoretical and experimental research works [1-5]. However, it is only recently that papers have appeared investigating The dissociative attachment processes to molecules in preliminary prescribed excited rotational-vibrational states [1], threshold singularities [3] and resonances [2,3] of these reactions have been examined. The cross sections dissociative attachment reactions of electron to diatomic molecules H_2, HD, D_2, HCl, DCl, F_2, HF, DF, Cl_2, Br_2, HBr, DBr, I_2, DI, HI, N_2, Li_2, Na_2 have been calculated. The main approximation in this approach consists in the fact that the interaction of an incident electron with electrons and nuclei a target molecule is replaced by interaction of an incident electron with each atoms as a whole and atom is considered to be the field center. So, the complicated many particle problem of calculation of the cross sections of electron scattering by diatomic molecules is reduced to a three-particle problem which is solved by method of quantum few-body theory of scattering proposed L.D.Faddeev and O.Y.Yakubovski [4] This method is applicable for the description of both the direct processes and the processes proceeding without the formation of intermediate long-lived states. Therefore, this approach is applied here to calculate the cross sections of an electron collision with diatomic molecules in the ground state and preliminarily prescribed arbitrary rotational-vibrational states. The results of calculations are presented and compared with the available experimental data and with the results of calculation using other approximation. Comparison of the performed calculations with experimental data shows that simulation of the interaction, in the framework of present above gives satisfactory agreement with experiment [1], coincidence of the orders of magnitude of cross sections, including the izotopic effects [5], and confirms the existence of the Efimov [3] effect in dissociative attachment processes.

References

[1] Schultz G.J. Rev.Mod.Phys.,v.45,1973,p.423; Gallup G.A., Fabricant I.I. Phys.Rev., v.A57, 1998,p.2596.

[2] Pozdneev S. Application of quantum theory of scattiring to the calculations of different processes in nuclear, atomic and molecular physics, Moscow, Janus-K, 2001; Dynamics of Elementary Atomic-Molecular Processes in Gas and Plasma, Nova Sci. Publ., v.212, 1996; Pozdneev S. JETP, v.99, N 5, 2004, p.915-933; J.Rus.Las.Res.,v.22, 2001, p.175; Bull. Lebedev Phys.Inst., N5, 2003, p.1.

[3] Efimov V. Nucl.Phys., A362, 45, 1981; A378, 581, 1982; Phys.Rev., C47, 1876, 1993; Vugalter S.A., Zislin G.M. Dokl AN USSR, 1982, v.267, p.784.

[4] Faddeev L.D., Merkuriev S.P. Quantum scattering theory for several particles systems, Kluwer, London, 1993.

[5] Demkov Yu.N., Ostrovskii V.N. Zero-range potentials and their application in atomic physics, Plenum, 1988; Phys.Lett., v.15, p.235, 1956.

Physics Education and outreach using ion and electron beams

P. Riccardi*, V. Romano and F. Pellegrino

Dipartimento di Fisica, Università della Calabria and INFN, gruppo collegato di Cosenza, Rende (CS)- Italy

*Pierfrancesco.riccardi@unical.it

Abstract: The need to communicate with the public is widely known within the broadest scientific community and education and public outreach have become important aspects in the working life of research scientists. We have recently reported on education and public outreach activities with schools using vacuum equipments [1], that favor a large involvement of researchers, supporting a sustained interaction of researchers with school pupils and teachers. Here, we would like to present some of the activities that used ion and electron beams, developed to create contact between schools in the region of Calabria and our physics department

[1] P. Riccardi, V. Romano, F. Pellegrino Vacuum 196 (2022) 110737

Swift heavy ion irradiation of bismuth nanowires pressurized in diamond anvil cells

C. Schröck[1,2*], I. Tzifas[1], K.O. Voss[1], L. Bayarjargal[2], W. Sigle[3], I. Schubert[1], M.E. Toimil-Molares[1], B. Winkler[2] and C. Trautmann[1,4]

[1]*Materials Research, GSI Helmholtz Center for Heavy Ion Research, Germany*
[2]*Institute of Geosciences, Goethe University Frankfurt, Germany*
[3]*Max-Planck Institute for Solid State Research, Stuttgart, Germany*
[4]*Department of Materials- and Geosciences, Technical University of Darmstadt, Germany*
[*]*c.schroeck@gsi.de*

The simultaneous exposure of materials to multiple extreme conditions is a field of increasing interest in modern high pressure research. A worldwide unique approach, applying concomitantly high-pressure using diamond anvil cells (DACs) and irradiation with swift heavy ions (SHI) of GeV energies has been pioneered at GSI Helmholtz Center Darmstadt [1] and revealed new effects such as the generation of new phases far from thermodynamic equilibrium or the stabilization of high pressure phases at ambient conditions [2].

In this report, we present activities to exploit intrinsic properties of nanomaterials beneficial for the manipulation of high pressure phase diagrams [3]. As material of interest bismuth was selected, due to its complex and well-characterized high-pressure phase diagram and its sensitivity to SHI irradiation. The experiments require the fabrication of bismuth nanowires by electrodeposition in etched ion-track membranes (example shown in Fig. 1) [4], compression of miniaturized samples in DACs and subsequent irradiation using relativistic heavy ions of typically several tens of GeV kinetic energy. Preliminary experiments including reference irradiation studies of bismuth nanowires at ambient conditions and high pressure x-ray diffraction studies will be presented. The aim of this project is to investigate to what extent size effects can be utilized in order to promote SHI-induced high p-T phase transitions and to provide insight into the underlying mechanisms of the combined pressure and irradiation effects.

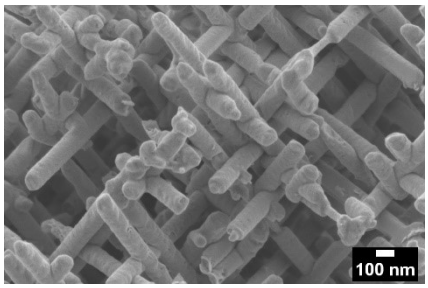

Figure 1: SEM image of a bismuth nanowire network

References

[1] Glasmacher, U.A. et al., Physical Review Letters, **96**(19), (2006), p. 195701
[2] Lang, M. et al., Nature materials, **8**(10), (2009), p. 793-797
[3] Machon, D. et al., Journal of Applied Physics, **124**(16), (2018), p. 160902
[4] Wagner, M.F.P. et al., Advanced Electronic Materials, **7**(3), (2021), p. 2001069

Mechanisms of ion irradiated MWNT antibacterial activity: experiment and calculation

A. Stepanov[1*], A. Shemukhin[2] A. Dimitrieva[1], and A. Nazarov[2], A. Popov[1], D. Yumanov[1], A. Kovalenko[1], E. Vorobyeva[2]

[1]*Hematological Laboratory, Chuvash State Agrarian University, Russian Federation, Russia*
[2]*Skobeltsyn Institute of Nuclear Research, Lomonosov Moscow State University, Russia*
[*]*for.antonstep@gmail.com*

The mechanism of the antibacterial effect of nanomaterials has not been sufficiently studied to date [1], on the basis of modern studies it can be argued that most nanoparticles are effective against most, both gram positive and gram negative bacteria [1-5]. Also, some papers describe the negative impact of nanostructures on viral particles [5].

At the moment, some antibacterial mechanisms have already been proven.

1. Fixation of nanoparticles on the cell walls of bacteria and penetration into it, which thereby affects the permeability of the wall and causes cell death [1,2,4,5], the mechanism of this action is described in [5] - electrostatic interactions between the conductive polymer and bacteria lead to the adhesion of microorganisms to the surface of the polymer. Then the diffusion of nanoparticles and particles of active counterions to the cytoplasmic membrane occurs, followed by their penetration into the cell, which ultimately leads to cell death, in [3,5] it is said that the direct destruction of the bacterial membrane leads to the death of the bacterial cell;

2. Destruction of the bacterial cell wall due to oxidative stress, which occurs as a result of an instant reaction with fatty acids, proteins and sugar molecules, which in turn causes a rapid stimulation of lipid peroxidation activity, which causes membrane disintegration, damage to it and the release of cell contents to the outside [1,2,4,5];

3. Interaction of positively charged groups of nanoparticles with a negatively charged bacterial membrane, which in turn causes osmotic disproportion and, as a consequence, prevents the growth of bacteria [4, 5].

In this work, we have calculated (method of molecular dynamics) and experimentally shown that for MWCNTs, the first and second mechanisms of antibacterial activity take place.

References

[1] R. Singh, M. S. Smitha, and S. P. Singh, *J Nanosci Nanotechnol*, 14 (2014) 4745-56
[2] J. R. Rajabathar, G. Periyasami, A. M. Alanazi, M. Govindasamy, P. Arunachalam, *Processes* 8 (2020) 1654
[3] L. Gabrielyan, H. Badalyan, V. Gevorgyan, et al. *Sci Rep* 10 (2020) 13145
[4] Y.N. Slavin, J. Asnis, U.O. Häfeli, et al. *J Nanobiotechnol* 15 (2017) 65.
[5] A. M. Díez-Pascual, *Int J Mol Sci.* 22 (2021) 10511

Si doping of beta-Ga_2O_3 defect calculation

A. Stepanov[1*], E. Okulich[2] and D. Tetelbaum[2]

[1]*Hematological Laboratory, Chuvash State Agrarian University, Russian Federation, Russia*
[2] *Lobachevskiy Nizhniy Novgorod State University, Russia*
[*]*for.antonstep@gmail.com*

Calculation of the band structure and other properties in β-Ga_2O_3 for Si implanted in the crystal instead of GaI, GaII was performed by the density functional theory method in the plane-wave basis (projector augmented wave - PAW) using Ga pseudopotentials, taking into account 3d valence electrons. The expansion in the plane-wave basis was carried out up to an energy of 520 eV. The hybrid exchange-correlation functional Heyd-Scuseria-Ernzerhof HSE [1] with mixing parameters α=0.35, μ=0.20 Å-1 was used for the calculation. To calculate the thermal stability of implanted defects, the Nudged Elastic Band method was used from first principles. Several nonequivalent positions of defects in the β-Ga_2O_3 lattice were considered. Defects were considered at concentrations of 5, 10, 15.20% by weight

Changes in the width and topography of the band structure and the mobility of charge carriers are obtained.

References

[1] 1. Heyd, Jochen, Gustavo E. Scuseria, and Matthias Ernzerhof, *The Journal of Chemical Physics*, 18 (2003) 8207-15

Radiation tolerance of GaN and Ga_2O_3: role of the defect generation rate

A.I. Titov[1], K.V. Karabeshkin[1], A.I. Struchkov[1], A. Azarov[2], P.A. Karaseov[1,*]

[1]*Peter the Great St.-Petersburg Polytechnic University, St-.Petersburg, Russia*
[2]*Centre for Materials Science and Nanotechnology, University of Oslo, Norway*
[*]*platon.karaseov@spbstu.ru*

Gallium nitride (GaN) and gallium oxide (Ga_2O_3) are semiconductors with wide bandgap of 3.4 and 4.5-5.3 eV, respectively. In contrast to GaN which has become a dominant material for a range of high-power and UV optoelectronic devices, research interest on Ga_2O_3 has not reached maturity, despite it is considered as one of the most promising candidates for next generation power electronics. Among existing Ga_2O_3 polymorphs, monoclinic β-Ga_2O_3 is the only one thermodynamically stable phase. However, metastable corundum α-phase is also attractive since it has a higher bandgap than β one.

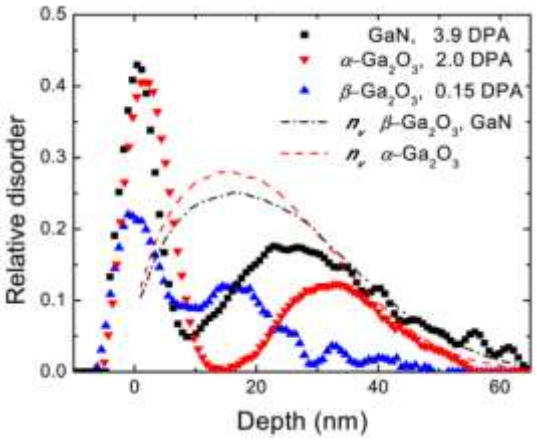

Figure 1. Depth profiles of relative disorder in GaN, α- and β-Ga_2O_3 implanted with 40 keV P ions to doses indicated. Profiles of ion-generated lattice vacancies predicted by TRIM simulations are shown by the dashed lines [2].

There are practically no systematic investigations of irradiation-induced defects in different Ga_2O_3 polymorphs, and the most of existing data are focused on defect formation in β-phase (see, for instance, [1]). Recently, we have demonstrated that ion-induced damage formation in GaN and Ga_2O_3 polymorphs exhibits different behavior. For example, Fig. 1 shows that despite the main features of depth distributions of ion-induced defects are similar for these materials the doses required to achieve the same damage level are quite different. In the present contribution, we analyze the role of the defect generation rate on the disorder formation in all three semiconductors. Specifically, GaN, α-Ga_2O_3 and β-Ga_2O_3 samples were irradiated at room temperature with 40 keV P^+ ions to various doses using different ion fluxes. The resulting radiation damage was measured using RBS/C technique.

We demonstrate that the radiation resistance of α- and β-Ga_2O_3 polymorphs is lower than that of GaN. At the same time, damage in β-Ga_2O_3 accumulates at the rate an order of magnitude higher than in α-phase. Furthermore, our results revealed different dose-rate effects (i.e. the dependence of defect accumulation on ion beam flux) in these materials. The mechanisms of radiation damage formation in these semiconductors will be discussed.

Work was supported by Russian Science Foundation grant # 22-19-00166.

References

[1] A. Azarov, et al. *Phys. Rev. Lett.* 128 (2022) 015704
[2] A.I. Titov. et al. *Vacuum* 200 (2022) 111005

A graphical user interface for SDTrimSP

P.S. Szabo[1,2,*], **D. Weichselbaum**[1], **H. Biber**[1], **C. Cupak**[1], **A. Mutzke**[3], **R.A. Wilhelm**[1], **and F. Aumayr**[1]

[1]*Institute of Applied Physics, TU Wien, Vienna, Austria*
[2]*Space Sciences Laboratory, University of California, Berkeley, USA*
[3]*Max Planck Institute of Plasma Physics, Greifswald, Germany*
[*]*szabo@berkeley.edu*

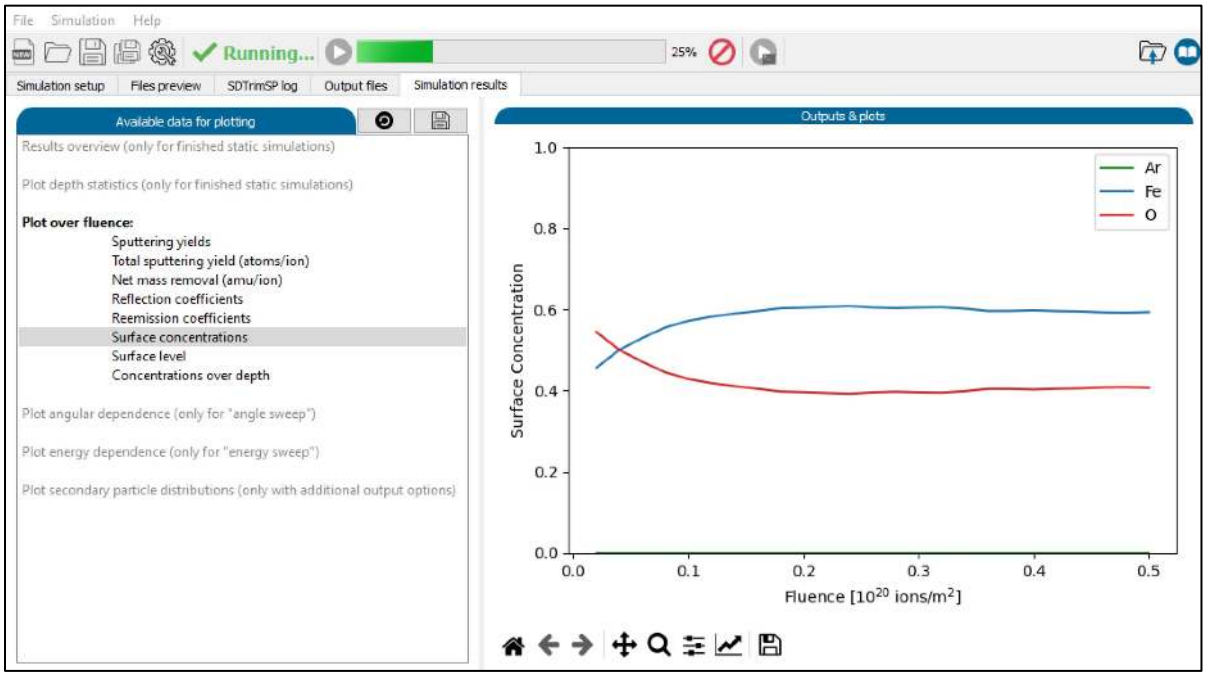

Figure 1: A screenshot of the GUI that shows an evaluation example for 2 keV Ar impacting an Fe_2O_3 sample under 60°. In particular, surface concentration changes due to preferential O sputtering are depicted here.

In comparison to the commonly used binary collision approximation code TRIM [1], the program SDTrimSP provides additional capabilities for simulating ion-solid interaction – mainly in the form of dynamic simulations that account for ion-induced target changes [2]. Furthermore, SDTrimSP has been found to perform favorably for the simulation of sputtering yields [3].

In order to make SDTrimSP easier to use, we have now developed a graphical user interface (GUI) companion program [4]. With this GUI, SDTrimSP simulations can be prepared, started and directly evaluated (see Fig.1). It can be used for the calculation of sputtering yields, ion reflection coefficients and ion-induced dynamic effects as well as for the investigation of implantation ranges or vacancy formation. The GUI will be made available online to allow access for a broad group of potential users.

References

[1] J.F. Ziegler, M.D. Ziegler, and J.P. Biersack, *Nucl. Instrum. Methods Phys. Res. B*, 268. (2010), 1818-1823
[2] A. Mutzke, et. al., *IPP Report*, 2019-02 (2019)
[3] H. Hofsäss, K. Zhang, and A. Mutzke, *Appl. Surf. Sci.*, 310 (2014), 134-141
[4] P.S. Szabo, et. al., submitted to *Nucl. Instrum. Methods Phys. Res. B* (2022)

Projectile dependence in dissociation of biomolecules by swift heavy ion irradiation

Tomoya Tezuka[1], Mizuki Hongo[1], Takuya Majima[1], Manabu Saito[1,2], and Hidetsugu Tsuchida[1,2,*]

[1]*Department of Nuclear Engineering, Kyoto University, Japan*
[2]*Quantum Science and Engineering Center, Kyoto University, Japan*
[*]*tsuchida@nucleng.kyoto-u.ac.jp*

Elucidation of biomolecular damage caused by ion beams is vital in particle beam cancer treatment. So far, protons and carbon ion beams have been used in particle beam therapy in cancer. Recently, a new irradiation method using two or more types of ion beams called multi-ion radiation therapy has been studied to optimize dose distribution around tumor cells [1]. In multi-ion radiotherapy, helium, carbon, oxygen, and neon ion beams are being considered. Based on this background, in this work, we irradiated solid-phase nucleotide molecules with various types of ion beams to understand the particle dependence of ion beams in the biomolecular dissociation. The damaged sites of the biomolecule were identified by secondary ion mass spectrometry.

The experiments were performed using 2.0-MV tandem Pelletron accelerator at Kyoto University. Projectiles were 0.5 – 3.5 MeV helium, 0.6 – 5.0 MeV carbon, and 1.0 – 5.0 MeV oxygen beams. The beam was incident on biomolecule targets and then secondary ions emitted from the target were measured by a time-of-flight secondary ion mass spectrometer. The target was uridine 5' – monophosphate (UMP), prepared on a silicon wafer by dropping high-concentration UMP solutions on a silicon wafer and then drying it under the atmosphere.

Figure 1 shows the TOF mass spectra of positive secondary ions emitted from the UMP target for 3.0-MeV He^+, C^{2+}, and O^{2+} irradiation, respectively. The peak intensities of secondary ions with damaged phosphate ($[PO+CH_3]^+$, $NaPO_2^+$, $[PO_3+C_2H_3O]^+$, and $[PO+R]^+$ ("R" indicates ribose)) becomes stronger in the case of C^{2+}, and O^{2+} irradiation. This result suggests that DNA strand breaks are more likely to occur with heavy ion irradiation. This trend is consistent with previous studies using DNA targets [2].

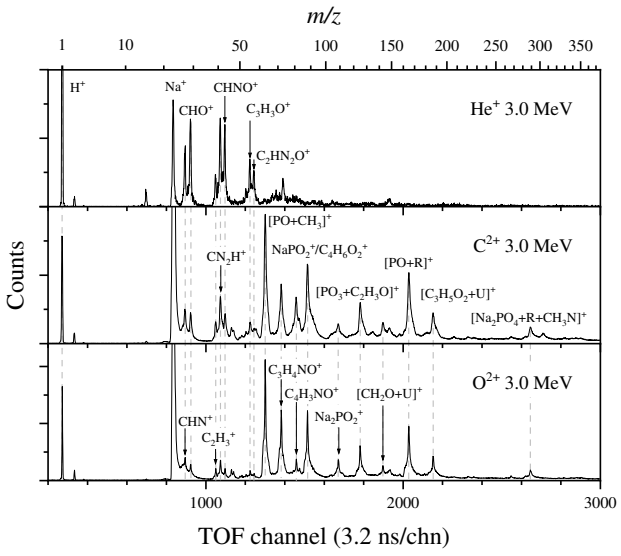

Figure 1: TOF mass spectra of positive ions emitted from the UMP target with 3.0-MeV He^+, C^{2+}, and O^{2+} impact, respectively.

References

[1] D.K. Ebner, S.J. Frank, T. Inaniwa, S. Yamada, T. Shirai, *Front. Oncol*, 11, 624786 (2021).
[2] A. Urushibara, N. Shikazono, P. O'Neill, K. Fujii, S. Wada, A. Yokoya, *Int. J. Radiat. Biol.* 84, 1, (2008).

Development of analytical methods in the sputtering theory of solids

L. Forlano[1] and A. I. Tolmachev[2]

[1] *University of Calabria, Cosenza, Italy*
[2] *Russian New University, Moscow, Russia*
tolmachev.alex@rambler.ru

In the last years analytical investigation of sputtering processes in solids under ion bombardment is practically substituted by computer simulation. Nevertheless, as before in progress are the new attempts to reduce explanation of basic sputtering characteristics to the analysis of some magic formula or integral. Theoretical treatment of sputtering is usually performed in the frames of some simplifying assumptions. Sigmund sputtering theory [1] uses the infinite medium approximation, disregards the target surface, and considers the angular distribution of sputtered atoms as isotropic. At low energies of sputtered atoms their energy distribution turns out to be proportional to the inverse energy squared,

$$f(u)\,du = C\,\frac{du}{u^2} \qquad for \qquad u = \frac{E}{E_0} \ll 1\,, \tag{1}$$

where E is the energy of sputtered particle and E_0 is the energy of ions. The energy distribution (1) disagrees with the law of conservation of energy, because total cascade energy becomes infinite. In refs. [2,3] the target surface is included in consideration and the angular distribution is expressed as a superposition of spherical functions. That modifies the energy distribution (1) and weakens the singularity at the point $u = 0$:

$$f(u)\,du = C\left(\ln\frac{1}{u}\right)^{-3/2}\frac{du}{u^2} \qquad for \qquad u \ll 1\,. \tag{2}$$

The energy distribution (2) leads to finite total energy of the atomic cascade. But the delta-type boundary condition for ions cannot be described adequately by the first two or three Legendre polynomials. In ref. [4] the method of discrete streams removed the problem of boundary condition, but the inverse Laplace transformation was performed only approximately.

In the present work the inverse Laplace transformation is expressed in the form of integral in the complex plane and it can be calculated with arbitrary accuracy. The analytical formula for the Laplace transform $g(s)$ can be divided in the real and imaginary parts after substitution $s = 1 + i\omega$. After calculation the integral we get the energy distribution of sputtered atoms not only for the case of low energies $u \ll 1$, but for the whole energy range $0 < u \leq 1$ [5]. Using the formula obtained we can analyze the dependence of sputtering yield on the ion energy, ion mass, atomic potential and inelastic energy losses of particles in the matter.

References

[1] P. Sigmund. Physical Review, **184** (1969) 383.
[2] J. B. Sanders and H. E. Roosendaal. Radiation Effects, **24** (1975) 161.
[3] M. Vicanek and H. M. Urbassek. NIMB, **30** (1988) 507.
[4] A. I. Tolmachev. NIMB, **93** (1994) 415.
[5] A. I. Tolmachev and L. Forlano. Technical Physics, **65** (2020) 851.

Effect of molecular axis orientation of 3.6 MeV Si_2^+ on secondary electron emission from carbon foils

Naruki Uno[1], **Takuya Majima**[1], **Manabu Saito**[1,2], **Hidetsugu Tsuchida**[1,2,*]

[1]*Department of Nuclear Engineering, Kyoto University, Japan*
[2]*Quantum Science and Engineering Center, Kyoto University, Japan*
[*] *tsuchida@nucleng.kyoto-u.ac.jp*

When swift cluster ion beams interact with matter, the unique irradiation effect occurs. This effect originates from the interference between the component atoms of the cluster, which is called vicinage effects. The vicinage effects have been observed in many physical phenomena [1]. The magnitude of vicinage effects depends on cluster size, geometric structure of the cluster, and molecular axis orientation. However, the origin of vicinage effects is not entirely understood. So, we experimentally investigated the effect of molecular axis orientation on the energy of secondary electrons.

The experiment was performed by using 2 MV tandem Pelletron accelerator at the Quantum Science and Engineering Center, Kyoto University. The projectile beam was 3.6 MeV Si_2^+, and the target was C foil with a thickness of 1.0 μg/cm^2. The backward emitted electrons to the beam direction were detected with a retarding field detector to measure the energy of electrons. When the projectile entered the target, Si_2^+ fragmented into two Si^{q+} ions with a charge state q and was separated by the Coulomb explosion. The fragments were deflected with an electric field applied by a parallel plate deflector and detected by a microchannel plate (MCP) with a phosphor screen anode. A CMOS camera recorded a two-dimensional image of two Si^{q+}. We obtain molecular orientation angle θ using the image data. The start trigger was a signal of the MCP, and we measured yields of secondary electrons in an event-by-event mode.

The molecular orientation angle θ = 0–30°, 60–90°, and 0–90° to the beam direction were defined as parallel, perpendicular, and random, respectively. The observed energy distribution of secondary electrons showed a maximum value near 18 eV. The secondary electron yield at energies below 18 eV depends on the molecular axis orientation of the incident Si_2^+. As shown in Table 1, this dependence was the same as the orientation effect of electronic stopping power calculated using the method described in Ref. [1].

Table 1: The relationship between yields of secondary electrons and the electronic stopping power. Y indicates yields of secondary electrons with an energy of 18 eV or less.

Orientation	Y	S_e (eV/Å)
Parallel	0.227 ± 0.008	288.5
Perpendicular	0.252 ± 0.010	329.2
Random	0.234 ± 0.005	319.1

References

[1] T. Kaneko, H. Kudo, S. Tomita, and R. Uchiyama, *J. Phys. Soc. Jpn*, 75 (2006) 1-6.

Surface treatment procedures to mitigate desorption processes induced by swift heavy ions

V. Velthaus[1,2 *], **C. Trautmann**[1,2], **and M. Bender**[1,3]

[1]*GSI Helmholtzzentrum fuer Schwerionenforschung, Planckstr. 1, 64291 Darmstadt, Germany*
[2]*Technische Universität Darmstadt, Alarich-Weiss-Str. 2, 64287 Darmstadt, Germany*
[3]*Hochschule RheinMain, Am Brückweg 26, 65428 Rüsselsheim, Germany*
[*]*v.velthaus@gsi.de*

Ion-induced desorption is a serious limitation for stable operation of high beam intensities in heavy ion synchrotrons. The desorption is mainly stimulated by lost ions that collide with the vacuum chamber wall and trigger the release of gas, predominantly hydrogen and carbon oxides. Due to the higher gas density, the beam loss is enhanced and the effect is self-amplifying. Next generation heavy ion accelerators like FAIR or SPIRAL2 are designed for intensities that are orders of magnitude higher than the intensity of existing machines. Hence, ion-induced desorption becomes a big challenge.

To better understand and control the influence of material and surface factors, desorption measurements with swift heavy ions (Ca and Au at 4.8 MeV/u) were conducted with focus on oxygen-free copper and tungsten samples. The surfaces were treated by different combinations of milling, lapping, polishing, etching and sputtering. Some of the samples were coated by carbon, titanium nitride. Additionally, some stainless steel samples coated with TiZrV were analyzed. For all tested samples desorption yields (number of released molecules per impacting ion) for H2, H2O, CO, CO2, O2 and Ar will be presented. For copper, surface cleaning by sputtering with 5 keV argon ions reduces the desorption yield significantly. Another promising method to reduce ion-induced desorption is thermal annealing at 400 °C for about 4 h under ultra-high vacuum conditions. Suitable annealing, cleaning and coating parameters will also be presented.

Molecular Dynamics Simulations of Silicon Vacancy and Nitrogen Vacancy Color Centers in Diamond

Wei Zhao[1], Zongwei Xu[1,*] , Fei Ren[1], Jintong Wu[1], and Tianze Sun[1]

[1] *School of Precision Instrument and Opto-Electronic Engineering, Tianjin University, China*

*zongweixu@tju.edu.cn

Diamond can be used in optical and electronic detection because of its low thermal conductivity, wide band gap and long spin coherence time. The internal point defects, including, silicon vacancy (SiV), nitrogen vacancy (NV), within the diamond produced by ion implantation modification, femtosecond laser processing or electron irradiation can be applied to quantum sensing, biomarkers or temperature monitoring. However, the much low yield of color center is still a critical problem to be solved. Molecular dynamics simulation can well explain the modification principle and defect formation mechanism of ion implantation for the color center's nanofabrication. It was found that SiV and NV color centers can be produced in silicon or nitrogen ion implanted diamond by molecular dynamics simulation. The color centers' yield was discussed by changing the key parameters of ion implantation into diamond with different incident angle and subsequent annealing setups. It was also found that silicon ion implantation into the stress-assisted substrate can improve the yield silicon-vacancy color center in diamond.

A novel method for preparing highly sensitive graphene room temperature gas detectors

J. Zeng[1,*], **P.C. Ma**[1,2], **S.X. Zhang**[1], **L.J. Xu**[1], **P.P. Hu**[1], **and J. Liu**[1]

[1] *Institute of Modern Physics, Chinese Academy of Sciences (CAS), Lanzhou 730000, PR China;*
[2] *University of Chinese Academy of Sciences (UCAS), Beijing 100049, PR China.*
[*] *zengjian@impcas.ac.cn*

The detection of poisonous gas is very important in industrial production and our daily life. Traditional metal oxide sensors always have high operating temperature and have the risk of igniting flammable gases. It is necessary to develop a new and efficient gas sensitive element. Graphene has a very high specific surface area and electron mobility. Theoretically, graphene can detect a single gas molecule [1], and it is sensitive to a concentration variation of gases at room temperature. Graphene meets the needs of further development of gas detectors in lower energy consumption, higher sensitivity, smaller size and flexible sensors.

Theoretical calculations show that using defected graphene can improve the performance of graphene gas detectors. Ion irradiation is an effective way to introduce defects in the materials. In this work, we investigate the irradiation effects of graphene gas detectors induced by highly charged ions (HCIs, 4.25 MeV $^{54}Xe^{17+}$) and find obvious gas sensing improvement in irradiated detectors (Fig. 1a). In 1 ppm NO_2 atmosphere, 27 times higher gas sensitivity was detected in irradiated detectors (Fig. 1b). Even in the low concentration (50 ppb), 12 times sensitivity improvement was achieved. Furthermore, we obtained optimal sensitivity enhancement of graphene gas detectors for the irradiation fluences ranging from 1×10^{13} ions/cm^2 to 7×10^{14} ions/cm^2.

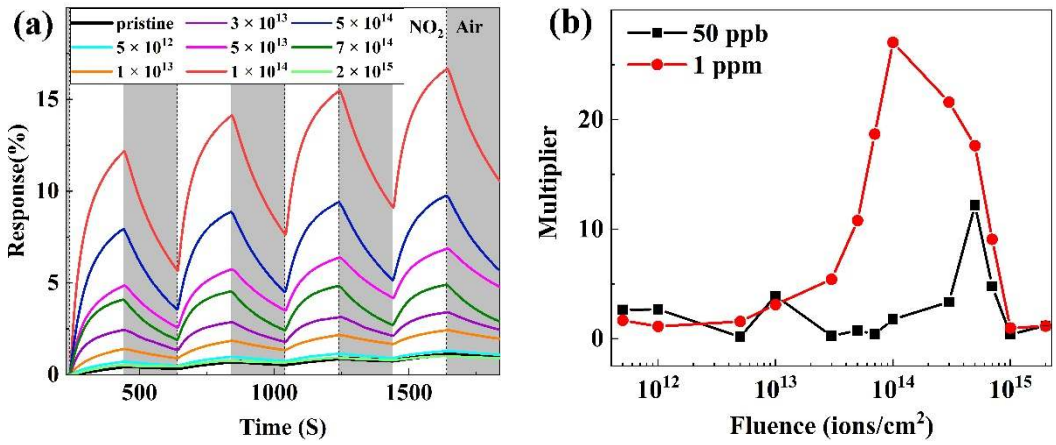

Figure 1: (a) response of the pristine and sensors irradiated with different ion fluences to 1ppm NO_2. (b) Evolution of gas sensing enhancement multiplier with increasing irradiation fluence for 50 ppb and 1 ppm NO_2 concentrations.

Our work paves a way to effectively improve the sensitivities of two-dimensional material-based gas detectors. This is especially important for the development of new generation detectors which work at room temperature.

References

[1] F. Schedin, A.K. Geim, S.V. Morozov, E.W. Hill, P. Blake, M.I. Katsnelson and K.S. Novoselov, *Nature Materials*, 6 (2007) 652-655.

Phase Stability of Pre-irradiated CeO_2 with Swift Heavy Ions under High Pressure up to 45 GPa

J. Lan[1,2], P. Zhai[1,2,*], S. Nan[3], L. Xu[1], J. Niu[3], C. Tian[1,2], Z. Li[1], W. Li[3], J. Liu [1,2], and R. Ewing[4]

[1]*Institute of Modern Physics, Chinese Academy of Sciences, Lanzhou, China*
[2]*School of Nuclear Science and Technology, University of Chinese Academy of Sciences, Beijing, China*
[3]*State Key Laboratory of Tibetan Plateau Earth System, Resources and Environment (TPESRE), Institute of Tibetan Plateau Research, Chinese Academy of Sciences, Beijing, China*
[4]*Department of Geological Sciences, Stanford University, Stanford, California, USA*
[*]*zhaipengfei@impcas.ac.cn; j.liu@impcas.ac.cn*

CeO_2 is often used as a non-radioactive surrogate of UO_2 and PuO_2 to simulate the radiation damage of nuclear fuel by fission fragments. At ambient conditions, CeO_2 exhibits a fluorite structure. The first-order phase transition occurs at about 31 GPa. One interesting question is how the radiation damage in a material affects its high-pressure behavior. The effect of defects on the high-pressure behavior of materials is fundamental to understanding and designing materials for extreme environments. Previous work has demonstrated that radiation damage can enhance phase stability or alter the transformation pathway [1,2]. It is necessary to explore this interesting issue in more materials.

In this work, the polycrystalline CeO_2 was first irradiated with 336 MeV Xe ions over a large fluence range of 3×10^{10}-2×10^{13} ions/cm^2. Then, the irradiated CeO_2 was compressed in diamond anvil cell up to ~45 GPa, using argon as the pressure-transmitting medium to avoid any possible reaction with the irradiated CeO_2 and to provide a quasi-hydrostatic condition. High-pressure Raman spectroscopy shows that low-fluence ion irradiated CeO_2 (3×10^{10} and 3×10^{11} ions/cm^2) exhibits nearly the same high-pressure behavior as unirradiated CeO_2; whereas, after high-fluence irradiation (3×10^{12} and 2×10^{13} ions/cm^2), the phase stability of CeO_2 is significantly enhanced, with the critical phase transition pressure increased from 31.7 to 37.3 GPa and only about 7% high-pressure phase transition fraction at 45.1 GPa (2×10^{13} ions/cm^2). In comparison with the high-pressure Raman results of pre-irradiated CeO_2 before and after 573, 1073 and 1273 K annealing in air, we propose that large interstitial-type defect clusters, such as dislocation loops formed in heavily-irradiated CeO_2, are predominately responsible for the increased phase stability at high pressures.

References

[1] M. Lang, F. Zhang, J. Lian, C. Trautmann, R. Neumann, and R. Ewing, *Earth and Planetary Science Letters*, 269(2008)291–295

[2] S. Park, C. Tracy, F. Zhang, C. Park, C. Trautmann, S. Tkachey, M. Lang, W. Mao, and R. Ewing, *Physical Chemistry Chemical Physics* 20(2018)6187-6197

Swift Heavy Ion Tracks in CeO_2

J. Lan[1,2], P. Zhai[1,2,*], S. Nan[3], L. Xu[1], J. Niu[3], C. Tian[1,2], Z. Li[1], W. Li[3], J. Liu [1,2,*], and R. Ewing[4]

[1]*Institute of Modern Physics, Chinese Academy of Sciences, Lanzhou, China*
[2]*School of Nuclear Science and Technology, University of Chinese Academy of Sciences, Beijing, China*
[3]*State Key Laboratory of Tibetan Plateau Earth System, Resources and Environment (TPESRE), Institute of Tibetan Plateau Research, Chinese Academy of Sciences, Beijing, China*
[4]*Department of Geological Sciences, Stanford University, Stanford, California, USA*
[*]*zhaipengfei@impcas.ac.cn; j.liu@impcas.ac.cn*

This work was motivated mainly by two factors. First, it was found that the ion track morphology in rutile TiO_2 is variable as a function of the ion path length in our previous work [1]. These results have been attributed to the outflow of the thermal-spike-induced molten phase and epitaxial recrystallization during rapid quenching [1]. We suggested that materials with strong recrystallization ability are the prime candidates for finding this variable morphology of ion tracks. Second, Ishikawa et al. [2] found that the spherical hillock of ion track in CeO_2 is crystalline. This indicates that recrystallization plays an important role in the formation of crystalline hillocks. However, it is still unclear whether the morphology of ion tracks in CeO_2 is influenced by the recrystallization effect as we predicted.

In this work, polycrystalline CeO_2 samples pre-deposited on TEM grid were irradiated with 550 MeV Bi ions under 45° incidence. The TEM results confirm that the ion track in CeO_2 evolves with the ion path length as previously observed in rutile TiO_2. The actual length of conical track near surface is estimated to be about 75 nm. It indicates that below this depth the "pure" bulk effect with more efficient recrystallization works (the remained damage is usually difficult to be observed by conventional TEM).

Furthermore, according to the similarity in ion track and strong recrystallization ability of fluorite-structured CeO_2 and UO_2, we infer that the track morphology near surface of UO_2 should exhibit the same behavior as CeO_2. It is known that fission tracks have never been observed in bulk UO_2 and it was previously explained that the electronic energy loss of fission fragments is below the threshold of track formation (22–29 keV/nm) in UO_2 [3]. However, our present work might provide some new insights into no fission tracks in bulk UO_2, i.e., the strong recrystallization suppresses the fission track formation in bulk of UO_2. This hypothesis is supported by one previous result of single crystalline UO_2 irradiated with 944 MeV Pb ions [4], where the RBS/C results show that only the extent of radiation damage in the first ~100 nm depth is high, whereas it is very low and almost constant in the deep, although the average electronic energy loss from the surface up to 5 μm is as much as 55 keV/nm.

References

[1] P. Zhai, S. Nan, L. Xu, W. Li, Z. Li, P. Hu, J. Zeng, S. Zhang, Y. Sun, and J. Liu, *Nuclear Instruments and Methods in Physics Research Section B: Beam Interactions with Materials and Atoms*, 457(2019)72–79
[2] N. Ishikawa, N. Okubo, and T. Taguchi, *Nanotechnology*, 26(2015)355701
[3] T. Wiss, Hj. Matzke, C. Trautmann, M. Toulemonde, and S. Klaumünzer, *Nuclear Instruments and Methods in Physics Research Section B: Beam Interactions with Materials and Atoms*, 122(1997)583–588
[4] F. Garrido, S. Moll, G. Sattonnay, L. Thomé, and L. Vincent, *Nuclear Instruments and Methods in Physics Research Section B: Beam Interactions with Materials and Atoms*, 267(2009)1451-1455

Trion Emission in WSe_2 Tuned by Swift Heavy Ion Irradiation

S. X. Zhang[1,*], **L. J. Xu**[1], **P. P. Hu**[1], **K. Maaz**[1], **J. Zeng**[1], **P. F. Zhai**[1], **Z. Z. Li**[1], **L. Liu**[1], **J. Liu**[1]

[1]*Materials Research Center, Institute of Modern Physics, Chinese Academy of Sciences (CAS), Lanzhou, 730000, P. R. China*

*zhangsx@imcas.ac.cn

Understanding and facilitating defects in two-dimensional transition metal dichalcogenides (TMDCs) are of fundamental importance for their application in optoelectronic devices and valleytronic devices. In this study, swift heavy ion (SHI) irradiation was applied to introduce defects in monolayer WSe_2 in a controlled manner. Disordered latent tracks were observed normally distributed on multilayer WSe_2, as shown in Fig. 1a. Temperature-dependent photoluminescence and transient absorption spectroscopy are employed to investigate the excitonic performances in defective WSe_2. Compared with exciton emission, the ratio of trion emission of WSe_2 has enhanced significantly for WSe_2 irradiated with elevated fluences, as shown in Fig. 1b. The recoiled atoms from the substrate SiO_2 contributed the probability of trion formation. SHI irradiation caused atomic mixing at the interface between WSe_2 and SiO_2 has been confirmed according to SRIM calculation[1], as shown in Fig. 1c. These results not only display that the fact that excitonic performance of TMDCs can be modulated, but also reveal that SHI irradiation is an effective technique that promotes applications of TMDCs in photonics and valleytronics.

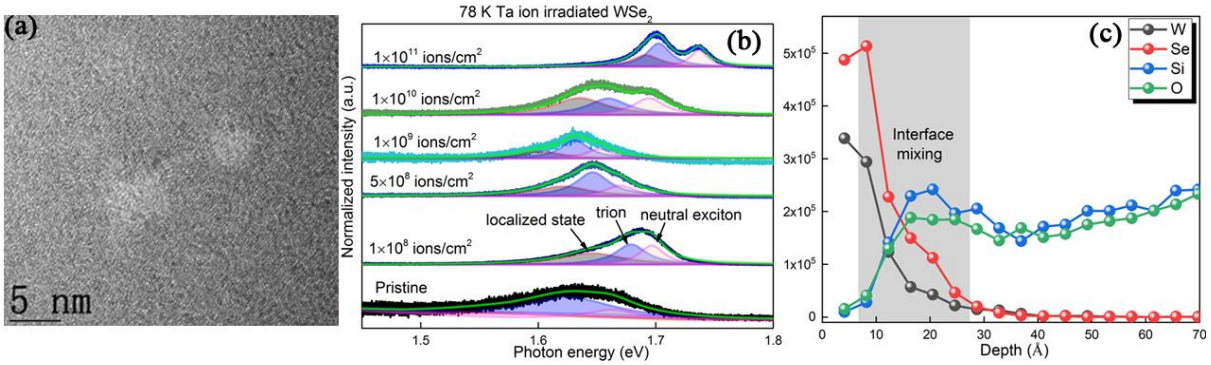

Figure 1 (a) Normally distributed disordered latent tracks in SHI irradiated multilayer WSe_2. (b) Evolution of exciton emissions with increasing ion fluences measured at 78 K. (c) 2.1 GeV Ta ion caused interface mixing according to SRIM code[1].

References:

[1] J.F. Ziegler, M.D. Ziegler, and J.P. Biersack, Nucl. Instrum. Methods Phys. Res. B, 268(11-12), 1818-1823(2010).

Dependence of the electronic stopping on the method of measurement

A.N. Zinoviev[1], **and P.Yu. Babenko**[1,*]

[1] *Ioffe Institute, St. Petersburg (Russia)*
[*] *babenko@npd.ioffe.ru*

The results of measurements of the electronic energy loss dE/dx by the backscattering method and the thin film transmission method differ significantly.

Using our code [1], we simulated the passing of protons in Au film with the thickness of d=200 Å. The trajectory length L of protons in Au films and the energy loss ΔE were calculated. Due to multiply scattering the values L and d are quite different at small collision energies.

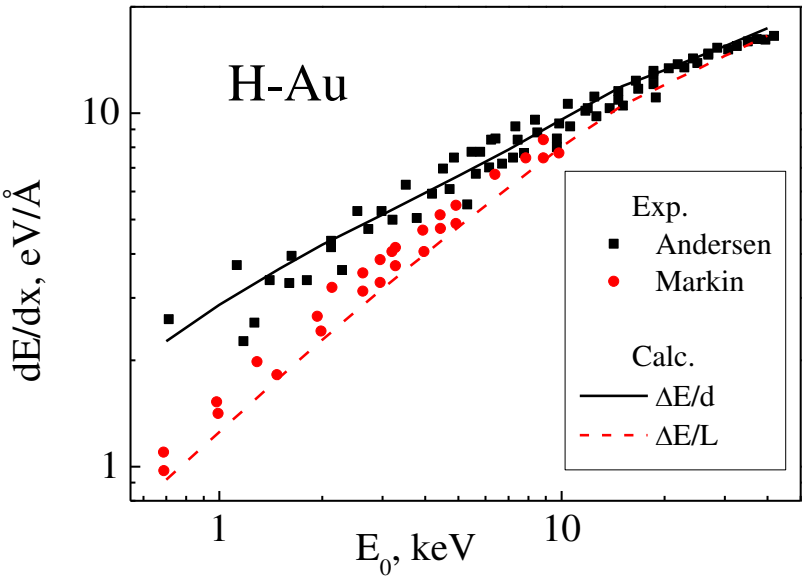

Fig.1 Inelastic energy loss as a function of the initial energy E_0.

Fig. 1 shows the experimental data on dE/dx obtained by transmission [2] and backscattering method [3]. The calculated ratio ΔE/d (solid line) coincides with results from [2] measured by transmission method. The ratio ΔE/L (dash line) gives dE/dx measured by backscattering method [3]. Therefore, the difference of values obtained by discussed methods is mainly connected with multiply scattering effects and with the interpretation of obtained results.

References

[1] D.S. Meluzova et al., *J. Surf. Invest.*, 13 (2019) 335.
[2] H.H. Andersen et al., *NIMB*, 194 (2002) 217.
[3] S.N. Markin et al., *Phys. Rev. B*, 78 (2008) 195122.

Fast electron contribution to electronic stopping

A.N. Zinoviev[1], **and P.Yu. Babenko**[1,*]

[1] *Ioffe Institute, St. Petersburg (Russia)*
[*] *babenko@npd.ioffe.ru*

In p-He and p-Ar collisions the emission of fast electrons was observed [1] (Fig. 1). Cross-sections of n-fold ionization σ_i^n, excitation cross-section σ_{ex} and electronic stopping cross-section S_e are related by formula

$$S_e = \sum_n \left(\sigma_i^n \left\{ \sum_{n=1,2,3,\ldots} I_n + n \cdot W_e \right\} \right) + \sigma_{ex} \cdot I_{ex} \qquad (1)$$

Here I_n is n-fold ionization potential, I_{ex} is excitation potential, W_e is the mean energy of emitted electrons. In the considered case the contribution of excitation is only 7% in p-He collisions and 8-10% in p-Ar collision and this term can be easily subtracted. Usually single ionization process is dominant and the values of W_e can be obtained from relation (1) using the experimental values of σ_i^n. The values of W_e obtained by this method are in good agreement with direct measurements of energy spectra of emitted electrons (see Fig. 1). The theory of dynamical ionization (DI) [2] predicts the proportionality of W_e to initial velocity v. In the considered cases such dependence occurs up to v<2 a.u. At larger velocities the Born approximation successfully describes the observed dependence.

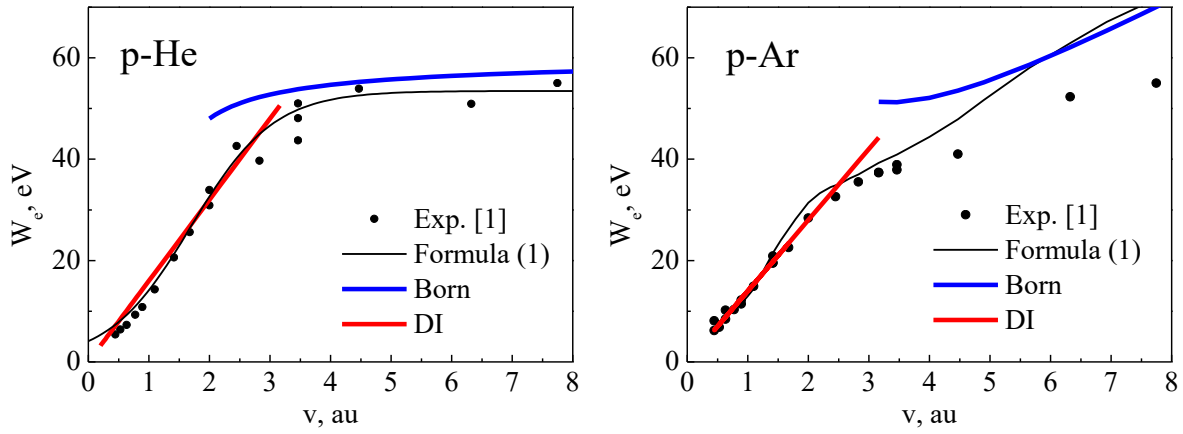

Fig.1. The dependence of W_e versus v. Points – experiment [1], black line - values obtained using formula (1). Predictions by the dynamical ionization theory and Born approximation are also indicated.

Let us consider the case of p-Ar collision, E =200 keV. In this case W_e= 45 eV, this value exceeds the ionization potentials by a factor of three. The emission of fast electrons in energetic ion-surface collisions can produce additional radiation effects during ion implantation and this phenomenon must be taken into account.

References

[1] M.E. Rudd, L.H. Toburen, N. Stolterfoht, *At. Data Nucl. Data Tables*, 18 (1976) 413.
[2] S.Yu. Ovchinnikov, G.N. Ogurtsov, J.H. Macek, Yu.S. Gordeev, *Phys. Rep.*, 389 (2004) 119.

On the problem of Be and W impurities in ITER plasma

A.N. Zinoviev[1], P.Yu. Babenko[1,*], M.I. Mironov[1], and A.P. Shergin[1]

[1] *Ioffe Institute, St. Petersburg (Russia)*
[*] *babenko@npd.ioffe.ru*

In the experiments on the tokamak ITER beryllium is planned to be the material of the first wall and tungsten – the material of the divertor. Beryllium was chosen due to the small Z which leads to low irradiation losses of Be ions in the plasma. The choice of tungsten was due to its low sputtering coefficient when bombarded by hydrogen isotopes and helium ions.

The fluxes of fast D and T atoms leaving the plasma can sputter the beryllium wall and, as our studies have shown, cause Be to enter the plasma at a level equal to 3-5% of the average ion plasma concentration. At present the difference in the sputtering coefficients of beryllium between theory and experiment reaches 50% for hydrogen irradiation, and 27% for deuterium. There is no experimental data for tritium. Particles with angles of incidence of 60-70 degrees from the surface normal are known to make a large contribution to sputtering. Therefore, it is important to know the angular dependences for sputtering coefficients. Unfortunately, such experimental data is scarce.

As our calculations show, sputtered Be atoms leave the wall with energies in the 5-100 eV range. More accurate information on the energy and angular distributions of sputtered Be atoms would allow us to increase the reliability of the estimates of the beryllium influx into the plasma. According to our estimation, sputtered atoms can easily reach the plasma separatrix region. In this region the plasma temperature is $T_e = T_i = 170$ eV, density is $2 \cdot 10^{13}$ cm^{-3}. In such conditions Be atoms are ionized up to bare nuclei and thermalized up to the energies of $E = T_i = 170$ eV. When approaching the divertor, they can be additionally accelerated by the plasma potential U and have the energy $E = T_i + ZU$. They will bombard the divertor and cause intensive surface erosion. According to [1], the density of gas-plasma target near divertor is $1.8 \cdot 10^{15}$ см$^{-3}$, its length along the magnetic line is 5-10 cm, the electron temperature is 10 eV, and the degree of plasma ionization is 50%. Our estimates show that when passing this target, the ions partially lose energy, their charge slightly decreases, but most of them reach the divertor and cause it to sputter. According to our estimates, if Be ions with a concentration of 5% are present in the plasma, the divertor sputtering due to Be ion irradiation is 25 times higher than in the case of hydrogen irradiation.

Therefore, sputtering coefficients of the divertor material by ions with different charge are highly necessary, as well as the energy and angular distributions of sputtered atoms. In addition to Be ions, the same information is needed for C and O ions, which usually enter the plasma due to sputtering of oxides and carbides on the wall, as well as for N, Ne, Ar, which can be used as the additives in the plasma to lower the electron temperature at the divertor.

References

[1] A.S. Kukushkin, H.D. Pacher, V. Kotov et. al., *Fusion Eng. Des.*, 86 (2011) 2865.

Reflected particles energy spectra during bombarding a tungsten surface with hydrogen atoms

V.S. Mikhailov[1, *], **P.Yu. Babenko**[1], **D.S. Tensin**[1] **and A.N. Zinoviev**[1]

[1] *Ioffe Institute, St. Petersburg (Russia)*
[*] *chiro@bk.ru*

The backscattered particles spectra (Fig.1) are calculated depending on the angle and energy for the perpendicular bombardment of tungsten by hydrogen atoms. The code [1] used binary collision approximation.

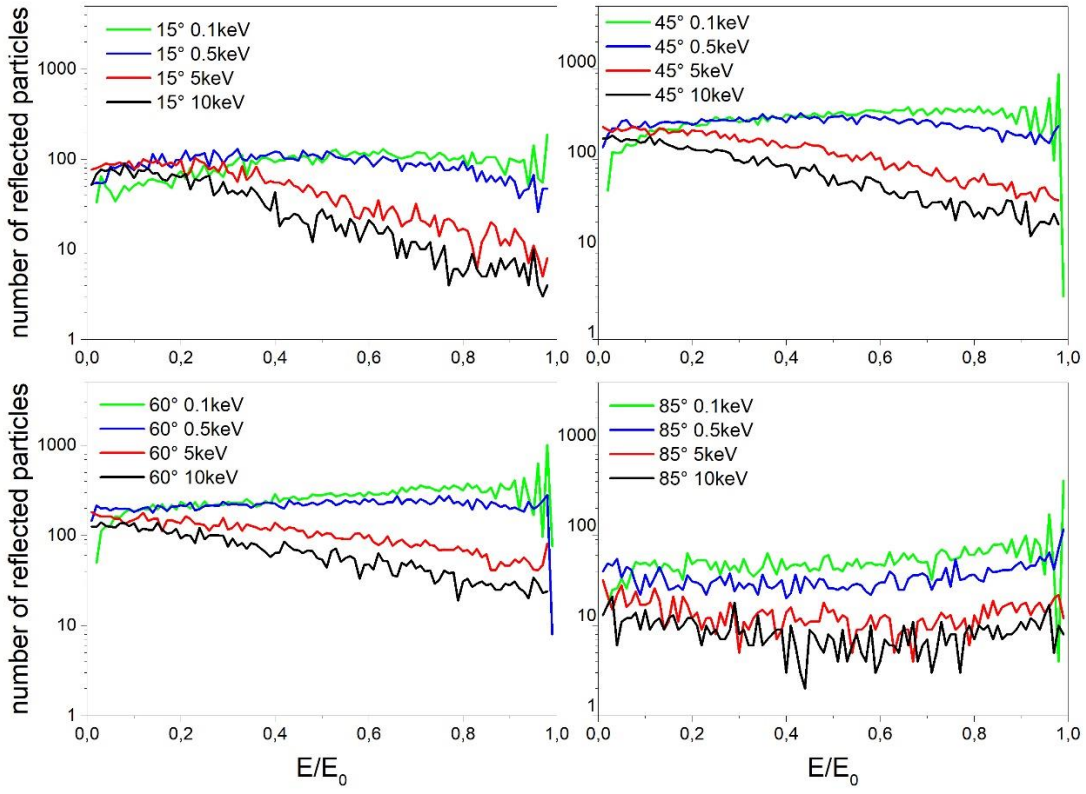

Fig.1. Backscattered particles spectra.

The abscissa represents the normalized energy. The y-axis represents the reflected particles number. The total number of bombarding particles was 10 million. The number of reflected particles is greater for lower energies, since the reflection coefficient decreases with increasing energy. These results can be useful for analyzing of fast hydrogen particles influx into the plasma and for neutral particle diagnostics

References

[1] D.S. Meluzova, P.Y. Babenko, A.P. Shergin, et al., *Synch. Investig*. 13, 335–338 (2019).

Hydrogen atoms reflection coefficient from the beryllium surface saturated with hydrogen

V.S. Mikhailov[1, *], **P.Yu. Babenko**[1], **D.S. Tensin**[1] **and A.N. Zinoviev**[1]

[1] *Ioffe Institute, St. Petersburg (Russia)*
[*] *chiro@bk.ru*

The hydrogen atoms reflection coefficients from hydrogen-saturated beryllium are calculated. The code [1] used binary collision approximation. The concentration ratio of hydrogen to beryllium in the solid was 20/13. The reflection coefficients dependence on the angle counted from the surface and energy of bombarding particles was calculated (Fig.1).

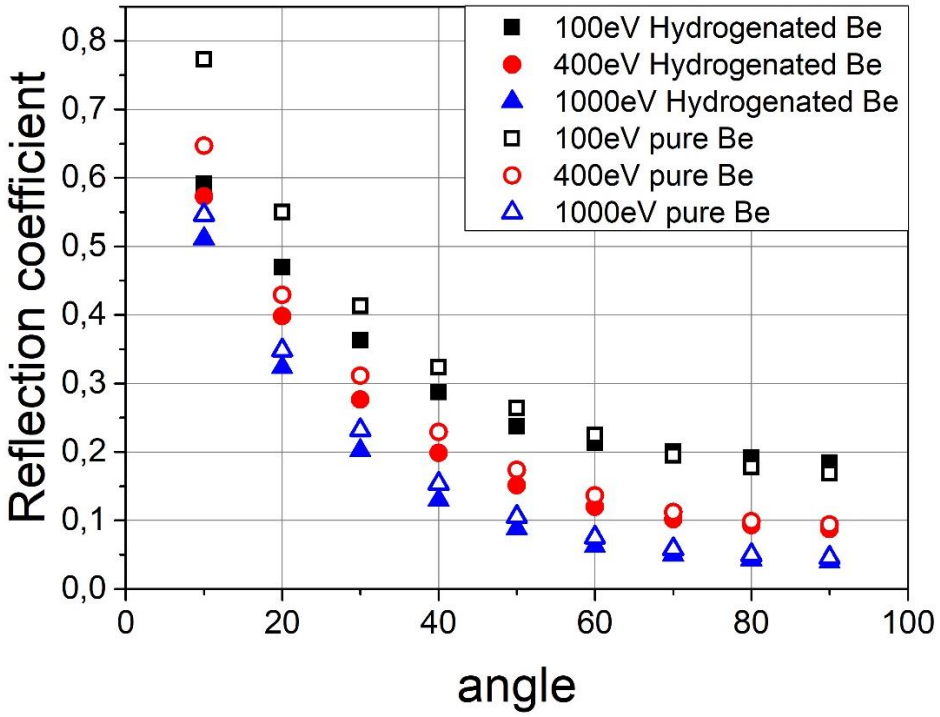

Fig.1. Hydrogen atoms reflection coefficients from pure and hydrogen-saturated beryllium

The difference in the reflection coefficients for hydrogenated and pure beryllium is significant at low angles of incidence. This difference decreases with increasing energy of the incident particles.

References

[1] D.S. Meluzova, P.Y. Babenko, A.P. Shergin, et al., *Synch. Investig*. 13, 335–338 (2019).

Channeling of hydrogen isotopes in gold and tungsten

D.S. Tensin[1,*], **P.Yu. Babenko**[1], **A.P. Shergin**[1], **and A.N. Zinoviev**[1]

[1]*Ioffe Institute, St.Petersburg, Russia*
[*]*daria.tensin@gmail.com*

Spatial distributions and ranges of H and D ions in Au(100) and W(100) were calculated. Two components of the depth distribution of ranges which appear with the increase in the energy of ions were observed (Fig.1): one is caused by near-surface scattering, and the other one characterizes channeled particles. A new phenomenon – formation of a stable spatial structure of the channeled part of the beam after the beam passes a short distance (Fig.2) – was found. Transition into adjacent channels occurs as the ions slow down. The spatial structure of the channeled ion beam completely falls apart near the stopping point of the particles. An experiment linking the obtained spatial distribution with angular distribution of emitted particles is proposed.

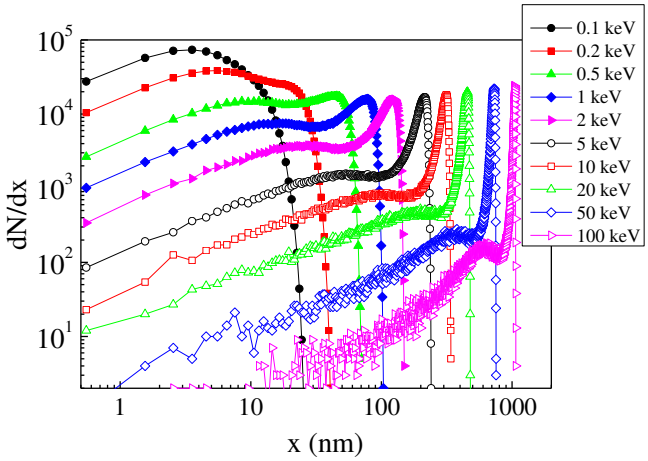

Figure 1: Depth distribution of ranges of 0.1-100 keV D ions in W(100) in the case of normal incidence.

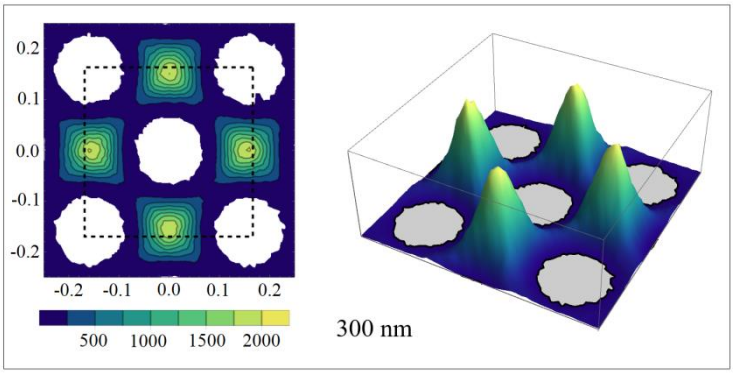

Figure 2: Spatial distribution of D ions at a depth of 300 nm inside W(100); initial energy of ions – 100 keV. Axes represent distance in nm. Color corresponds to a number of particles registered at a particular spot. Dashed square – area irradiated with D ions.

Modeling the interaction of hydrogen and helium isotopes with the first wall of a tokamak reactor

D.S. Tensin[1,*], **P.Yu. Babenko**[1], **A.P. Shergin**[1], **and A.N. Zinoviev**[1]

[1] *Ioffe Institute, St Petersburg (Russia)*
[*] *daria.tensin@gmail.com*

Computer simulation was used to study the interaction (reflection, implantation, ranges, energy release) of hydrogen, deuterium, tritium, and helium atoms with beryllium, carbon, and tungsten, which are promising materials of a tokamak-reactor first wall. A program code developed by the authors [1] was used to perform simulations of ion collisions with the surface.

Using the DFT method [2], interaction potentials of plasma atoms (H, D, T, He) and atoms of the first wall materials (Be, C, W) were calculated. An unexpectedly strong influence of the well in interaction potentials on the reflection processes was found. It has been shown that at initial energies below 200 eV, the presence of a potential well drastically changes the reflection coefficients – from almost a 100% reflection to a noticeable absorption of particles by the surface.

The influence of the surface structure (crystal, polycrystal, amorphous) on the values of reflection coefficients as well as their dependence on the energy and the angle of incidence of plasma atoms were studied. Satisfactory agreement with the available experimental data is demonstrated.

Ranges, energy release and nuclear stopping powers were calculated. It is shown that the nature of the energy release is very different from the existing concept – at energies up to 100 keV, the maximum energy release occurs near the surface, and the Bragg peak dominates only at energies above 500 keV. This phenomenon is explained by how the stopping power depends on the particle energy.

It has been shown that tritium atoms penetrate deeper into the surface than deuterium atoms with the same energy, regardless of the surface material. As a result, dangerous accumulation of tritium during prolonged wall irradiation in a tokamak reactor is predicted. Using the DOUBLE-MC code [3], the energy spectra of deuterium and tritium atoms leaving the plasma in a tokamak reactor were calculated. It has been shown that tritium accumulation is also present when the surface is irradiated with a flux of atoms with a wide energy spectrum.

References

[1] D.S. Meluzova, P.Yu. Babenko, A.P. Shergin, A.N. Zinoviev, *J. Surf. Invest. X-ray*, 13 (2019) 335.
[2] A.N. Zinoviev, K. Nordlund, *Nucl. Instr. Meth. B*, 406 (2017) 511.
[3] V.I. Afanasyev, F.V. Chernyshev, A.I. Kislyakov et. al., *Nucl. Instr. Meth. A*, 321 (2010) 456.

Molecular dynamics simulations of tungsten and beryllium sputtering near threshold

D.S. Tensin[1,*], **A.N. Zinoviev**[1], **P.Yu. Babenko**[1], **and A.P. Shergin**[1]

[1]*Ioffe Institute, St.Petersburg, Russia*
[*]*daria.tensin@gmail.com*

In this work a code for molecular dynamics simulations of tungsten sputtering was developed. The code uses a modern embedded atom method potential developed by Marinica et al. [1] (denoted there by "EAM-4"), stiffened for cascade simulations in the manner described in the work [2]. The atomic structure of tungsten was constructed using a model of an ideal amorphous solid simulated by a program code [3]. Sputtering of beryllium was simulated using LAMMPS. Analytical bond-order potential from [4] was chosen for Be-Be interaction. Interaction of an incident ion with W and Be target atoms was described by a potential obtained through density functional theory calculations [5]. Sputtering yields for the Ne-W system calculated using our code are in good agreement with experimental data [6].

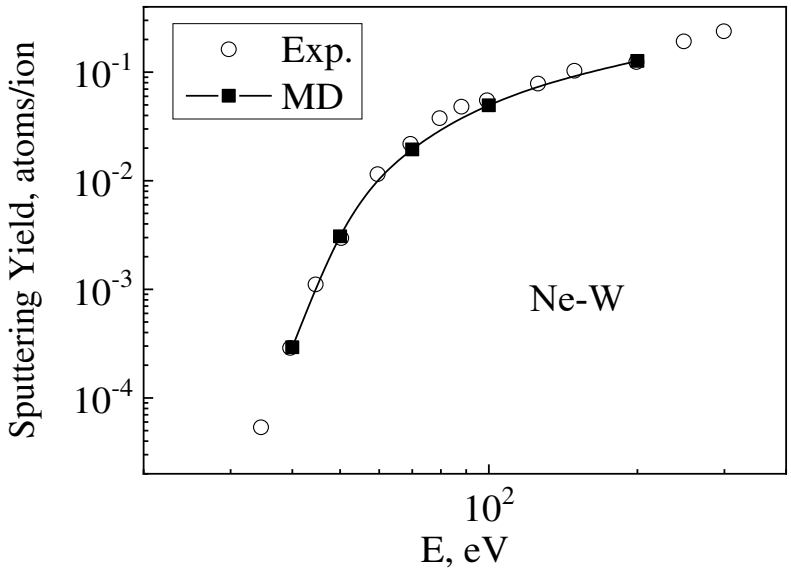

Figure 1: Sputtering yield for W surface versus initial energy of incident Ne atom. Experimental data from [6].

References

[1] M-C. Marinica et.al., *J.Phys.Cond.Matt.*, 25 (2013) 395502
[2] A.E. Sand et.al., *Journal of Nuclear Materials*, 470 (2016) 119
[3] https://users.cecs.anu.edu.au/~u9300839/
[4] D.S. Meluzova et.al., *NIMB*, 460 (2019) 4
[5] C. Björkas et al, *J.Phys.Cond.Matt.*, 21 (2009) 445002
[6] R. Behrisch, W. Eckstein, Sputtering by Particle Bombardment. Berlin. Springer. 2007.

Nuclear stopping powers for DFT potentials

A.N. Zinoviev[1,*], **P.Yu. Babenko**[1], **K. Nordlund**[2]
[1] *Ioffe Institute, St. Petersburg (Russia)*
[2] *Helsinki University, Helsinki (Finland)*
[*] *zinoviev@inprof.ioffe.ru*

As shown in [1] the potentials calculated in the framework of DFT using Dmol approach for choosing wave function basis are in good agreement with scattering experiments. For these potentials, calculations of nuclear stopping powers (dE/dx) were carried out [2]. To correct the parameters of the potential well, we used data on the dissociation energies of diatomic molecules.

The obtained values differ by 12-50% from the data given by the SRIM code [3], where the ZBL potential is used. For the case of a small attractive well (see Fig. 1a), the data have been successfully fitted using universal coordinates proposed in [4].

In the presence of deep potential well (Fig. 1b) an additional peak appears on the dependence of losses at small energies. Obtained data for H-Be, H-C and H-W collisions are important for modeling plasma-wall interaction in thermonuclear research.

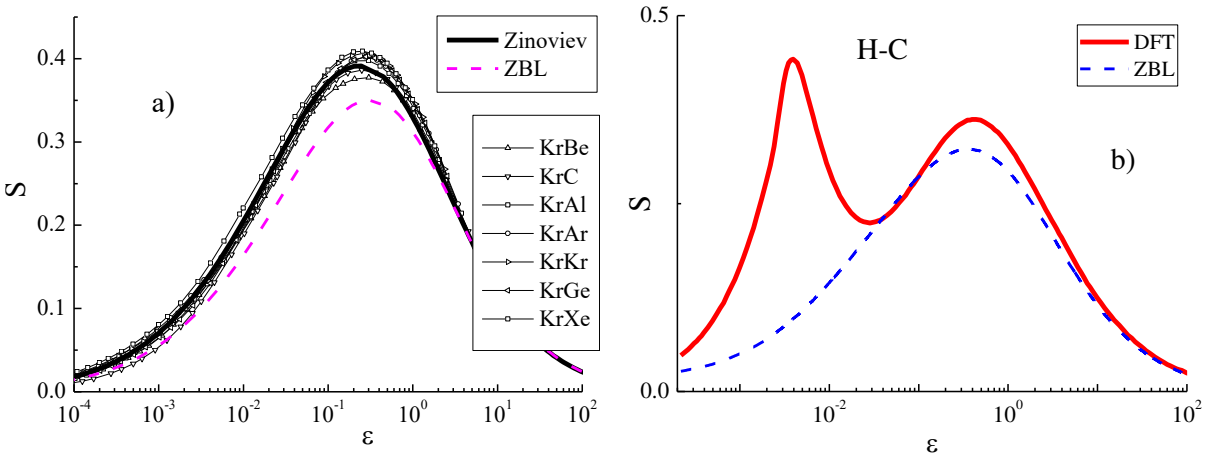

Fig.1. Nuclear stopping powers in universal coordinates in comparison with data obtained using ZBL and Zinoviev potential: a) Kr-Be, C, Al, Ar, Kr, Ge, Xe collisions, b) H-C case.

References

[1] A.N. Zinoviev, K. Nordlund, *Nucl. Instr. Meth. B*, 406 (2017) 511.
[2] A.N. Zinoviev, P.Yu. Babenko, K. Nordlund, *Nucl. Instr. Meth. B*, 508 (2021) 10.
[3] J.F. Ziegler, J.P. Biersack, SRIM, http://www.srim.org.
[4] J. Lindhard, V. Nielsen, M. Scharff, *Mat. Fys. Medd. Dan. Vid. Selsk.*, 36 (1968) 1.

The potential determination for the H-Au system from experimental data

P.Yu. Babenko[1], **A.N. Zinoviev**[1,*], **V.S. Mikhailov**[1], **D.S. Tensin**[1] **and A.P. Shergin**[1]

[1] *Ioffe Institute, St. Petersburg (Russia)*
[*] *zinoviev@inprof.ioffe.ru*

A technique is proposed for determining the parameters of the interatomic interaction potential in the case of particles scattering by a solid. The potential of the Zinoviev type [1] was taken as the basis one. To determine the parameters of the potential, the description of the experimental energy spectra of scattered particles [2] for different scattering angles β relative to the normal using our code [3] is used.

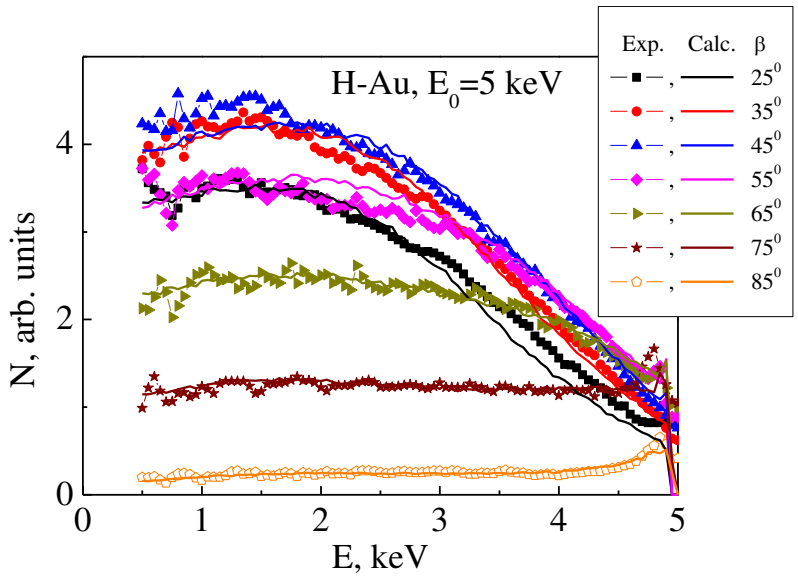

Fig. 1. Energy spectra of scattered protons.

From fig. 1 it can be seen that, by varying the potential parameters, it is possible to achieve agreement between the experiment and the calculation with an accuracy of 7%. The resulting potentials are characterized by a strong decrease in the screening constant compared to collisions in the gas phase.

References

[1] A.N. Zinoviev, *NIMB*, 269 (2011) 829.
[2] H. Verbeek, *J. Appl. Phys.*, 51 (1980) 1783.
[3] D.S. Meluzova et al., *J. Surf. Invest.*, 13 (2019) 335.

Photoionization of a Quantum Grating formed by a Single Atom

S.F. Zhang[1,2,*], **B. Najjari**[1,], **and X. Ma**[1,2]

[1] *Institute of Modern Physics, Chinese Academy of Sciences, Lanzhou 730000, China*
[2] *University of Chinese Academy of Sciences, Beijing 100049, China*
[*] *zhangshf@impcas.ac.cn*

When an atom passes through a macroscopic diffraction grating its wave function acquires a regular space structure and its collision by another particle can be thought of as scattering, of the latter, on a grating composed of a single atom (termed as “quantum-grating" or “QG” for short). We will report on photoionization of such a ‘quantum grating’ (see Fig. 1)[1]. It is shown that, unlike photoionization of a ’normal’ atom or molecule, in the case of an atomic QG there is no ‘mirror symmetry’ correspondence between the momentum spectra of the photoelectrons and recoil ions. Moreover, the spectra of recoil ions display both one- and two-particle interference while the electron spectra are sensitive only to the latter. Besides, the recoil-ion spectra contain a direct information about the diffraction grating, however the electron spectra do not in general. The reason for the “striking disparities" between the electron and recoil ion spectra is due to the large difference between the electron and nuclear masses which has a qualitatively different impact on the photoionization process for an atomic QG compared to the ‘normal’ atomic case.

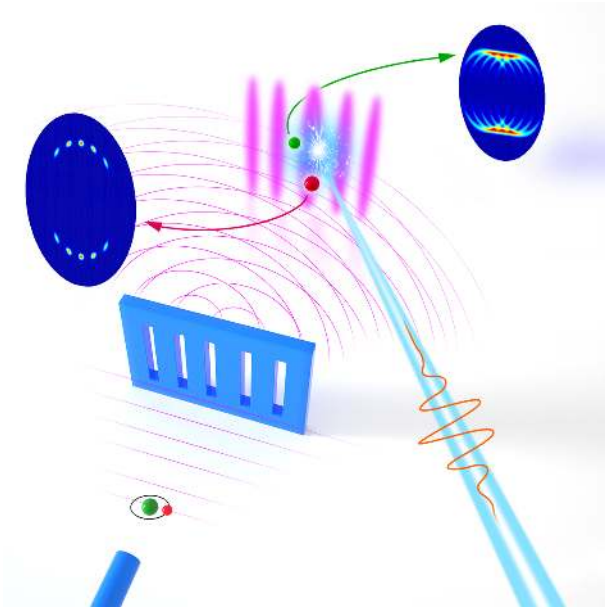

Figure 1: Illustration for the photoionization of Quantum Grating.

Moreover, the atomic QG can profoundly manifest itself also when it is probed in other basic atomic collision processes (e.g. ionization by charged particles, radiative and non-radiative electron capture to bound/continuum states and projectile-electron loss) as well as in processes involving photo absorption and Compton scattering.

References

[1] S. F. Zhang, B. Najjari, and X. Ma, *Journal of Physics B: Atomic, Molecular and Optical Physics*, 2021, 54, 15LT01

Selective Bond Cleavage of ArCO by Electron Impact

S. Yan[1,2,*], **D. Liu**[3], **S. B. Zhang**[3], **and X. Ma**[1,2,*]

[1] *Institute of Modern Physics, Chinese Academy of Sciences, Lanzhou 730000, China*
[2]*University of Chinese Academy of Sciences, Beijing 100049, China*
[3]*School of Physics and Information Technology, Shanxi Normal University, Xi'an 710119, China*
[*]*yanshuncheng@impcas.ac.cn, x.ma@impcas.ac.cn*

Chemical reaction manipulation is one ultimate goal of chemistry investigation, and many control techniques in atomic/molecular scale have been developed to maximize the production of the desired product and minimize the yield of the side product, e.g. achieving the selective bond cleavage [1-3]. This direction is important in low-temperature plasma, astrochemistry, as well as heterogeneous catalysis. Recently, several theoretical calculations predicted that the cross-section of a specific molecular fragmentation pathway will be enhanced by embedding the molecule into a cluster [4, 5] and ionizing/exciting the neighboring atom.

We carried out the ArCO fragmentation experiment by 480 eV electron impact at reaction microscope, where two ions and one electron were measured in coincidence. As shown in Fig.1, the yield ratio of $Ar^+/C^+/O$ ion pair to $Ar^+/O^+/C$ ion pair is larger than 6, which is 5 five times larger than that of C^+/O ion pair to O^+/C ion pair in isolated CO case. The characteristic of the electron energy spectrum and Newton diagram in our experiment suggests that the polarization between Ar^{2+} ion and CO will produce the transient $(ArCO)^{2+}$ ion, the following emission of an O atom and Coulomb explosion of ArC^{2+} metastable ion will induce Ar^+/C^+ ion pair, this mechanism enhances the specific fragmentation pathway $CO \rightarrow C^+ + O$.

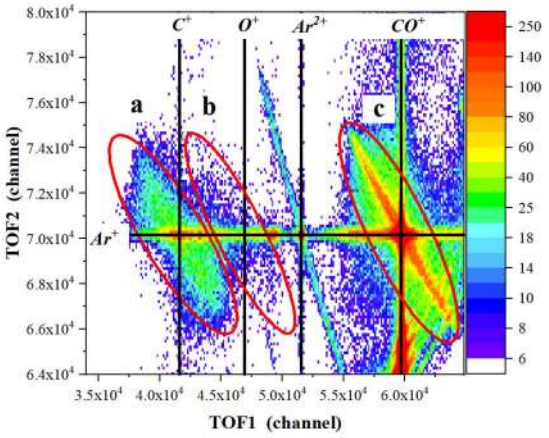

Figure 1. Two-dimensional TOF correlation map.

This experimental work is supported by the National Key Research and Development Program of China (No. 2017YFA0402300), the National Natural Science Foundation of China under Grant Nos. U1832201, 11934004 and 11974230.

References

[1] W. Eberhardt, T. K. Sham, R. Carr, et al., *Physical Review Letters*, (1983) 50: 1038
[2] M. Lemeshko, R. V. Krems, J. M. Doyle, et al., *Molecular Physics*, (2013) 111: 1648
[3] M. G. Hu, Y. Liu, M. A. Nichols, et al., *Nature Chemistry*, (2021) 13: 435
[4] L. S. Cederbaum, *The Journal of Physical Chemistry Letters*, (2020) 11: 8964
[5] Y. C. Chiang, S. Engin, P. Bao, et al., *Physical Review A*, (2019) 100: 052701

Index of authors